TALLINN UNIVERSITY OF TECHNOLOGY
School of Information Technologies

Aleksandr Nikolajev 153763IVEM

EVALUATION OF LED AS LIGHT SENSOR

Master's thesis

Supervisor: Paul Annus

PhD

Tallinn 2017

TALLINNA TEHNIKAÜLIKOOL
Infotehnoloogia teaduskond

Aleksandr Nikolajev 153763IVEM

VALGUSDIOODIDE EVALVEERIMINE VALGUSSENSORINA

Magistritöö

Juhendaja: Paul Annus
PhD

Tallinn 2017

Author's declaration of originality

I hereby certify that I am the sole author of this thesis. All the used materials, references to the literature and the work of others have been referred to. This thesis has not been presented for examination anywhere else.

Author: Aleksandr Nikolajev

04.05.2017

Abstract

Master thesis is on the topic of "Evaluation of LED as Light Sensor", which describes the possibilities of using light-emitting diodes as both light sources and light detectors. The paper describes how light-emitting diodes were analysed as light sensors, how the measurements were performed and what their characteristics were. The work overviews current technologies which use light-emitting diodes as both emitters and detectors, analyses capabilities of the several designs and describes two designs which were made where light-emitting diodes are used as receivers, their calculations, simulation results and prototypes testing results.

This thesis is written in English and is 68 pages long, including 6 chapters, 54 figures and 5 tables.

Annotatsioon

Valgusdioodide evalveerimine valgussensorina

Magistritöö teemal "Valgusdioodide evalveerimine valgussensorina" kirjeldab valgusdioodide kasutamise võimalusi nii valgusallikate kui valgusdetektoritena. Dokumendis kirjeldatakse, kuidas analüüsiti valgusdioode kui valguse sensoreid, kuidas mõõtmised teostati ja millised olid nende tunnused. Töö antakse ülevaade tehnoloogiast mis kasutab valgusdioode nii saatja kui vastuvõtja funktsioonis, analüüsitakse lahendusvariante. Täpsemalt kirjeldatakse kahte vastuvõtja varianti, esitatkse nende arvutuste, simulatsioonide ja prototüüpide katsetulemused.

Lõputöö on kirjutatud inglise keeles ning sisaldab teksti 68 leheküljel, 6 peatükki, 54 joonist, 5 tabelit.

List of abbreviations and terms

AC	Alternating Current
ADC	Analogue-Digital Converter
BOM	Bill of Materials
DC	Direct Current
IC	Integrated Circuit
LD	Laser Diodes
LED	Light Emitting Diode
OA	Operational Amplifier
PCB	Print Circuit Board
PWM	Pulse Width Modulation
RGB	Red Green Blue
SMD	Surface-Mount Technology
SNR	Signal-to-Noise Ratio
THT	Through-Hole Technology
TIA	Transimpedance Amplifier
UART	Universal Asynchronous Receiver/Transmitter
UV	Ultraviolet
VLC	Visual Light Communication

Table of contents

List of Figures

List of tables

1 Introduction

Nowadays, light-emitting diodes had become part of our life. The light-emitting diode (LED) is a light source which contains p-n junction inside and emits light when it is forward biased. LEDs received their popularity comparing to the traditional light sources because they are small in size, rugged, reliable during execution, bright and efficient [1]. In addition, LEDs have longer lifespan than the traditional light sources [2]. The continuous development of the LED technology has granted many types of LEDs, with different powers and sizes. The choices of the colour for the LEDs are also very wide, present LEDs could be any colour, especially if it is RGB LED which can change it's colouring any moment depending on the control signal. In 2014 the Nobel Prize in Physics was presented to the group of scientists who developed in 1990 efficient blue LED [3]. Such a large variety of LEDs gave the possibility to use them in many applications, including healthcare and environment. Today it is hard to imagine human life without this invention.

But due to the fact that LED was designed specifically for emitting light one can forget that fundamentally they are photodiodes as well and they can work as light detectors [4]. Although they are not optimized for this task, like specifically designed photodiodes, transistors and resistors, they are still very effective at it. The idea of LEDs working as light detectors was widely published in 1970-s by Forrest W. Mims [5], [6], but yet final utilization of LEDs like detectors didn't find its popularity until now.

1.1 Working principle of LED as photodiode

To start with, it should be explained what is the working principle of the photodiode. A photodiode is a semiconductor device which has p-n junction like most of the diodes and intrinsic layer between p and n layers [7]. The photocurrent is produced by generating electron-hole pairs due to the absorption of the light in the intrinsic or depletion region and the amount of the generated photocurrent is proportional to the absorbed light.

The working principle states that when photons of energy which are greater than 1.1 eV hit the diode, electron-hole pairs are created. The intensity of photon absorption, which is also known as the inner photoelectric effect, depends on the energy of photons. The lower the energy of photons, the deeper the absorption is.

When the absorption occurs in the depletion region of the p-n junction, these hole pairs are swept from the junction. This results in holes move toward the anode and the electrons move toward the cathode which produces photocurrent.

Light emitting diodes work opposite way. When the current passes through the diode, the carriers start to move. Electrons and holes in semiconductor recombine and the emission of photons starts [1]. As the reaction human sees the diode emitting light. But LEDs have the same p-n junction where the carriers can be externally affected both by current or, what is more important, light. This brings to the conclusion the LED should behave the same way as the photodiode due similarity of the internal structure and effects of external light. As a result, when the LED is exposed to light, it starts to generate light current.

1.2 State-of-the-art

One of the technologies which gave the push in LED development as a light detector was Visual Light Communication (VLC). Currently, wireless technologies play a significant role in our lives [8], and an analysis of the use and transfer of data predicts that in the future the use of wireless technologies will only increase [9]. Since this technology shows promising results [10]-[13], it is assumed that in the future it will be used in high performance networks.

Development and evolution of the data transmission through light, search for cheap solutions and with reducing circuit complexity engineers returned to the idea of using light-emitting diodes as photodetectors. Due to its ubiquitous and cost, simple commercial LED is now easy to find.

LEDs as sensors were able to find their place in the VLC technology [4], [14]. Currently, the novel idea is to use LED as a transceiver for data transmission and data receiving. It provides a new low-speed and wireless "ad hoc" networking for short distances [14] and this technology is able to communicate with speed of less than megabit per second at the distances of few meters and it will be very useful in such cases as home networks, deploying sensor networks, smart illumination or some consumer devices like smart toys

or car diagnostics [4], [15]-[16]. The concept of the idea is presented in Figure 1 and one of the prototypes is in the Figure 2.
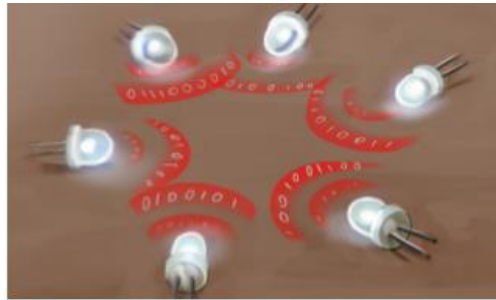
Figure 1. Concept art of LED as a transmitter which shows the communication and data transmission between the diodes using light [14].
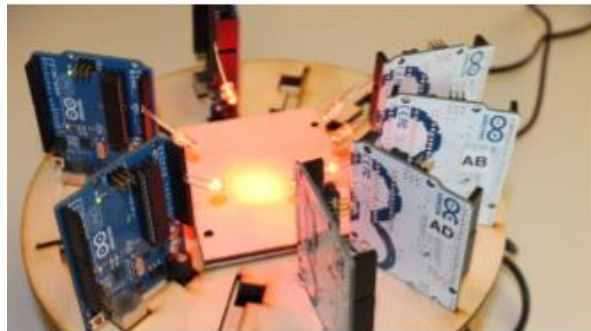
Figure 2. The prototype which consists of multiple ATmega328P evaluation boards which communicate with each other through the LEDs [14]. The chosen LEDs are red 5mm Kingbrigth L-7113SEC-J3 with peak wavelength 640nm and field of view 20°. VLC adhoc network has PHY and MAC layers which use LEDs in bidirectional communication as both transimmer and receiver. All boards connected to the computer which gives a signal to the boards to deliver the payload. The system could operate reliably at distances up to 2m.

Additionally, LED has been used in the detection of solar radiation and daylight [17]-[21].

One of the most unique features which provides LED working as light detector is his ability to sense only the certain range of wavelength [21]-[24]. This ability is widely used in those cases where there is a need to choose only certain wavelengths, and this highlights the LED comparing to other photodetectors. In case of the photodiodes it would be needed to develop an additional optical filter, which would allow to capture only certain wavelengths, and in the case of the LED it is "integrated." It should be noted that there are discussions and analysis showing that the LED responds to wavelengths which it emits itself and shorter [4], [25]-[26], but other measurements show that the sensitivity

of the LED has a shift comparing to radiation [21], [24]. The measurements of the sensitivity of the LEDs from various sources are shown in the Figure 3 - Figure 6.
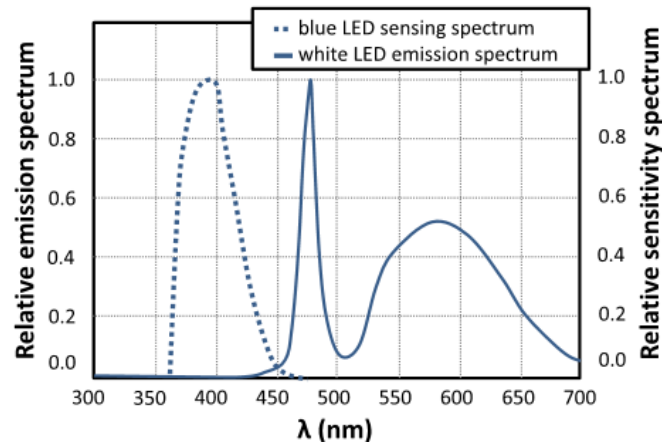
Figure 3. Emission and sensing spectra of phosphor-coated blue LED [21].
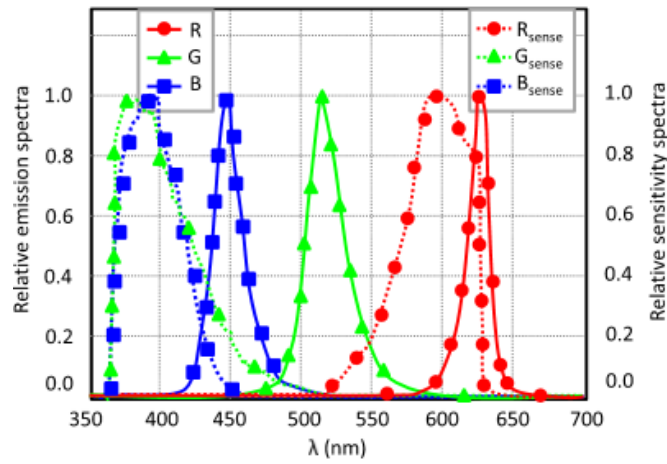
Figure 4. Illustration of emission and sensitivity spectra of red, green and blue LEDs at room temperature [24].
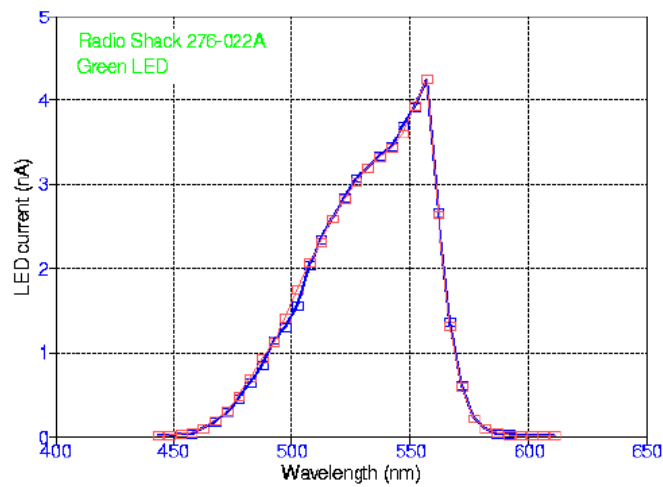
Figure 5. Detection of the green LED [28].

16
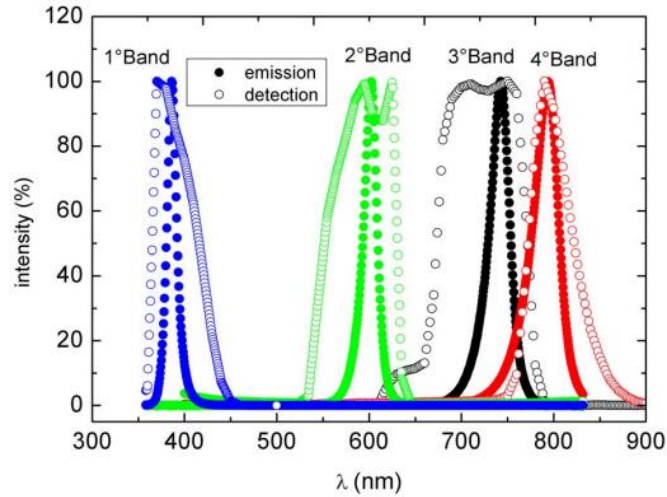
Figure 6. Normalized emission and detection spectra of the selected LEDs [32].

Sensitivity of the LED is lower than the photodiodes or phototransistors have [27], but this drawback can be corrected in several ways. One of them is to use operational amplifiers [28]. One of the available circuits is shown in Figure 7.
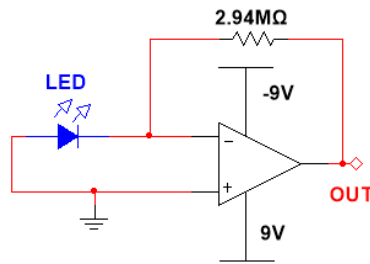
Figure 7. Operational amplifier based circuit [28]. The LED is connected in series to the input of the operational amplifier.

In this circuit the input is connected in series with the negative pin of the operational amplifier which should ideally have 0 current flows. The operational amplifier has a negative feedback through resistor with very high resistance. The circuit works as current-to-voltage converter. The LED generates photocurrent when it senses light and the voltage on the output of the operational amplifier start to grow. Ideally, the equation should like:

$$V_{out} = I_{photo} \cdot R \tag{1}$$

Although, this one of the simplest ways to improve LEDs sensitivity, it is not good enough due to very low sensitivity of the LED and, as a result, low generated photocurrent. Only few were able to adopt this circuit to LED [27]. In addition, output would have nonlinear response due to logarithmic relationship to the received light energy. Also, high resistance

of the feedback resistor develops significant thermal DC voltage drift due to the temperature coefficient of the amplifier [29].

There are also a variety of amplifier connections which could improve the work certain specifications of the device and the final choice should be based on linearity, offset, noise and bandwidth considerations. In Figure 8 - Figure 10 multiple circuits are presented, each one is designed to improve certain specification.
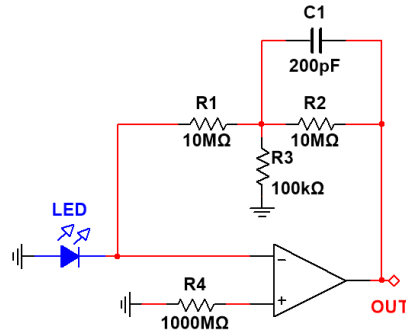
Figure 8. Circuit with DC error compensation [29]. DC error is one of the primary noise limitation with the commonly prefered high feedback resistances. To resolve this this effect, additional capacitor added to bypass feedback resistor. In addition, resistor tree is also recommended to replace high value resistor. Resistors may have more reasonable values but they introduce more noise. However, stray capacitance across the feedback is reduced due to added physical spacing because of the multiple elements. The equalent resistance for the feedback is described through next equation:

$$Req \; = \; R1 \; + \; R2 \; + \; (\frac{R1 \cdot R2}{R3}) \tag{2}$$
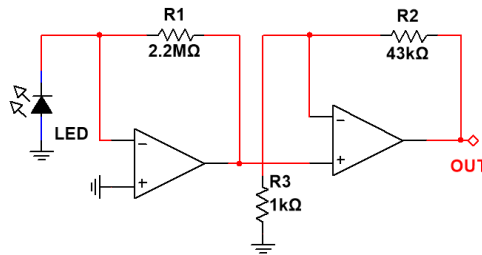
Figure 9. Circuit for greater bandwidth [29]. The parasitic capacitance around the body of the resistor always remain and affects tha bandwidth of the device. To reduce this effect lower feedback resistance should be used which will also reduce converter gain. The second amplifier is added following current-to-voltage converter. The equation for the output of the circuit is considered next:

$$V_{out} = (1 + \frac{R_4}{R_3}) \cdot R_1 \cdot I_{photo} \tag{3}$$

However, one must remember that inceasing bandwidth of the device will reduce its Signal-to-Noise ratio.
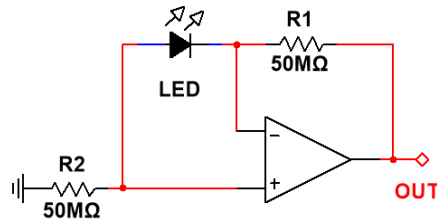
Figure 10. Circuit with improved Common-Mode-Rejection of coupled noise [29]. The photocurrent drives the non-inverting inout in that path which creates second voltage signal. The resulting gain is doubled if resistors R_1 and R_2 are equal. This also removes DC voltage from the diode and,as a result, photodiode leakage current is avoided. Additionaly, improvement in the common-mode rejection of coupled noise is added. The equation for the output voltage:

$$V_{out} = (R_1 + R_2) \cdot I_{photo} \tag{4}$$

These circuits were first designed for photodiodes but they still can be relevant for use with LEDs but using modern operational amplifiers.

The possibility to use operational amplifiers to design optical transceiver which allows the LED to work both as transmitter and receiver made possible to use the LED in Universal Asynchronous Receiver/Transmitter (UART) communication [30]. The solid advantage is that the LED could be switched faster from forward-bias when it emits light to reverse-bias when the light sensitivity is higher. The operational amplifiers are used to amplify the received signal and compare to the reference value. The circuit of the design is presented in Figure 11. This design was also tested in the simulation environment and the results of the simulation could be found in Appendix 7 – Simulation of the original EDN Networks design.
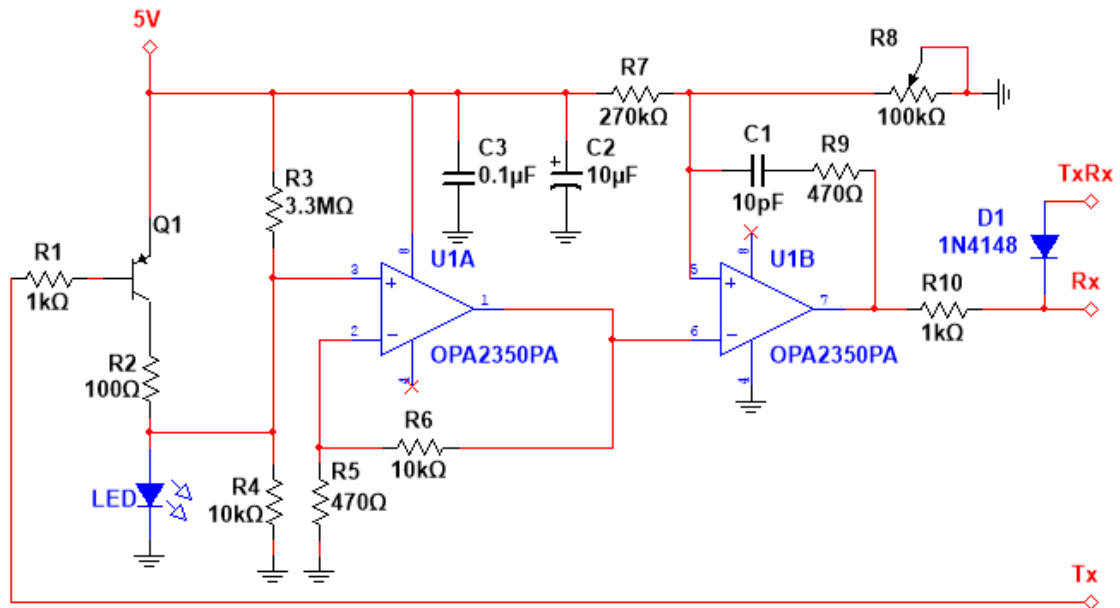
Figure 11. LED transceiver circuit proposed in EDN Network [30]. The transmitted signal is sent by Tx pin which opens and closes transistor Q1 which makes the LED blink. When the device is in the receiving mode, the transistor Q1stays constantly closed and the generated photocurrent flows through the resistor R4 which works as current-to-voltage converter. Operational amplifier U1A is used as the signal amplifier and U1B converts the output of the U1A to logical level signals. The reference voltage for the U1B is set with the potentiometer R8. The chain of R9 and C1 gives the hysteresis. Pin TxRx is used to isolate the Rx pin from Tx while the device is transmitting the signal.

Another way to make a photodetector out of the LED is to use CMOS analog I/O of the microcontroller. The idea is based on the model of the reverse biased LED shown in Figure 12 where it works as a capacitor in parallel with current source which optically induces photocurrent [4], [31]. When the diode is in reverse mode, it charges the capacitance. After that, I/O pin which was Vcc switches to input mode which gives the possibility for diode to discharge its current through the pin. This principle is described in Figure 13.
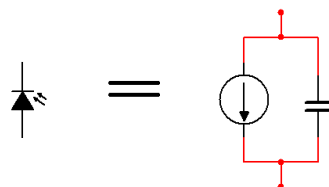
Figure 12. Model of the LED when it works as light detector [4]. The model consists of the current source and capacitor in parallel.

20
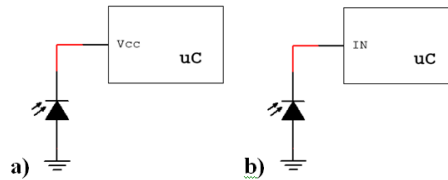
Figure 13. Stages of work of the LED when it's working as the light detector [4]. In stage a) the capacitor is charged through the pin which was set to the Vcc value. In stage b) the pin is set to measure the voltage and capacitor starts to discharge through the pin. The speed of discharge varies from the amount of light sensed by the LED.

This gives two ways for the microcontroller to measure the amount of light. First is when the measurement is taken for constant periods and with threshold voltage set. The speed of discharge of the LED is dependent on the amount of light. When the LED is illuminated by low amount of light, it discharges slower and not able pass the threshold value. The curve is shown in Figure 14. This can be considered as logical '0'. On the other hand, when it is illuminated by other light source, the process of discharging goes faster which results in faster voltage drop which is shown in Figure 15. As a result, this is logical '1' [4]. The design was tested in the simulator and the results could be observed in Appendix 8 – Simulation of the design proposed by Mitsubishi Electric Research laboratories.
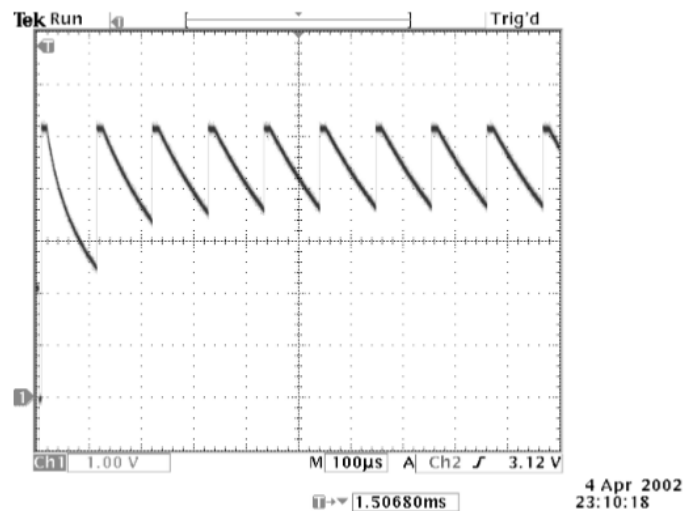
Figure 14. Voltage on the input of the microcontroller when the LED is not being illuminated [4]. This is the receiving the signal sequence when the microcontroller measures the amount of light. The microcontroller is taking measurements with the static period of 100 microseconds and totally it executes 40 light measurements. When the amount of light which is sensed by the device is low, the discharging speed of the LED is also small and it is not able to cross the reference voltage during 100 microsecond period.
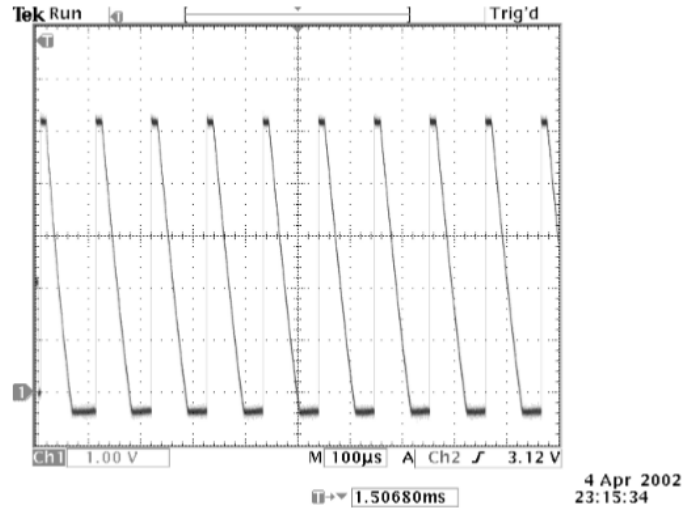
Figure 15. Voltage on the input of the microcontroller when the LED is being illuminated [4]. In this case the amount of light sensed by the LED is enough to fully discharge during 100 microsecond period.

Second way to measure the amount of light is by measuring time of discharge [31]. Like in first method, LED is charged by the supply from the I/O pin, then it switches to the input mode and starts measuring time. When the voltage discharges from logical '1' to logical '0' level, the timing stopes and depending on the measured time, microcontroller considers what amount of light did the LED sensed. The t_{period} time of the measurement can be calculated as:

$$t_{period} = t_2 - t_1 \tag{5}$$

Here t_2 is measurement start time and t_1 is measuremnt stop time. The example of measurement is shown in Figure 16.
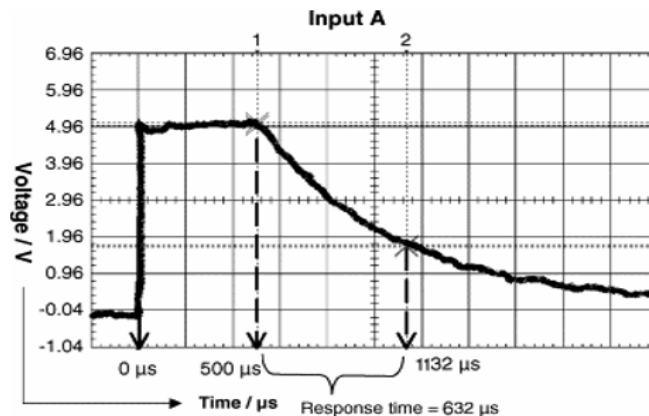
Figure 16. Voltage on the input of the microcontroller when the timing principle being used [27]. From 0 to 500 microseconds the capacitance of the LED is charged. After 500 microseconds the microcontroller switches to input mode and starts measuring the time while the diode discharges through the input till it reaches logical '0'. After measuring the time microcontroller calculates amount of light which was sensed by the LED.

22

Both of these methods show that they are able to sense light when being illuminated. In addition to the light measurement, microcontroller can also perform additional tasks. But these circuits are designed only for sensing of light and if it's needed to make LED working in bidirectional way, then both pins of the LED should be connected to I/O. This type of connection is shown in Figure 17 [4].
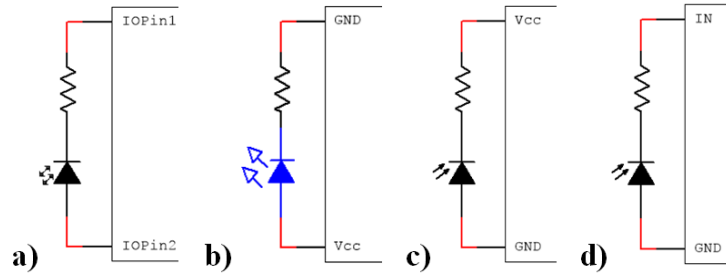
Figure 17. LED connection with the microcontroller for bidirectional work [4]. Working modes of the LED: a) general look how the LED should be connected for bidirectional work. b) the LED is switched to the light emitting or data transmission mode. c) the LED is switched to receive mode. It charges through the I/O pin which outputs Vcc voltage. D) the LED is switched to receive mode. It discharges through the I/O pin which is switched to input and the microcontroller measures the voltage value.

The final circuit has found its popularity in various applications, including developing technology of VLC, healthcare, security, environment and it is clear that LED based sensing devices have a broad range of applicability. Still, the range of work of such devices is quite low since the sensitivity of the LED is much lower comparing to other photodetection elements [27]. The fact that optical sensitivity of the various LEDs is not well known gives its certain complexity in designed circuit's where LEDs work as light detectors or both light detectors and emitters.

1.3 Problem statement

During the research there were described many possible ways to use light-emitting diodes as light detectors. LEDs play main role in visual light communication technology and they have found their place in meteorology and radiometry due to their unique abilities. Although, the popularity of LEDs as light sensors continues to grow and there were certain tests performed there is still lot of work to be done. Strictly, at the moment there is not too much information regarding optical sensitivity properties of the light emitting diodes. For example, how linear is the sensitivity of the LEDs to ambient light, what wavelengths are they sensitive to and how it may vary. Previously, it was found that the

LEDs are most sensitive to the smaller wavelengths than they illuminate [21], [24]. But other sources report that certain LEDs are sensitive to their own wavelengths and, in some cases, even bigger ones [32]. This brings to conclusion that several diodes of the same colour may react differently and this aspect could be analysed.

Everything comes to idea that LEDs should be analysed with accordance to the standards [33]-[36] in the same way and manner as if it was photodiode, phototransistor or photoresistor which were originally designed as photodetectors. In order to perform such analysis, suitable light detector should be chosen as an ultimate reference which the test element should be compared with. The simplest circuit is described in Figure 18.
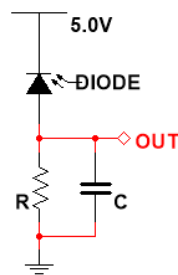
Figure 18. Circuit to test sensitivity of the LED. The diode is reverse-biased and the circuit is designed to sense ambient light only [36].

Another possible solution which could be used in order to test LEDs reaction on diffent wavelengths is by using monochromator [28]. This is a perfect way to find out which wavelengths are best detected by different LEDs which could be important in designing photometers in future.

In order to test the light sensors, an appropriate light source should be used [2]. There is large variety of the light sources presented in nowadays, but most of them are based on LEDs due to multiple advantages, such as longer lifetime. Though, there are still challenges persist, for example, the output of the light source is dependent on the temperature of the testing environment which could heavilty inlfuence the results of the sensor. Additionally, there are other cases, like correct light intensity determination, callibration of the light source, positioning light source in front of the sensor and so on. Engineer and resercher should be aware of these aspects in order to perform the measurements correctly.

The next way to evaluate the light sensors could be done using the integrating spheres [37]. These spheres are designed for evaluation of LEDs as light sources. Though, if the first measuremnts were taken using the original sensor in the sphere, then this sensor

24

could be replaced with the LED sensor and additional measurements could be taken. Afterwards, the final results are compared and certain conclussions could be done, how the LED sensor differs from the original sensor.

Additional important parameter to be analyzed is how LED sensor will behave itself in noisy environment or, strictly speaking, to ambient light. LEDs are gaining their popularity in VLC technology where light is used as an environment where information is transmitted. However, the area and the place where it is used may vary and conditions may change any time, so it is important to know if the light illuminated by other sources could interrupt the work of the device and how heavily. In radio frequency environment many modulation techniques were used in order to improve signal-to-noise ratio of the devices and these modulations could be also used when transmitting information through the light [14]. By incresing SNR the sensitivity of the final device is also improved which may result in longer distance of work. Present VLC communicators with LEDs as the receivers work on quite small distances, just few meters [14]. Applying suitable modulation could improve the result.

In addition to modulation, there other possible solutions to improve LED detector sensitivity. One of them is by concentrating the light on the spot where LED is located. In this case, laser diodes (LD) perfectly fit for this task. Moreover, LDs are the same LED but with additional lenses which means that they still could be used for light detection. Currently, research in IEEE databse revealed that lasers in VLC are used basically with photodiodes or other detectors as the receivers [9]-[11].

But LDs are more suitable for communication only between 2 nodes while sometimes there could be a need to distribute the same information between the nodes. LEDs light illumination beam can have different degree and by taking LED with the widest beam degree it may be possible to send one package of information to the multiple nodes.

The idea of measuring amount of light using different circuits was described previously, some of the circuits were presented [4], [27], [29]. Circuits may use operational amplifiers or microcontrollers with built-in ADCs, but all these designs have one common idea of using the reverse-biased LED. Analysis of work in different cases brought to idea that there could be possible way to illuminate the light and sense the ambient light by the LED at the same time. The idea is based on the fact that LED generates photocurrent depending on the amout of light it senses.

To conclude, the list of problems and ideas described in this paper is minor showing that there is still a lot to be done in this field. Currently, the main task is to start evaluating

light-emitting diodes sensitivty characteristics and compare them to existing light sensors. This is only the first step in understanding what LEDs can actually do, but in the nearest future this information will help in designing circuits where play main role in light detection.

1.4 Purpose of the work

The main purpose of the work is to investigate the capabilities of the LEDs as light sensor, investigate little-analysed features which were left unchecked in the previous researches or confirm the work of other researches which were made. This work aims to analyse the LEDs in order to give brief technical data for future projects. Additionally, the device which uses LED as both emitter and detector could be designed using the information received from the research.

1.5 Objectives

The master's thesis work has main objectives which are described below.

1. Study illuminance sensitivity of the LEDs using different light sources and different load resistances.

2. Study wavelength sensitivity of the LEDs using monochromator and spectrometer. Confirm the results which were made before, discover the new results with the LEDs which were not analysed previously.

3. Study angular response of the LEDs and describe how this could be used and in what tasks.

4. Study LED sensitivity when the diode is forward-biased and reverse-biased.

5. Develop the prototype VLC communication device.

2 Measurements performed and devices used.

There are multiple measurements should be performed in order to analyze characteristics of the light sensors [33], [38] and in this work next experiments will be performed:

- Illuminance analysis

- Wavelength analysis

- Angular response analysis

- Forward-biased and reverse-biased sensitivity analysis

The device under test was built using the same circuit as it was described in Figure 18. The advantage of such circuit is that it uses minimum amount of elements and in further development it can be improved using the various amplifiers to improve its work.

In order to perform these measurements there were multiple devices used. The full description for the measurement devices could be found in Appendix 1 – Full description of the measurement devices. The list of the used devices is next:

- Agilent 34410A Digital Multimeter

- Agilent E3631A DC Power Supply

- Agilent E3634A DC Power Supply

- Keithley 2612 SYSTEM SourceMeter

- Zurich Instruments MFLI Lock-in Amplifier

- Zurich Instruments HF2IS Impedance Spectroscope

- Monochromator UM-2

- OCEAN OPTICS Spectrometer USB4000

- TM-202 Lux-meter

- Multiple rails with scaling, platforms and lenses

In addition to the measurements which were described before it could be possible to evaluate the temperature influence on the characteristics of LED and one way to achieve it is to use integrating sphere TeraLED unit which analyzes the properties of the LED when it is switched as light source, but replace internal sensor in the device with the LED. But in this work the device turned out to be uncalibrated and there was no other solution to perform temperature-controlled measurements.

In order to analyze light sensors there were multiple light sources selected, most of them are different types and with different spectral characteristics. The spectrums of different light sources are presented in Appendix 2 – Spectrums of different light sources. The list of the used light sources is presented:

1. Warm fluorescent lamp OSRAM DULUX S 9W/41-827 [39]

2. Cold fluorescent lamp 9W/827

3. Halogen lamp 12V 10W

4. Halogen lamp SC Electric JC G4 12V 35W [40]

5. Halogen lamp Xenon capsule PRO-LITE Xenon Ultra 2 Pin 12 20W [41]

6. Car Xenon Lamp

7. White Bright LED FLR-50T04-HW7

8. Violet Bright LED YSL-R531R3D-D2

2.1 Illuminance analysis

Illuminance is a measure of photometric flux per unit area, or visible flux density [42]. It is typically expressed in lux which is lumens per square meter. The key feature of the lux is that it takes into account the human's eye visual system [43]. It is known that humans visual system is more sensitive to certain wavelengths than others, and so that every wavelength is given a different weight. This weighting factor is known as luminosity function. In luminosity function the peak wavelength is at 555 nm. And the main idea is to find out how the light sensor is sensitive to the ambient light from humans vision site.

This analysis allows to determine that the amount of photocurrent generated by the photodiode is linear to illuminance falling on the diode [44]. Because the diode consists of an active p-n junction which is also operated in reverse bias, the reverse current starts to flow while the light reaches the junction. Photodiodes are not sensitive as phototransistors, though, their linearity can be useful in other applications such as Lux meters.
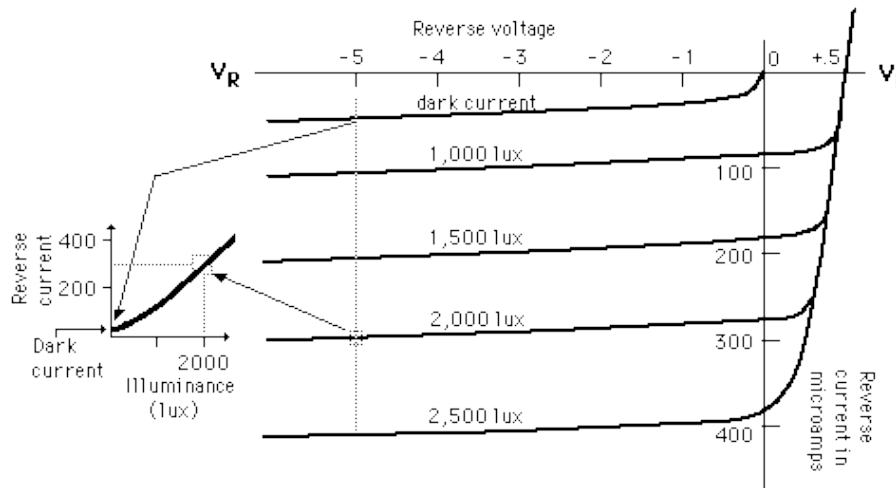
Figure 19. Dependence of the reverse current from the illuminance [44].

The further analysis was divided in 3 parts in order to find out what currents are generated and what parameters and how they influence the output currents. It should be noted that the temperature of the environment greatly affects the work of the photodiode but due to lack of the specific device which is capable to perform such measurements this part wasn't done. The ambient temperature should be considered the same as in room which is 25 degrees in Celsius.

2.1.1 Illuminance versus light current analysis

This part of the measurement which should show the dependence of the amount of light current generated by illuminance which falls on the diode. As it was described before the amount of the current on the output should be proportional to the given amount of the illuminance and in case of the photodiode it should have linear dependence. But the linearity appears once the illuminance is significantly above the dark current region [44] (see Figure 19). The expected results is that LEDs output current should have linear dependence on the amount of illuminance like other photodiodes.

There are several ways to obtain the dependence off light current from illuminance. But first of all the illuminance at certain point should be calculated. There are two approaches to calculate the Illuminance [45]:

- Lumen Method – this method determines average light levels in large open areas

- Point Calculations – determines light levels at the a specific point on an object or surface

The second method is more suitable since this experiment requires knowledge of the illuminance at the certain point. And the illuminance with this method could be calculated using the next formula [46]:

$$E = \frac{I}{d^2} \cdot \cos\theta, \tag{6}$$

where E- illuminance on the surface, I - luminous intensity of the source in the direction of the surface, d - distance from the source to the surface and the θ - is the angle between the light ray coming from the source to point.

Using that equation it is possible to calculate the distance for each required illuminance point and measure the output current values at these points.

Though this is theoretically possible way of performing measurements the values of luminous intensity for each light source may vary or that data maybe missing in datasheets. And the next way to perform measurements is with help of the device which is capable of showing the illuminance – Lux meter. Or professional spectrometer which has the function of converting irradiance to illuminance.

In these measurements the final choice was made in using the provided Lux meter TM-202 in order to measure the illuminance at each point. The measurements should be performed with various light sources in order to see how they influence the LEDs. The load resistance value should remain the same and it is recommended that the value would be small enough, so that influence of the input impedance of the measuring device would be small.

2.1.2 Illuminance with different load resistances analysis

In this measurement the main idea is the same as with previous one but the measurements should be performed with only few chosen LEDs and using different load resistances. The idea is to confirm that LED performs itself as an ideal current source when the light strikes it and the output current doesn't change with the load resistance. It also should be taken into consideration that the measuring device has its own internal impedance which influences the output of the device under test. And the higher is the load resistance the higher is the influence. So, when the voltage on the load resistance is measured the output current of the LED should be recalculated with the input impedance taken into account. The final equation should be:

$$I_{out} = \frac{U_{load}}{\frac{R_{load} \cdot Z_{input}}{R_{load} + Z_{input}}}, \tag{7}$$

where I_{out} – output current, U_{load} – voltage on the load resistance, R_{load} - load resistance value and the Z_{input} – input impedance value of the measuring device.

2.1.3 Light current versus supply voltage analysis

This is the final part of the illuminance measurement where the influence of the voltage supply on the output current is analysed. In this case the illuminance remains constant and only supply voltage is changed. The load resistance should remain the same and only one light source is used. It is expected that the output current will increase with the voltage supply but the linearity behaviours could be different.

2.2 Wavelength sensitivity analysis

Wavelength sensitivity analysis is needed in order to understand to which wavelength multiple types of LEDs are sensitive to. It was previously discussed that this idea could be useful in certain applications where there is a need to react only to certain wavelengths or colours of light.

In this part there is a need to prepare a certain setup which is able to output only determined wavelength at the desired spot and that the spectral irradiance should remain

the same for each wavelength value. The idea shown in Figure 20 where vertical equal traces represent equal irradiance value.
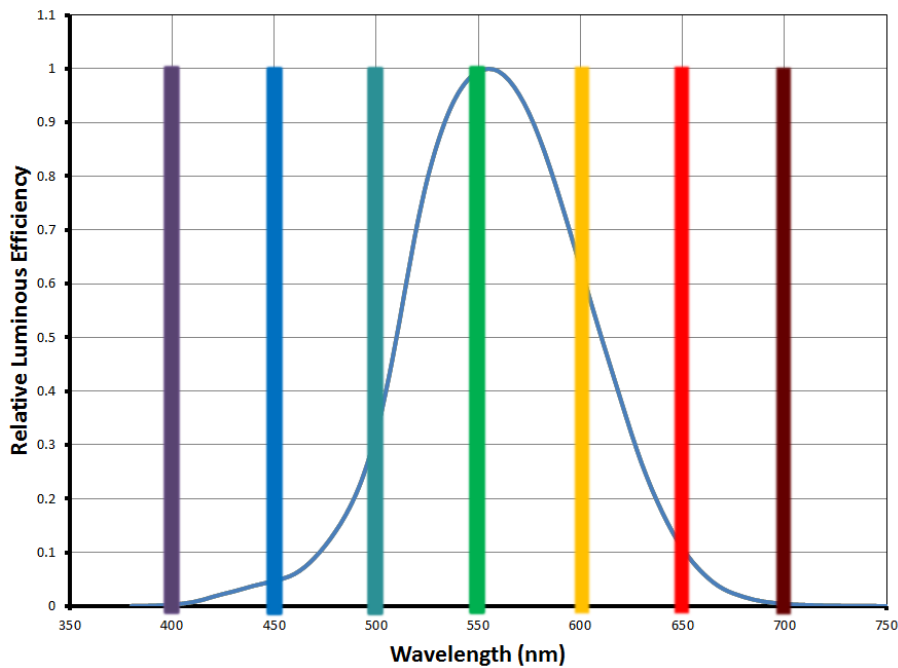
Figure 20. Ideal irradiance source with luminosity function [43]. Irradiance with each wavelength value should be equal in order to get ideal light source.

But since each light source has its own spectrum which is in most cases far from being ideal there is a need in monochromator which can divide light source on separate wavelengths and output only specific one and spectrometer to see how high is the irradiance of the wavelength.

The first part is to calibrate the monochromator to see at which degree point which wavelength on the output. The second part is to adjust the light source that the output for each wavelength would be equal. There are two ways to achieve this:

1. Change the power for the light source. Decreasing the power decreases the brightness of the light source which also decreases the irradiance at certain wavelength point. Note that increasing the power of the light source and exceeding its limits could cause damage to the light source.

2. By opening or closing input slit of the monochromator if one has such capability. If there is a capability to regulate the width of the input slit this is one of the safest ways to adjust the output of the monochromator.

32

After these parts are done the measurements can be started with group of LEDs. Though, it should be noted that light sources due to their spectrums have their limits and in order to continue measurements there could be a need to replace the light source with different one. If the light source is replaced or the current setup was disturbed for some reason the calibrations should be repeated.

In these measurements there were two halogen lamps, one halogen with xenon capsule and xenon lamp in order to measure the spectral response from 395 to 700 nm which covers visible light area. Halogen lamp 10W was covering area from 480 to 700 nm. Others were chosen to cover the rest of the area. The step between each measurement was 5 nm, so totally there were 62 steps. The step size was chosen based on the digital power supply precision and spectrometers accuracy and should give high accuracy measurements.

The results are presented as relative spectral response which are calculated with the next equation:

$$R = \frac{V_{out} - V_{dark}}{V_{max} - V_{dark}} \cdot 100\%, \tag{8}$$

where R – relative spectral response, V_{out} – voltage output on the load resistance at the particular wavelength, V_{dark} – voltage on the load resistance from the dark current and the V_{max} – the maximum voltage output value detected on the load resistance among all wavelengths.

It is expected that the wavelength response is shifted from peak wavelength emitted in direction of shorter wavelengths.

2.3 Angular response analysis

The main idea is to determine relative sensitivity of the LED at each degree of the incident light and find out what is the area where the sensitivity is maximum. In order to determine the angular response of any light sensor the special construction should be made which allows to:

1. Rotate the light sensor from $-90°$ to $+90°$ in one axis.

2. Tilt the light sensor in second axis from $-90°$ to $+90°$ and repeat the rotation.

3. Repeat the tilting until you won't cover whole sensor

Such construction allows to build full 3D model of area of the sensitivity for each of the LEDs and light sensors.

Another way to build 3D model of area of the sensitivity is next:

1. Rotate the light sensor from $-90°$ to $+90°$ in one axis.

2. Rotate the light sensor itself on 90 degrees and repeat rotation in one axis.

This would result in obtaining only two lines for both axis and the whole 3D model should be rebuilt by rotating the half of the line around one axis only on quarter and merge the results. The resulting 3D model would only approximate the area of the sensitivity of the LED but if both lines do look similar in comparison the approximation would have high accuracy.

It is estimated that the results of the rotation from $-90°$ to $+90°$ degrees should have response close to Lambert's cosine law [47] and each group of LEDs should have similar reaction.

2.4 Forward-biased and reverse-biased sensitivity analysis

The main idea of this analysis is to determine how current direction and value influence the sensitivity of the of the LED sensor. For this case there should be build a setup where both LEDs should have similar structure which was showed in Figure 18, but without the capacitor in parallel with the load resistance since it could influence the input and output signals. The resulting circuit is presented in Figure 21. The instrument which could be used is lock-in amplifier which would sense only certain signal of certain frequency. It would be an advantage if the instrument would have both lock-in structure and signal generator in one.
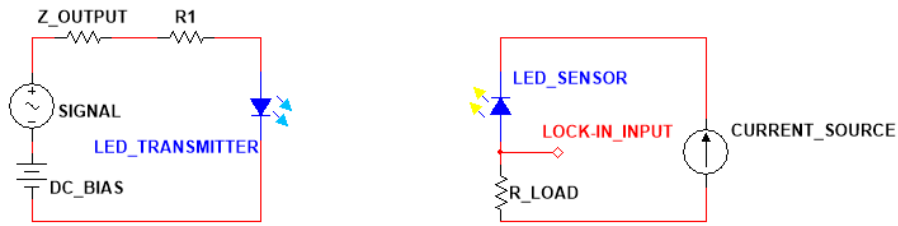
Figure 21. LED transmitter and receiver circuit.

The LED which would be transferring the signal should have DC voltage bias, so that it won't transfer only positive half-waves of the signal. The signal amplitude and the frequency should be set in the external frequency generator or in lock-in internal generator. The amplitude summed with DC bias shouldn't be too high otherwise the resulting from the resistance in series current may damage the LED transmitter.

As for the LED sensor part, it should contain current source which would generate current and set the LED sensor at certain current point. The example picture is shown in Figure 22.

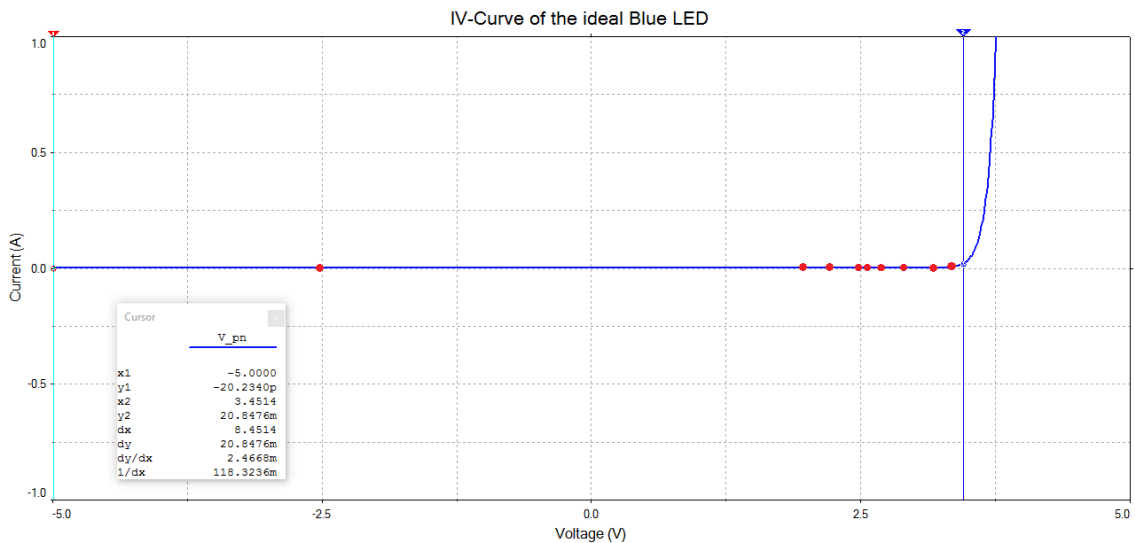Figure 22. IV-curve of the diode with current points.

It is estimated that when the LED sensor is reverse-biased the sensitivity to the light signal increases and vice versa. Only certain LEDs needs be chosen for this measurement which should be figured out through the previous experiments:

1. One LED which showed the highest sensitivity

2. One white colour LED because of its future perspective

3 Light emitting diodes selection

The main advantage of the LEDs over the photodiodes is that they should be cheaper and sensitive only to specific light colour. So the idea is to find LEDs which are one of the cheapest ones but they also should be provided by one manufacturer in order that there won't be large differences in the parameters. In addition to the LEDs under test there should be photodiode additionally acquired which is sensitive to visual light. Such photodiodes have different purposes and can be used, for example, in Lux meters.

There were two groups of 5mm light emitting diodes selected provided by Adafruit and SparkFun. They were discovered in official YE International online store.

The reference photodiode was found in ELFA Distrelec online store and is provided by Everlight Electronics.

3.1 SparkFun light emitting diodes

As it was written in the description the 'LED Rainbow Pack' contains total number of 12 diffused 5mm LEDs which can give red, orange, yellow, green, blue and violet colours. This pack is good because it doesn't only contain large variety of different colour LEDs but also large number of them which is good for statistical data. The features of the LEDs which were taken from provided datasheet [48] are described in the next Table 1.

Colour	Brightness	Wavelength	V_{DROP}
BASIC RED	150 - 200 mcd	620 - 625 nm	2.0 – 2.4 V
BASIC YELLOW	150 - 200 mcd	587 - 591 nm	2.0 – 2.4 V
BASIC BLUE	300 - 400 mcd	465 - 467 nm	3.2 – 3.4 V
BASIC GREEN	150 - 200 mcd	570 - 575 nm	2.0 – 2.4 V
BASIC ORANGE	200 - 300 mcd	600 - 610 nm	2.0 – 2.4 V
BASIC VIOLET	50 - 100 mcd	395 - 400 nm	3.0 – 3.6 V

Table 1. Parameters of the SparkFun LEDs.

Note that the main webpage doesn't provide information about forward current but further investigation showed that the forward current is 20mA [49] and 50% viewing angle up to 60°. In further research the group of SparkFun light emitting diodes will be called shortly "Basic LEDs".

3.2 Adafruit light emitting diodes

Unlike SparkFun Rainbow Pack, these Adafruit light emitting diodes were provided separately. Multiple LEDs with different colours were obtained: Red, Yellow, Green, Blue, Violet and White. The main differences from the SparkFun LEDs are that they don't have optical filters of specific colours installed and their brightness should be significantly higher.

The white LED should be described separately since it is considered as the unique one. White coloured LED is rapidly replacing traditional light sources which had the main task to illuminate rooms, streets and so on. And unlike other LEDs in the group it works as a bright blue light source which has phosphor covering which generate both blue and yellow colours [50] and all together they imitate white colour. Since this particular colour is rapidly taking its place in human's everyday life it should be analysed with higher priority.

The features of the LEDs which were taken from provided datasheets and web store page descriptions [51]-[58] are described in the next Table 2.

Colour	Forward Voltage	Forward Current	Maximum Forward Current	Brightness	Wavelength	Viewing Angle
Bright Red	1.8-2.2 V	20 mA	30 mA	1500 mcd	640 nm	20°
Bright Yellow[1]	3.0-3.4 V	20 mA	20 mA	18000-20000 mcd	523 nm	15°
Bright Green	3.2-3.8 V	20 mA	30 mA	8000 mcd	520 nm	20°
Bright Blue	3.2-3.8 V	20 mA	30 mA	6000 mcd	465 nm	20°
Bright Violet	3.4 V	20 mA	25 mA	350 mcd	400 nm	15°
Bright White	3.0 V	20 mA	20 mA	15000 mcd	Cool White	24°

Table 2. Parameters of the Adafruit LEDs.

In further research the group of Adafruit light emitting diodes will be called shortly "Bright LEDs".

3.3 Reference photodiode from Everlight

This particular photodiode was chosen as a reference because of its capability of being responsive only to visual light. It has responsivity close to the human eye spectrum, the good output linearity across wide illumination range and the sensitivity variation across various light source is very low [36]. As an additional benefit is that this light sensor incorporates both photodiode and current amplifier integrated circuit which significantly increases devices sensitivity to ambient light.

The features of the photodiode which were taken from provided descriptions are described in the Table 3.

---

[1] During research it was found out that there were made mistakes in the datasheet, such as, wavelength value was incorrect as it belongs to green colored LED, not yellow, and that this datasheet was designed for green LED. It is now unknown are the other values for the marked LED are correct.

	Supply Voltage	Peak Sensitivity Wavelength	Sensitivity Wavelength Range	Angle of half Sensitivity	Dark Current
Reference Photodiode	1.8 – 5.5 V	550 nm	390 – 700 nm	143°	1 – 100 nA

Table 3. Parameters of the Ambient Light Sensor ALS-PDIC144-6C/L378 [36].

In further research the ambient light sensor ALS-PDIC144-6C from Everlight will be called "Reference photodiode".

3.4 Other light sensors

During the research of the angular response and wavelength sensitivity two additional white LEDs were analysed. The difference between them and previously described LEDs is that they have different shape and more powerful than others. The main idea was to analyse their angular response and how their construction improves their sensitivity at different angels. Additionally, they were used during the analysis of the wavelength response to confirm that white LEDs are only sensitive to certain wavelengths.

The first warm white LED is Lucky Light model HP30MW6C which is round shape high-power LED. This particular model has next Table 4 [59]:

Colour	Forward Voltage	Forward Current	Reverse Current[1]	Luminous Flux	CCT	Viewing Angle
Warm White	3.3 V	150 mA	10 uA	25 lm	3000	135°

Table 4. Parameters of the power LED Lucky Light model HP30MW6C [59].

---

[1] This is the maximum reverse current which can be observed when the reverse voltage is 5 V.

The second model HPR20D-19K10YW-D square shape high-power LED by Huey Jann. There is little information regarding its features [60]. The most Table 5 are next:

Colour	Forward Voltage	Forward Current	CRI	Luminous Flux	CCT	Viewing Angle
Warm White	10.5 V	1050 mA	85	688 lm	3300	120°

Table 5. Parameters of the power LED Huey Jann model HPR20D-19K10YW-D [60].

If they were being used in research procedure they will mentioned by their model names or construction shape.

4 Results of the measurements

4.1 Illuminance analysis

The results of the measurements where the reaction of LED on being illuminated by the light source is studied. Multiple light sources were used in order to perform the analysis and 2 groups of LED were being observed and a reference photodiode in addition.

First of all, preparation of the test environment was made. The rail with two platforms was prepared where the light source was standing still on one side. The other part was being moved. The lux meter was set on the second platform and moved in order to find out the positions of the measurement points. The second possibility was made when instead of the distance the voltage of the light source is changed. At this point both platforms remain constant, but by changing the voltage the spectrum emitted by the light source is also changed. The example picture of the setup is presented in Figure 23.
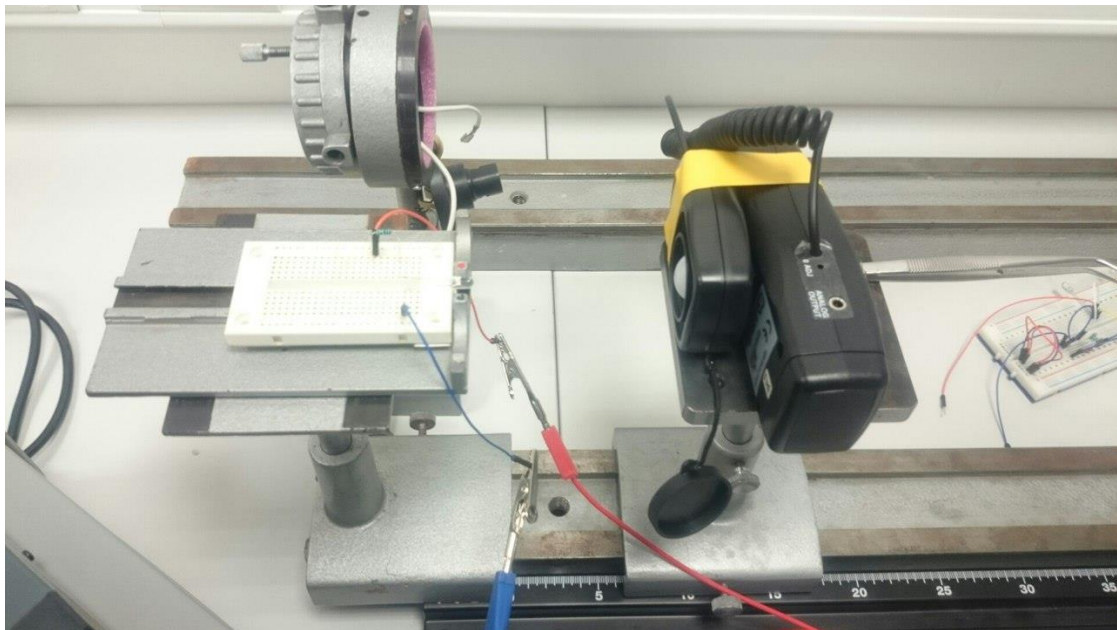
Figure 23. Setup with the moving platforms where white bright LED is used as the light source and lux meter is used to take find different Illuminance values. These positions are written down and then used in LED as a light sensor measurements. The measurements should be performed with the light switched off due to ambient light noise.

The total number of measurement points was 19 with different Illuminance values which is enough to draw the results graph in logarithmic scale. The illuminance values were

taken from 10 to 1000 lx. Multiple diodes with different colors were tested. The expected results are that the LEDs from the "Bright" group should be more sensitive and generate more photocurrent than the similar color from "Basic" group. The sensitivity varies with each light source due to different light spectrum they emit. Additionally, the voltage of the light sources was being changed instead of the distance, but since this also changes emission spectrum the reaction on the same light source should be different.

The next measurements were done:

- **Warm Fluorescent Lamp 9W**: Current vs Illuminance. The first load resistance was chosen the same as with the reference photodiode 5K1, but due to low output voltage it was replaced. The new load resistor was 1M 1% (1MOhm). The voltage supply for the LED (photodiode) circuit was set to 3V. To change the illuminance value the rail with metrics was used with moving platform on it. This measurement was more stable and with higher load resistor value than previous measurement. Capacitor was removed due to high capacitance and high time constant.
- **Halogen lamp 10W**: Current vs Illuminance. The load resistor was 1M 1% (1MOhm). The voltage supply for the LED (photodiode) circuit was set to 3V. To change the illuminance the voltage of the Halogen lamp was changed. The distance between the lamp and the LEDs remained constant.
- **Halogen lamp 10W**: Current vs Illuminance. The load resistor was 1M 1% (1MOhm). The voltage supply for the LED (photodiode) circuit was set to 3V. To change the illuminance the distance between the light source and LED sensor was changed. The voltage remained 12V.
- **Halogen lamp 10W**: Current vs Supply Voltage. The illuminance remained constant: 1000 lux. The load resistor was 1M 1% (1MOhm). The steps between each voltage measurements were 0.5V.
- **Halogen lamp 10W**: Current vs Illuminance. The load resistors were changing: 1K, 10K, 100K, 1M and 10M. The voltage supply for the LED (photodiode) circuit was set to 3V. To change the illuminance the voltage of the Halogen lamp was changed. The distance between the lamp and the LEDs remained constant. Only next LEDs were analysed: Yellow Basic, Yellow Bright and White Bright.
- **White LED FLR-50T04-HW7 60mW**: Current vs Illuminance. The load resistor was 1M 1% (1MOhm). The voltage supply for the LED (photodiode) circuit was set to 3V. To change the illuminance the voltage of the white LED was changed. The distance between the source and the LEDs remained constant.
- **White LED FLR-50T04-HW7 60mW**: Current vs Illuminance. The load resistor was 1M 1% (1MOhm). The voltage supply for the LED (photodiode) circuit was set to 3V. To change the illuminance the distance between the light source and LED sensor was changed. The voltage remained 12V.
- **Cold Fluorescent Lamp 9W**: Current vs Illuminance. The load resistor was 1M 1% (1MOhm). The voltage supply for the LED (photodiode) circuit was set to

3V. To change the illuminance the distance between the light source and LED sensor was changed.

In order to measure the voltage on the output of the device the digital multimeter was used set to take 150 samples. The input impedance was set to default value which is 10MOhm. This was considered during results calculation, so the actual load resistance with 1MOhm and 10MOhm resistors would be 910KOhm and 5MOhm respectively.

The results of the measurements are shown in Figure 24 - Figure 27. They only represent the results which were made using two light sources, which are Halogen lamp and White LED, and show two the most sensitive LEDs from each of the group. All other measurement results with other LEDs can be found in Appendix 3 – Results of the Illuminance measurements.
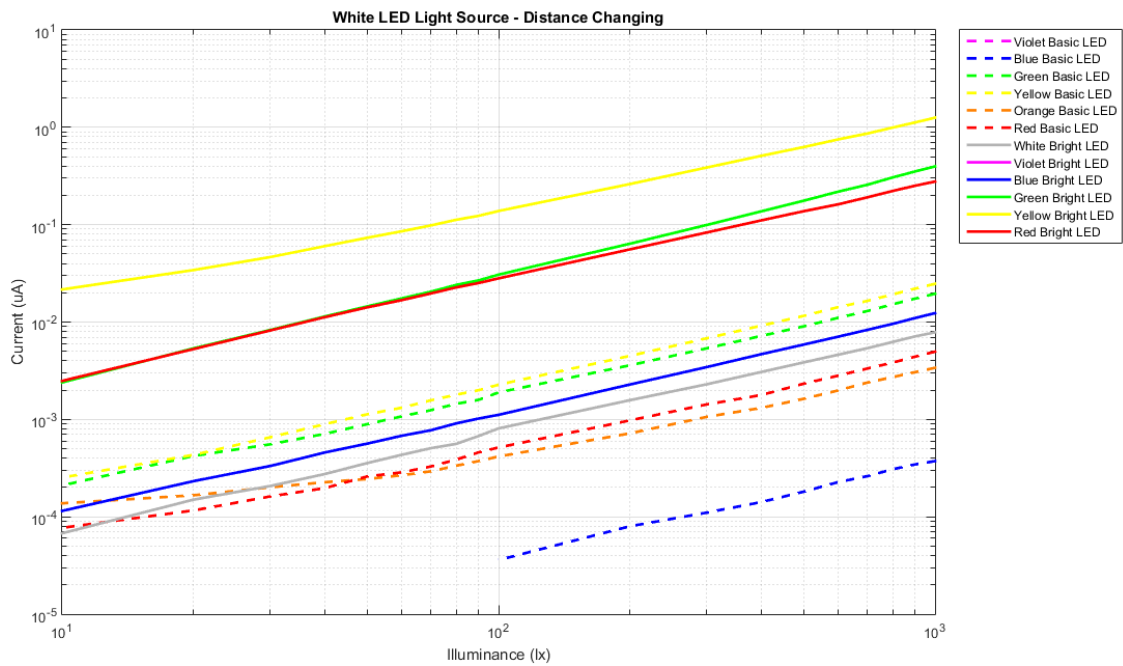
Figure 24. Illuminance versus Current when the white LED is used as the light source. In order to change the illuminance value at the certain point, the distance between the LED sensor and the light source was changed.
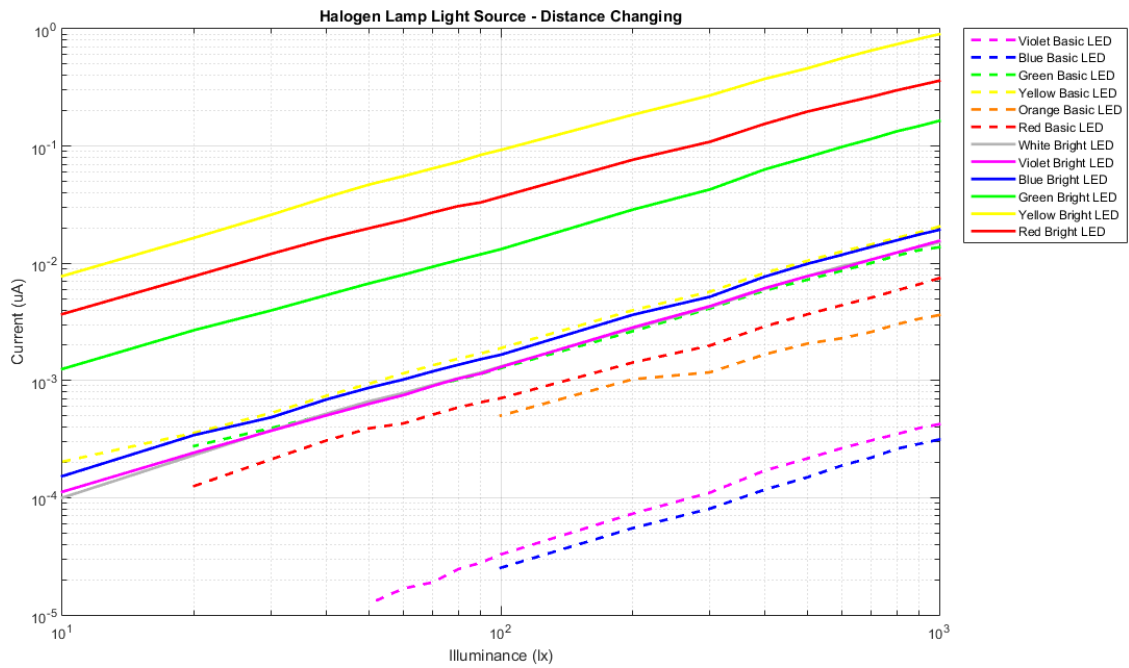
Figure 25. Illuminance versus Current when halogen lamp is used as the light source. In order to change the illuminance value at the certain point, the distance between the LED sensor and the light source was changed.

As it can be seen, with different light sources all LEDs react differently. In both cases the most sensitive LED turned out to be the yellow one from the "Bright" group. The yellow from the "Basic" was also the most sensitive in his group. The reason can be in the spectral sensitivity, that they were sensitive to the highest point in the light source's spectrum. However, halogen lamp had strong red and infrared red and the red LED was expected to be more sensitive in this case. Additional reason can be that the yellow have higher luminous intensity which in sum with previous statement results in higher sensitivity. With "Basic" LEDs additional role may play optical filter which they have in order to emit certain light color.
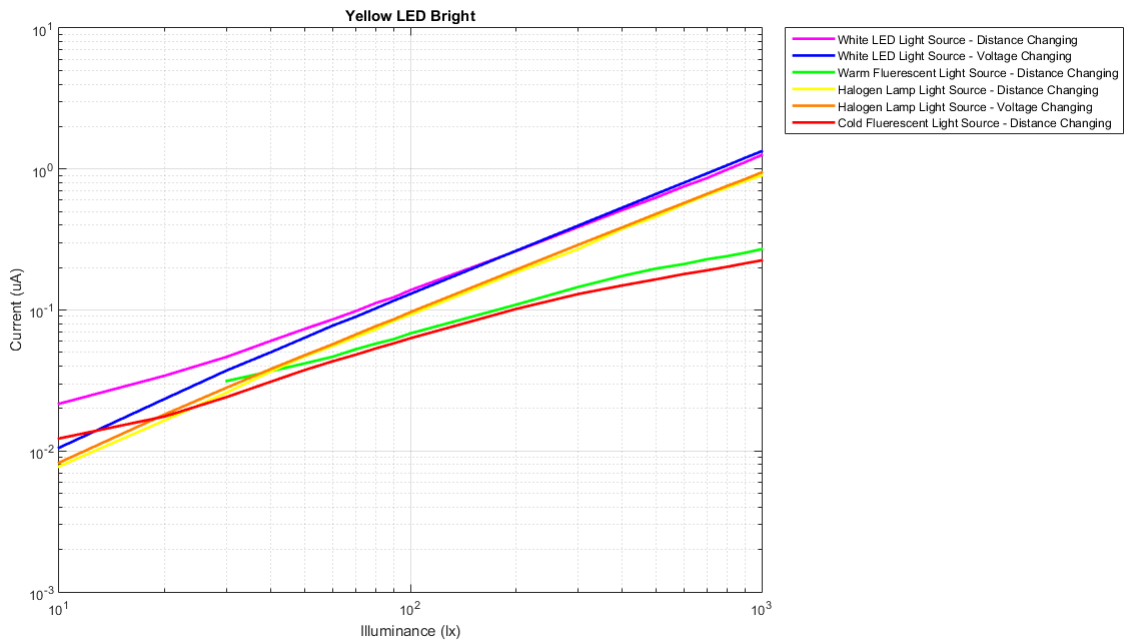
Figure 26. Illuminance versus Current of the Yellow "Bright" LED with different light sources. Two types of light sources were used by changing both distance and voltage.
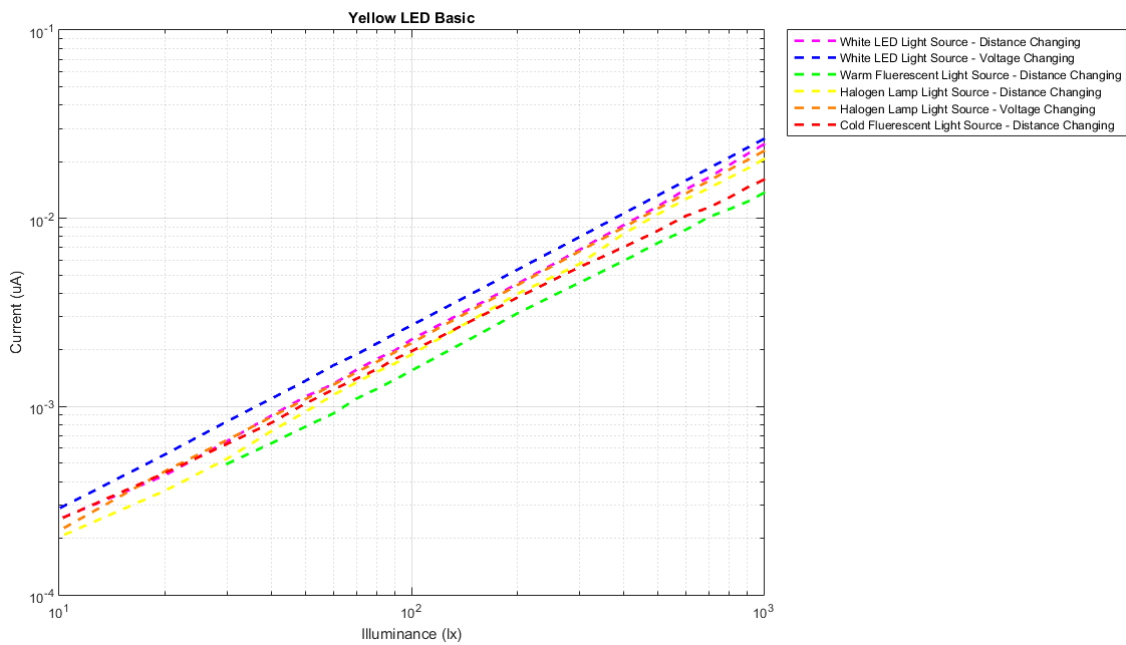
Figure 27. Illuminance versus Current of the Yellow "Basic" LED with different light sources. Two types of light sources were used by changing both distance and voltage.

In these results it can be noted that these LEDs were the most sensitive to white bright LED. It appears that yellow LEDs are more sensitive in this area where the white LED has emission peak. However, some LEDs had different reaction, for example, red and orange ones were more sensitive to halogen lamp which has strong red and infrared part. Violet, blue and white ones were the most sensitive to the cold fluorescent lamp.

45

Overall, it appears that most of the LEDs have linear output current dependence on the illuminance like a typical photodiode. It should be mentioned that LEDs from "Bright" group started to lose linearity with any of the fluorescent lamp at high illuminance levels. The possible reason may be that the fluorescent lamp is powered with impulse power supply which influences the emission spectrum. The orange one loses linearity only at low illuminance values which means the generated photocurrent is already close to the dark current at these levels. Blue and violet from the "Basic" group showed the least sensitivity to any of the light sources showing small potential with the cold fluorescent lamp. Though, the noise levels were still too high.

The next results of the measurements with different load resistances for the yellow "Bright" LED shown in Figure 28. The rest of the results with other 2 LEDs are shown in Appendix 3 – Results of the Illuminance measurements. The main idea was to confirm that LEDs like photodiode work as current source while being illuminated by the light. The illuminance value varied by changing the voltage of the light source and the voltage supply for the sensor circuit remained constant 3 V. The halogen lamp was used as the light source.
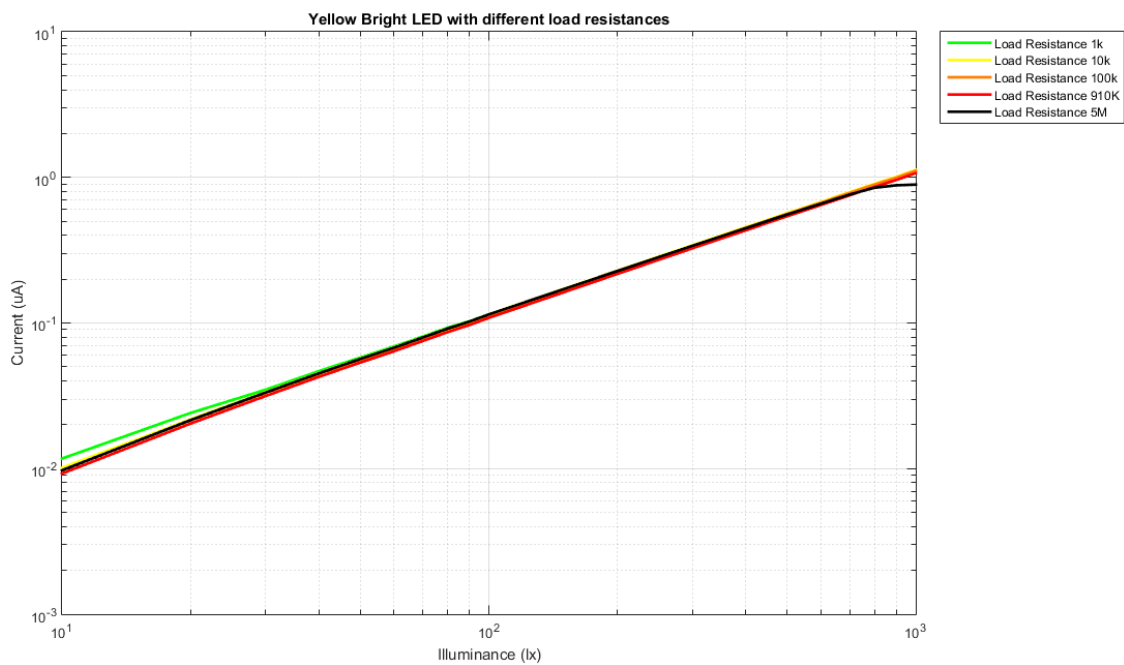
Figure 28. Output current dependence with different load resistances for the Yellow "Bright" LED.

From the results which were received for all of the tested LEDs it can be concluded that the output photocurrent doesn't depend on the load resistance value, however, from the

Yellow "Bright" LED results it could be observed that with such high resistance as 5MOhm the LED starts to saturate and not able to output higher current. Since the Yellow "Bright" LED showed itself as the most sensitive light sensor among other LEDs and all the output currents levels are the same, it can be concluded that this also applies to all other LEDs. With Yellow "Basic" and White "Bright" LEDs behave as expected on high illuminance values. With lower values the noise levels affect the results.

Last but not least, the output current also depends on the supply voltage of the light sensor. This time the illuminance value remained constant and only supply voltage was changed from 0 to 5 V. The first load resistance which was used for the measurements was 5.1KOhm, but due to high noise levels it was changed to higher values. Due to lower light sensitivity of the "Basic" LEDs, their load resistance was 5MOhm. The halogen lamp was used as the light source. The "Bright" group had 910KOhm load resistance. The results for the Yellow "Bright" and Green "Bright" are presented in Figure 29 and Figure 30 respectively. The rest of the results are for overlook in Appendix 3 – Results of the Illuminance measurements.
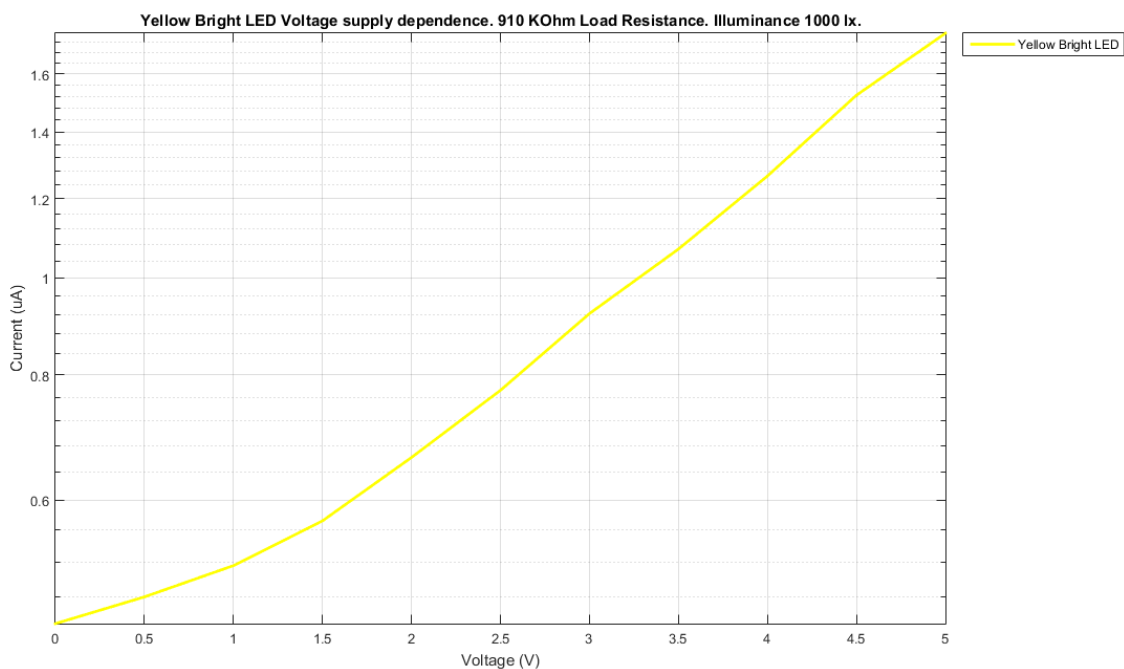
Figure 29. Output current dependence with the different supply voltage for the Yellow "Bright" LED.
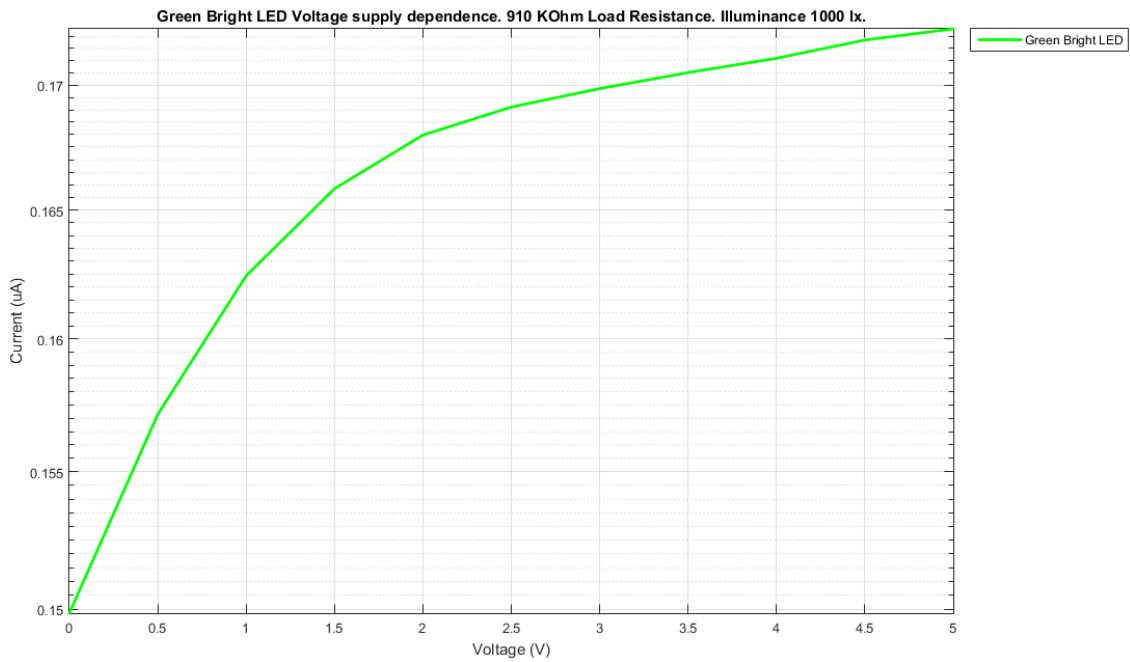
Figure 30. Output current dependence with the different supply voltage for the Green "Bright" LED.

The results show that each LED color from different groups has different dependencies. Most of the show linear output current growth with the voltage supply rising, like red ones, violet, orange. Some of them show linear response only at higher values of the supply voltage, like Yellow "Bright" LED. The Green and White "Bright" LEDs showed response similar to what the reference photodiode has, both in datasheet and measurements. The blue colored LEDs showed weak responses in previous results and high noise levels were observed during this research, so because of this the final results for the blue LEDs are still uncertain. Overall, analysis of the results shows that starting from the certain point the output photocurrent linearly increases with the supply voltage.

4.2 Wavelength analysis

The relative wavelength response of each LED was analysed. The two groups of LEDs, "Bright" and "Basic", and two additional white LEDs HP30MW6C and HPR20D-19K10YW-D were tested. Three LEDs of one colour from each group was analysed in order to get statistics data. Multiple light sources were tested before using but only two of them were found suitable for the measurements. Both of them were halogen lamps with different wattage ratings, 10W and 35W respectively, powered from DC 12V.

The main task was to measure the wavelength response of the LEDs in visual light spectrum which is from 400 nm to 700 nm. In order to complete it, at least two light sources need to be used where one is served to measure wavelength response starting from 700 nm and going to lower wavelengths while its emission spectrum allows it. Halogen lamp 10W was chosen for this part due to its good emission spectrum near red and infrared area. But due to weak blue and near ultraviolet part of the spectrum it was possible to measure only from 480 nm to 700 nm.

For the rest 80 nm other light source was needed. Ideally, it should be light source which emits ultraviolet from the beginning and powered from DC power supply. Unfortunately, it was not possible to find such ultraviolet lamp, so alternatives were considered. One of them is using xenon arc lamp [61] which has stable ultraviolet part of the spectrum, but only two types of lamps were found for the short period. One of them was Xenon Ultra 12V 20W lamp supplied by Pro-Lite [41], but during the measurements this lamp didn't show better results in comparison to regular halogen lamp. The next xenon lamp, which was tested, was the one which are installed in cars. The picture of this xenon lamp is shown in Figure 31.
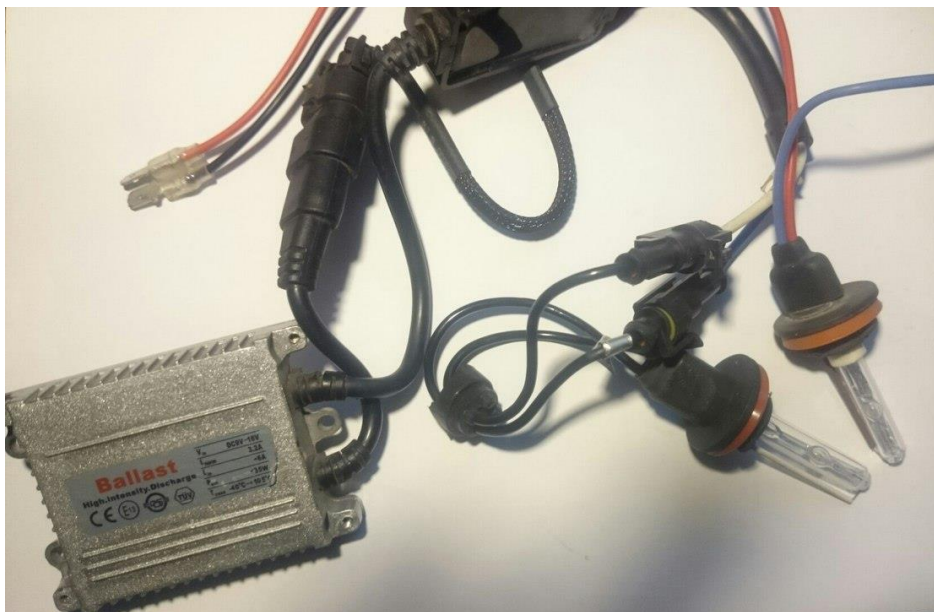
Figure 31. Car xenon lamp with the power supply.

This lamp showed good spectrum emission down to 400 nm which was perfect for the analysis but due to the fact that this xenon lamp is powered by external impulse power supply which creates voltage up to 25 kV [62], the spectrum was not stable and discreet

which made the measurements too unstable and inaccurate. Eventually, this xenon lamp wasn't used due to its lack of stability.

Returning back to the halogen lamp, it should be once again mentioned that they still have near ultraviolet and ultraviolet part of the spectrum, however, too weak. But due to the fact that they still have it, the decision was made to try more powerful halogen lamp which is 35W. During initial tests the LEDs were capable to sense violet and ultraviolet part of the spectrum. The final decision was that in order measure relative response of the LEDs from 400 nm to 480 nm the Halogen lamp 12V 35W would be used.

Before measuring the wavelength sensitivity, calibration procedure should performed first. During the calibration procedure, instead of LED, the sensor of the spectrometer was installed at the output of the monochromator. Due to monochromator was missing module with the slit inside, an improvised slit was attached to its output. By varying the voltage of the light source the irradiance on the output of the monochromator should be equal at every wavelength. It is predictable, that with the emission spectrum of the halogen lamp the longer wavelength would require lowering of the voltage in order to lower the irradiance. At the same time each wavelength value which is shown by spectrometer is written down with the degrees shown on the monochromators drum, so when the certain wavelength needs to be selected, the drum of the device is rotated at the certain degree. Overall, each wavelength will how its own voltage of the supply and degree of the monochomator's drum. With the first 10W halogen lamp voltage was adjusted this way that for each wavelength irradiance the spectrometer would show average radiant intensity 10000 Counts. With the 35W halogen lamp due to its weak ultraviolet emission the spectrometer would show lower value, average radiant intensity 3500 Counts. The integration time for both cases was set 20ms. The examples of the spectrometer output for both halogen lamps are shown in Figure 32 and Figure 33 respectively.
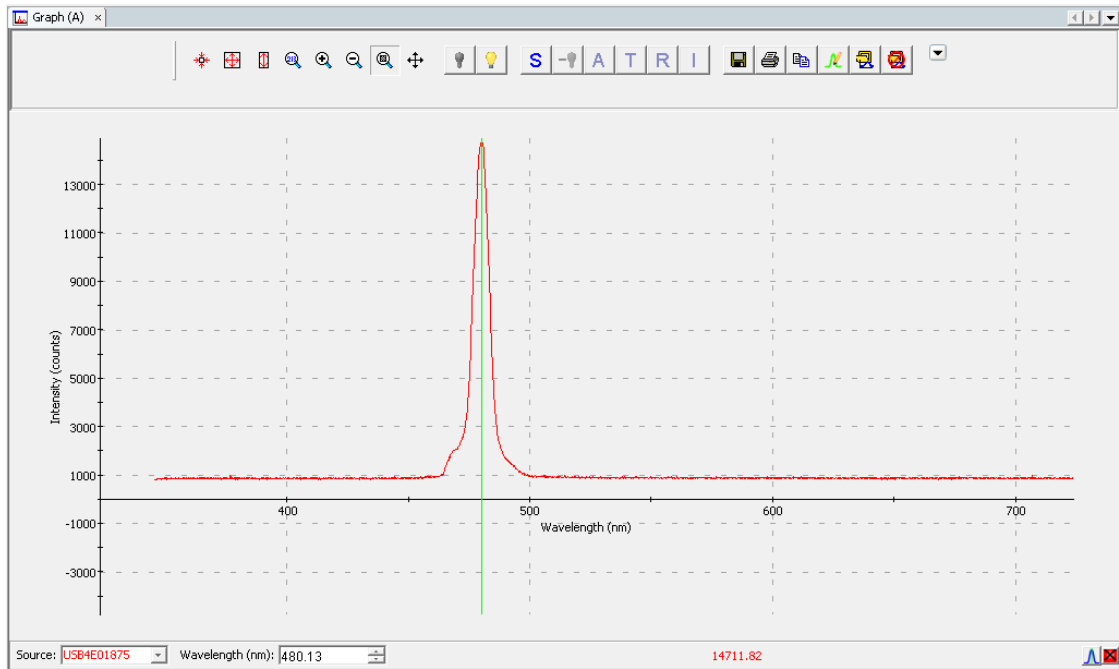
Figure 32. Intensity of irradiance of the wavelength 480 nm. In order to reduce the intensity to 10000 Counts the voltage of the light source needs to be reduced or input slit of the monochromator covered.
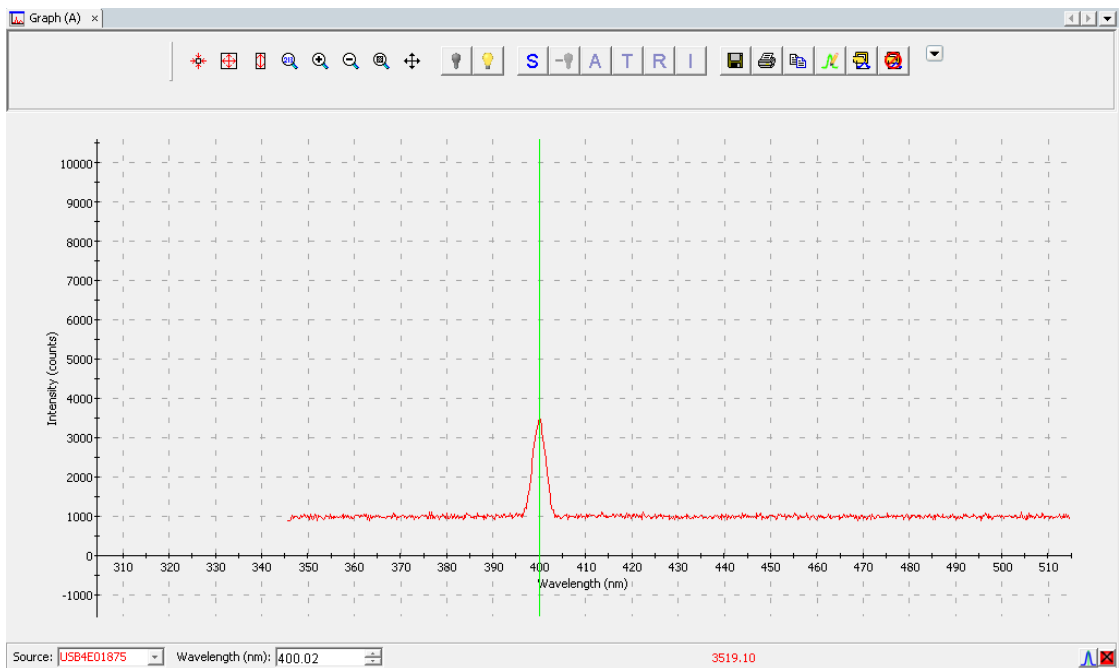
Figure 33. Intensity of irradiance of the wavelength 400 nm.

After the calibration was finished, the sensing probe of the spectrometer is removed and LED is connected instead. The load resistor was 10MOhm but due to fact that it was connected to the digital multimeter which also had 10MOhm input resistance in parallel, the final load resistance was 5MOhm. The digital multimeter was set to take samples for

100 seconds for more accurate results and calculate the average value. In order to reduce the influence of the ambient light, the LEDs were covered with the black box. The setup can be viewed in Figure 34.

Figure 34. The setup for the wavelength response measurement. The platform with the LED is behind the white paper, under the black box.

The results of the measurements of different LEDs from "Bright" group are presented in Figure 35 and Figure 36. All other results could be found in Appendix 4 – Results of the Wavelength response measurements.
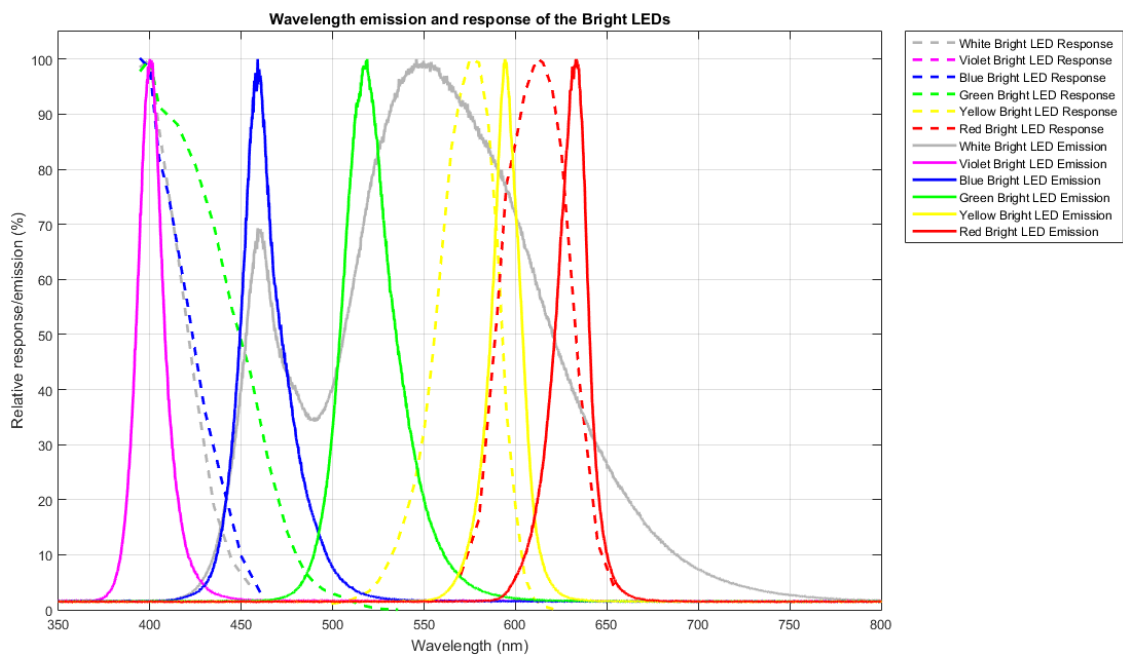

Figure 35. Wavelength emission and response of the "Bright" group LEDs.
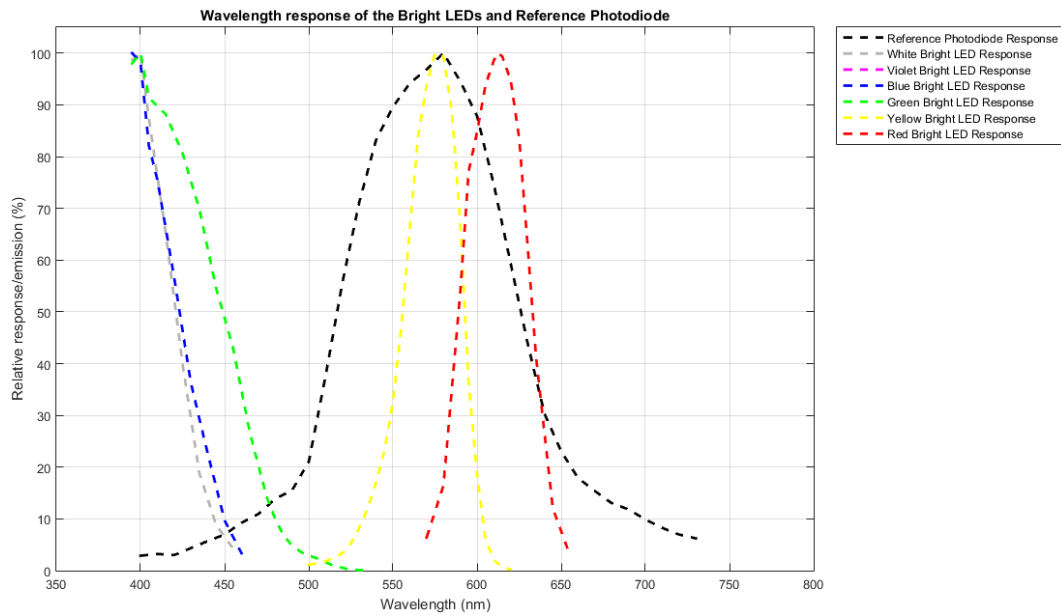
Figure 36. Wavelength response of the "Bright" group LEDs compared to the reference photodiode.

As it can be noted from the results, the peak wavelength response of the LEDs is shifted from the peak emission and it always sensitive to shorter wavelengths. The lower wavelength LED emits, the larger can be observed. However, the largest shift in the "Bright" group can be observed with the green one. The only result which is missing for the "Bright" group is the response for the violet LED, but due to results from other LEDs, it is rightly to note that the area of the sensitivity could be found in UV area of the spectrum which exceeds the capabilities of the used light sources.

For the LEDs from "Basic" group could be observed the same behavior which was observed with "Bright" group. However, for yellow and green sensitivity wavelength range seems to be wider than for the similar color LEDs from other group. The only missing data was for the blue and violet "Basic" LEDs due to their low sensitivity and high noise levels. Like with violet "Bright" LED it is right to mention that the wavelength response could be found in UV area of spectrum.

Comparing the wavelength response with the reference photodiode, it can be concluded that width of the wavelength range is approximately 3 times shorter which gives the possibility to use LEDs in the devices where only certain wavelength needs to be sensed, while photodiode requires additional optical filters to be installed in order to perform the same task. And each LED is sensitive only to certain colors where wavelength is shorter than one they emit. This means that the task, where same color LEDs need to use the light

53

environment to exchange the data will, will be quite challenging due to the fact that they are almost insensitive to their own light. The probable solution for this is to use RGB LEDs where blue ones could be used as the transmitters and green ones as the receivers of the data.

To conclude, the LEDs showed the expected results and behaved the same way as it was described in the references [21], [24].

4.3 Angular response analysis

In order to measure LEDs angular response, a special construction was built which rotates the LED from $-90°$ to $+90°$ in one axis. The LED could be set in two positions which gives the possibility to analyze the angular response in two axis. On the other platform the light source is placed which emits constant intensity light through the slit. The light source is typically the white LED, but for some LEDs which were not sensitive enough, it was replaced with violet one. The construction setup could be observed in Figure 37.
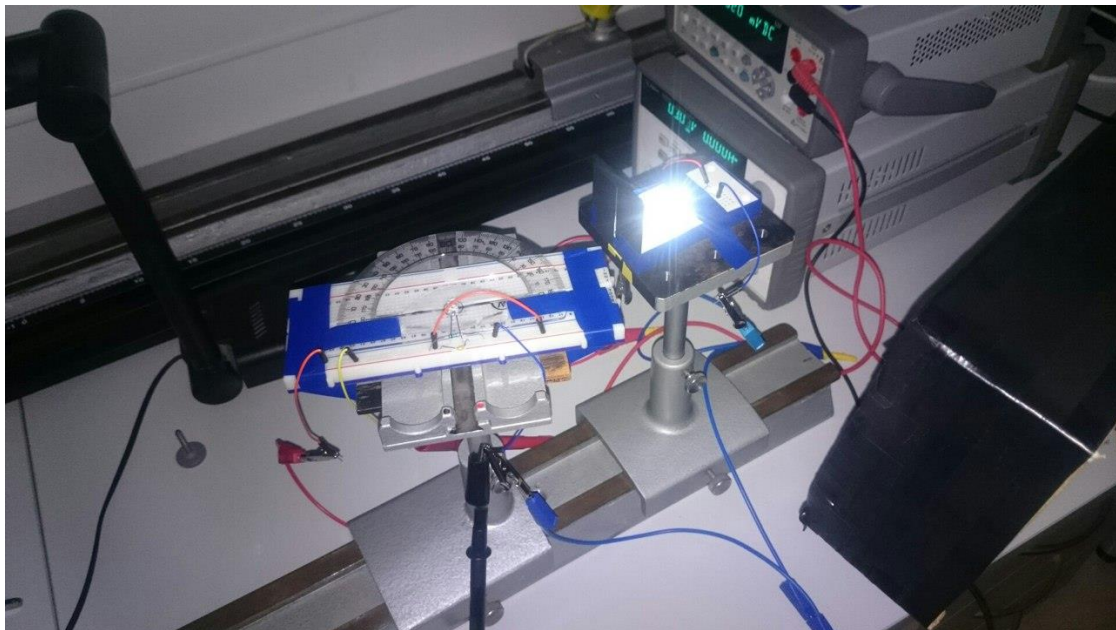
Figure 37. Setup for angular response measurements.

After measuring the angular response of the LED in both axis the 3D picture was being rebuilt. The results for the Yellow "Bright" and Yellow "Basic" LEDs are shown in Figure 38 and Figure 39. All other measurement results could be found in Appendix 5 – Results of the Angular response measurements.
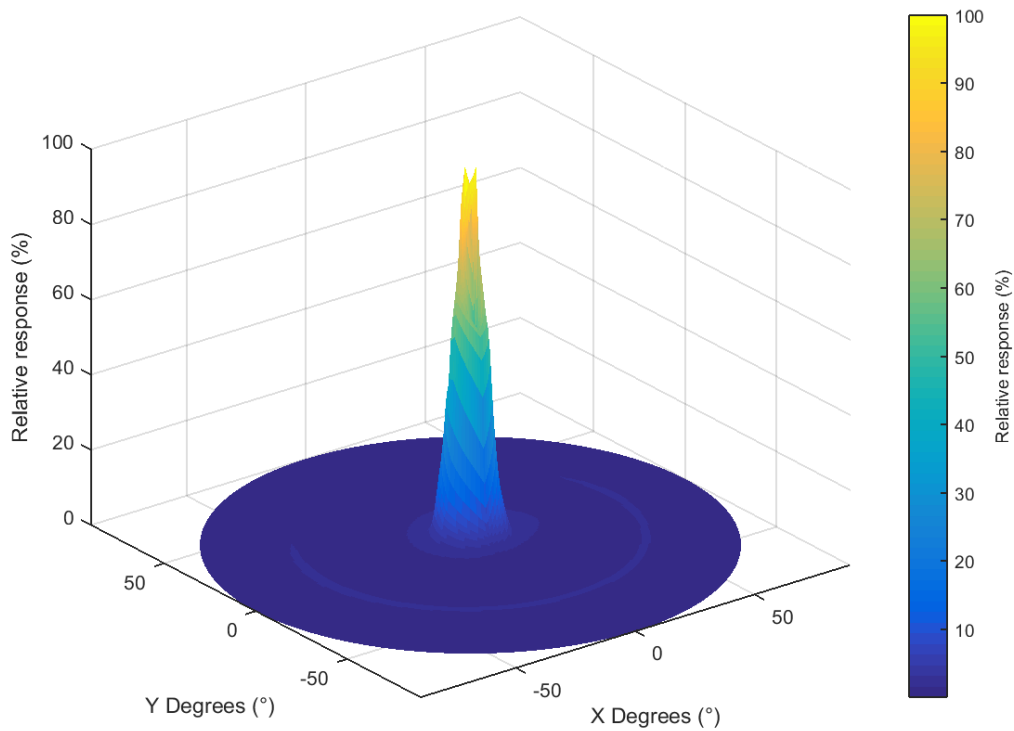
Figure 38. Angular response of the Yellow "Bright" LED.

It seems that few results tend to have few inaccuracies, such as few spikes were sensitivity is shown to be better, though, ideally it should be only one. It is especially seen in cases with the "Bright" LEDs. The reasons for such unordinary reaction are several, but primarily this is the result of the geometrical design of the LEDs. Additionally, it also could be the error caused by the unstable fixture of the prepared measurement instrument. Though, comparing the results, it is seen that LEDs which have wider sensitivity area, tend to have less errors, so this basically applies to the "Bright" group, which have narrowest sensitivity angle. But the received results still show the bigger picture, what are the sensitivity areas for each of the group of LEDs.
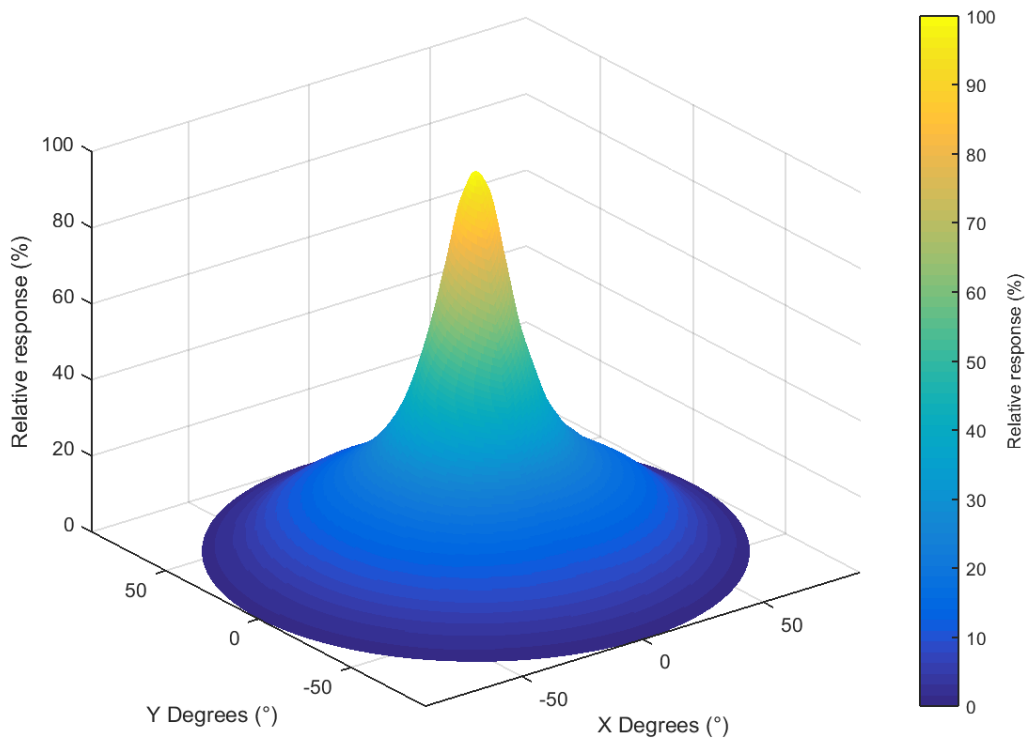
Figure 39. Angular response of the Yellow "Basic" LED.

From the given results it could be observed that the response of the LEDs from "Basic" group is wider than the one the "Bright" group possesses. The main reason for such difference could be found in the constructional features of the LEDs. They use specific reflector [1], where crystal is situated, which also serves for the heat dissipation. The "Bright" group is designed to emit very narrow beam as it was described in datasheets while the output beam for the "Basic" ones is wider. Due to these factors, the LEDs were designed this way to emit beam of the certain width and, hence, their sensitivity area is relatively the same as the angle of the emitted beam. The only exception is the blue-colored LED from both groups which has greater area of sensitivity comparing to other color LEDs. These conclusions brought to the idea of using the LED of different construction in order to check this idea. That is the main reason why two additional white LEDs were included where one has flat rectangle construction and the other one has round lens. It is expected that due to their shapes the area of sensitivity should be considerably wider and may even exceed the beam angle they emit. These results of the additional measurements could be observed in Figure 40 and Figure 41.
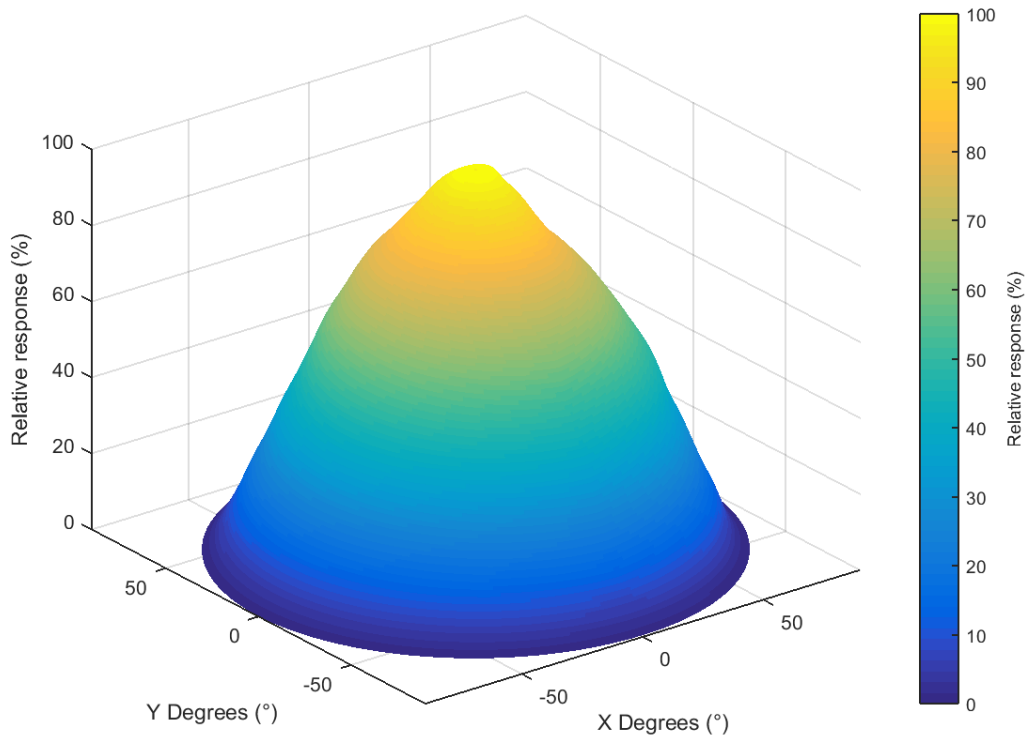
Figure 40. Angular response of the square-shaped White LED.
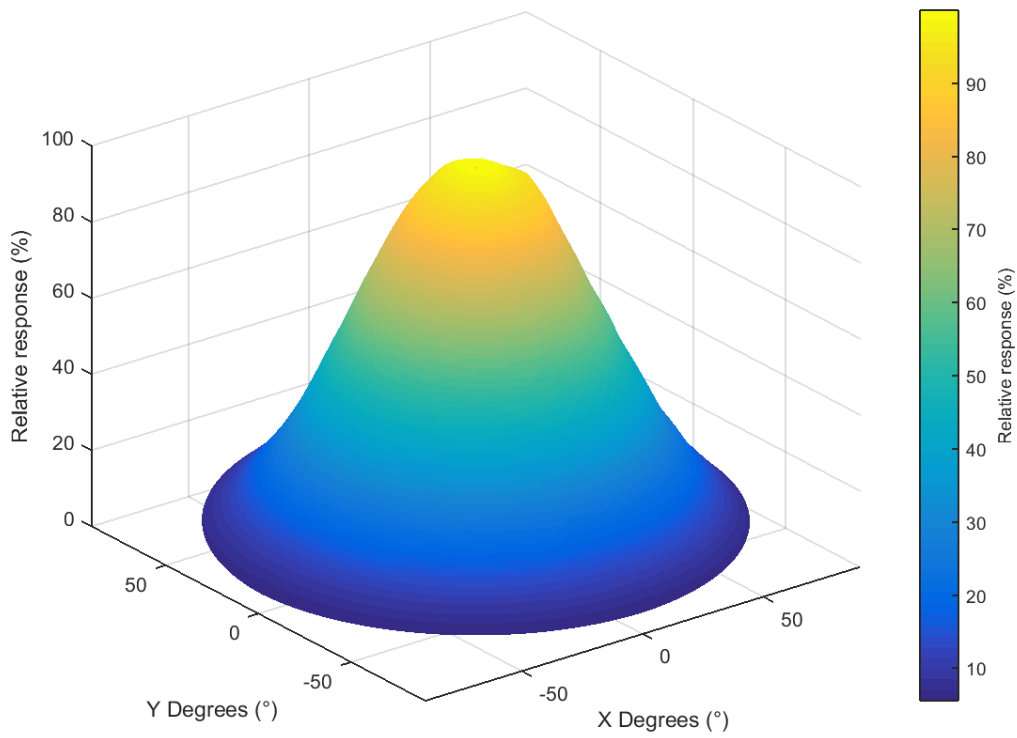
Figure 41. Angular response of the White LED with round lens.

As it was expected, the relative response area of these two white LEDs is considerably greater than that which could be provided by 5mm LEDs. Moreover, the results show that it is possible to sense the signal even when the LED with round lens is turned on 90° towards the light source. It seems that the light which reaches the lens starts to scatter inside reaching the sensitive area of the LED. Due to this fact, it gives the possibility to use LEDs in area where wide covering area is needed or in situations where LEDs are used as the transmitters but turned to each other on very wide angle.

To conclude, the 5mm LEDs from the "Bright" and "Basic" groups didn't show the behavior which was expected from them, but, instead, showed that their area of sensitivity is very narrow. These results show it is good idea to use such LEDs in tasks where only narrow area should be covered and high ambient light noise resistance is needed. However, when the wider area coverage is needed, then LEDs with round lenses or flat surface could be applied. The results show that the only LEDs which show behavior closest to the Lambert's cosine law are these last two white LEDs.

4.4 Forward-biased and reverse-biased sensitivity analysis

In order to analyze how sensitivity is affected by the forward-biased and reverse-biased LED, there is a need in the instrument which is able to lock-in to certain frequency and measure the voltage or current on the output. The lock-in amplifier can be such instrument.

The first prototype is shown in Figure 42 and its realization in Figure 43 and Figure 44. The generator with DC bias is connected to the transmitting LED with 100 Ohm resistor R1 in series. The voltage value was chosen such that wouldn't exceed the current limitations of the LED which were described in datasheet. The load resistor R2 of the receiving resistor can vary, it was tested with both high resistance and low resistance values. The voltage supply V3 sets the receiving LED to forward or reverse bias.
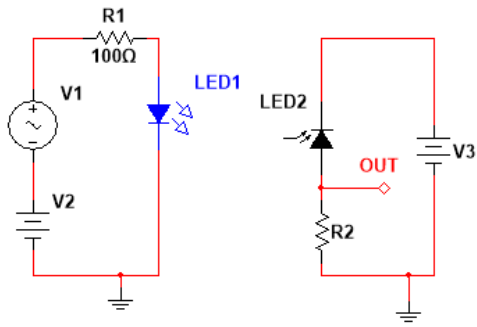
Figure 42. First circuit which was used with lock-in amplifier.
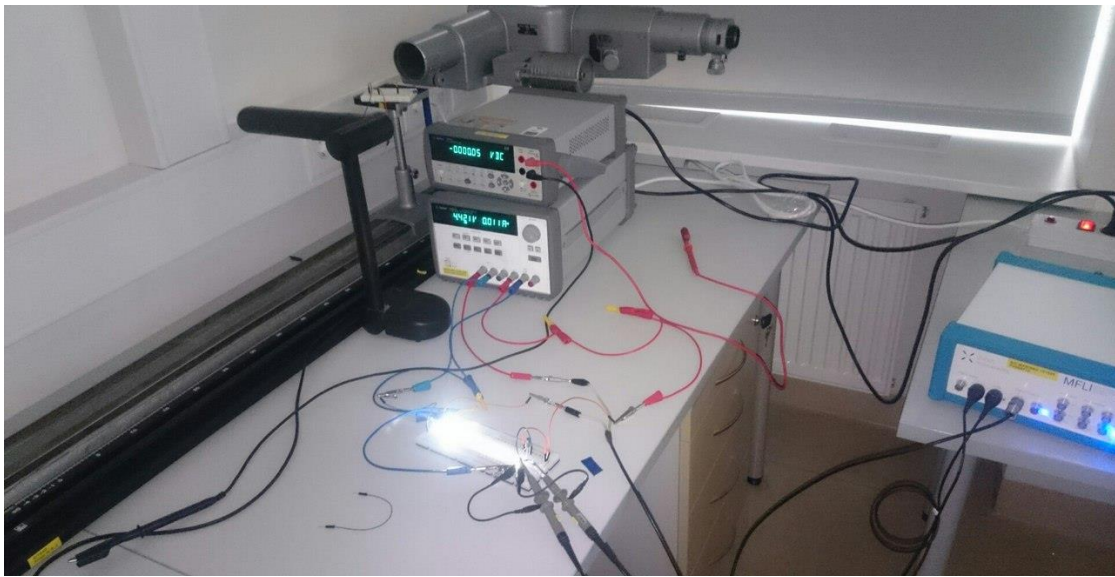
Figure 43. First circuit realization with all the equipment installed.
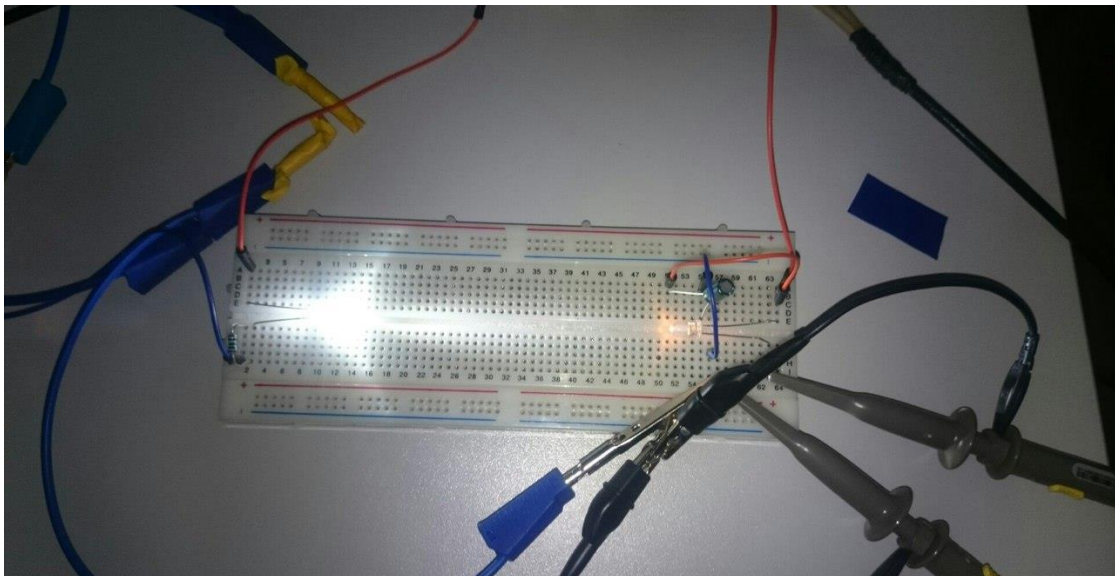
Figure 44. Closer look at the circuit. The capacitor is not the part of the circuit, it was left from the previous measurements.

The first analysis showed that the circuit requires improvements in order to reduce noise generated by the signals. The next prototype was made using the circuit shown in Figure 21 which uses current source instead of voltage supply. This time the PCB was created instead of breadboard and the main idea was reduce the size of the probe and power supply wires in order to reduce noise. The resulting PCB could be viewed in Figure 45.
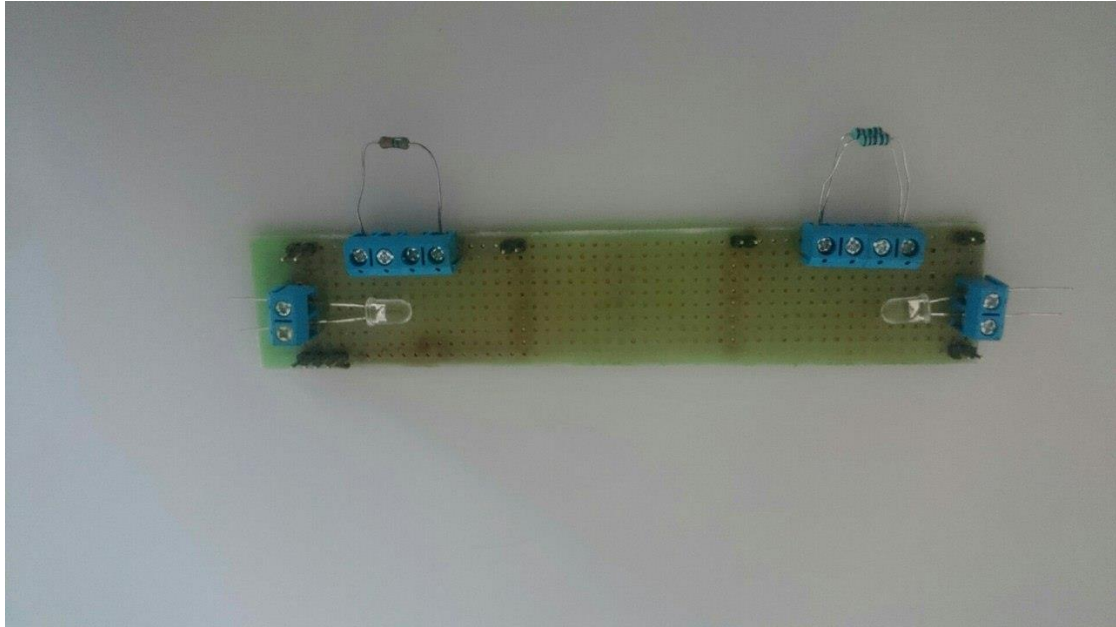
Figure 45. New version of the circuit designed in PCB.

This circuit uses shorter wires to connect to the lock-in amplifier which reduces the noise affects on the output of the device. The load resistor value was constant 10KOhm, determined from the maximum capabilities of the current source meter. The DC bias voltage was set to 4 V and the sinusoidal signal was used with peak-to-peak 2 V. The lock-in amplifier was set to pass only AC part of the signal. There were 2 LEDs tested in total, yellow and white, both from "Bright" group. The measurements were next:

- White LED as a light source and Yellow LED as a light sensor. Influence of the forward and reverse current on the yellow LED sensitivity. Influence of the signal frequency on the sensitivity of the yellow LED with forward and reverse current applied.

- White LED as a light source and White LED as a light sensor. Influence of the forward and reverse current on the white LED sensitivity. Influence of the signal

frequency on the sensitivity of the white LED with forward and reverse current applied.

- Violet LED as a light source and White LED as a light sensor. Influence of the forward and reverse current on the white LED sensitivity. Influence of the signal frequency on the sensitivity of the white LED with forward and reverse current applied.

The violet LED was used due to the fact that the white LED was most sensitive to the wavelength which violet emits which was confirmed from the previous wavelength analysis. It is expected that with the higher reverse current and lower frequency the sensitivity of the LED would be better.

The analysis was performed with accordance to the next steps:

1. The current value of the current source was set to one value
2. The frequency of the signal for one current value varied from 1 kHz to 1 MHz. Increasing the frequency of the signal showed significant growth of the noise levels.
3. When the certain current and frequency values are set, the first measurement is taken without blocking the lights path to obtain the received signal value.
4. The next step was to block the lights path to acquire values when there is no signal. In short, these results could be considered as a noise.
5. Set the frequency to the next value and repeat previous two steps.
6. Repeat previous four steps at each current value of the current source ranging from **1nA** till **10uA** when the LED is reverse-biased and from **1nA** till the limit when no signal could be sensed when the LED is forward-biased.

The results of the work for the Yellow "Bright" LED are shown in Figure 46 **-** Figure 48**.** The rest of the results could be found in Appendix 6 – Results of the forward-bias and reverse-bias sensitivity measurements.

61
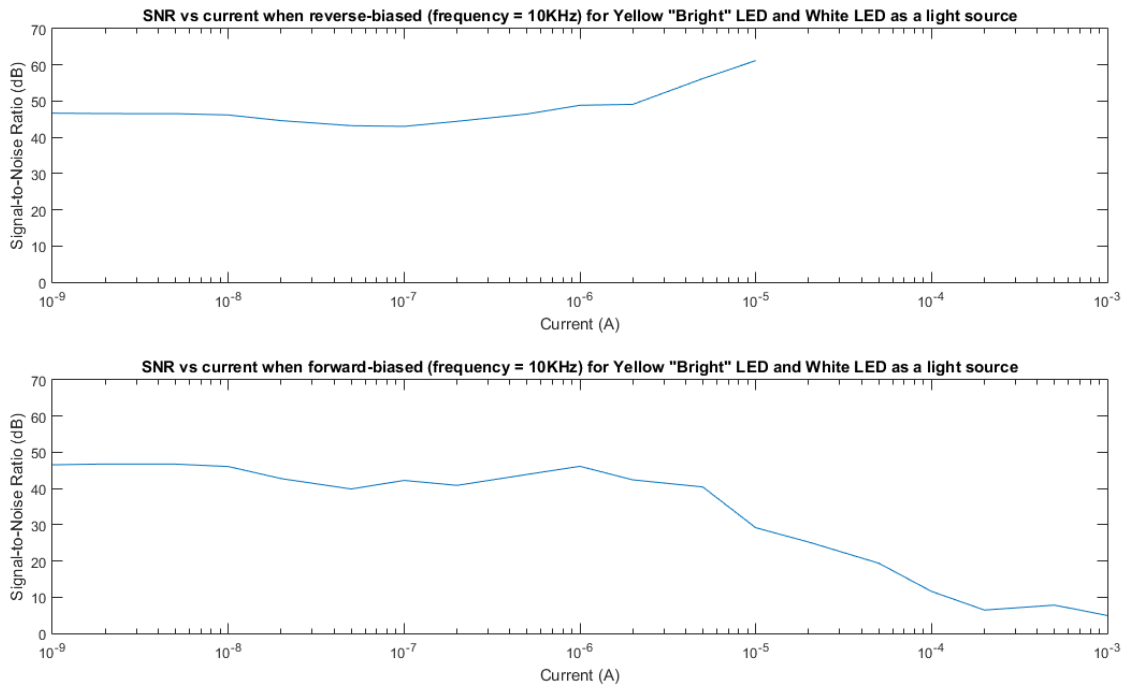
Figure 46. Signal-to-Noise Ratio of forward and reverse-biased LED with constant frequency of the signal.
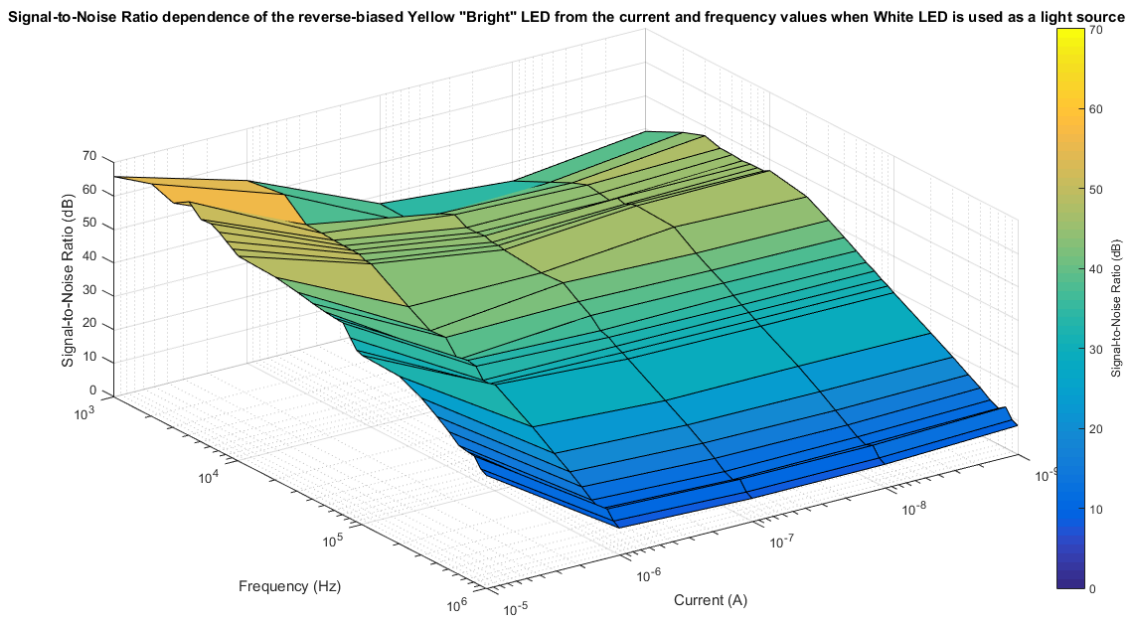
Figure 47. Signal-to-Noise Ratio of reverse-biased LED with variable frequency of the signal.
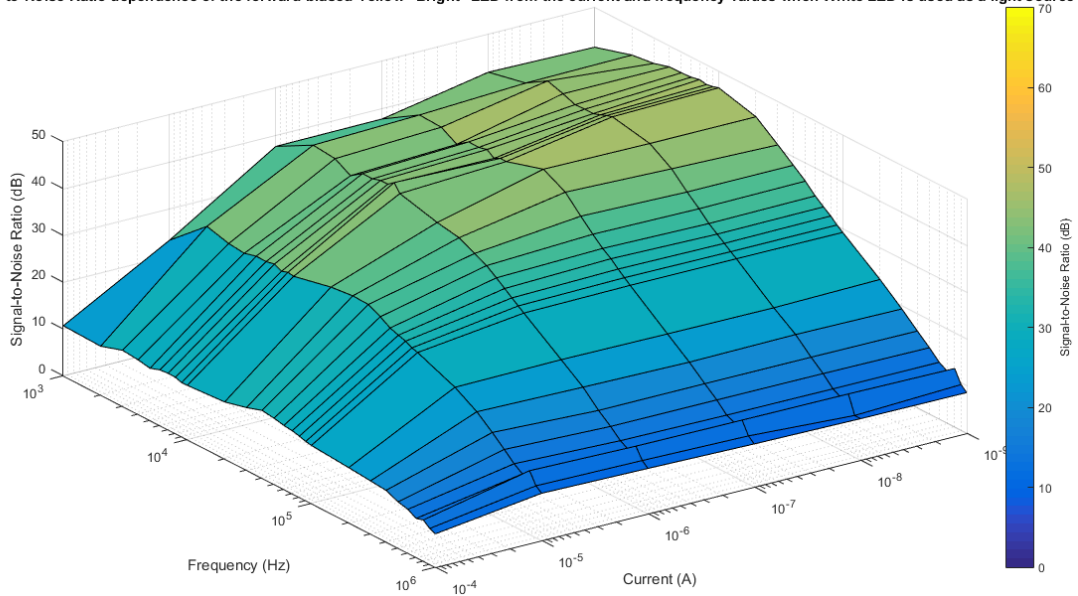
Figure 48. Signal-to-Noise Ratio of forward-biased LED with variable frequency of the signal.

It should be noted that the results had a high variance due to the fact that the light couldn't be perfectly blocked, so additional results filtering was performed. But even after that, the results show the LEDs behave as expected, but with additional notes. It seems that reverse-biased LED becomes more sensitive when the higher current value is applied but only to the light source which emits wavelength which the LED sensor is the most sensitive to. The reaction was observed with the White "Bright" LED when it was set against the other white colored LED. The results show that there was no improvements with the sensitivity at higher reverse current values, moreover, there was small recession and instability monitored. When the same experiment was made with Yellow "Bright" LED, the improvements were noticed since Yellow has notably high sensitivity with the white LEDs. In order to confirm the theory, the decision was made to repeat the measurements with the White "Bright" LED, but this time the violet LED should be used as the light source. Final results show that with violet LED the white LED sensor start to behave the same way as the yellow one and with higher reverse current the sensitivity started to grow.

As for the situation when the diode is forward-biased, his behavior fully coincides with one which was predicted, at higher current values the sensitivity starts to drop significantly. While the current value is small enough, the sensitivity stays unaffected on the same level as with small current values when the diode is reverse-biased. So this

means that it is still possible to use LED as a light sensor while small forward current value is applied.

Regarding the frequency measurements, the reaction on the increase of the frequency was predicted before and the results show that the Signal-to-Noise ratio drop with the increase of the frequency, though, it stays unknown what caused the fade of SNR at lower frequencies. This is the result of the junction capacitance of the LED which works as a low-pass filter for the signal. When the frequency is high enough, the output value on the load resistance starts to fall. One way is to increase the load resistance value but this will also increase noise levels. Another way is to apply reverse voltage on the LED which reduces the internal junction capacitance and, as a result, increases the cut-off frequency.

To conclude, the results of the measurements confirm that, though, it is possible to use forward-biased LED as a light sensor, it sensitivity is heavily reduced with higher forward current, so it is more reasonable to organize the circuit which would switch the LED from forward-biased state to the reverse-biased. As a result, the SNR level raises and the cut-off frequency improves.

5 Visual light communication device

The received results of the measurements could be used in the designing of the improved VLC device. The idea is to analyze the circuits of the previously designed devices which were found in the references, choose the most suitable one by its parameters and improve its design. There were multiple circuits available, each on has its own working principle which was previously described. But all of them use microcontrollers in order to work and it is possible to use modern parts to improve their work.

5.1 Device selection

There were two circuits chosen for the selection, each with certain cons and pros. The task is to evaluate and compare both of them, make certain conclusions, after what the final decision should be made what circuit would be selected.

5.1.1 Analysis of the LEDComm device

The first circuit, which was analyzed, was proposed by Mitsubishi Electric Research laboratories [4]. This circuit was also used in other works [4], [14] and the main benefit of such design is its simplicity. The whole work is done by the microcontroller while it needs only 2 external components one of which is LED itself. The data analysis is done by the microcontroller which reads analog value with the help of ADC. There are multiple samples taken to determine whether the light is being sensed or not. Each sample has length of 100us. So far, it was stated that the speed of the communication was 250 bit/s. Modern microcontrollers include improved ADC-s like, for example, the new MSP432 family from Texas Instruments has which are capable to have conversion rate of 1 Msps [63]. Theoretically, if the new sample length is 1us the communication speed could be improved up to 25 kbit/s. That is the huge improvement, but, so far, that is much as it can go unless the better ADC is implemented. Another way to overcome this limitation is to reduce the amount of samples which should be taken. By default it takes 40 samples to define if the LED is being emitted or not, but if this value is decreased the theoretical communication speed increases proportionally, though, this may result in errors.

Before reading the analog value on the LED it is switched to reverse bias in order to load the junction capacitance. Its value heavily influences the work of the device and the higher

it is the slower is the charging speed which, as a result, decreases the final speed of communication. In fact, different LEDs have different junction capacitance, for example, white ones have it higher than the red ones [64]. So, in order to increase the speed of work of the device, suitable LED should be chosen.

The next drawback is the limited current. The LED is driven from the general pin directly which requires the high current value which not every microcontroller can provide.

Last, but not least, the reaction on the ambient light which can be considered as noise is quite sensitive. Due to no filtering part the output of the LED sensor will always remain on the same level which will disrupt the communication link. Though, it is still depends on the LED itself and where it is situated because now it is known that most of the LEDs have very narrow angular response.

To conclude, the LEDComm device showed itself to be the quite reliable and simple since it uses the least amount of components and heavily depends on the microcontroller. Modern microcontrollers continue to evolve improving the ADC resolution and conversion time which could improve the work of the device. However, it is recommended to add few additional components to increase noise resistance, decrease lack of microcontrollers output current and influence of junction capacitance of the LED.

5.1.2 Analysis of the UART device

The second circuit which was analysed was mentioned EDN Network article and based on UART communication [65]. The principal schematic was presented earlier in Figure 11. This circuit uses more components than previous one and doesn't have such a high dependence on the microcontroller it is being connected to. The benefit of such design is that in order to send signal it is forward-biased and for receiving signal it switches to reverse-bias. Additionally, it has two operational amplifiers one of which amplifies the signal and second one works as a comparator with additional positive feedback. This circuit uses IR LED for emitting and sensing purposes and worked with the speed of 250 kbps. This is 1000 times faster than default speed of LEDComm. And this number could be improved with the help of modern components.

What is more, unlike with LEDComm, this circuit uses transistor to drive the LED which means that the current value flowing through the LED will be higher and as the result, working distance would be longer.

Like in previous case, junction capacitance plays important role in working speed of the device. When the transistor is opened the junction capacitance of the LED is charged through resistor R2. But when it is closed the diode discharges through the resistor R4. It should be noted that the values of these resistors are different and R4 value is in 100 times higher which means that the discharge sequence would be longer. This is the first limitation which was found.

The potentiometer is used to set the input threshold of the comparator. It is likely to mention that using potentiometer is not reliable since it wears of fast, it is noisy, have inertia problems [66]. When the device is switched on it should be ready to go at once without the need to be adjusted. If the there is a need to dynamically change the value it could be done by the microcontroller without any moving parts.

As it was mentioned before, the device uses UART serial communication to transmit the data. Since only one LED is used to both transmit and receive signal, both Tx and Rx pins are connected to the LED sensor. While the diode is transmitting the signal, the same signal is being read at the Rx pin. The combination of R10 and D1 is being used to decrease the influence of the transmission. This combination is questionable since the Rx pin could be disabled or the interrupt handler, if it is used, could be disabled internally in the microcontroller. Taking that into consideration, it is possible that this combination could be removed.

Like with LEDComm device, this is one is also influenced by the ambient light, though, it uses IR LEDs for communication and this gives advantage against ambient light sources which have weak IR part of the spectrum. But if the LEDs would be replaced by those which work in visual light area this could cause problems.

To sum up, this circuit shows greater capabilities and based on the adding of more external components to improve incoming signal and ready to go when connected to the UART section of the microcontroller. It appears that this circuit has more sensitivity capabilities, but the communication speed depends on more components and limitations

of the serial communication link. But with certain component upgrades and additional updates it should be possible to improve the work of the circuit.

5.1.3 Final selection

After brief analysis of both of the circuit the final decision was made to improve the second circuit which was proposed by EDN Network. The circuit showed both higher speed and sensitivity since it uses more external components to amplify the received signal. Another advantage is that it's more universal and could be connected to most of the microcontrollers and doesn't have heavy dependence on the microcontroller's internal peripherals. Last but not least, it uses UART to communicate with other devices instead of using internal ADC which frees more resources for other tasks.

5.2 Device improvement

With accordance to the previously described negative sides of the circuit, there were few improvements made in order to increase the performance of the device. In order to control how the changes affect the device the new circuit was tested and simulated in the "Multisim" environment. The software provided large database of different components from various producers, but some custom ones were added in order to improve the layout. When the device was transmitting the signal, the default blue color LED was used for the simulation. During the receive part, the LED was replaced with several optocouples in order imitate the LED working as the light sensor. The final circuit is presented in Figure 49.
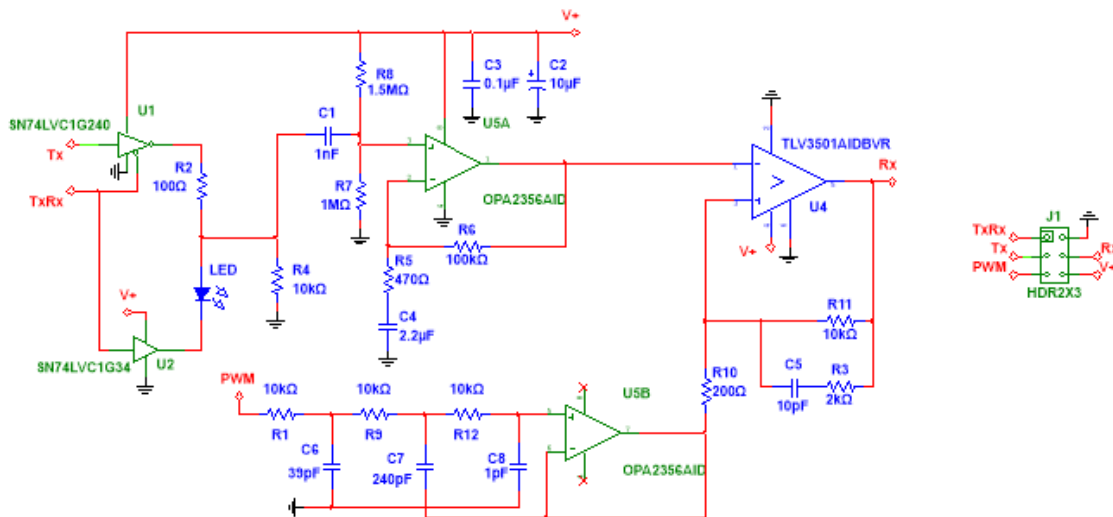
Figure 49. Circuit of the light communication device.

The list of the improvements which were made is described below.

1. The transistor Q1 which was presented in previous variant of the device was replaced with two IC-s U1 and U2. The first IC U1 serves as inverting buffer [67] with 3-state output. It is controlled by two signals Tx and TxRx. When the device is sending the package, TxRx is set to 'logical 0' and the Tx signal is passed to the LED. The junction capacitance of the LED now will discharge the same way through the resistor R2 which increases the final speed of transmission. When device is receiving the package, TxRx is set to logical 'logical 1'. This sets the U1 inverting buffer to high impedance state of the output and the photocurrent generated by the LED will pass through R4 resistor. The buffer [68] U2 follows the signal TxRx which sets the LED in forward-bias or reverse-bias. In reverse bias the junction capacitance of the LED decreases which compensates the transmission speed loss due to high load resistance value of the R4.

2. The AC coupling was added to remove the DC component from the signal. The idea is to reduce the noise of the ambient light which can influence the work of the device by generating constant photocurrent. The AC coupling consists of C1, R7 and R8. This circuit sets another DC bias level to the input of the OA U3A which equals 40% of the power supply and passes frequencies of the signal which are higher than 159 Hz. The AC coupling has very low influence on the load resistor R4 due to high resistance value.

69

3. In order to amplify only AC part of the signal, the capacitor C1 was added to the non-inverting amplifier. Like in previous case, in order to amplify the signal with frequency of 159 Hz the capacitor value was chosen 2.2uF. Due to only AC part being amplified the DC part will remain the same on the output of the amplifier.

4. Operational amplifiers OPA2350 [69] were replaced with OPA2355 [70] which are related products and serve in the same applications but have higher bandwidth and unity gain frequency and much higher slew rate. This allows the devices to communicate with higher speed exceeding 250 kilobits per second.

5. Instead using potentiometer in the design, the circuit presents PWM signal to DC converter [71]. It is based on the Chebyshev's type 3rd order active low-pass filter [72] which would attenuate all high frequency components of the signal and leave only DC component. By controlling the duty cycle of the PWM signal it is possible to change the DC component itself and set more accurate reference voltage for the comparator than the potentiometer can provide with the least microcontroller pins in use. The higher the frequency of the PWM signal, the higher is the accuracy, but the requirement is that the frequency of the signal wouldn't be lower than 4 MHz. The higher the attenuation the better, but the only restriction was to use only one OA. This is the main reason why filter was chosen Chebyshev's type with pass band ripple set to 1 specifically, since it has the steepest roll-off, but also has ripple in the pass band. However, since there are no frequency components which apply in the pass band area, except noise values, the effects of the ripple are not taken into consideration.

6. The second OPA2350 which was working as the comparator was replaced with the TLV3501 [73] which was originally designed to work as the comparator and has higher speed of work comparing to one which was in the original design. The resistors R11 and R10 set the hysteresis voltage. The C5 and R3 chain adds hysteresis for the AC part of the signal and additional forcing effect which speeds up the switching of the comparator. The reference voltage is adjusted by the 'PWM to DC converter' and controlled directly by the microcontroller. The default setup should be made to set the reference voltage on the positive input of the comparator higher than the DC signal on the negative input.

7. The chain from the original circuit consisting of R10 and D1 was considered as optional and removed in this design. It is possible to isolate the receiving part of the microcontroller with the software. Or the receiving part could also be used to echo back the signal which is being sent and control it. Additionally, with the new design it is now possible to perform self-calibration by the microcontroller to adjust proper reference voltage for each signal frequency and reduce bit error rate.

The calculation part is described in the Appendix 9 – Calculation of the improved design components. The simulation of the circuit is shown in the Appendix 10 – Simulation of the improved design of the communication device. The picture of the PCB designed in 'Ultiboard' environment is shown in Figure 50. More detailed pictures and 3D models of the board are presented in Appendix 11 – Print Circuit Board of the improved communication device. The bill of materials which were used in the design could be found in Appendix 12 – Bill of materials for the improved communication device.
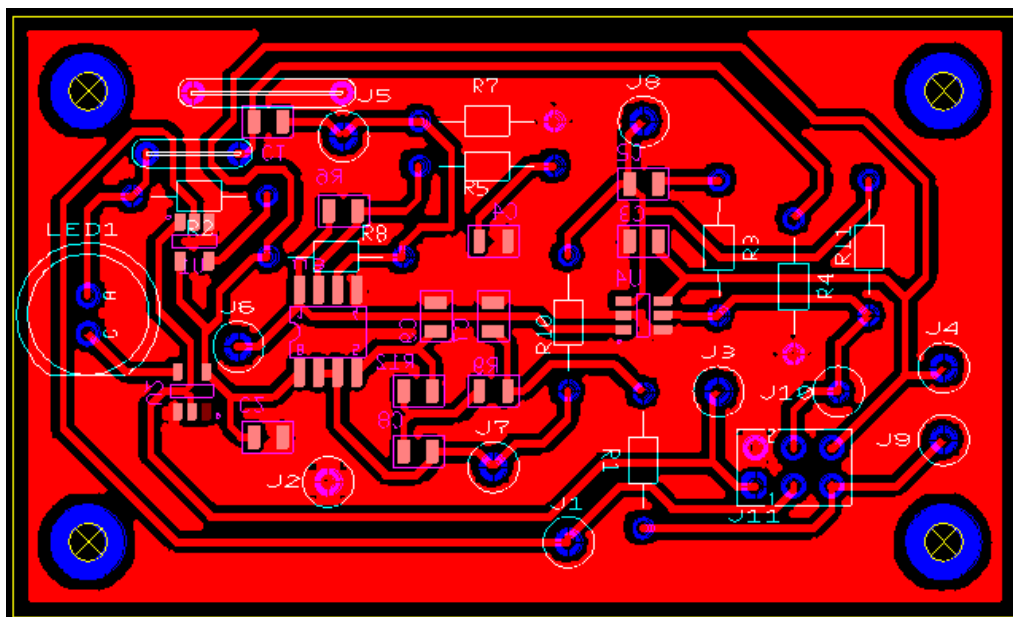
Figure 50. Overall look of the PCB for the communication device.

Overall, the new design of the device shows great improvements in the speed of the transmission, slight sensitivity increase of the LED sensor, reduced noise influence and is now more cost-effective due to idea of using the special purpose components. The final circuit is now larger than the original one and now microcontroller has the possibility to control several parts of the circuit with help of one additional pin. The simulation shows

71

promising results and the first prototype may exceed the capabilities of the original design.

5.3 Results of the communication device prototype

The components for described improved design were bought and the prototype of the communication device was constructed. The pictures of the device could be observed in Figure 51.
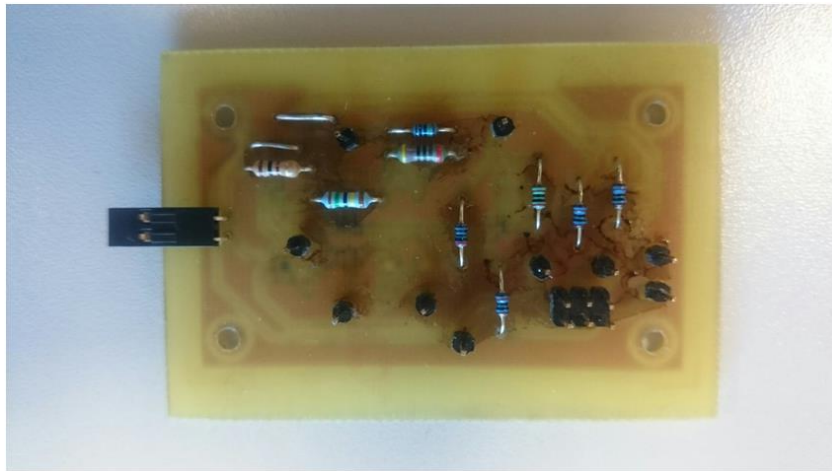
Figure 51. Top view of the communication device.

The results of the device work could be viewed in Appendix 13 – Results of the tests of the communication device.

The results show that device was able to achieve very high speed which was previously observed during the simulation part only at very close distances. By increasing the distance between the signal source and the device the frequency of the signal needed to be decreased. At distances higher than 85 mm the useful signal level generated by the LED was close to the noise level and the distortions could be observed on the output. In total, the device showed good speed of communication, however, due to very short distances of communication the practical use for the device is questionable.

The possible reasons why the device didn't behave as intended:

- The resistance value of the load resistor is extremely low for this application. The resistor's value was taken from the original design. The value wasn't changed due

to the fact that it is connected to the AC coupling which already has very high resistance values in order to not influence the load resistance. Increase in resistance would mean that the resistances of the AC coupling also need to be increased, but further increase of the resistance would cause more noises.

- Very high amplification for the first operational amplifier which amplifies the AC signal. Due very high amplification the amplifier oscillates and starts to generate noise signal.

- One of the possible reasons can also be degradation of the operational amplifier characteristics which were caused by inaccurate soldering during PCB construction procedure.

Additional factor which played significant role was the model ideality. During simulation procedure the noise levels on the input and output of the amplifier were not sufficient, though, during measurements of the prototype the results showed that noise levels are quite high. Additionally, the virtual circuit didn't show any signs that it could lose stability and start to oscillate. This brings to conclusion that simulation used more ideal models which didn't take into account additional variables which could oscillate or reduce the circuit parameters.

To conclude, the test of the design showed that it is not suitable for LED communication applications and other solutions should be considered.

5.4 Transimpedance amplifier

Lessons learned from the previous communication device design show that using 10kOhm resistance for current conversion is not enough. Additionally, the noise levels in the design doesn't allow to receive light at long distances. This actually brings to idea of using transimpedance amplifiers.

Transimpedance amplifiers are commonly used to work with light sensors and perform current-to-voltage conversion [74]. The circuits with transimpedance amplifiers are considerably simple and consist of the amplifier, feedback resistor and the photodiode. Additional components are needed only to reduce the noise influence of the device and improve its stability.

The Figure 52 shows the LED based light sensor using operational amplifier OPA380 from TI.
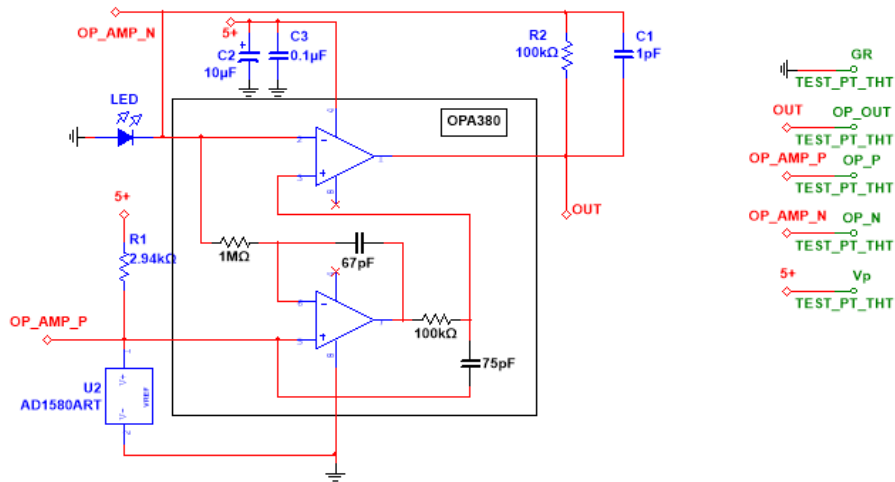
Figure 52. Transimpedance amplifier for LED on OPA380.

The calculations for the circuit were made and shown in Appendix 14 – Calculations of the transimpedance amplifier. The simulation part showing how the circuit is performing is shown in Appendix 15 – Simulation results of the transimpedance amplifier. The PCB for the design could be found in Appendix 16 – Print Circuit Board of the transimpedance amplifier and the Figure 53 shows the overall view. The rules which were used for the PCB of the communication device were also applied here. The BOM could be found in Appendix 17 – Bill of materials for the transimpedance amplifier.
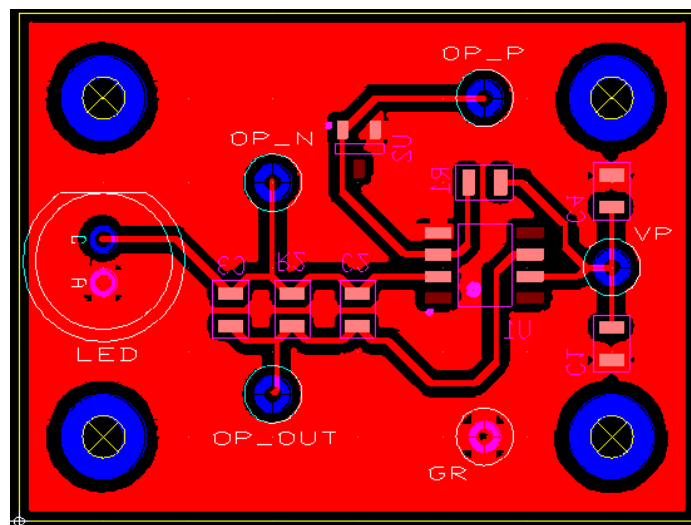
Figure 53. Overall look of the PCB for the transimpedance amplifier.

To sum up, calculations and the simulation show that the device should have good SNR level and high bandwidth up to 1 MHz which is lower than the previous device possessed but instead it should increase the sensitivity and, as the result, the distance between the transmitter and receiver.

5.5 Results of the transimpedance amplifier prototype

The components for described design were bought and the prototype of the transimpedance amplifier was constructed. The pictures of the device could be observed in Figure 54.

Figure 54. Top view of the transimpedance amplifier.

The results of the device work could be viewed in Appendix 18 – Results of the tests of the transimpedance amplifier.

Comparing the measurements from the device and the results received during simulation, it could be noted that the measured output voltages of the device are lower than estimated which means that the currents generated by the LED are lower. The possible reason is that the higher currents were registered with higher illuminance.

The results show that the device was able to achieve same speeds as the previous one, however, at speed of 1.5MHz the output signal was already changing to sinusoidal shape. The sensitivity of the device, though, was greatly improved and the device was able to give good output signal at the distance of 0.5m between the devices. At 1m, however, the output of the signal is already too noisy.

In order to increase the sensitivity of the device, the 100kOhm feedback resistor was replaced with 3.3MOhm and the feedback compensation capacitor removed. The gain increase should be approximately in 33 times, but this would result in decrease of the bandwidth and cause higher noise levels on the output. But the results show that at lower frequencies, such as 1kHz and 125kHz, the sensitivity of the device was increased further and at the distance of 1m the good output signal could be observed. In case of 1.5MHz signal, due to decreased cut-off frequency and increased noise levels, the signal was attenuated low enough that cannot be observed on the output.

Additionally, in case when 100kOhm feedback resistor was used, lock-in amplifier was used to see how the characteristics of the device would improve if lock-in feature would be added. The received measurements show that adding such feature would increase the SNR of the device and allow to increase the distance between the devices more than just using simple square-shaped signal.

To conclude, the amplifier showed promising results and this means that the further sensitivity increase of LED should be focused on advancement of the transimpedance amplifiers. By using modern amplifiers such as LTC6268 [75] by Linear Technology would significantly increase the transimpedance gain or bandwidth of the device depending on the feedback resistance value. Additionally, by using signal modulations or using lock-in features such as used in communications would also improve the features of the final device. Finally, it is possible to merge the previously developed communication device and transimpedance amplifier to create an unique device which would be able both send and receive the signal.

6 Summary

The task of this master thesis was to research the capabilities of LEDs as light sensors. Two test groups were used:

1. The 'Bright' group which was consisted of the Super Bright LEDs supplied by Adafruit. For more details about their specifications refer to Chapter 3.2.

2. The 'Basic' group which was consisted of the Basic LEDs supplied by SparkFun. For more details about their specifications refer to Chapter 3.1.

Additionally, in wavelength analysis and angular response analysis two additional white power LEDs were used supplied by Lucky Light and Huey Jann. For more details about their specifications refer to Chapter 3.4.

The results of the analyses of the conducted experiments are next:

- **Illuminance analysis**.

  o Among light sources warm and cold fluorescent lamp, halogen lamp and white LED (number 1, 2, 3 and 7 respectively) the yellow coloured LEDs in both 'Bright' and 'Basic' test groups appeared to be the most sensitive.

  o Output photocurrent has linear dependence on the illuminance value with three exceptions:

    1) The 'Bright' group had unlinear behavior if either warm fluorescent lamp (number 1) or cold fluorescent lamp (number 2) were used. The possible reason can be the influence of the impulse power supply of the fluorescent lamp while other light sources were powered from the DC voltage, but this point requires further investigation.

2) Blue coloured LED from the 'Bright' group showed that it has linear response even to both warm and cold fluorescent lamps.

3) Orange coloured LED from the 'Basic' group showed that it has unlinear response with all 4 light sources (number 1, 2, 3 and 7).

o Output photocurrent value doesn't depend on the load resistance.

1) High load resistance value may cause current saturation.

o Higher voltage supply value results in higher photocurrent output, except:

1) Blue LED from the 'Bright' group showed linear decrease of the photocurrent when the voltage supply increased.

2) Blue LED from the 'Basic' group showed unpredictable due to low sensitivity to Halogen lamp (light source number 3) and high noise level.

3) In order to control the behaviour of blue ones, it is possible to repeat the tests in future with the light source to which they are more sensitive to.

- **Wavelength analysis**.

    o This analysis showed that all of the LEDs from 'Basic' and 'Bright' groups including white ones from Lucky Light and Huey Jann are sensitive only to wavelength shorter than their peak emission wavelength.

    o The shift between the response and emission peaks in each color LED is not similar even if the LEDs are from the same test group.

    o The results of the LEDs which were used in this research coincide with the results of the references which also showed that peak sensitivity wavelength is shorter than peak emission wavelength.

        1) Other references state that peak emission and response wavelengths can be equal, so this statement worth of investigation.

78

It is possible in future to analyze other LED and find if this idea is true.

- **Angular response analysis**.

  o It was observed that angular response of each of the LEDs depends both on the shape of the LEDs and their internal construction.

  o It was observed that in most of the cases the angular response is close to emission beam degree. However, there was one exception:

    1) Unlike the other LEDs in both 'Basic' and 'Bright' groups, the blue ones showed notably higher angular response which could be analyzed further.

  o Only model supplied by LuckyLight was capable to sense the incoming light at the angle of 90°.

  o Models supplied by Huey Jann and LuckyLight showed response closest to Cosine law.

- **Forward-biased and reverse-biased sensitivity analysis**.

  o The analysis showed that LED light sensor was able to sense incoming light signal when forward-biased.

  o Reverse-biased connection could improve sensitivity of the LED. There was one exception:

    1) The results, when both LEDs of the white colour from 'Bright' group were used, show that no notable SNR improvement was registered and the higher reverse current could cause instability and oscillations.

- **Visual Light Communication device simulation and prototypes**.

  o Several devices were analysed and simulated, one of them was modified and two prototypes were built.

- The first device which was based on EDN Network design was capable to receive the signal at the desired speed only at very short distances.

- The second device which was based on transimpedance amplifier showed that it is capable to receive the signal at longer distances.

  1) Adding additional features such as lock-in or signal modulation could improve sensitivity and the working distance of the device.

- It can be concluded that TIA is more suitable for amplifying the incoming light signal and in future both devices could be combined in order to obtain the design which could both emit and receive light signals.

Overall, the research showed that LEDs behave the same way as the photodiodes and generate photocurrent when exposed to light. Using available measurement instruments it became possible to analyse characteristics of different colour light-emitting diodes, confirm the previously discovered capabilities and more deeply analyze features which were not well known. However, some of the LEDs, such as blue colored ones from each of the test group, showed unique behavior in multiple measurements. Future research could be done in order to find out if these types LEDs would behave the same way and what may be the cause of such phenomenon.

To conclude, though, the LEDs were designed for specific purpose, which is light emitting, they show great and unique capabilities in light sensing comparing to originally designed photodiodes or phototransistors, which brings to conclusion that LEDs could be used in future designs of dual-use nature instead of photodiodes in order to reduce the complexity of the devices.

References

[1] E.Fred Schubert, "LIGHT-EMITTING DIODES", second edition, Preface, page X, Cambridge University Press, 2006. Available: http://www.ifsc.usp.br/~lavfis2/BancoApostilasImagens/ApConstantePlanck/ApCtePlanck2013/LIGHT-EMITTING%20DIODES.e-0521865387-2e.pdf (23.04.2017)

[2] Martin Buck, "Considerations for light sources: For semiconductor light sensor test", Mixed-Signal Testing Workshop (IMSTW), 2015 20th International, 24-26 June 2015. Available: http://ieeexplore.ieee.org/stamp/stamp.jsp?arnumber=7177862 (23.04.2017)

[3] The Royal Swedish Academy of Sciences , "Blue LEDs – Filling the world with new light", The Nobel Prize in Physics, 2014. Available: https://www.nobelprize.org/nobel_prizes/physics/laureates/2014/popular-physicsprize2014.pdf (23.04.2017)

[4] Paul Dietz, William Yerazunis, Darren Leigh, "Very Low-Cost Sensing and Communication Using Bidirectional LEDs", MITSUBISHI ELECTRIC RESEARCH LABORATORIES, July 2003. Available: https://www.forth-ev.de/filemgmt_data/files/TR2003-35.pdf (23.04.2017)

[5] M. Mims, Siliconnections: Coming of Age in the Electronic Era. New York, NY, USA: McGraw-Hill, 1986

[6] Mims, Forrest M., III, LED Circuits and Projects, Howard W. Sams and Co., Inc., New York, NY, pp. 60-61, 76-77, 122-123.

[7] AZoOptics , "Photodiode – Working Principle and Applications", May 29 2014. Available: http://www.azooptics.com/Article.aspx?ArticleID=809 (23.04.2017)

[8] Yang Liu; Hung-Yu Chen; Kevin Liang, "Visible Light Communication Using Receivers of Camera Image Sensor and Solar Cell", IEEE Photonics Journal (Volume: 8, Issue: 1, Feb. 2016), Article #: 7800107. Available: http://ieeexplore.ieee.org/stamp/stamp.jsp?arnumber=7355280 (23.04.2017)

[9] C. H. Chang et al., "A 100-Gb/s multiple-input multiple-output visible laser light communication system" J. Lightw. Technol., vol. 32, no. 24, pp. 4723–4729, Dec. 2014. Available: http://ieeexplore.ieee.org/stamp/stamp.jsp?arnumber=6937061 (23.04.2017)

[10]   B. Janjua et al., "Going beyond 4 Gbps data rate by employing RGB laser diodes for visible light communication" Opt. Exp., vol. 23, no. 14, pp. 18746–18753, Jul. 2015. Available: https://www.osapublishing.org/DirectPDFAccess/937DAD94-

9546-E73A-764FECB2904C6805_321836/oe-23-14-18746.pdf?da=1&id=321836&seq=0&mobile=no (23.04.2017)

[11]   Y. C. Chi et al., "450-nm GaN laser diode enables high-speed visible light communication with 9-Gbps QAMOFDM" Opt. Exp., vol. 23, no. 10, pp. 13 051–13 059, May 2015. Available: https://www.osapublishing.org/DirectPDFAccess/9384B38F-B3E5-27EF-F53D585B22CA5856_318517/oe-23-10-13051.pdf?da=1&id=318517&seq=0&mobile=no (23.04.2017)

[12]   W. Y. Lin et al., "10 m/500 Mbps WDM visible light communication systems" Opt. Exp., vol. 20, no. 9, pp. 9919– 9924, Apr. 2012. Available: https://www.osapublishing.org/DirectPDFAccess/93A40820-9728-1838-B36D3EEC8412C15B_231999/oe-20-9-9919.pdf?da=1&id=231999&seq=0&mobile=no (23.04.2017)

[13]   C. W. Chow, C. H. Yeh, Y. Liu, and Y. F. Liu, "Digital signal processing for light emitting diode based visible light communication" IEEE Photon. Soc. Newslett., vol. 26, pp. 9–13, Oct. 2012. Available: http://web.it.nctu.edu.tw/~cwchow/journal/leos2012.pdf (23.04.2017)

[14]   Stefan Schmid; Giorgio Corbellini; Stefan Mangold; Thomas R. Gross, "LED-to-LED visible light communication networks", MobiHoc '13 Proceedings of the fourteenth ACM international symposium on Mobile ad hoc networking and computing, July 29–August 1, 2013. Available: https://s3-us-west-1.amazonaws.com/disneyresearch/wp-content/uploads/20140729173943/p1-schmid1.pdf (23.04.2017)

[15]   S. Schmid, G. Corbellini, S. Mangold, and T. Gross. "An LED-to-LED Visible Light Communication system with software-based synchronization". In Optical Wireless Communication. Globecom Workshops (GC Wkshps), 2012 IEEE, pages 1264–1268, Dec. 2012. Available: http://people.inf.ethz.ch/schmist/papers/OWC12.pdf (23.04.2017)

[16]   Giorgio Corbellini ; Kaan Aksit ; Stefan Schmid ; Stefan Mangold ; Thomas Gross, "Connecting networks of toys and smartphones with visible light communication", IEEE Communications Magazine (Volume: 52, Issue: 7, July 2014), pp 72 – 78. Available: https://s3-us-west-1.amazonaws.com/disneyresearch/wp-content/uploads/20150412230901/Connecting-Networks-of-Toys-and-Smartphones-with-Visible-Light-Communication-Paper.pdf (23.04.2017)

[17]   Y.B. Acharya, A. Jayaraman, S. Ramachandran and B. H. Subbaraya, "Compact light-emitting-diode sun photometer for atmospheric optical depth

measurements", Applied Optics (Vol. 34, No. 7, 1 March 1995), pp 1209. Available: https://www.prl.res.in/~library/Acharya_YB_1209_95_abst.pdf (23.04.2017)

[18]   Youngryel Ryu; Dennis D. Baldocchi; Joseph Verfaillie; Siyan Ma; Matthias Falk; Ilse Ruiz-Mercado; Ted Hehn; Oliver Sonnentaga, "Testing the performance of a novel spectral reflectance sensor, built with light emitting diodes (LEDs), to monitor ecosystem metabolism, structure and function", Agricultural and Forest Meteorology 150 (2010), pp 1597–1606. Available: http://environment.snu.ac.kr/wp-content/uploads/2016/03/Ryu_2010_AFM3.pdf (23.04.2017)

[19]   Forrest M. Mims III, "Sun photometer with light-emitting diodes as spectrally selective detectors", Applied Optics (Vol. 31, No. 33, 20 November 1992), pp 6965-6967. Available: http://userpages.umbc.edu/~martins/PHYS650/02860Mims.pdf (23.04.2017)

[20]   Jeffrey Czapla-Myers; Kurtis Thome; Stuart Biggar, "Automated Ground-Based Vicarious Calibration of MODIS", Remote Sensing Group, 24 March 2005. Available: http://mcst.gsfc.nasa.gov/sites/mcst.gsfc/files/meetings_files/mcst_2005_03_24_thome_poster.pdf (23.04.2017)

[21]   Shuai Li ; Ashish Pandharipande ; Frans M. J. Willems, "Daylight Sensing LED Lighting System", IEEE Sensors Journal (Volume: 16, Issue: 9, May1, 2016), pp 3216 – 3223. Available: http://ieeexplore.ieee.org/stamp/stamp.jsp?arnumber=7389352 (23.04.2017)

[22]   Shuai Li ; Ashish Pandharipande, "Color sensing and illumination with LED lamps", 2014 IEEE Fourth International Conference on Consumer Electronics Berlin (ICCE-Berlin), Date of Conference: 7-10 Sept. 2014. Available: http://ieeexplore.ieee.org/stamp/stamp.jsp?arnumber=7034294 (23.04.2017)

[23]   Ashish Pandharipande ; Shuai Li, "Illumination and light sensing for daylight adaptation with an LED array: Proof-of-principle", Industrial Electronics Society, IECON 2013 - 39th Annual Conference of the IEEE, Date of Conference: 10-13 Nov. 2013. Available: http://ieeexplore.ieee.org/stamp/stamp.jsp?arnumber=6700134 (23.04.2017)

[24]   Shuai Li ; Ashish Pandharipande, "LED-Based Color Sensing and Control", IEEE Sensors Journal (Volume: 15, Issue: 11, Nov. 2015), pp 6116 – 6124. Available: http://ieeexplore.ieee.org/stamp/stamp.jsp?arnumber=7152829 (23.04.2017)

[25]   James Bryant, "LEDs are Photodiodes Too", Rarely Asked Questions – Issue 108, August 2014. Available: http://www.analog.com/library/analogdialogue/archives/48-08/raq_108.html (23.04.2017)

[26]   Clark J. Radcliffe, "Chapter 7: Measuring Light with an LED". Available: http://www.egr.msu.edu/classes/me456/radcliff/handouts/Lecture_09-Chap7.pdf (23.04.2017)

[27]   Martina O'Toole; Dermot Diamond, "Absorbance Based Light Emitting Diode Optical Sensors and Sensing Devices", Sensors 2008, 8, 2453-2479. Available: https://www.google.ee/url?sa=t&rct=j&q=&esrc=s&source=web&cd=4&cad=rja&uact=8&ved=0ahUKEwiEktKH77HPAhVDhSwKHXgqDtYQFggtMAM&url=http%3A%2F%2Fwww.mdpi.com%2F1424-8220%2F8%2F4%2F2453%2Fpdf&usg=AFQjCNExd3by9AGgAbxBPbWzowuffrr6uQ&sig2=pWk9RG2MXv_GYXHVCDlbVA (23.04.2017)

[28]   Tanya M. Sansosti, "LED's as Light Detectors", Optics Rotation Project, Spring 2002. Available: http://laser.physics.sunysb.edu/~tanya/report2/ (23.04.2017)

[29]   Burr-Brown Corporation, "PHOTODIODE MONITORING WITH OP AMPS", January, 1995. Available: http://www.ti.com/lit/an/sboa035/sboa035.pdf (23.04.2017)

[30]   Kyle Holland, "LED doubles as emitter and detector", LI-COR Inc, Lincoln, NE, August 2001. Available: http://www.edn.com/design/analog/4340435/LED-doubles-as-emitter-and-detector (23.04.2017)

[31]   Graeme, Jerald, Photodiode Amplifiers: Op-amp Solutions, McGraw-Hill, 1996, pp. 4-7.

[32]   Emanuele Taralli ; Roberto Filippo ; Giorgio Brida ; Mauro Rajteri ; Simon R.G. Hall ; Agnieszka Bialek ; Claire Greenwell ; Nigel Fox, "LED-based field radiometer for sensor web in-situ measurements", Metrology for Aerospace (MetroAeroSpace), 2015 IEEE, Date of Conference: 4-5 June 2015. Available: http://ieeexplore.ieee.org/stamp/stamp.jsp?arnumber=7180675 (23.04.2017)

[33]   Institute of Electrical and Electronics Engineers and Electron Devices Society, Eds., "IEEE standard for sensor performance parameter definitions". New York, NY: IEEE, Inst. of Electrical and Electronics Engineers, 2014. Available: http://ieeexplore.ieee.org/stamp/stamp.jsp?arnumber=6880296 (04.05.2017)

[34]   Dr. Christine Rüth; Andreas Vogler; Wilhelm Karsten , "Ambient Light Sensors General Application Note", Opto Semiconductors, 29 June 2006. Available: http://www.osram-os.com/Graphics/XPic3/00039056_0.pdf/Ambient%20Light%20Sensors%20(General).pdf (23.04.2017)

[35]   Andrew Bierman; Jean Paul; Yiting Zhu; N. Narendran, "LED Testing Standards Overview", Capturing the Lighting Edge, 13 Aug. 2012. Available:

http://www.lrc.rpi.edu/education/outreachEducation/pdf/CLE4/PM3_Photometry.pdf
(23.04.2017)

[36]   Everlight, "Ambient Light Sensor - DIP 3mm T-1", ALS-PDIC144-6C/L378
datasheet, November 2015. Available: http://www.everlight.com/file/ProductFile/ALS-
PDIC144-6C-L378.pdf (24.04.2017)

[37]   Mentor Graphics, "Thermal and Radiometric Characterization of LEDs",
TERALED User's Manual, 2009. Available: http:\site.svg-tech.com\clients\svg-
tech\Downloads\TERALED6262014103329AM4.pdf (23.04.2017)

[38]   Dr. Christine Rüth; Andreas Vogler; Wilhelm Karsten, "Ambient Light
Sensors", General Application Notes, June 2006. Available: http://www.osram-
os.com/Graphics/XPic3/00039056_0.pdf/Ambient%20Light%20Sensors%20(General).
pdf (24.04.2017)

[39]   Osram, "Short CFLni, with 2-pin base for CCG operation", Osram Dulux S
family datasheet, April 2017. . Available:
https://www.osram.com/appsinfo/pdc/pdf.do?cid=GPS01_1027844&vid=PP_EUROPE
_Europe_eCat&lid=EN (24.04.2017)

[40]   Satcom, "SC-Electric Halogen Lamp JC/G4 12 35W", satcom.ee. Available:
http://www.satcom.ee/en/a/halogen-lamp-jc-g4-12v-35-w (24.04.2017)

[41]   Pro-Lite, "Xenon Ultra 2 Pin Low Voltage Capsule 12V", Product Data
Specification. Available: http://www.farnell.com/datasheets/45637.pdf (24.04.2017)

[42]   Alex Ryer, "Light Measurement Handbook", Chapter 7, 1997-2000. Available:
http://www.dfisica.ubi.pt/~hgil/fotometria/HandBook/ch07.html (25.02.2017)

[43]   Robert Keim, "Understanding Illuminance: What's in a Lux",
allaboutcircuits.com, January 2016. Available:
https://www.allaboutcircuits.com/technical-articles/understanding-illuminance-whats-
in-a-lux (23.04.2017)

[44]   C. R. Nave, "Photodiode Characteristics", HyperPhysics, Electricity and
Magnetism, 2012. Available: http://hyperphysics.phy-
astr.gsu.edu/hbase/Electronic/photdet.html (23.04.2017)

[45]   Matthew Ziff, "Lighting Calculations", Interior Architecture Program, Winter
2011. Available:
https://www.interiorarchitecture.ohiou.edu/ziff/ARTI%20288/288Lecture23-2011.pptx
(1.05.2017)

[46]   Electrical Knowhow, "Point by Point Method for Lighting Design", electrical-
knowhow.com, 2013. Available: http://www.electrical-knowhow.com/2012/12/point-
by-point-method-for-lighting.html (23.04.2017)

[47]   Alex Ryer, "Light Measurement Handbook", Chapter 6, 1997-2000. Available: http://www.dfisica.ubi.pt/~hgil/fotometria/HandBook/ch06.html (23.04.2017)

[48]   SparkFun, "LED MIXED PACK", Rainbow pack datasheet. Available: https://cdn.sparkfun.com/datasheets/Components/LED/SFE-03-0010-LEDInsertCards-RainbowPack-03-Outlines.pdf (23.04.2017)

[49]   SparkFun, "5mm Red LED YSL-R531R3D-D2", YSL-R531R3D-D2 datasheet. Available: https://www.sparkfun.com/datasheets/Components/LED/COM-09590-YSL-R531R3D-D2.pdf (23.04.2017)

[50]   Lighting Research Center, "How is white light made with LEDs", NLPIP Lighting Answers, Volume 7, Issue 3, May 2003 . Available: http://www.lrc.rpi.edu/programs/nlpip/lightingAnswers/led/whiteLight.asp (1.05.2017)

[51]   Ye International, "Super Bright Red 5mm LED", yeint.ee. Available: http://yeint.ee/elektroonika-1/led-komponendid/led-valgusdioodid/super-bright-red-5mm-led # https://www.adafruit.com/product/2700 (1.05.2017)

[52]   Ye International, "Super Bright Yellow 5mm LED", yeint.ee. Available: http://yeint.ee/elektroonika-1/led-komponendid/led-valgusdioodid/super-bright-yellow-5mm-led

[53]   Ye International, "Super Bright Green 5mm LED", yeint.ee. Available: http://yeint.ee/elektroonika-1/led-komponendid/led-valgusdioodid/super-bright-green-5mm-led (23.04.2017)

[54]   Ye International, "Super Bright Blue 5mm LED", yeint.ee. Available: http://yeint.ee/elektroonika-1/led-komponendid/led-valgusdioodid/super-bright-blue-5mm-led # https://www.adafruit.com/product/1793 (23.04.2017)

[55]   Ye International, "UV/UVA 400nm Purple LED 5mm Clear Lens", yeint.ee. Available: http://yeint.ee/elektroonika-1/arendusvahendid/led-indikaaatorid/led-ultraviolett/uvuva-400nm-purple-led-5mm-clear-lens (23.04.2017)

[56]   Lucky Light, "5mm Round With Flange Type Purple LED", YSL-R531R3D-D2 datasheet, May 2008. Available: https://cdn-shop.adafruit.com/datasheets/1793datasheet.pdf (23.04.2017)

[57]   Ye International, "Super Bright White 5mm LED", yeint.ee. Available: http://yeint.ee/elektroonika-1/led-komponendid/led-valgusdioodid/super-bright-white-5mm-led (23.04.2017)

[58]   Shenzhen Furuier, "5mm Standard Round White LED", FLR-50T04-HW7 datasheet, March 2011. Available: https://cdn-shop.adafruit.com/datasheets/FLR-50T04-HW7+(2012.02.22).pdf (23.04.2017)

[59]   Lucky Light, "0.5W Warm White High Power LED", HP30MW6C datasheet, July 2007. Available: http://www.luckylight.cn/UploadFiles/pdf_2014120114174890951.pdf (23.04.2017)

[60]   Huey Jann, "High Power 10W LED", HPR20D-19K10xWx-D datasheet, July 2009. Available: http://www.tme.eu/gb/Document/50269a726b9c4e648b1889ee19a2bb86/HPR20D-19K10xWx-D.pdf (23.04.2017)

[61]   Photon Technology International, "Lamp Emission Spectra", 2005. Available: http://mmrc.caltech.edu/Stark/Xe%20lamp%20spectra.pdf (23.04.2017)

[62]   AA1Car, "High Intensity Discharge Headlights". Available: http://www.aa1car.com/library/hid_headlamps.htm (23.04.2017)

[63]   Texas Instruments, "MSP432P4xx SimpleLink™ Microcontrollers", Technical Reference Manual, March 2015. Available: http://www.ti.com/lit/ug/slau356f/slau356f.pdf (25.02.2017)

[64]   JavaScience, "LED Frequency Response", February 2013. Available: http://www.jensign.com/Discovery/LEDFrequencyResponse/ (23.04.2017)

[65]   Mosaic Documentation Web, "Understanding Serial Communications". Available: http://www.mosaic-industries.com/embedded-systems/instrumentation/rs232-serial-rs485-protocol-uart-usart/understanding-serial-communications (23.04.2017)

[66]   J.T.Barett, "The Disadvantages of a Potentiometer". Available: http://sciencing.com/disadvantages-potentiometer-6144904.html (1.05.2017)

[67]   Texas Instruments, "Single Buffer/Driver With 3-State Output", SN74LVC1G240 datasheet, January 2001 [Revised December 2013]. Available: http://www.ti.com/lit/ds/symlink/sn74lvc1g240.pdf (23.04.2017)

[68]   Texas Instruments, "SN74LVC1G34 Single Buffer Gate", SN74LVC1G34 datasheet, December 2003 [Revised April 2016]. Available: http://www.ti.com/lit/ds/symlink/sn74lvc1g34.pdf (23.04.2017)

[69]   Texas Instruments, "OPAx350 High-Speed, Single-Supply, Rail-to-Rail Operational Amplifiers MicroAmplifier Series", OPA2350 datasheet, September 2000 [Revised December 2015]. Available: http://www.ti.com/lit/ds/symlink/opa350.pdf (23.04.2017)

[70]   Texas Instruments, "OPAx356 200MHz, CMOS OPERATIONAL
        AMPLIFIER", OPA2356 datasheet, November 2001. Available:
        http://www.ti.com/lit/ds/symlink/opa356.pdf (23.04.2017)

[71]   David M. Alter, "Using PWM Output as a Digital-to-Analog Converter on a
        TMS320F280x Digital Signal Controller", Application Report, September 2008.
        Available: http://www.ti.com/lit/an/spraa88a/spraa88a.pdf (23.04.2017)

[72]   M.E. Van Valkenburg, "Analog Filter Design", Chapter 8.6, pp. 250-251.
        Available: https://www.ece.uic.edu/~vahe/spring2016/ece412/Chebyshev.pdf
        (23.04.2017)

[73]   Texas Instruments, "TLV350x 4.5-ns, Rail-to-Rail, High-Speed Comparator in
        Microsize Packages", TLV3501 datasheet, March 2005 [Revised April 2016].
        Available: http://www.ti.com/lit/ds/symlink/tlv3501.pdf (23.04.2017)

[74]   John Caldwell, "1 MHz, Single-Supply, Photodiode Amplifier Reference
        Design", TI Designs – Precision: Verified Design. Available:
        http://www.ti.com/lit/ug/tidu535/tidu535.pdf (23.04.2017)

[75]   Linear Technology, "4GHz Ultra-Low Bias Current FET Input Op Amp",
        LTC6268-10/LTC6269-10 datasheet, 2015. Available:
        http://cds.linear.com/docs/en/datasheet/626810f.pdf (27.04.2017)

[76]   Agilent Technologies, "Agilent 34410A/11A 6 ½ Digit Multimeter", User's
        guide, Fifth edition, June 2012. Available:
        http://www.sophphx.caltech.edu/Lab_Equipment/34410%20User%20Guide.pdf
        (23.04.2017)

[77]   Agilent Technologies, "Agilent E3631A Triple Output DC Power Supply
        Specifications", E3631A datasheet, October 2002. Available:
        http://www.pd.infn.it/elettronica/Strumenti/HP_E3631A.pdf (23.04.2017)

[78]   Hewlett Packard, "HP E363xA - Series Programmable Power Supplies",
        Technical Data, October 1998. Available:
        http://www.testequipmenthq.com/datasheets/Agilent-E3634A-Datasheet.pdf
        (23.04.2017)

[79]   Keithley Instruments, "Series 2600 System SourceMeter", User's Manual, May
        2006. Available: http://www.imperial.ac.uk/media/imperial-college/research-centres-
        and-groups/centre-for-bio-inspired-technology/7291001.PDF (23.04.2017)

[80]   Zurich Instruments, "MFLI Lock-in Amplifier", Product Leaflet, January 2017.
        Available: https://www.zhinst.com/sites/default/files/zi_mfli_leaflet_online.pdf
        (23.04.2017)

[81]   Zurich Instruments, "HF2IS Impedance Spectroscope", Product Specification, August 2014. Available: https://www.zhinst.com/sites/default/files/zi_hf2is_leaflet_0.pdf (23.04.2017)

[82]   "Устройство и принцип действия призменного монохроматора УМ – 2", Theoretical introduction. Available: http://niimf.narod.ru/UM2.pdf (23.04.2017)

[83]   Ocean Optics, "USB4000 Fiber Optic Spectrometer", Installation and Operation Manual, 2008. Available: http://oceanoptics.com/wp-content/uploads/USB4000OperatingInstructions.pdf (23.04.2017)

[84]   Tenmars, "Lux/ Fc Light Meter", TM – 202 User's Manual. Available: http://www.elicrom.com/content/TM-204-MANUAL-USERS.pdf (23.04.2017)

[85]   Texas Instruments, "Precision, High-Speed Transimpedance Amplifier", OPA380 datasheet, November 2003 [Revised September 2007]. Available: http://www.ti.com/lit/ds/symlink/opa380.pdf (23.04.2017)

[86]   Analog Devices "1.2 V Micropower, Precision Shunt Voltage Reference", AD1580 datasheet, 2011. Available: http://www.farnell.com/datasheets/1506114.pdf?_ga=1.84581209.179113036.1481872966 (23.04.2017)

[87]   Hooman Hashemi, "Transimpedance Amplifiers (TIA): Choosing the Best Amplifier for the Job", Application Report, November 2015. Available: http://www.ti.com/lit/an/snoa942/snoa942.pdf (23.04.2017)

Appendix 1 – Full description of the measurement devices

- Agilent 34410A – digital multimeter [76] from Agilent which has $6\frac{1}{2}$ digits precision and capable to communicate with the PC via USB. For this device the program was made in LabView software which would take numerous samples, calculate average value and standard deviation. The input impedance was set to default value which is 10MOhm.

- Agilent E3631A – triple output DC power supply [77]. The main advantage of this power supply is that it is digital and capable to change voltage or current with high precision. The limits are is that first output can have maximum output voltage of 6V and current 5A, and the second output can have voltage ± 25V and current 1A.

- Agilent E3634A – DC power supply [78]. This power supply is more powerful than previous one and could have output voltage 25V with current 7A or voltage 50V with current 4A.

- Keithley 2612 SYSTEM SourceMeter [79]. This device is capable to work as current source and output desired current or voltage. The source meter could have voltage up to 200 V on the output and current up to 10 A.

- Zurich Instruments MFLI Lock-in Amplifier [80]. It is digital lock in amplifier which is able to cover up to 5MHz, 60 MSa/s and 16-bit precision, have current and differential voltage inputs. And like Agilent digital multimeter it is possible to work in LabView with it.

- Zurich Instruments HF2IS Impedance Spectroscope [81]. It is digital lock in amplifier which is able to cover up to 50MHz, 210 MSa/s and 128-bit digital signal processing, have 2 independent lock-in units and 2 signal generators. And like Agilent digital multimeter it is possible to work in LabView with it.

- Monochromator UM-2 [82]. This is monochromator has two modes. One is capable to output only desired wavelength from the light source on the input and other allows to watch full spectrum of the light source on the output. In order to change mode the output module should be replaced.

- OCEAN OPTICS Spectrometer USB4000 [83]. Portable spectrometer which covers 200-1100 nm range with optical resolution of 0.1nm to 10nm and has ability to connect to certain devices and accessories. It is rather fast and has integration time 3.8 ms – 10 s.

- Tenmars TM-202 Lux/Fc Light Meter [84]. Portable lux-meter which has accurate spectral response close to photopic luminosity function and $3\frac{1}{2}$ digits precision and up to ±6% accuracy depending on the light source.

Appendix 2 – Spectrums of different light sources

Figure 2 - 1. Spectrum of the Halogen lamp 12V 10W (Output power is 10W).
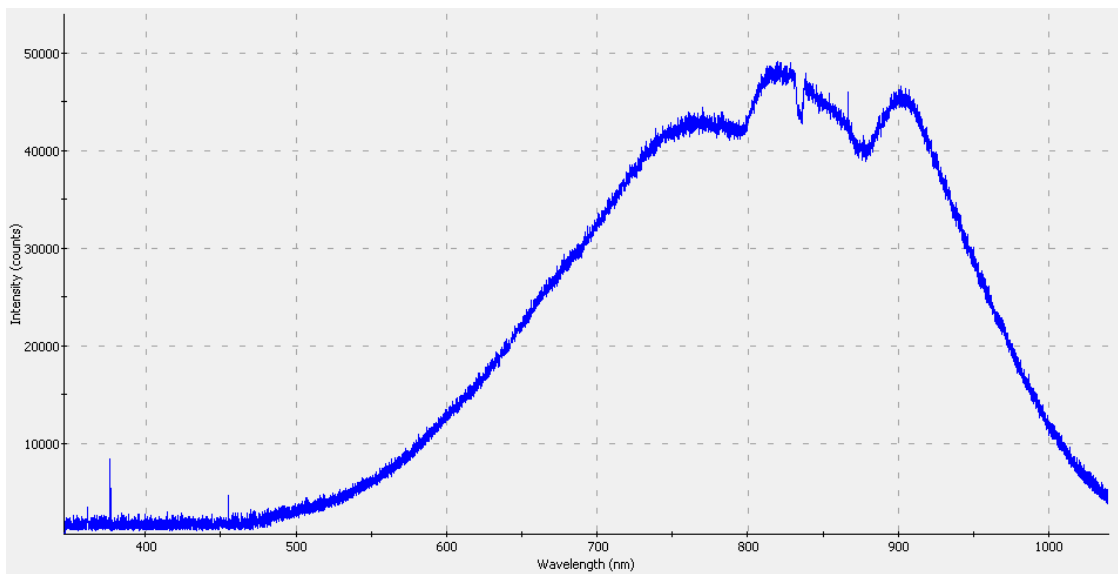
Figure 2 - 2. Spectrum of the Halogen lamp 12V 10W (Output power is 1.275W).
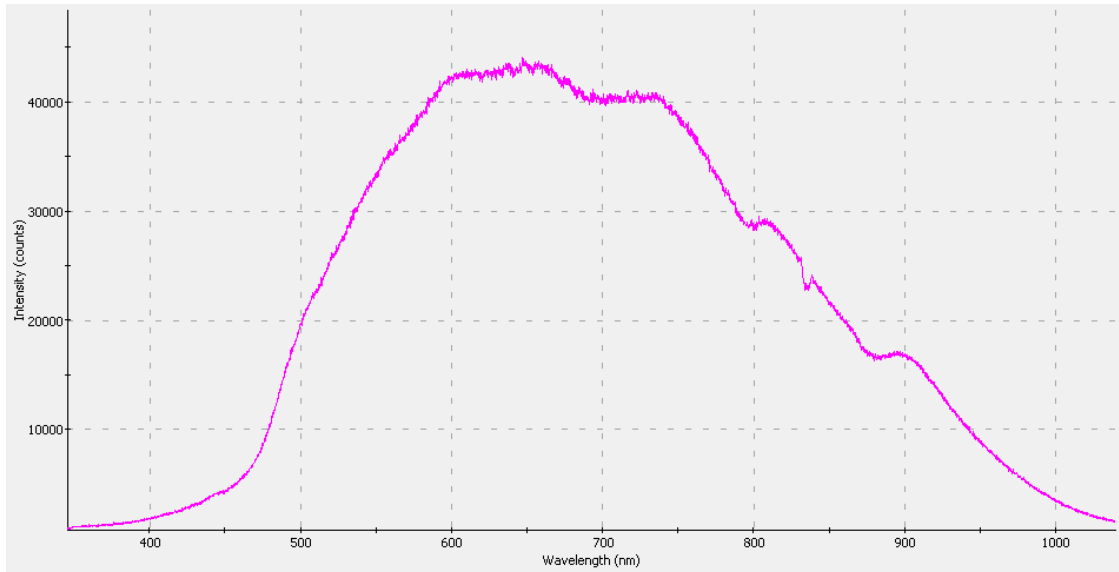
Figure 2 - 3. Spectrum of the Halogen lamp 12V 35W (Output power is 35W).
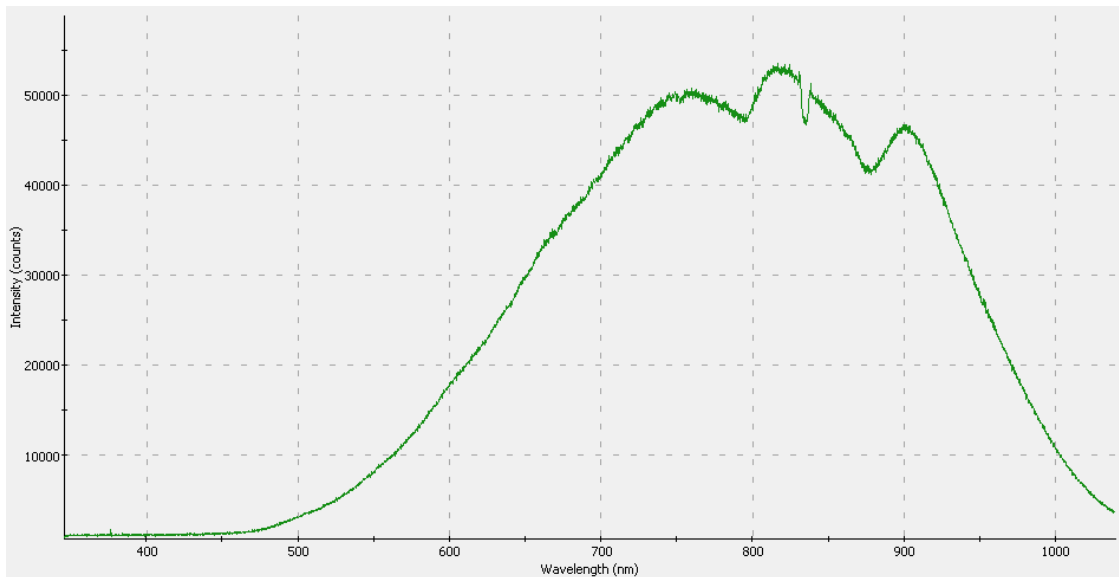
Figure 2 - 4. Spectrum of the Halogen lamp 12V 35W (Output power is 4.463W).
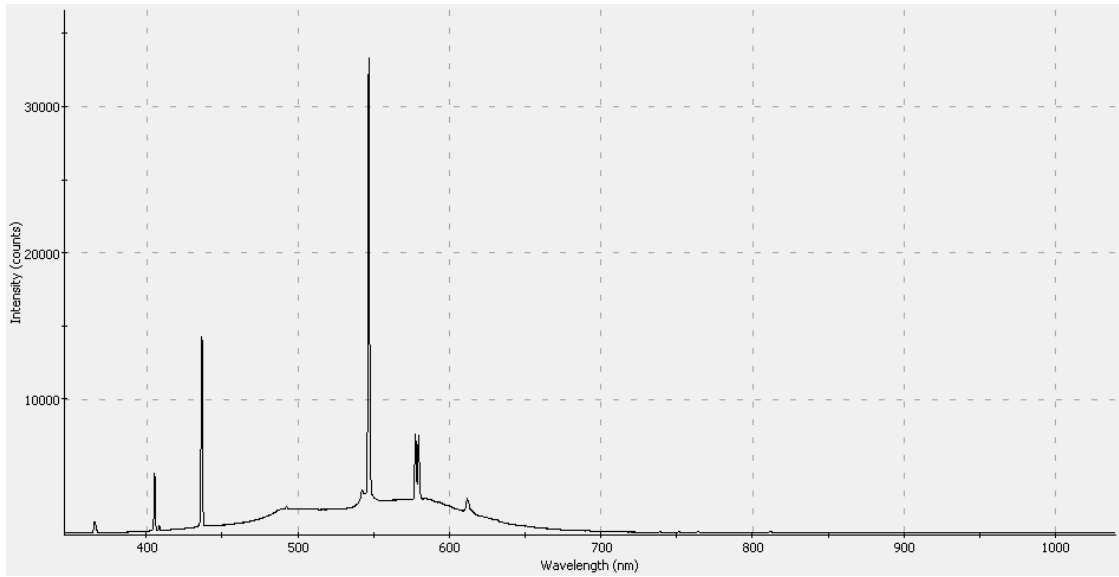
Figure 2 - 5. Spectrum of the Cold Fluorescent Lamp (Averaged).
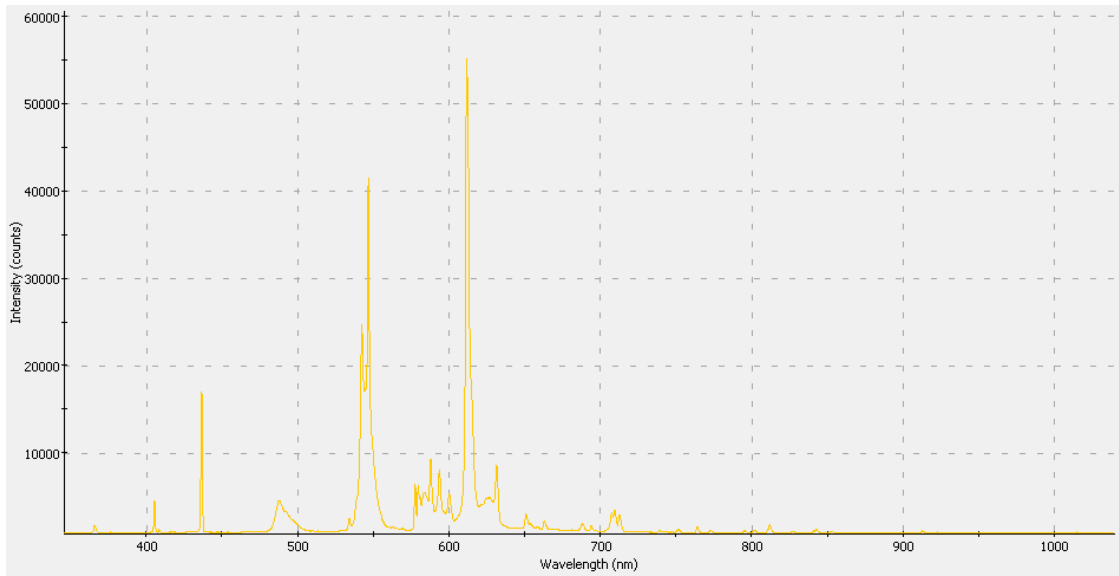
Figure 2 - 6. Spectrum of the Warm Fluorescent Lamp (Averaged).
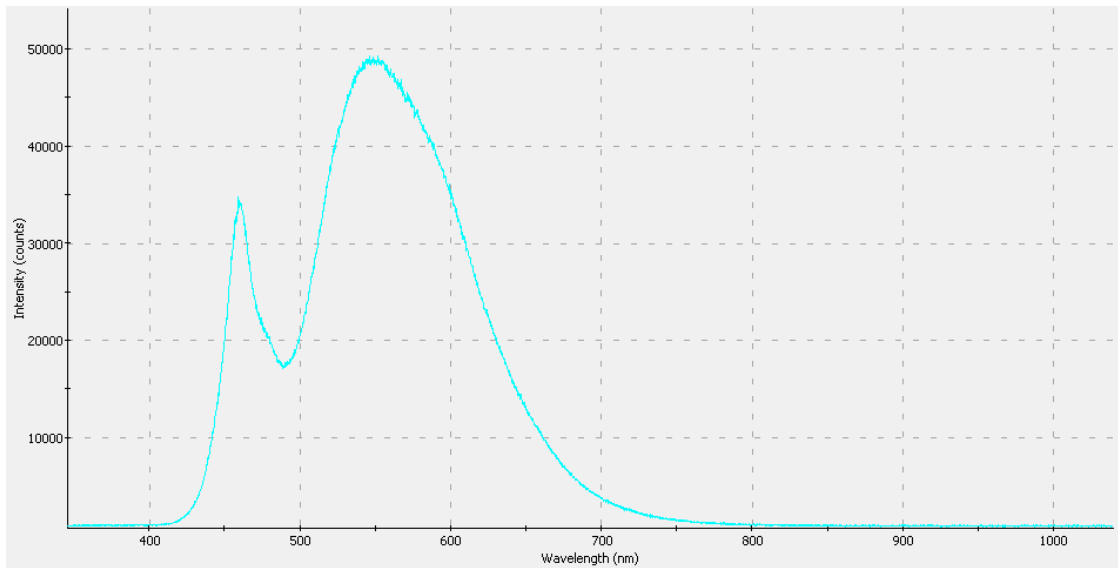
Figure 2 - 7. Spectrum of the White Bright LED (Output power is 60mW).
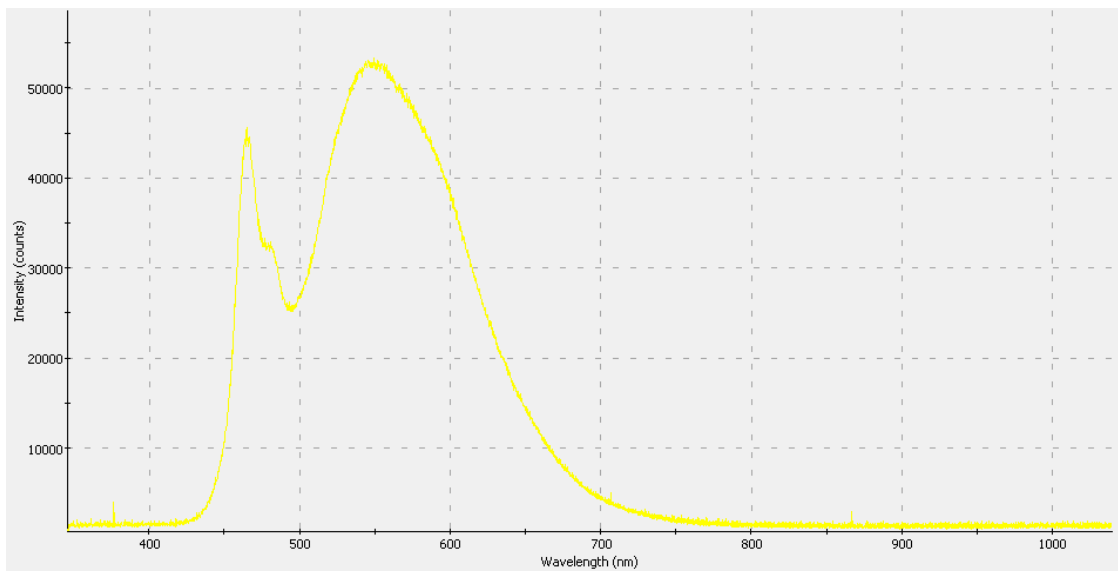
Figure 2 - 8. Spectrum of the White Bright LED (Output power is 0.25mW).

Appendix 3 – Results of the Illuminance measurements
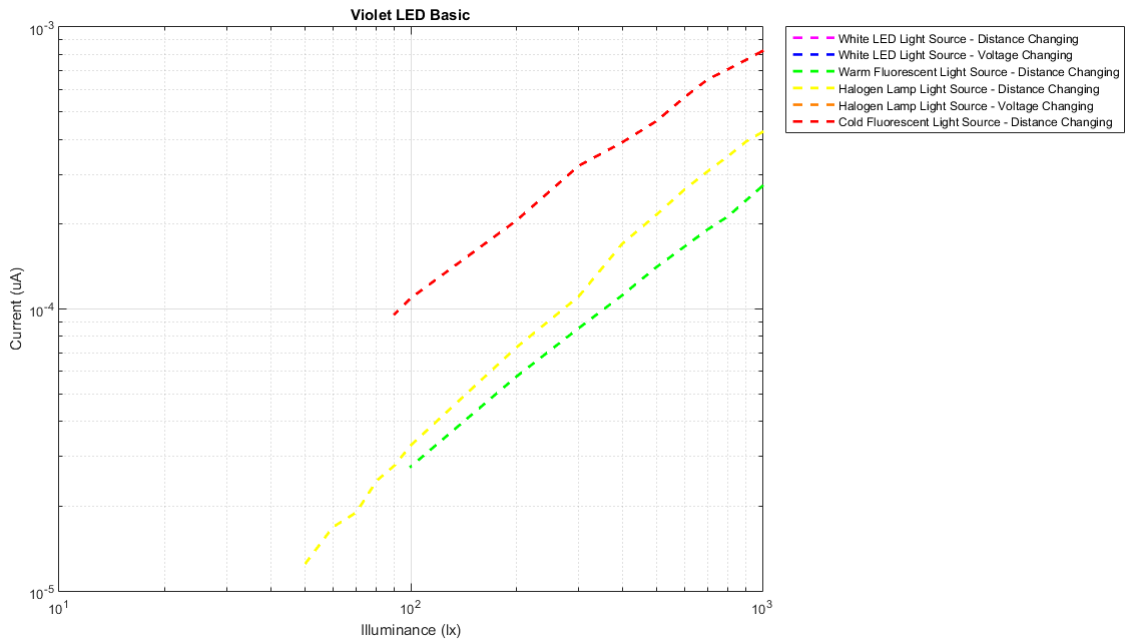
Figure 3 - 1. Illuminance versus Current. Reaction of Violet 'Basic' LED on different light sources.
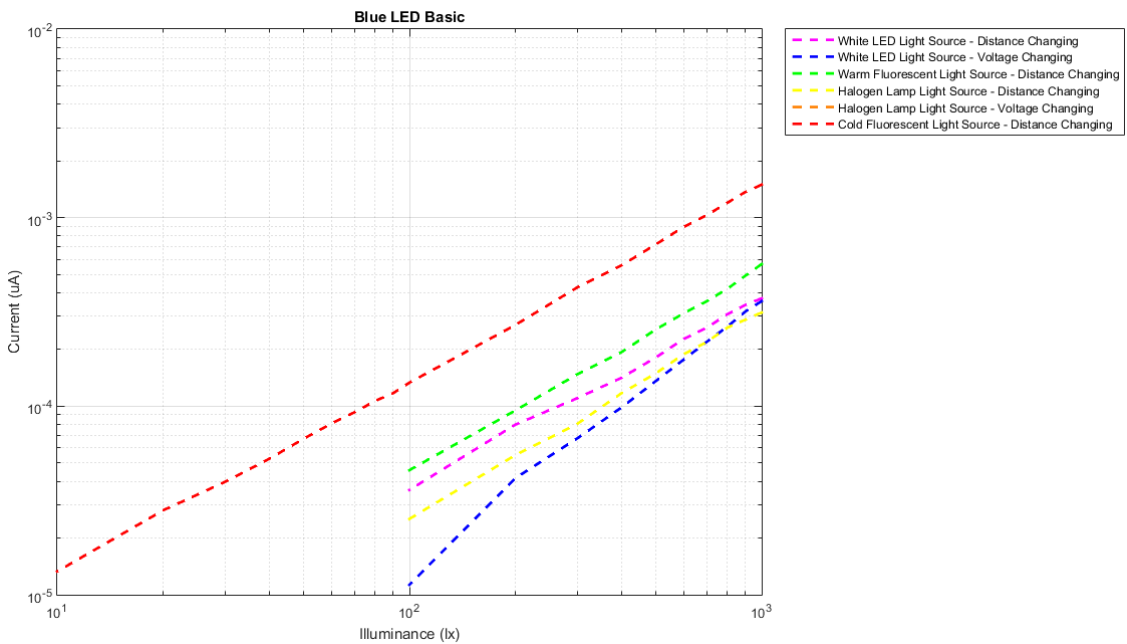
Figure 3 - 2. Illuminance versus Current. Reaction of Blue 'Basic' LED on different light sources.
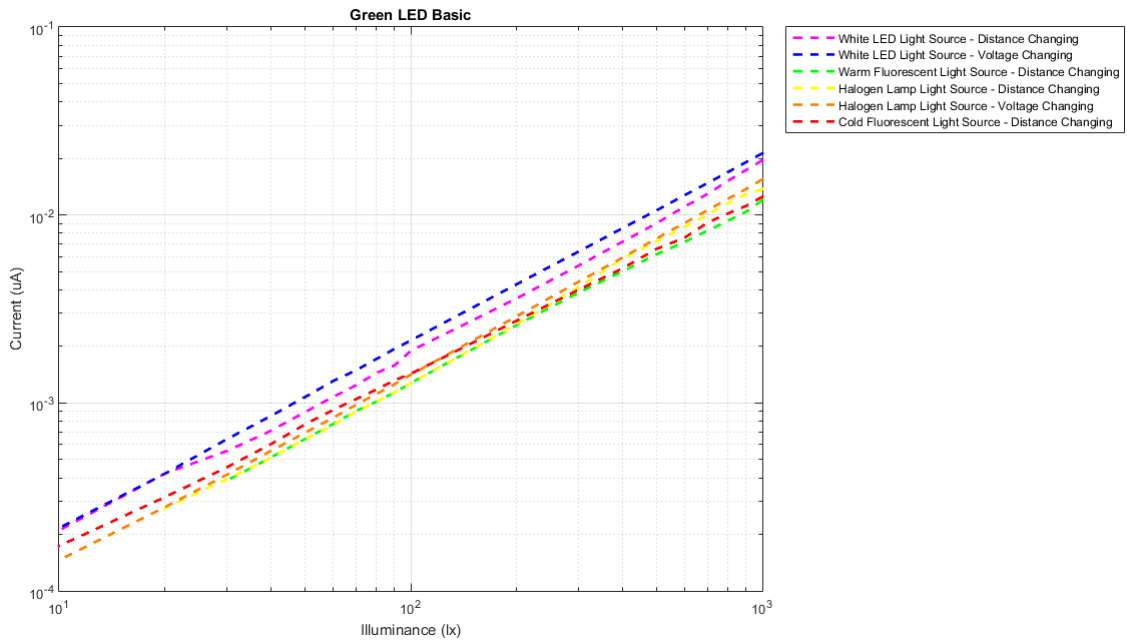
Figure 3 - 3. Illuminance versus Current. Reaction of Green 'Basic' LED on different light sources.
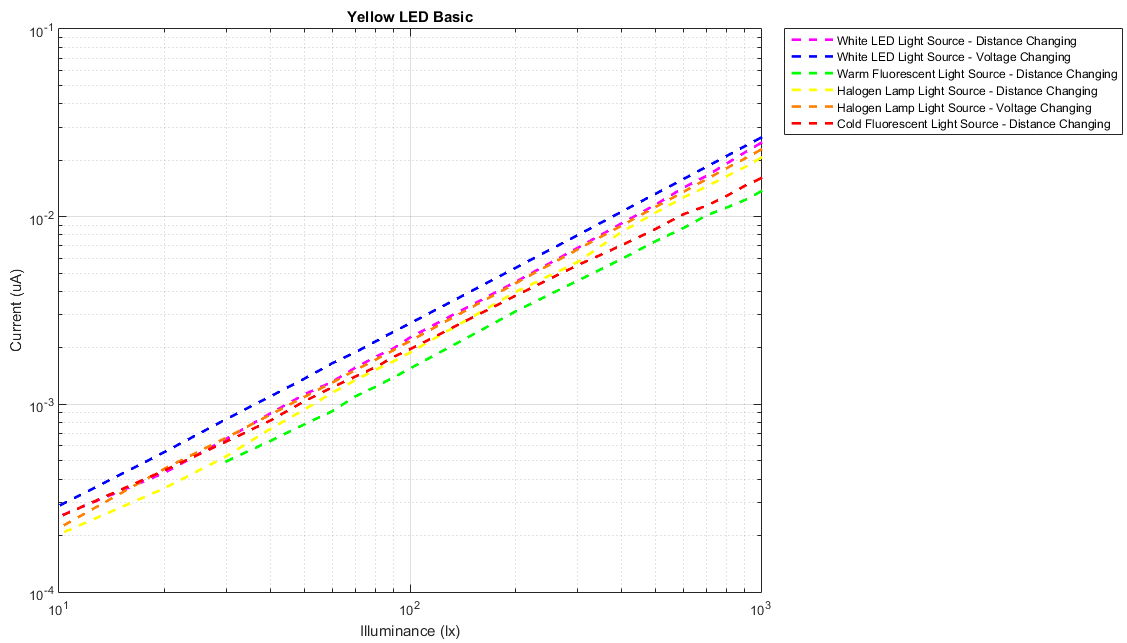
Figure 3 - 4. Illuminance versus Current. Reaction of Yellow 'Basic' LED on different light sources.
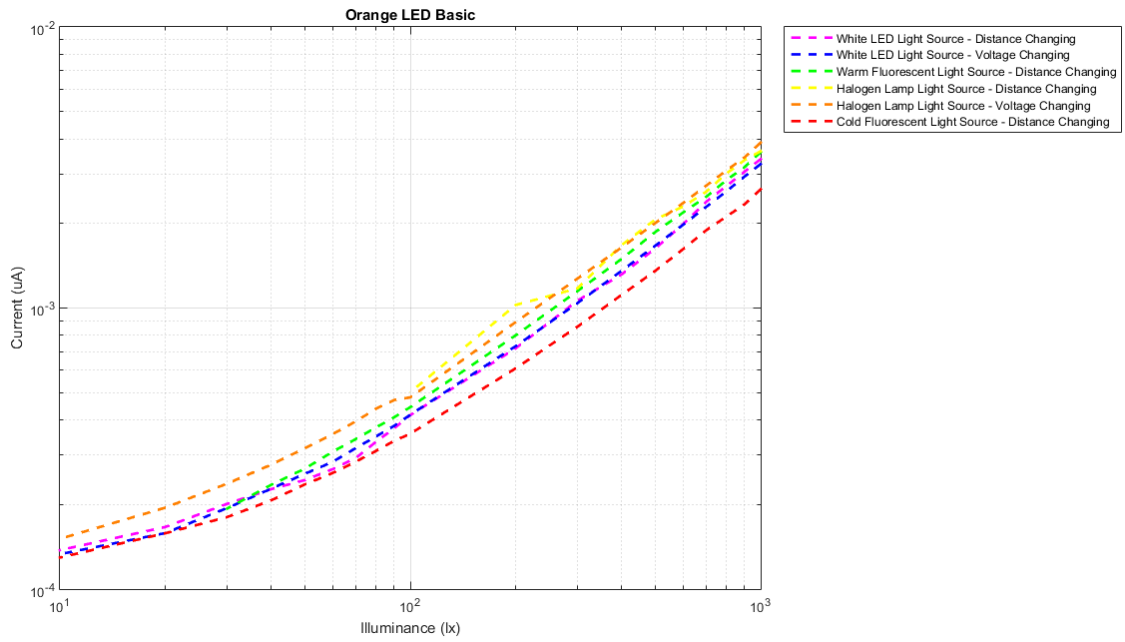
Figure 3 - 5. Illuminance versus Current. Reaction of Orange 'Basic' LED on different light sources.
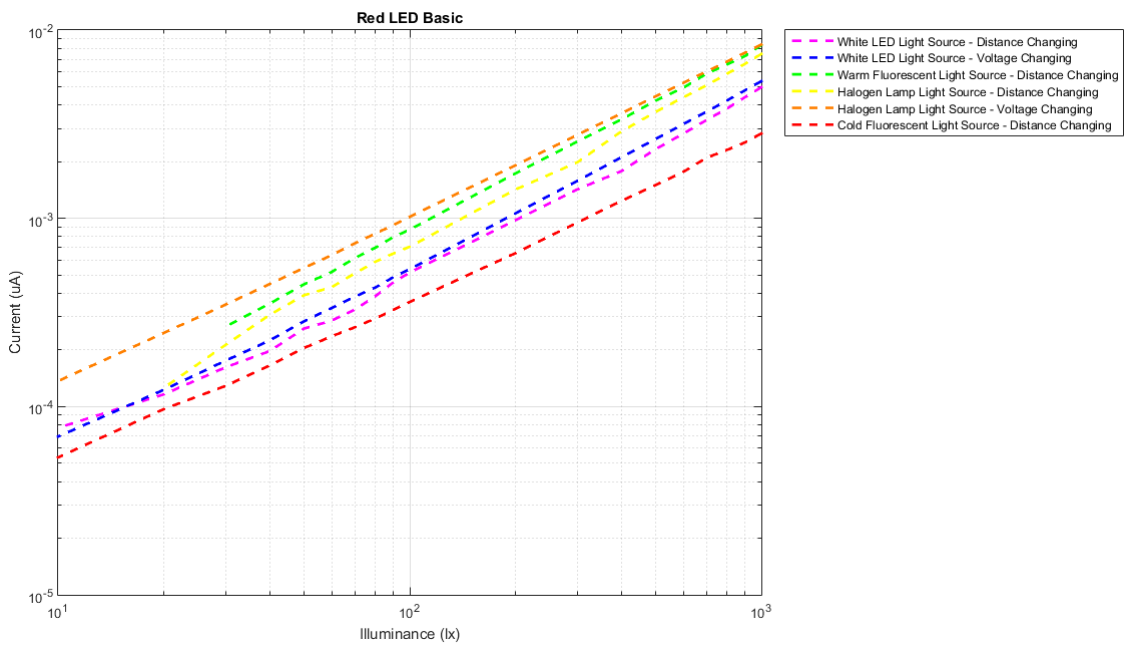
Figure 3 - 6. Illuminance versus Current. Reaction of Red 'Basic' LED on different light sources.
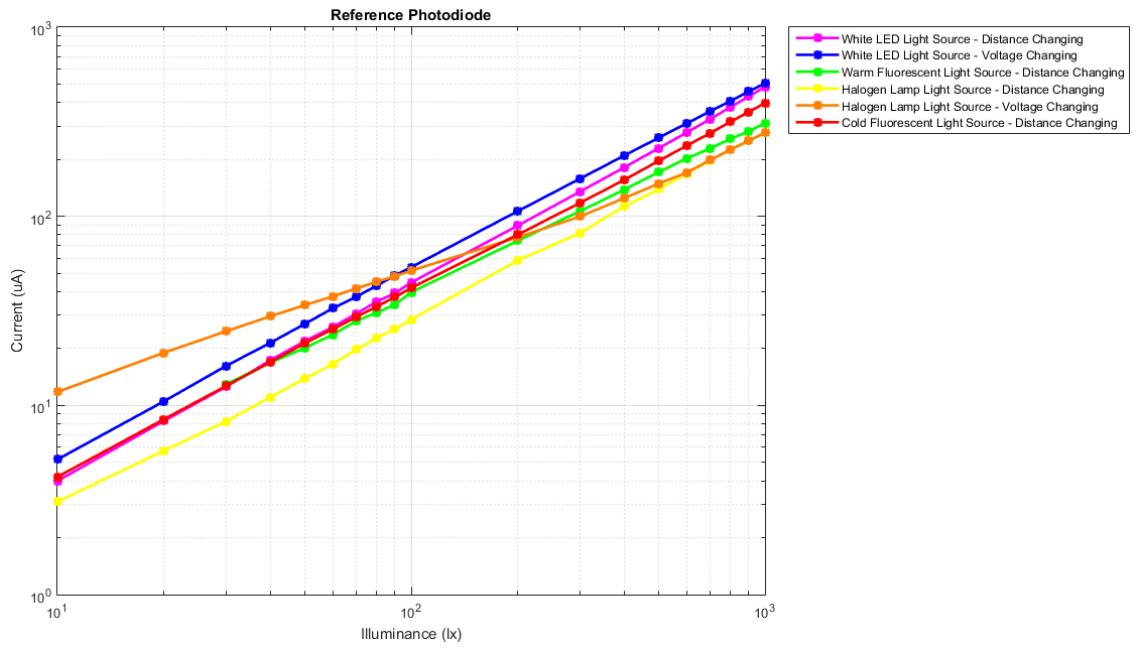
Figure 3 - 7. Illuminance versus Current. Reaction of Reference Photodiode on different light sources.
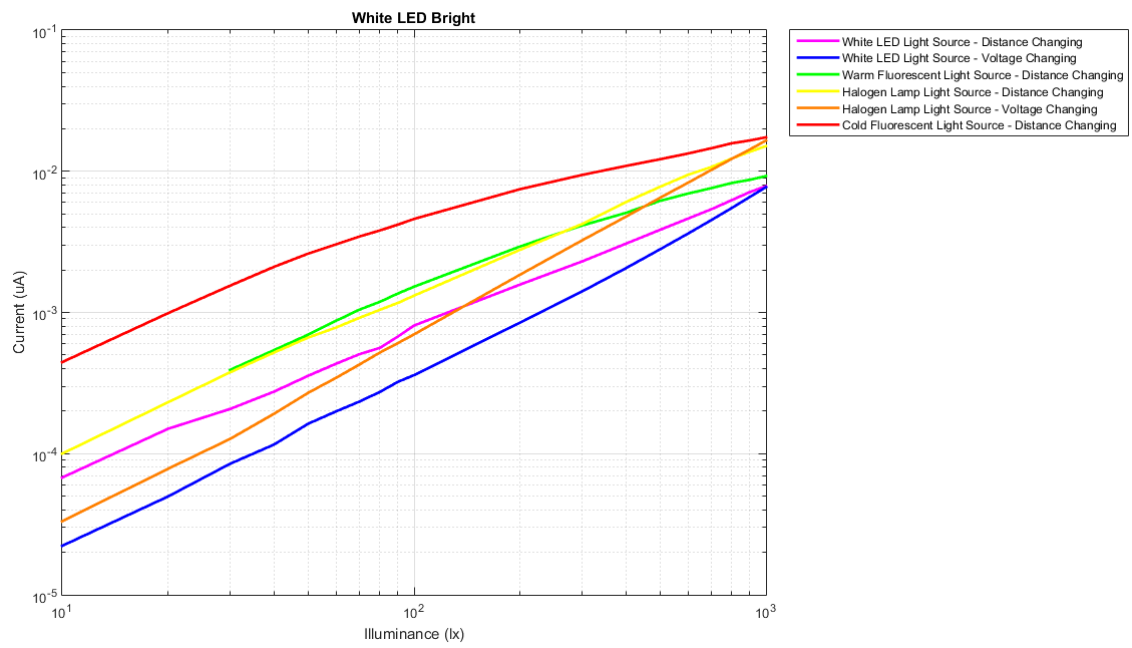
Figure 3 - 8. Illuminance versus Current. Reaction of White 'Bright' LED on different light sources.
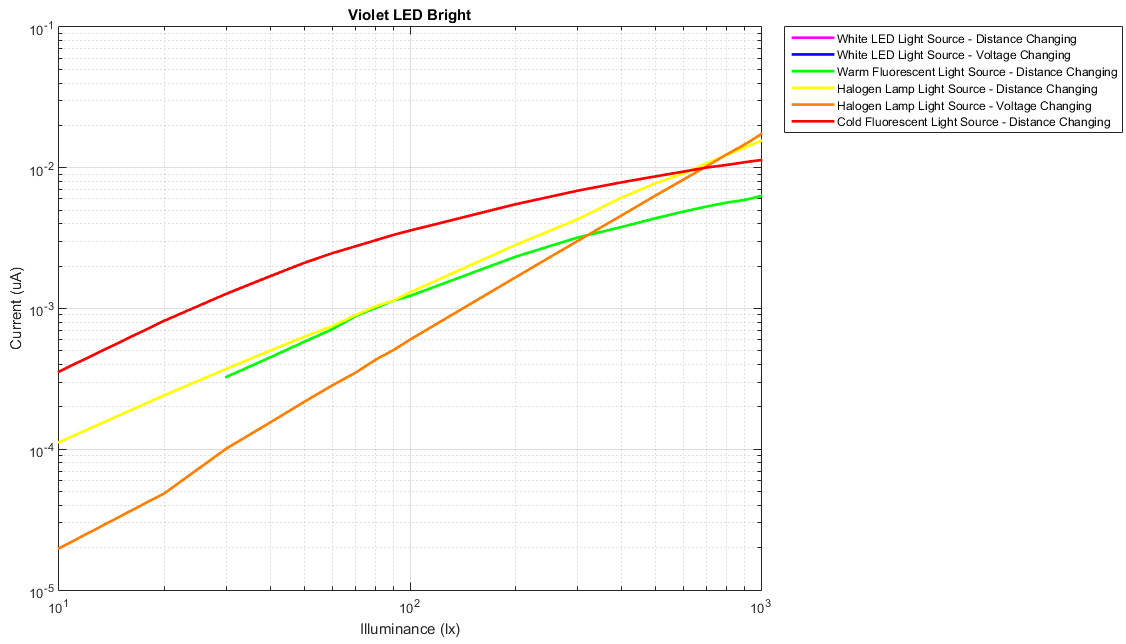
Figure 3 - 9. Illuminance versus Current. Reaction of Violet 'Bright' LED on different light sources.
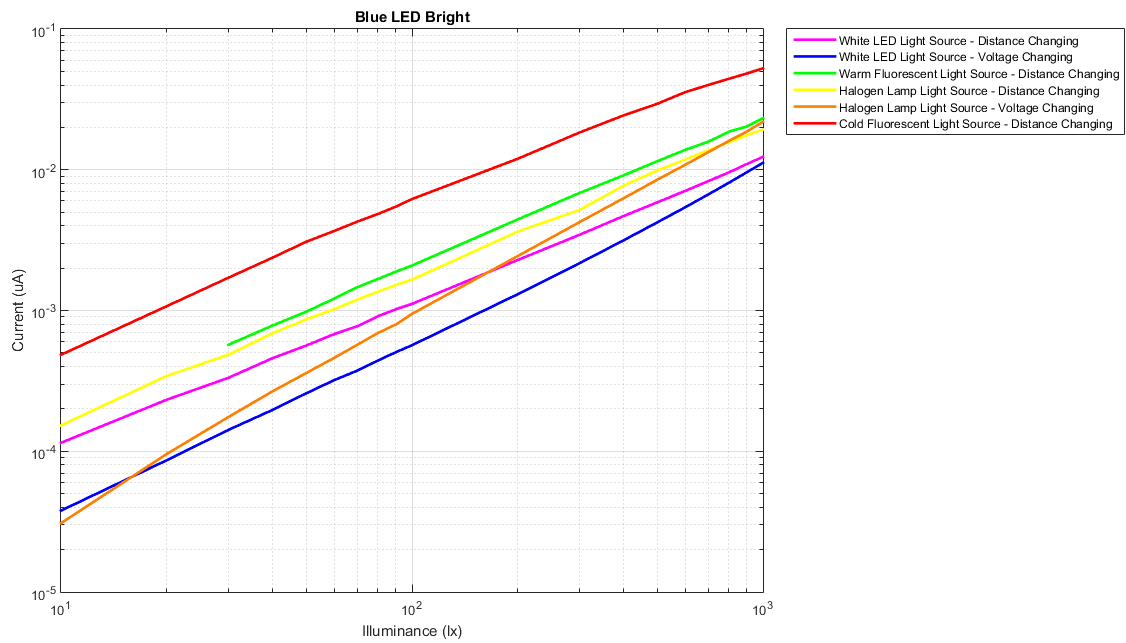
Figure 3 - 10. Illuminance versus Current. Reaction of Blue 'Bright' LED on different light sources.
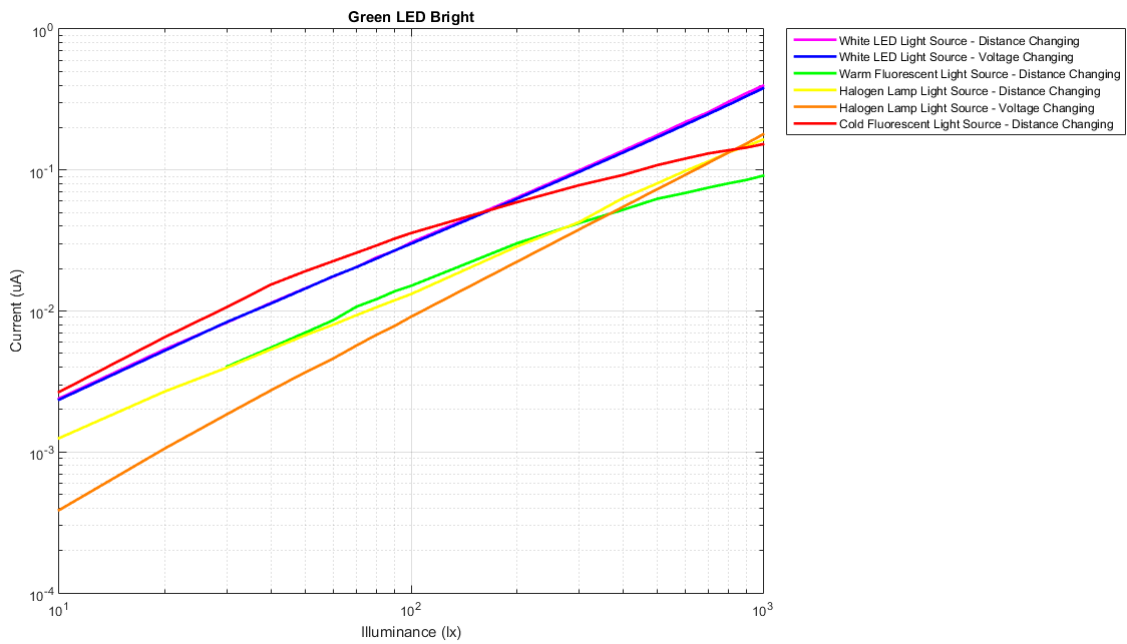
Figure 3 - 11. Illuminance versus Current. Reaction of Green 'Bright' LED on different light sources.
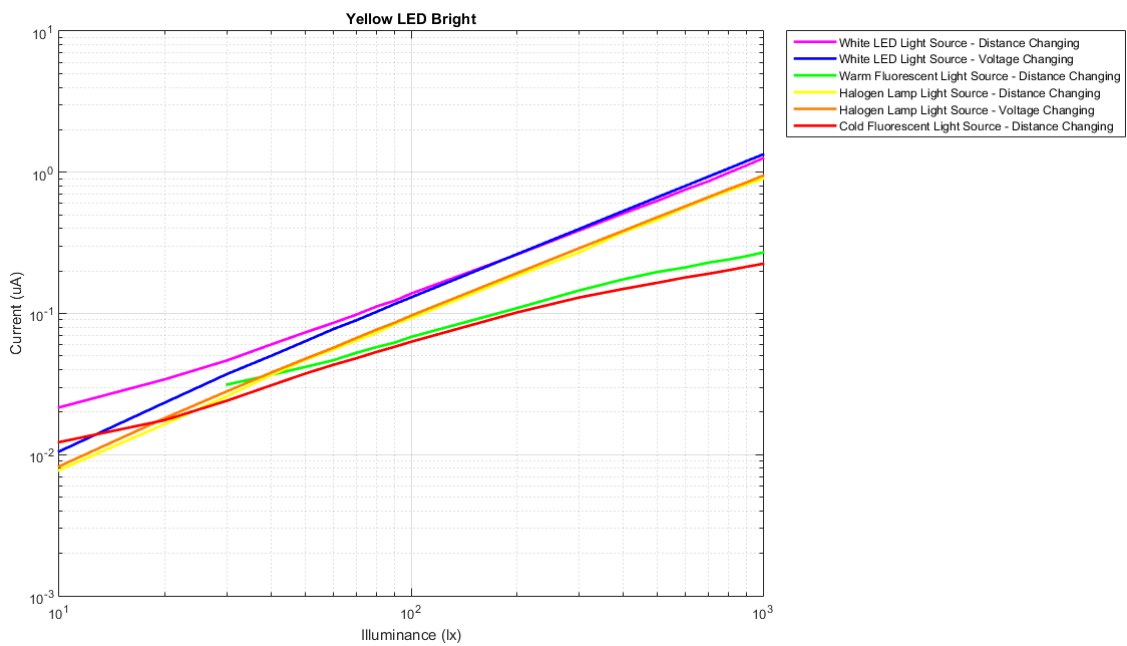
Figure 3 - 12. Illuminance versus Current. Reaction of Yellow 'Bright' LED on different light sources.
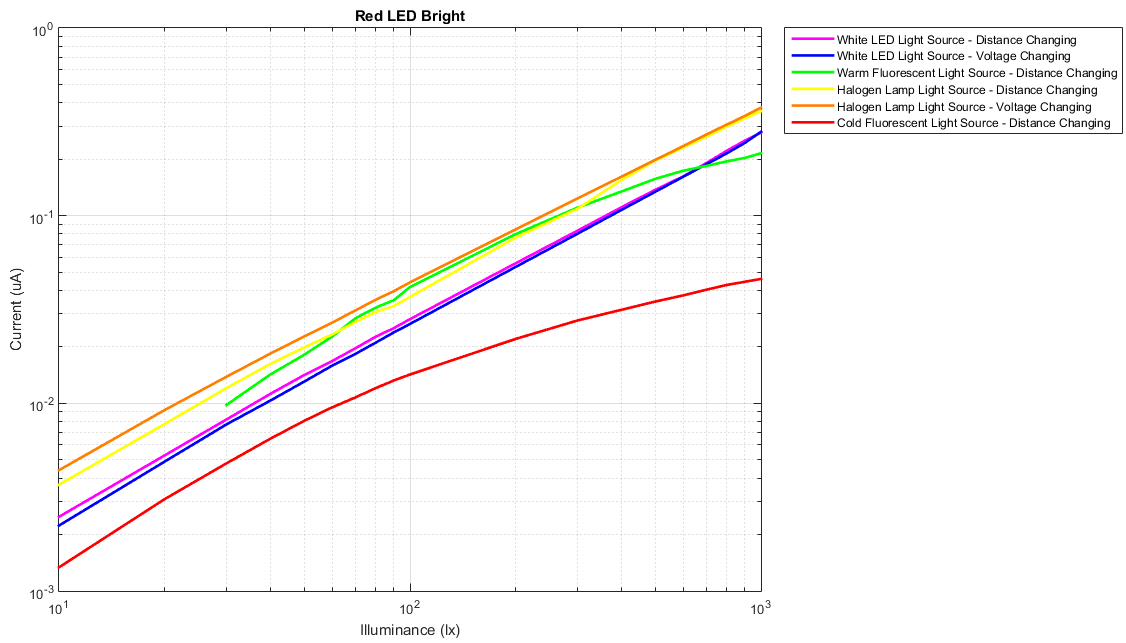
Figure 3 - 13. Illuminance versus Current. Reaction of Red 'Bright' LED on different light sources.
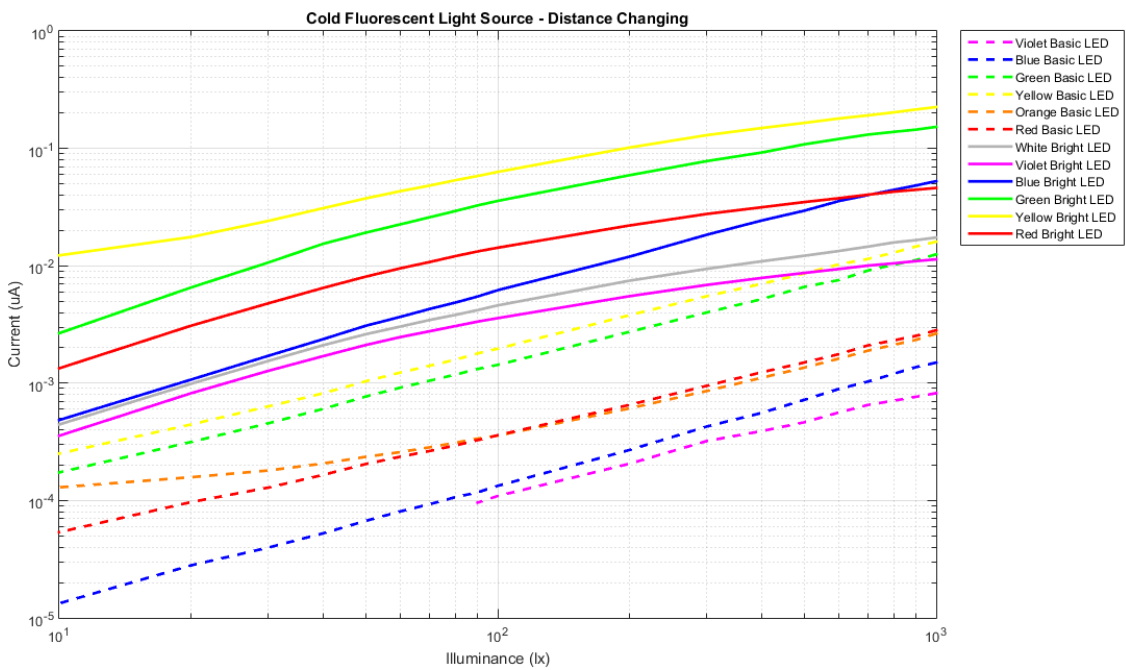
Figure 3 - 14. Illuminance versus Current. Reaction of different LEDs on Cold Fluorescent Light Source – Distance Changing.
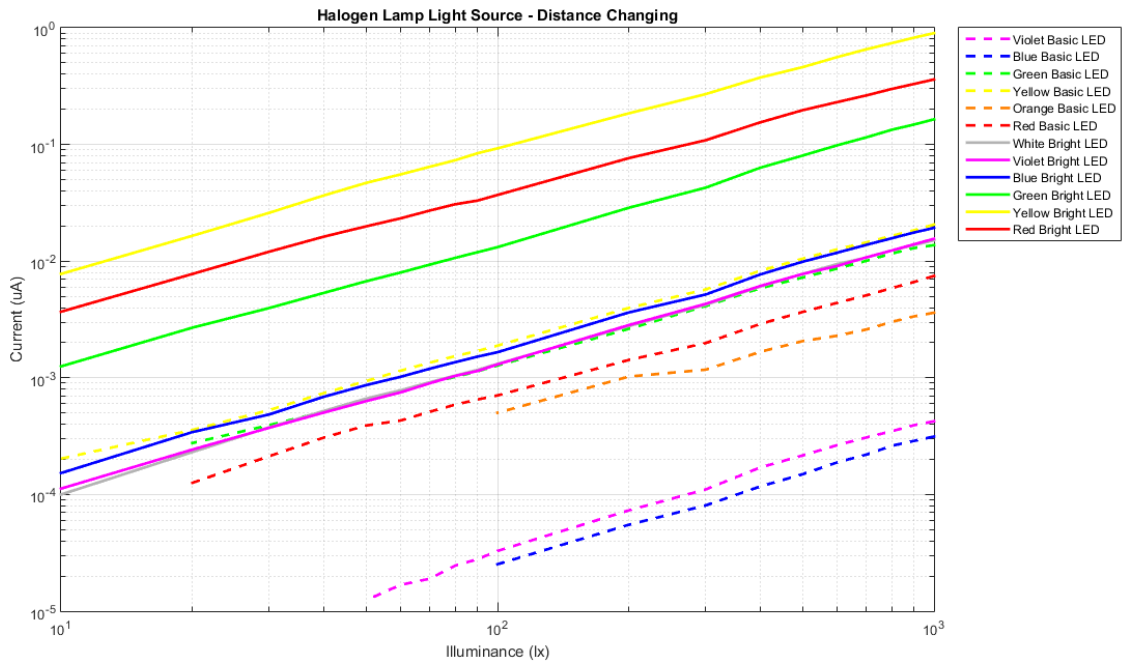
Figure 3 - 15. Illuminance versus Current. Reaction of different LEDs on Halogen Lamp Light Source – Distance Changing.
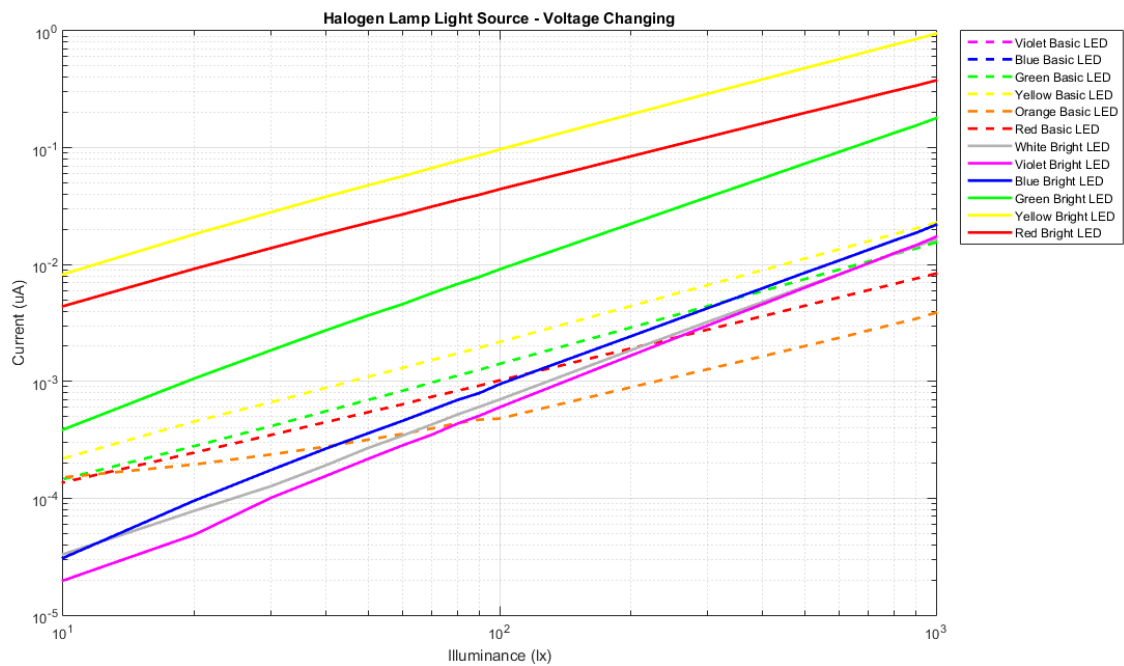
Figure 3 - 16. Illuminance versus Current. Reaction of different LEDs on Halogen Lamp Light Source – Voltage Changing.
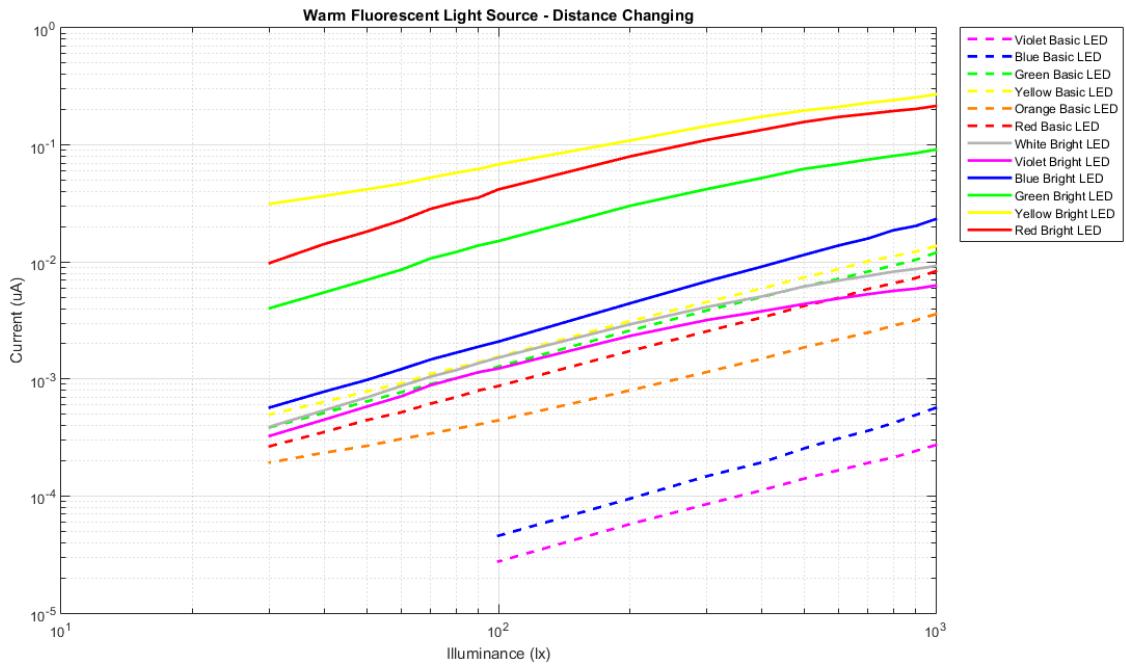
Figure 3 - 17. Illuminance versus Current. Reaction of different LEDs on Warm Fluorescent Light Source – Distance Changing.
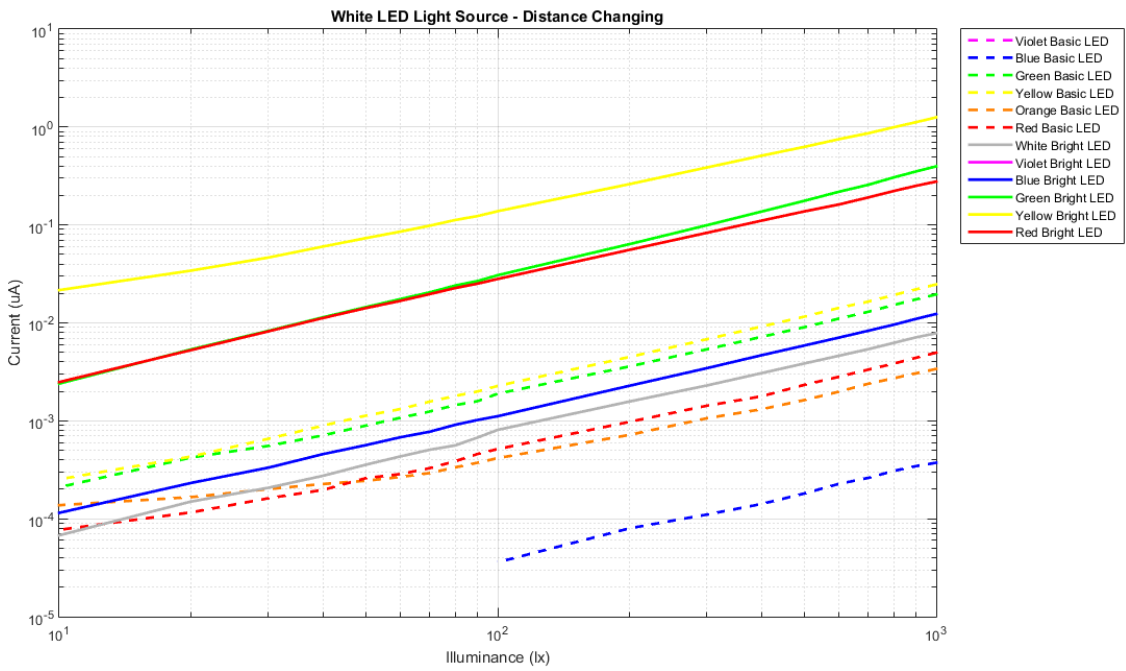
Figure 3 - 18. Illuminance versus Current. Reaction of different LEDs on White LED Light Source – Distance Changing.
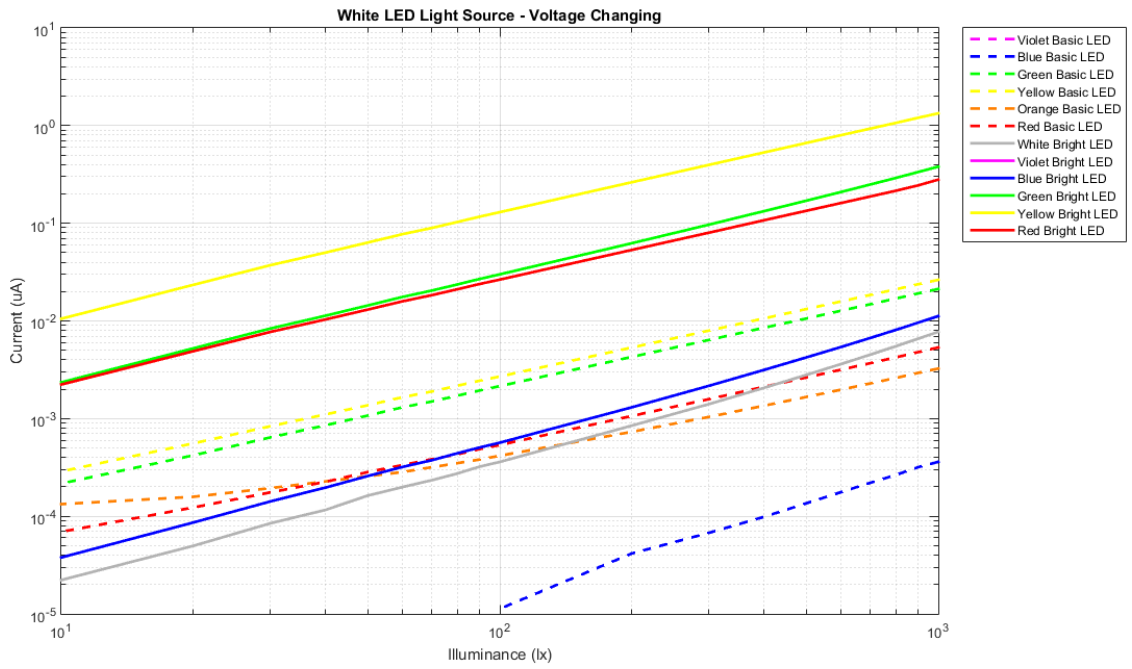
Figure 3 - 19. Illuminance versus Current. Reaction of different LEDs on White LED Light Source – Voltage Changing.
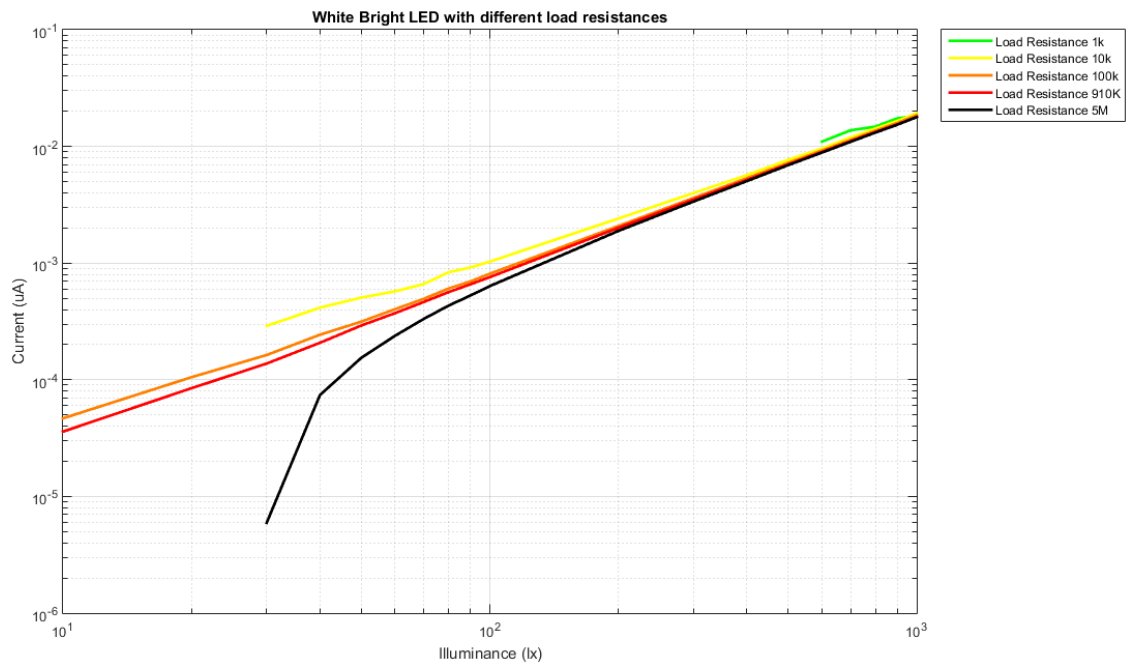
Figure 3 - 20. Illuminance versus Current of the White 'Bright' LED with different load resistances.
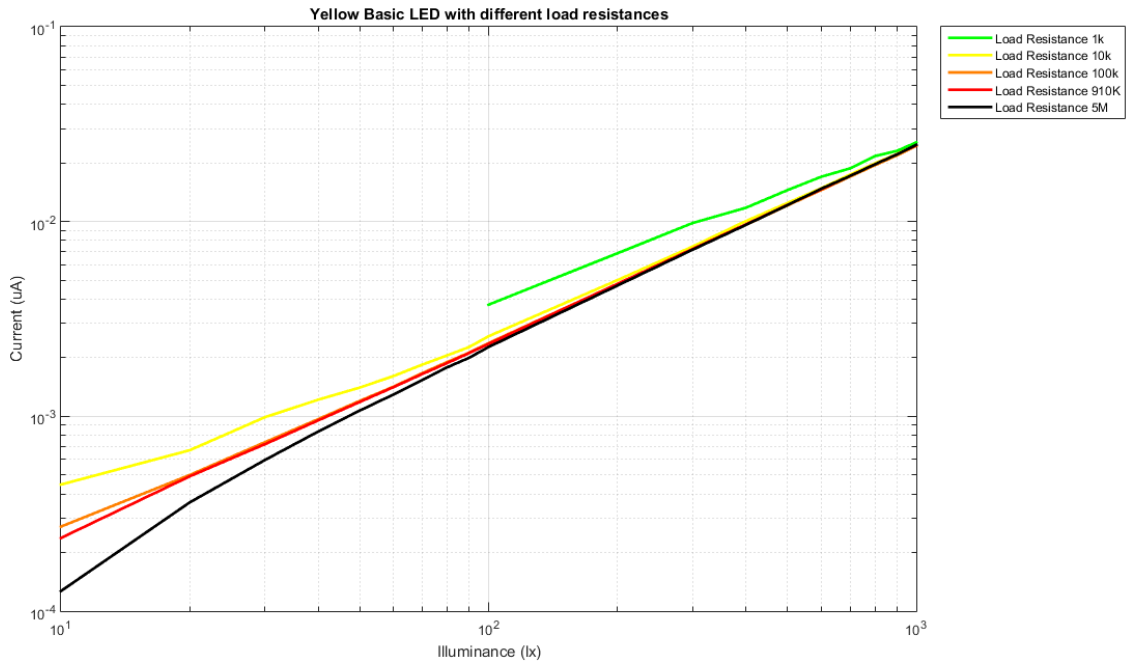
Figure 3 - 21. Illuminance versus Current of the Yellow 'Basic' LED with different load resistances.
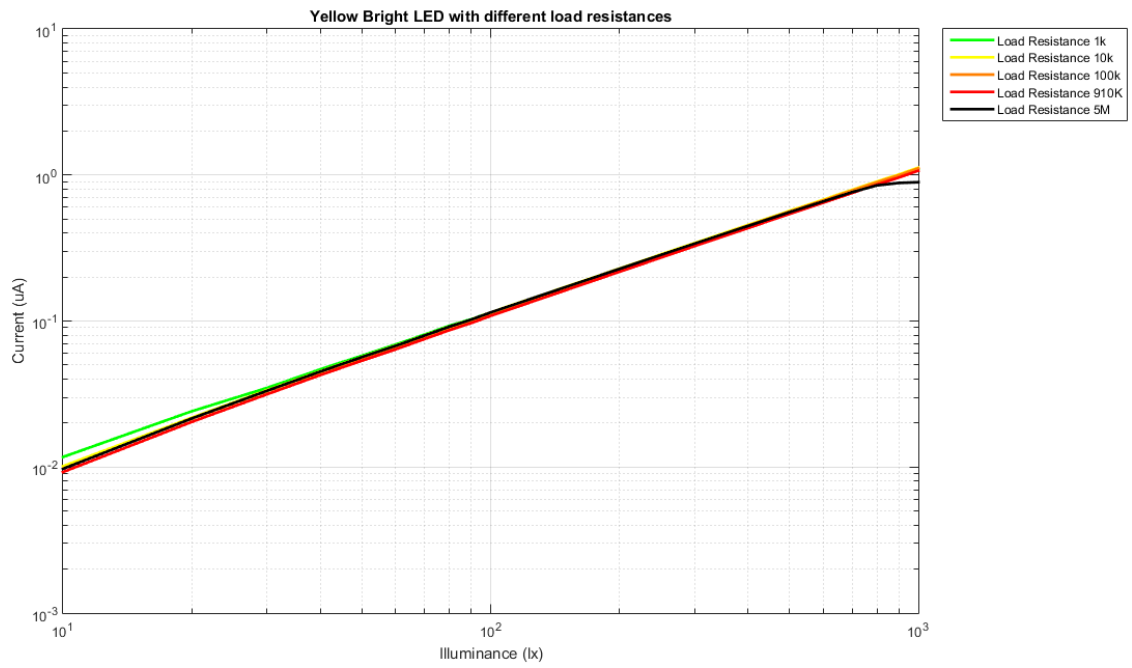
Figure 3 - 22. Illuminance versus Current of the Yellow 'Bright' LED with different load resistances.
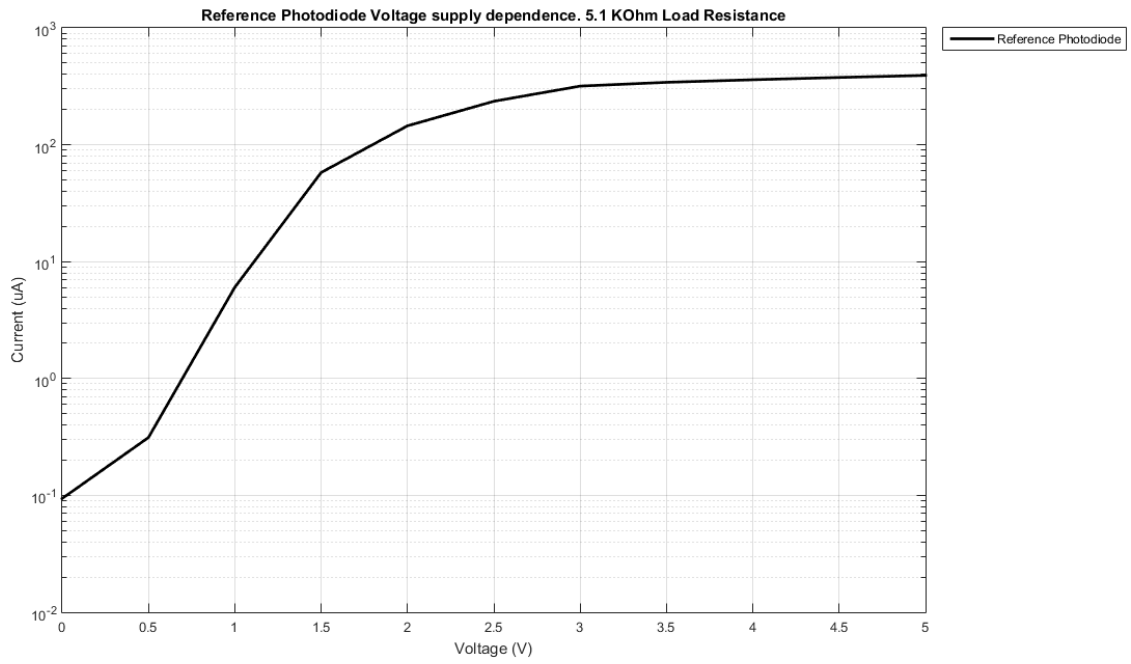
Figure 3 - 23. Current dependence from the power supply of the Reference Photodiode.
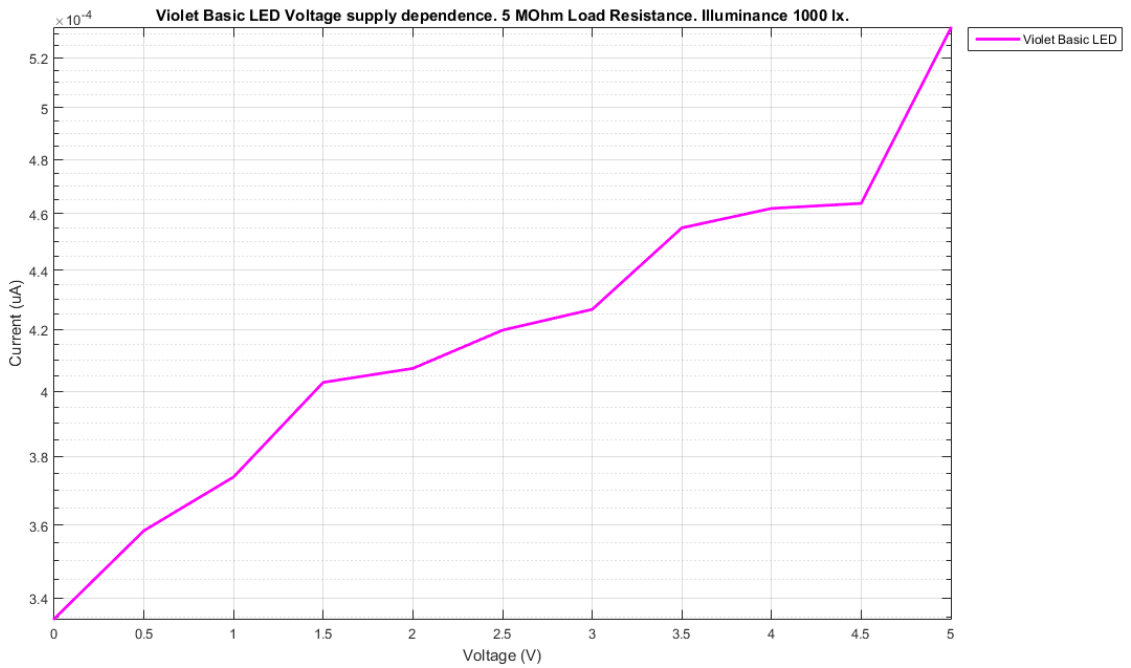
Figure 3 - 24. Current dependence from the power supply of the Violet 'Basic' LED.

107
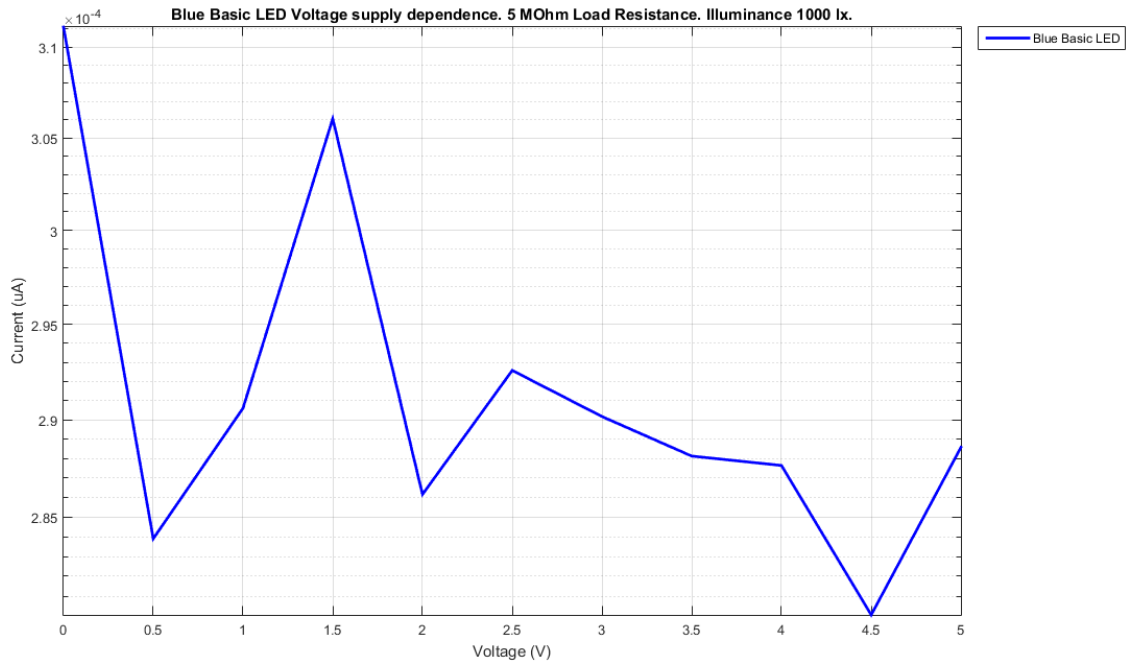
Figure 3 - 25. Current dependence from the power supply of the Blue 'Basic' LED.
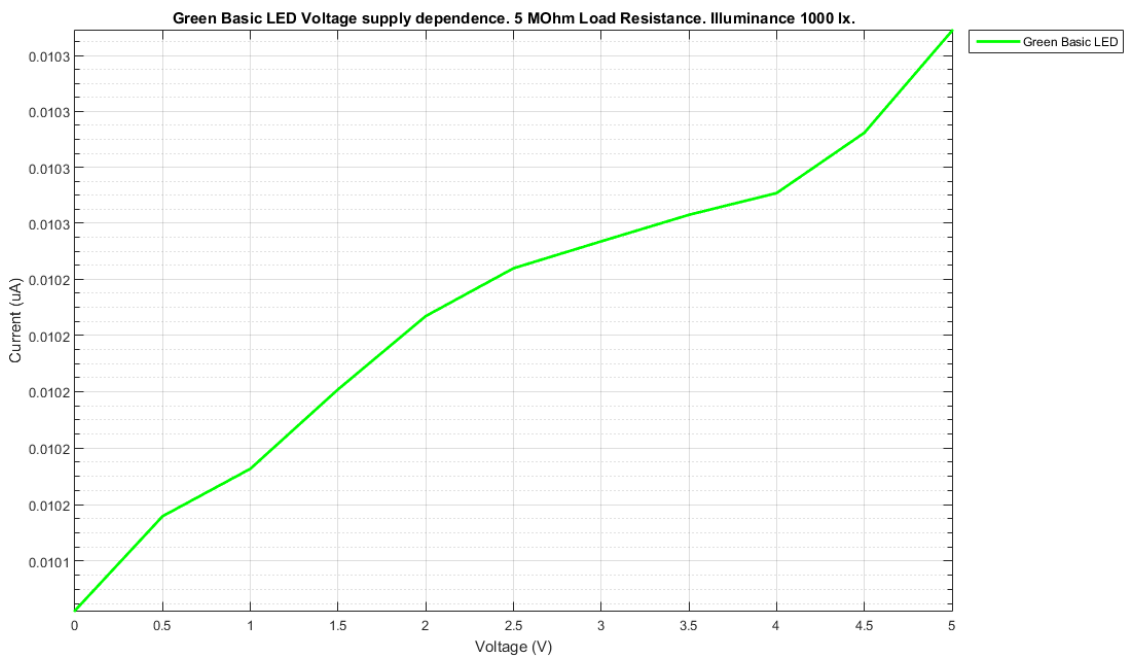
Figure 3 - 26. Current dependence from the power supply of the Green 'Basic' LED.

108
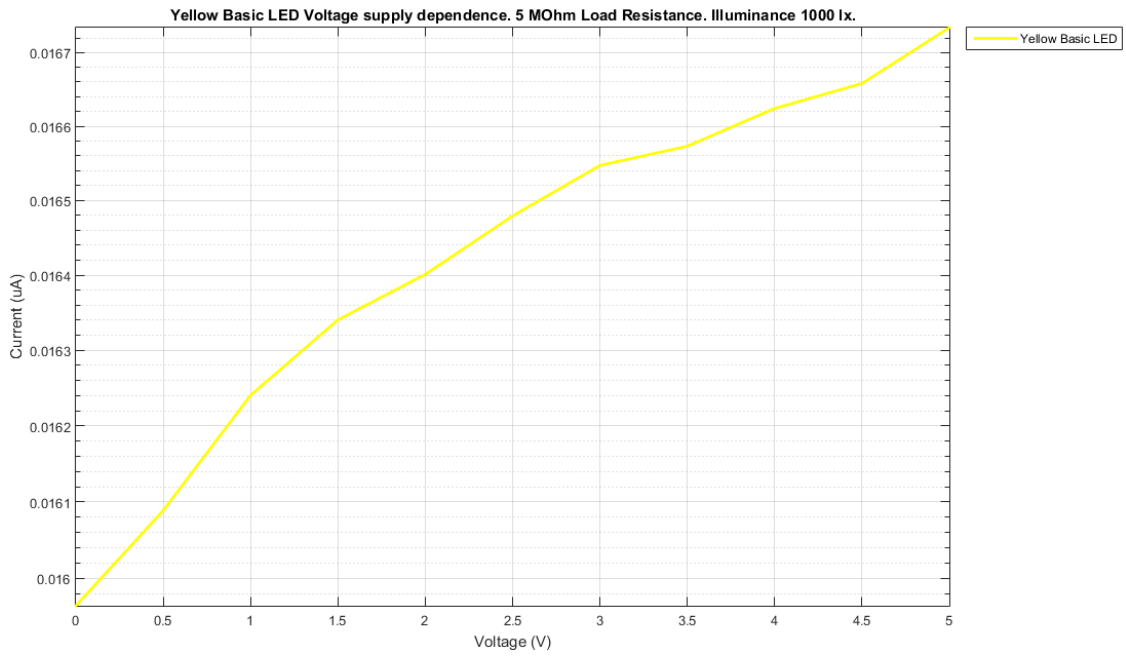
Figure 3 - 27. Current dependence from the power supply of the Yellow 'Basic' LED.
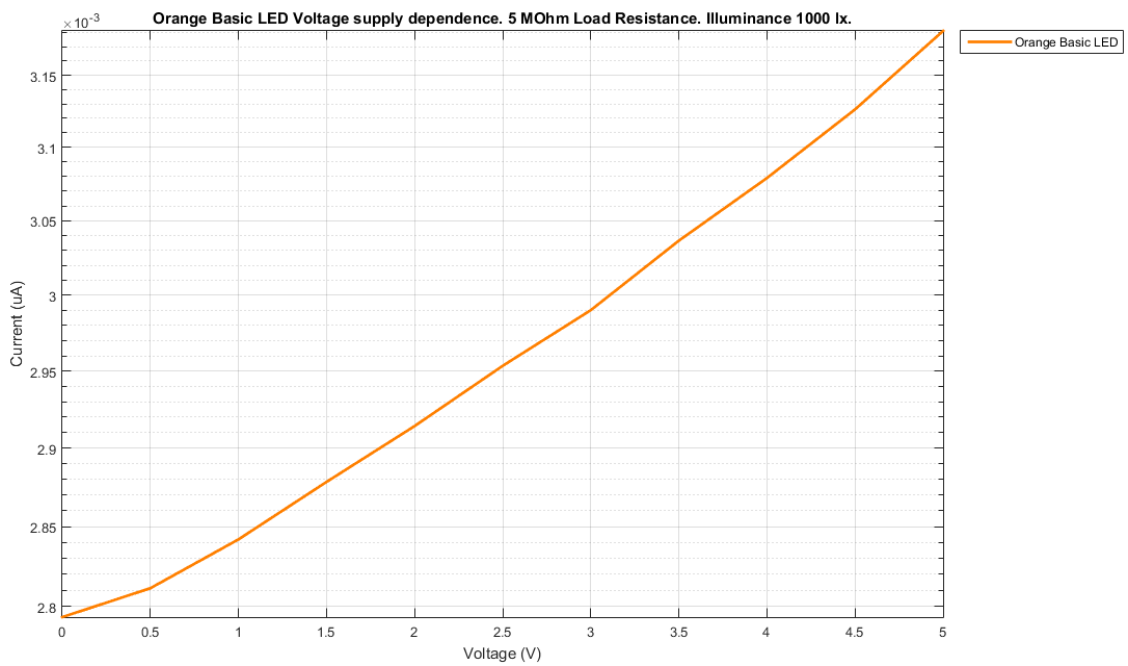
Figure 3 - 28. Current dependence from the power supply of the Orange 'Basic' LED.

109
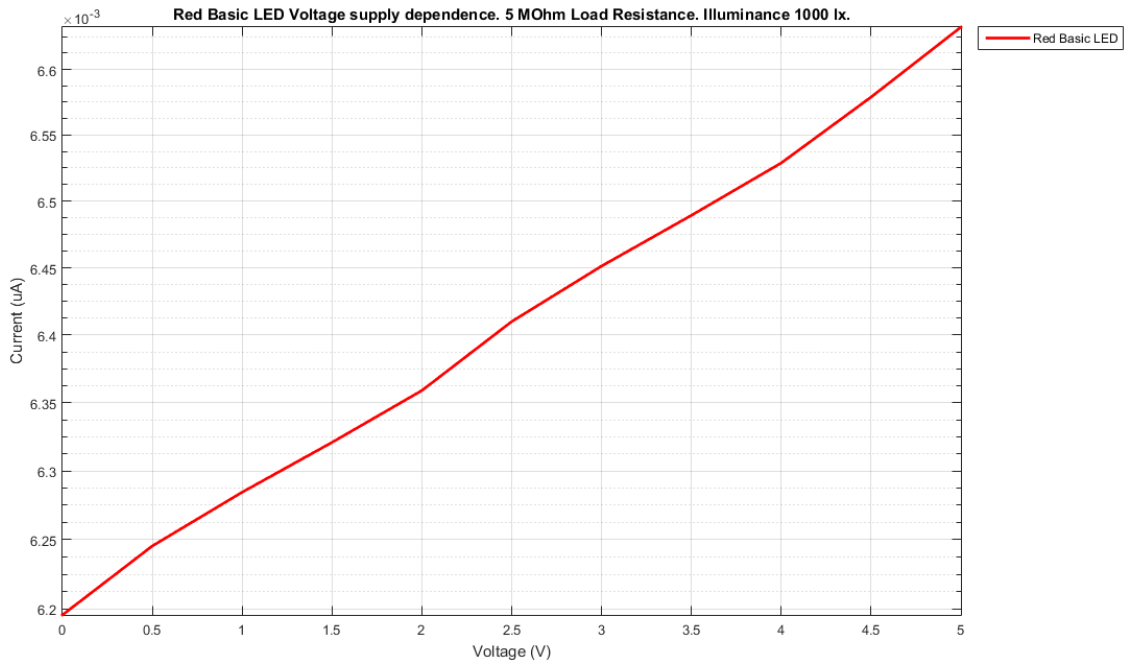
Figure 3 - 29. Current dependence from the power supply of the Red 'Basic' LED.
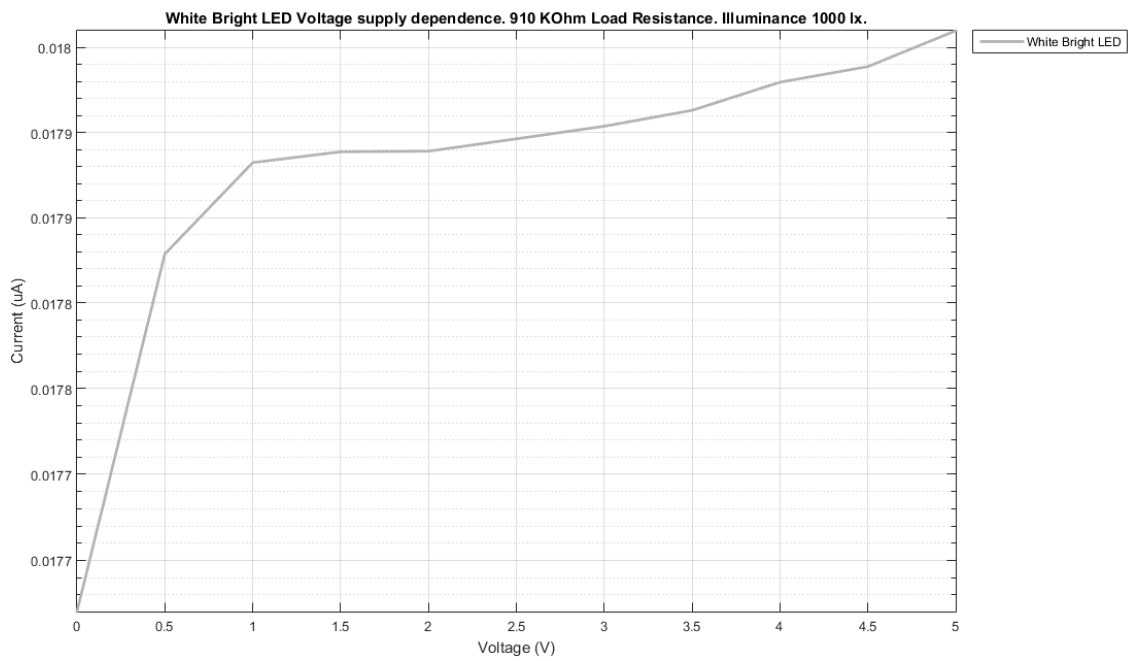
Figure 3 - 30. Current dependence from the power supply of the White 'Bright' LED.

110
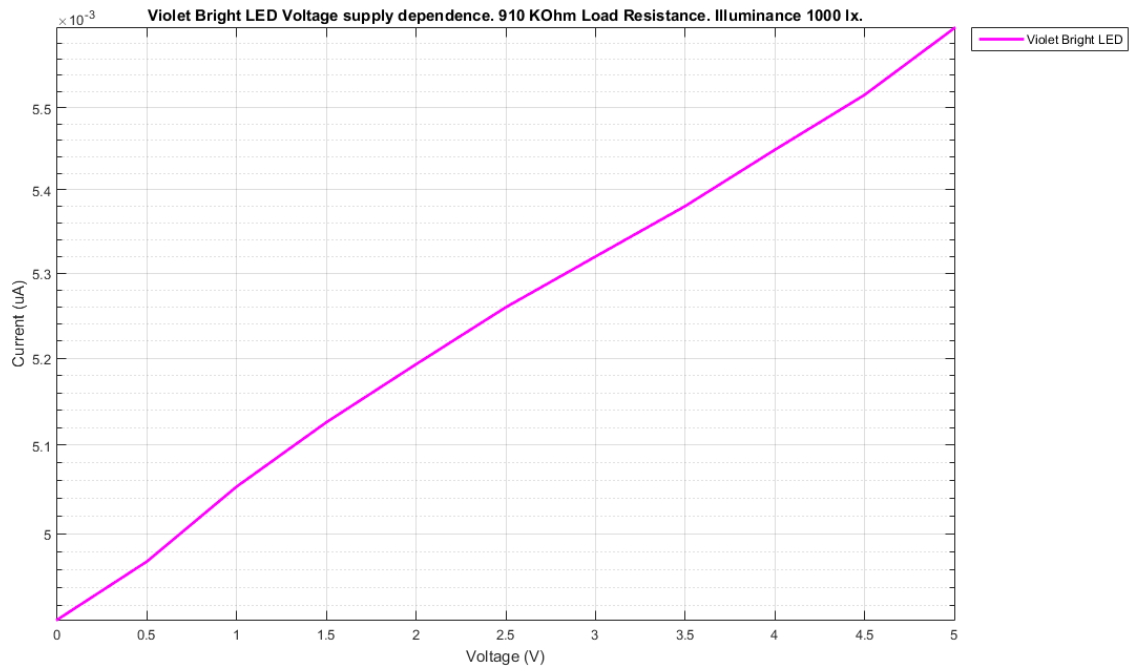
Figure 3 - 31. Current dependence from the power supply of the Violet 'Bright' LED.
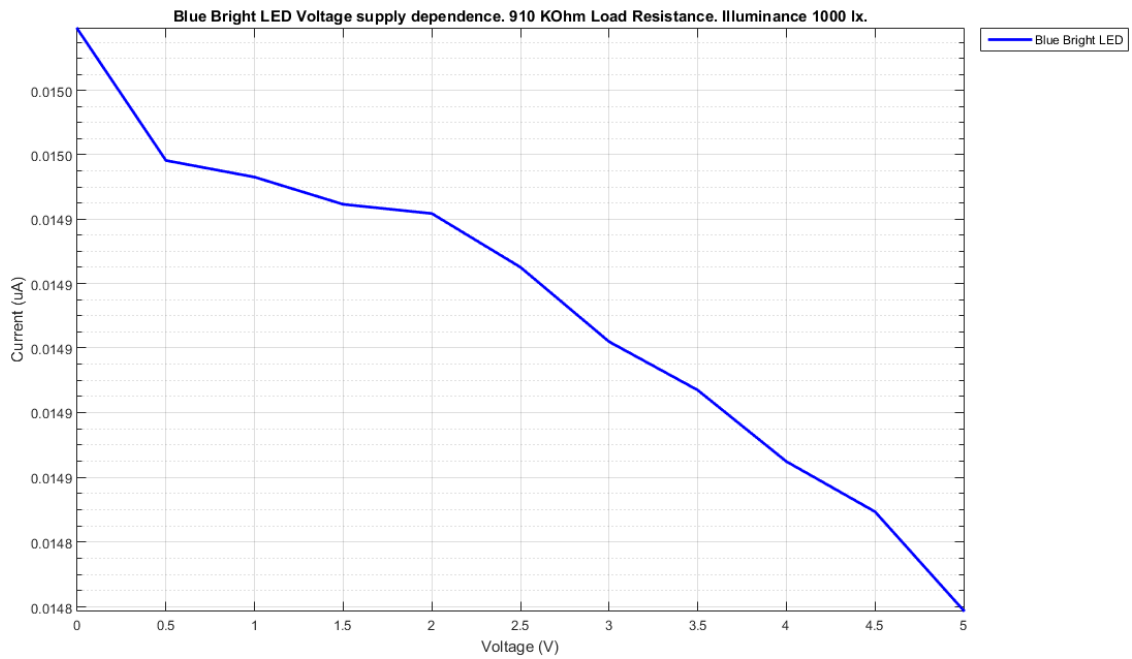
Figure 3 - 32. Current dependence from the power supply of the Blue 'Bright' LED.
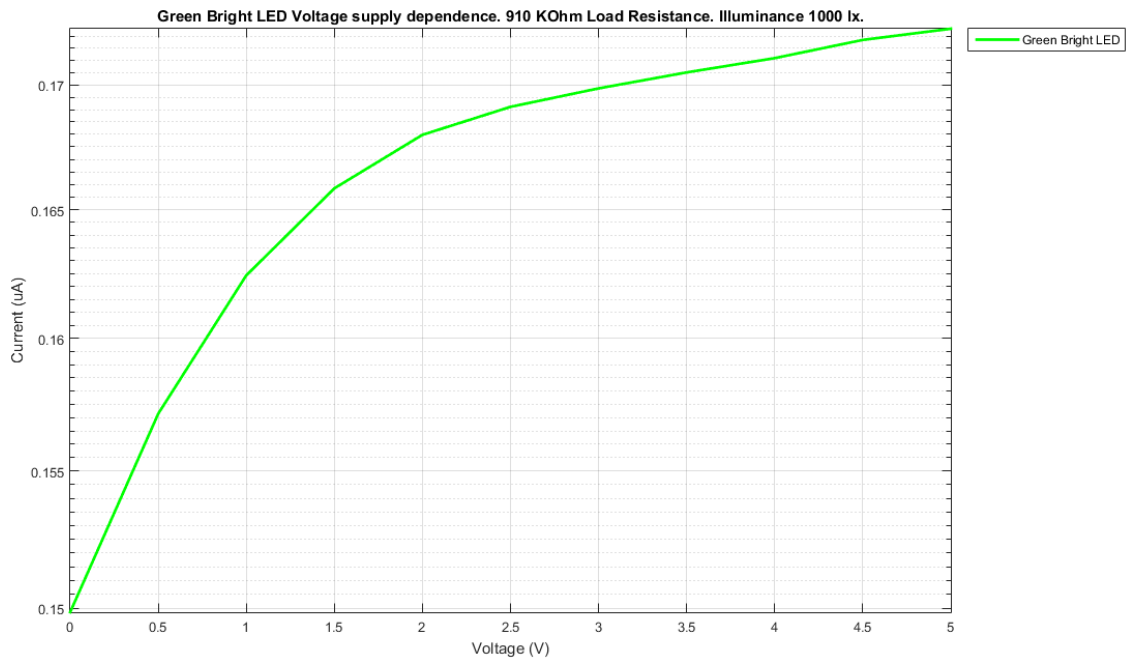
Figure 3 - 33. Current dependence from the power supply of the Green 'Bright' LED.
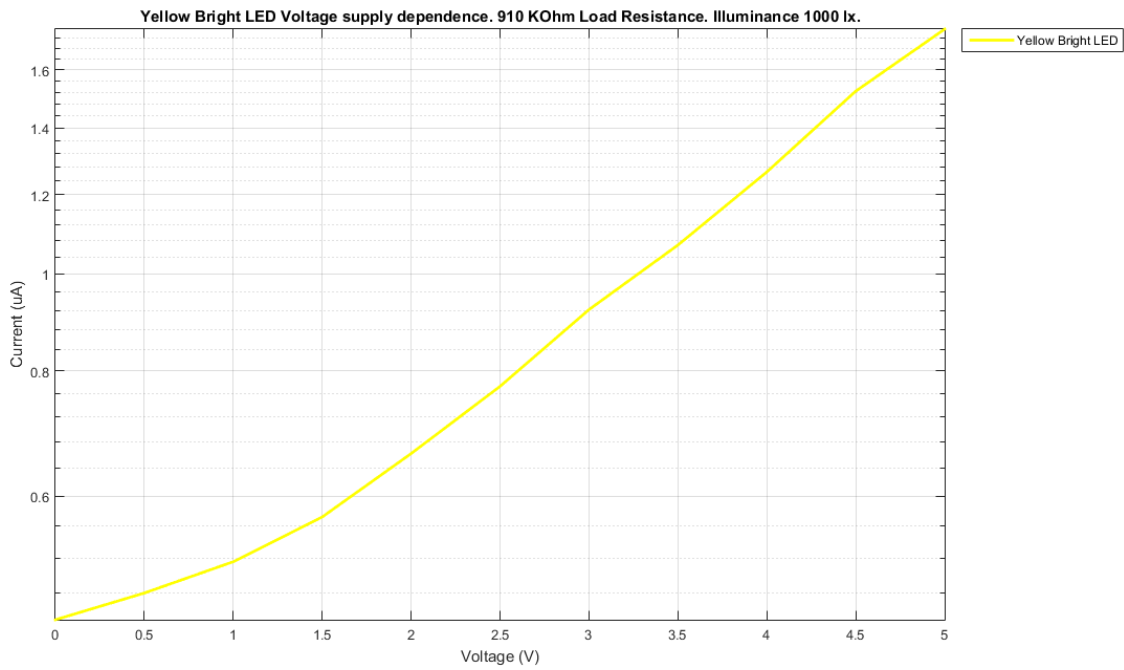
Figure 3 - 34. Current dependence from the power supply of the Yellow 'Bright' LED.

112
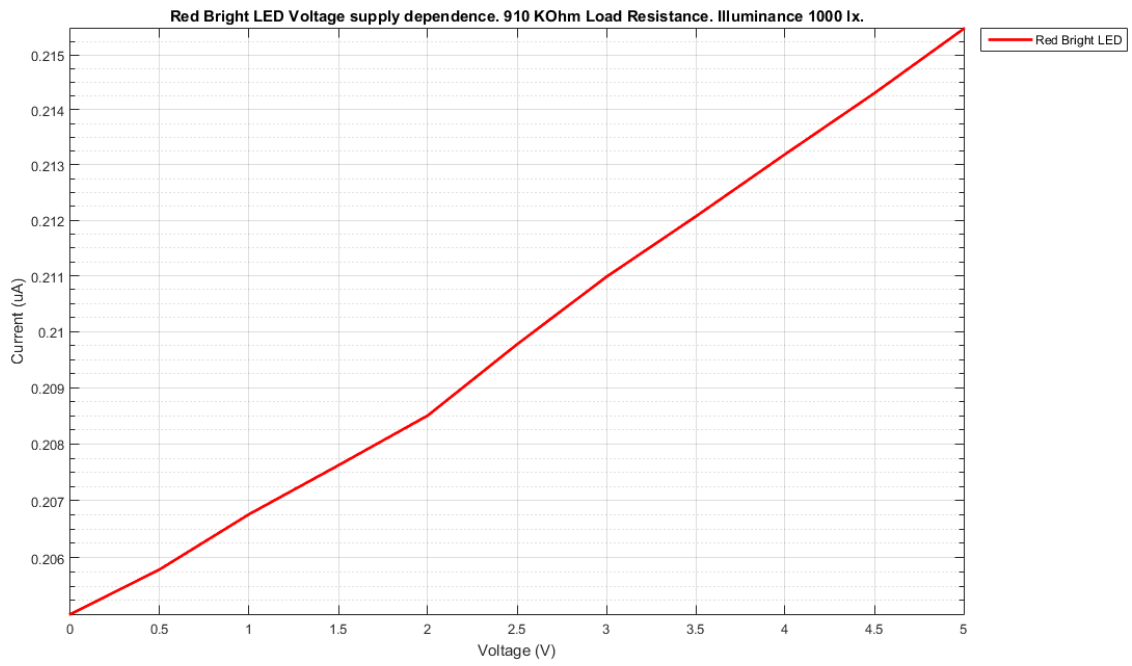
Figure 3 - 35. Current dependence from the power supply of the Red 'Bright' LED.

Appendix 4 – Results of the Wavelength response measurements
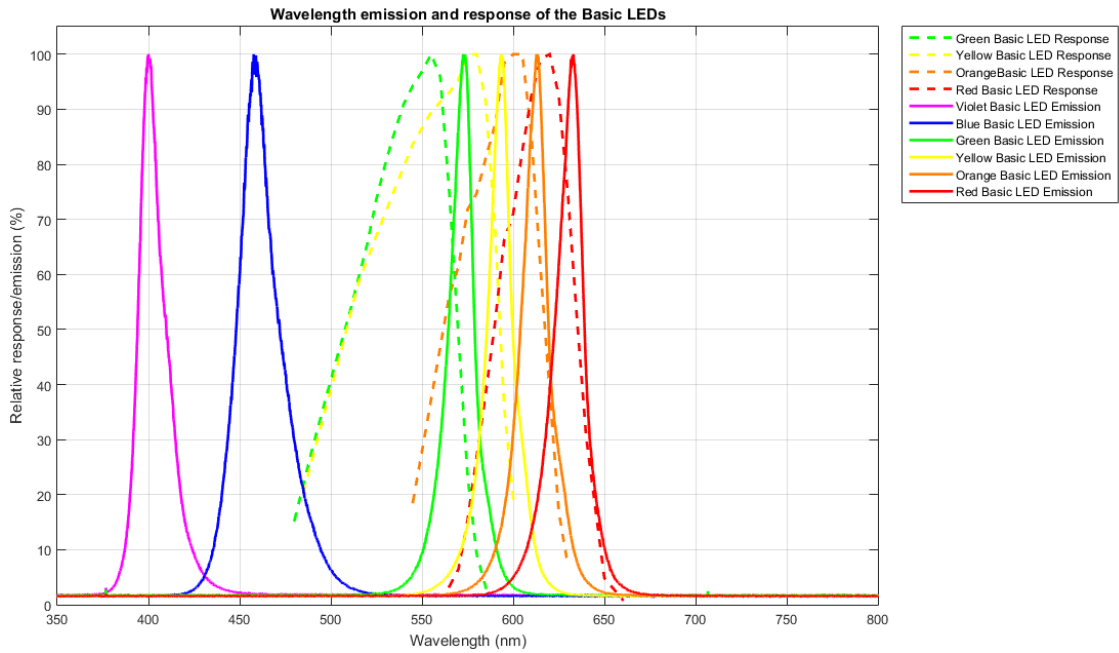
Figure 4 - 1. Wavelength emission and response of the LEDs from 'Basic' group.
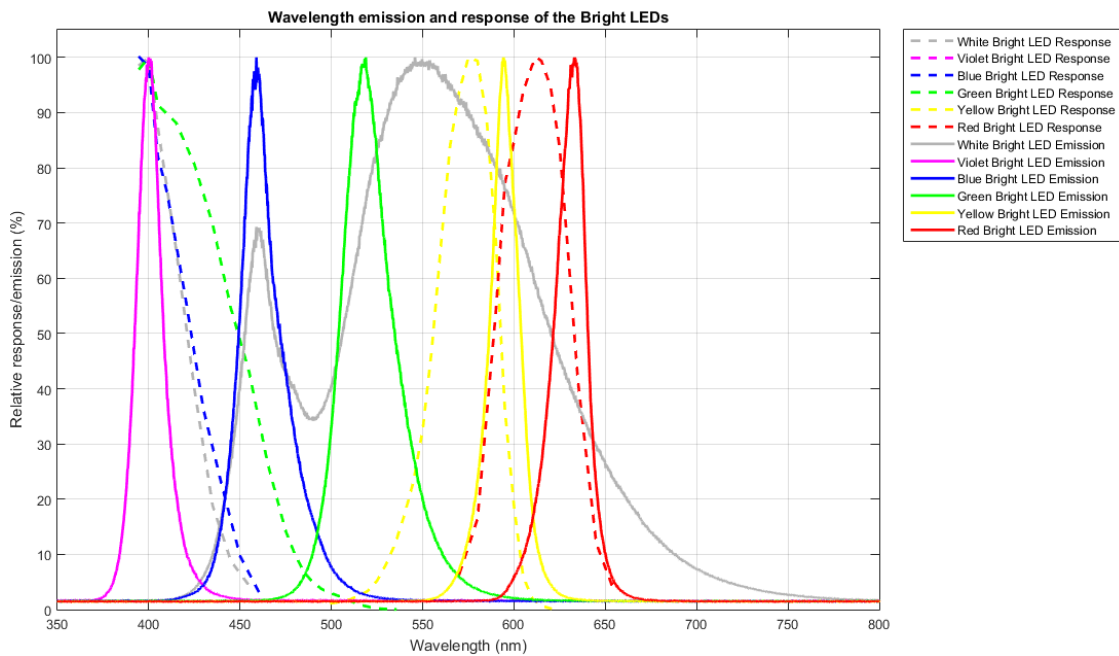
Figure 4 - 2. Wavelength emission and response of the LEDs from 'Bright' group.
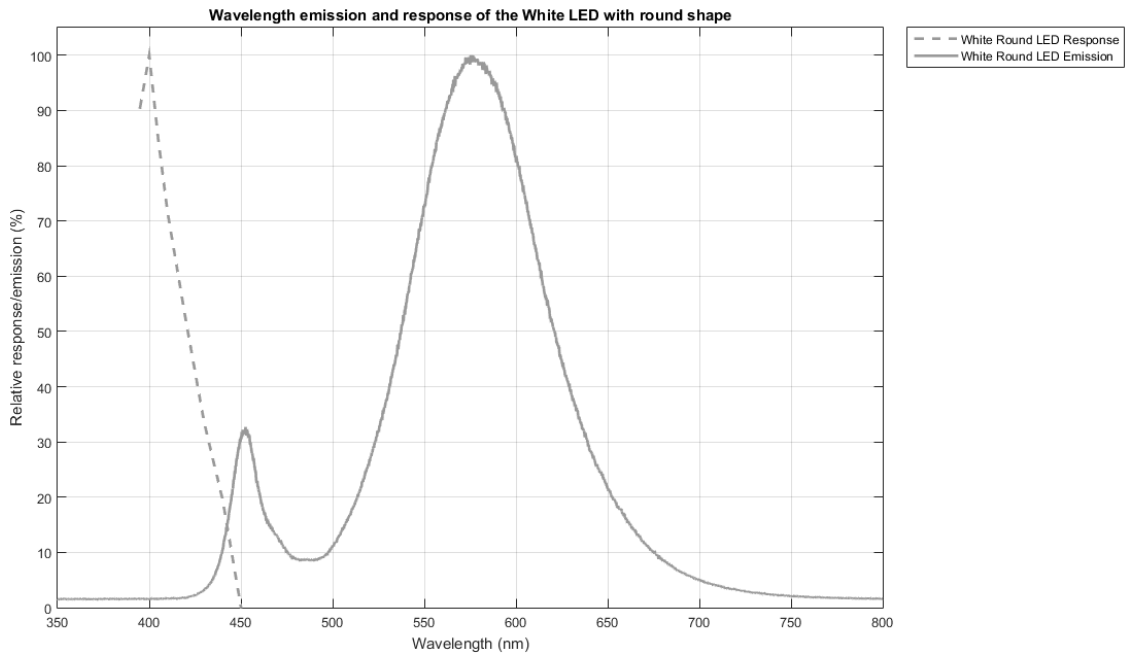
Figure 4 - 3. Wavelength emission and response of the round shape White LED.
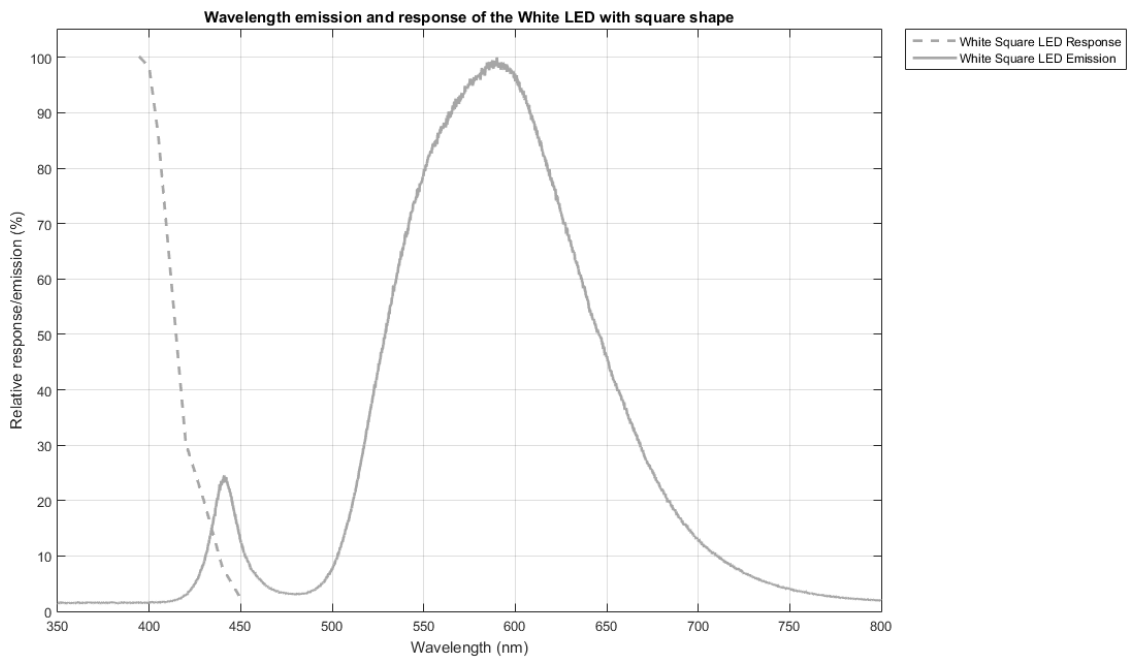
Figure 4 - 4. Wavelength emission and response of the square shape White LED.

115
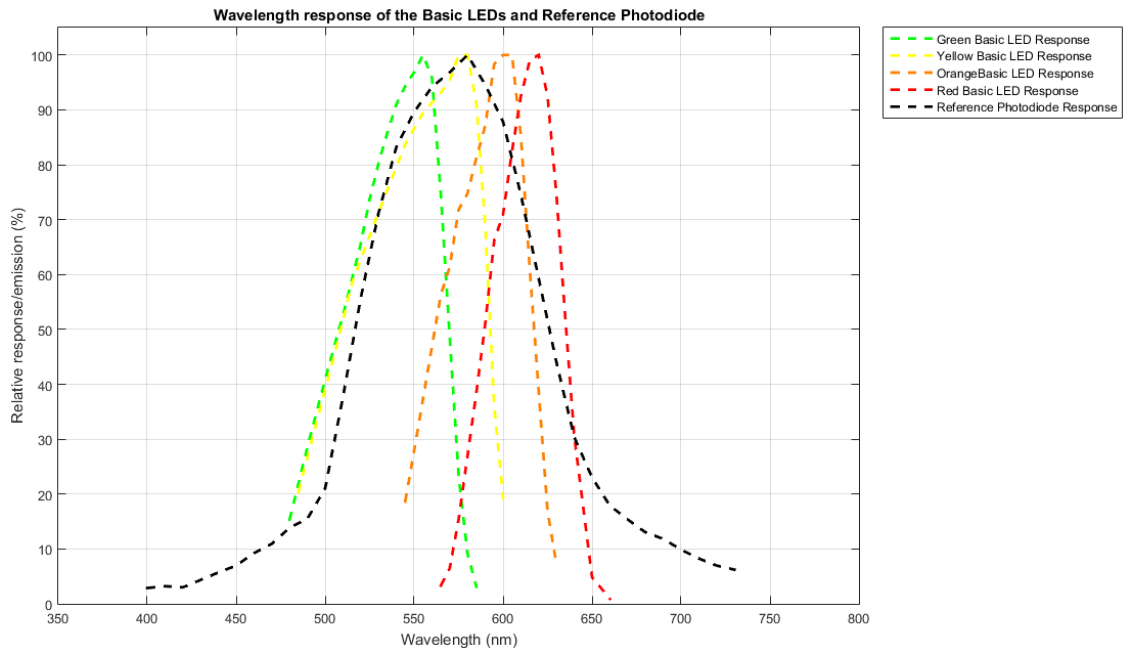
Figure 4 - 5. Wavelength response of the LEDs from 'Basic' group and Everlight Photodiode.
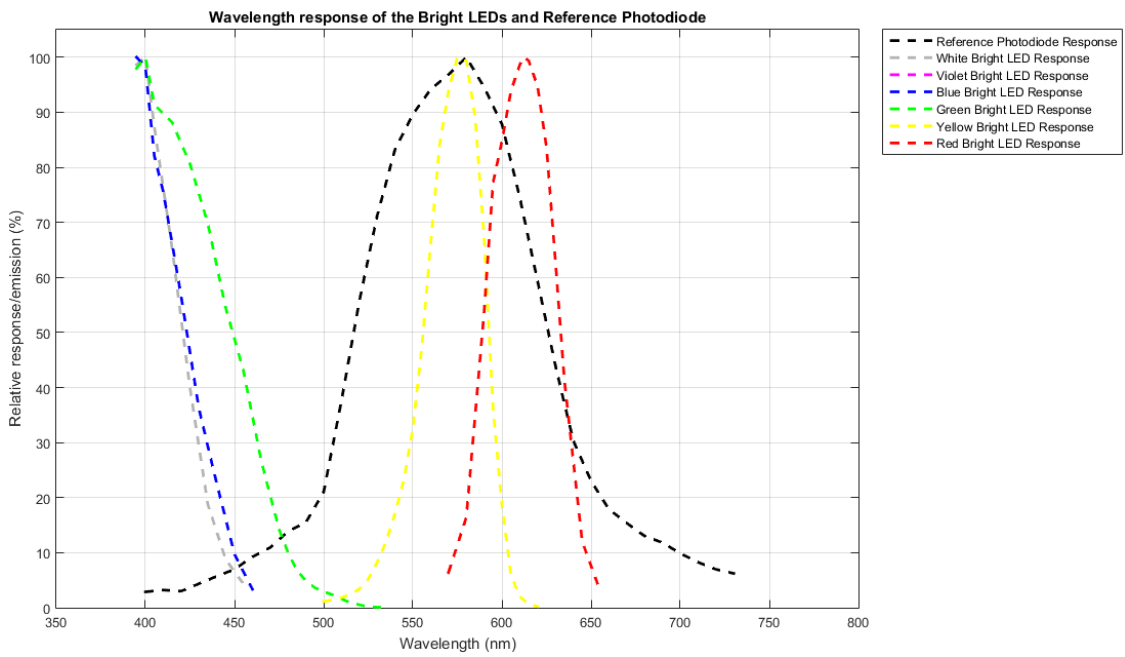
Figure 4 - 6. Wavelength response of the LEDs from 'Bright' group and Everlight Photodiode.

Appendix 5 – Results of the Angular response measurements
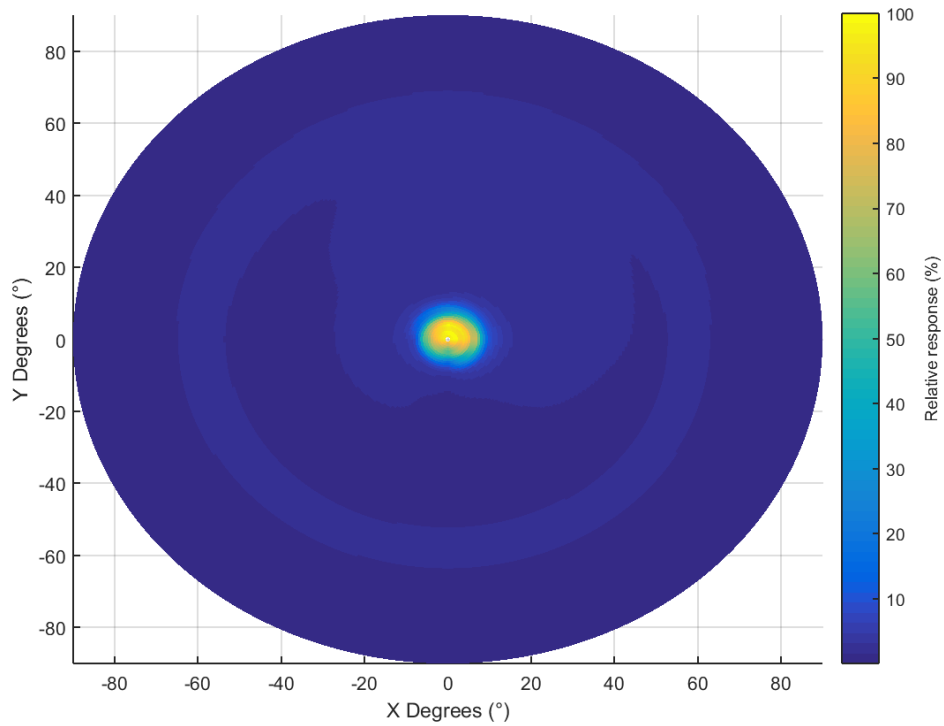
Figure 5 - 1. Top view of the 3D model of the angular response of the Red "Bright" LED.
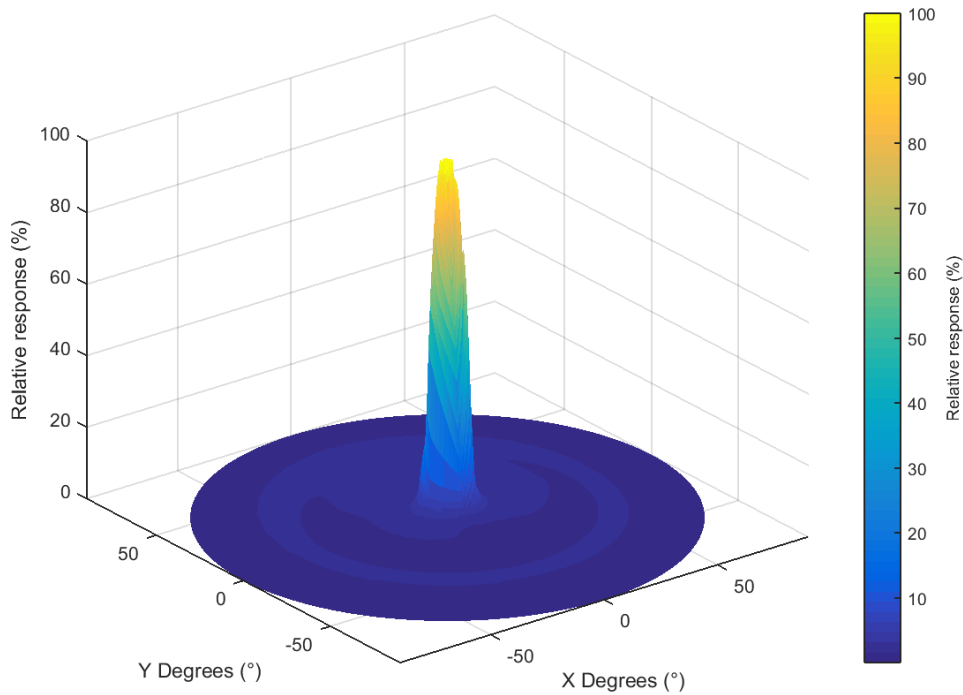
Figure 5 - 2. 3D model of the angular response of the Red "Bright" LED.
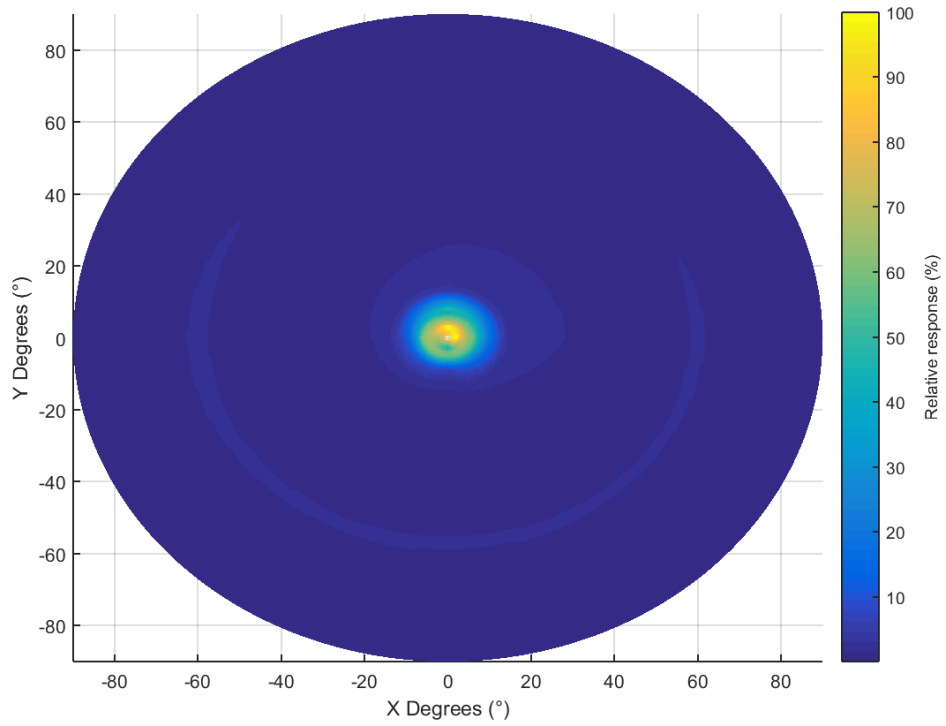
Figure 5 - 3. Top view of the 3D model of the angular response of the Yellow "Bright" LED.
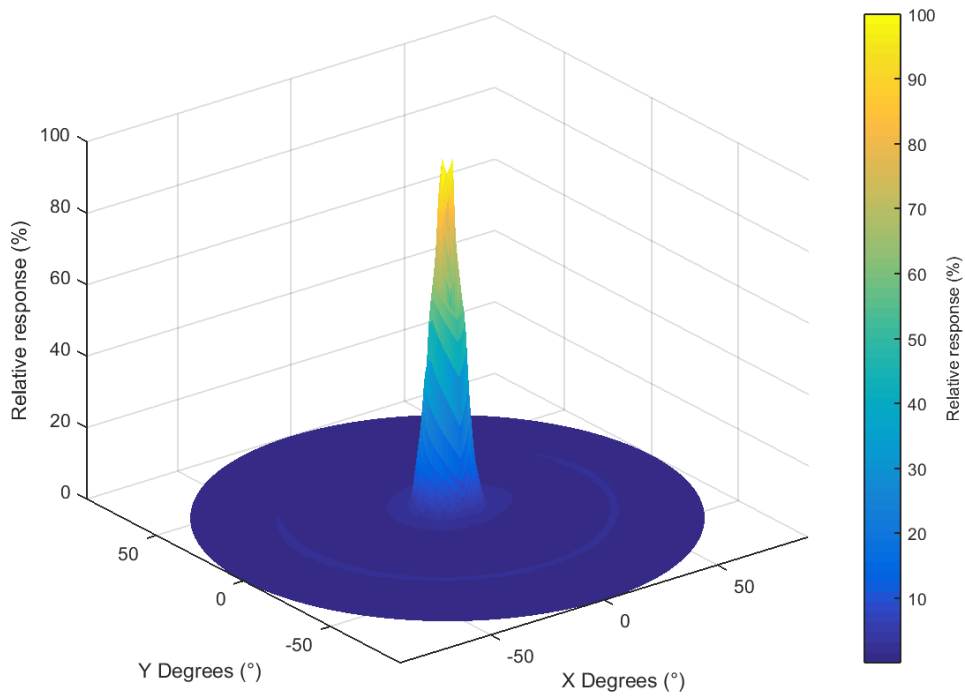
Figure 5 - 4. 3D model of the angular response of the Yellow "Bright" LED.
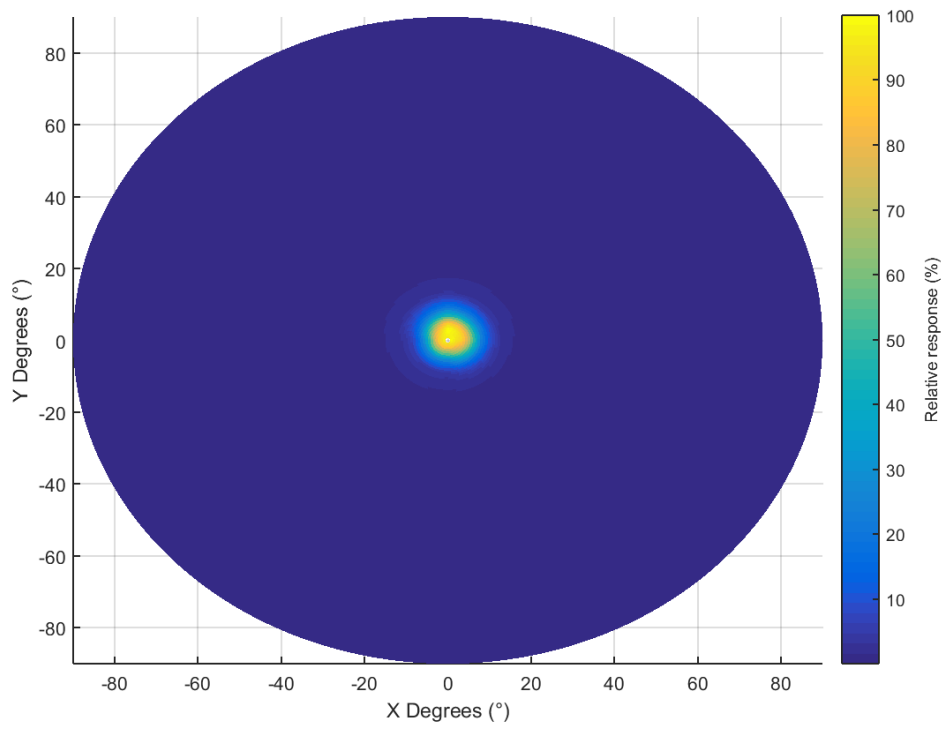
Figure 5 - 5. Top view of the 3D model of the angular response of the Green "Bright" LED.
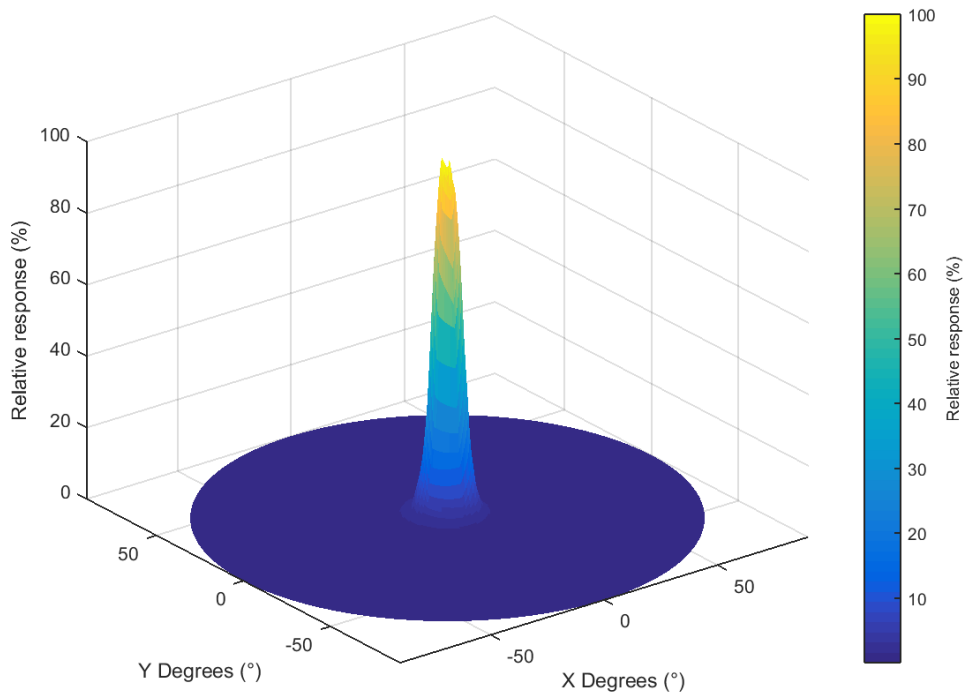
Figure 5 - 6. 3D model of the angular response of the Green "Bright" LED.

119
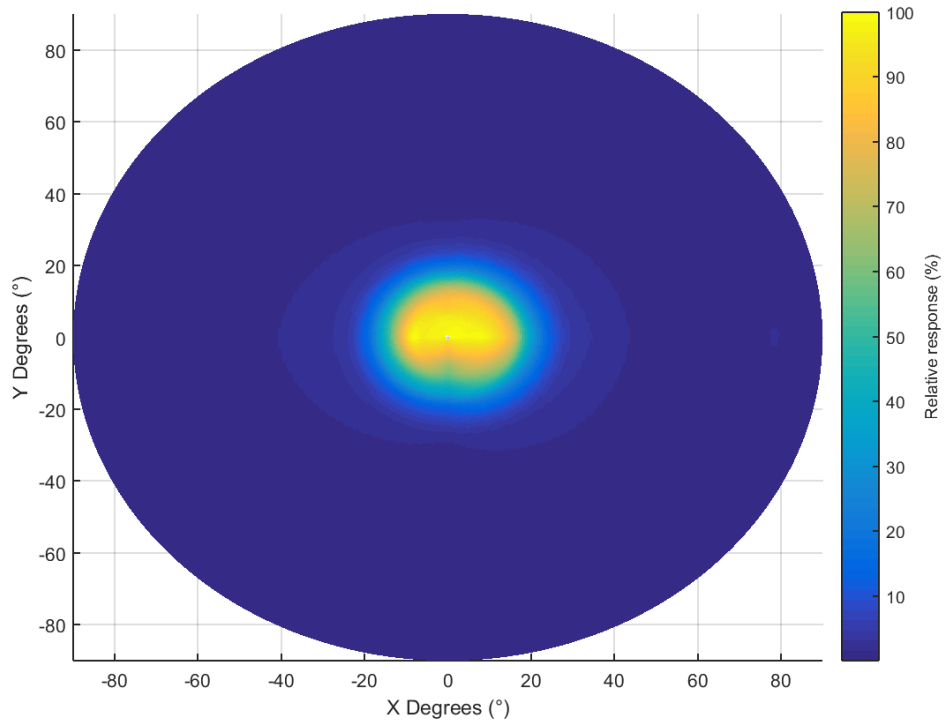
Figure 5 - 7. Top view of the 3D model of the angular response of the Blue "Bright" LED.
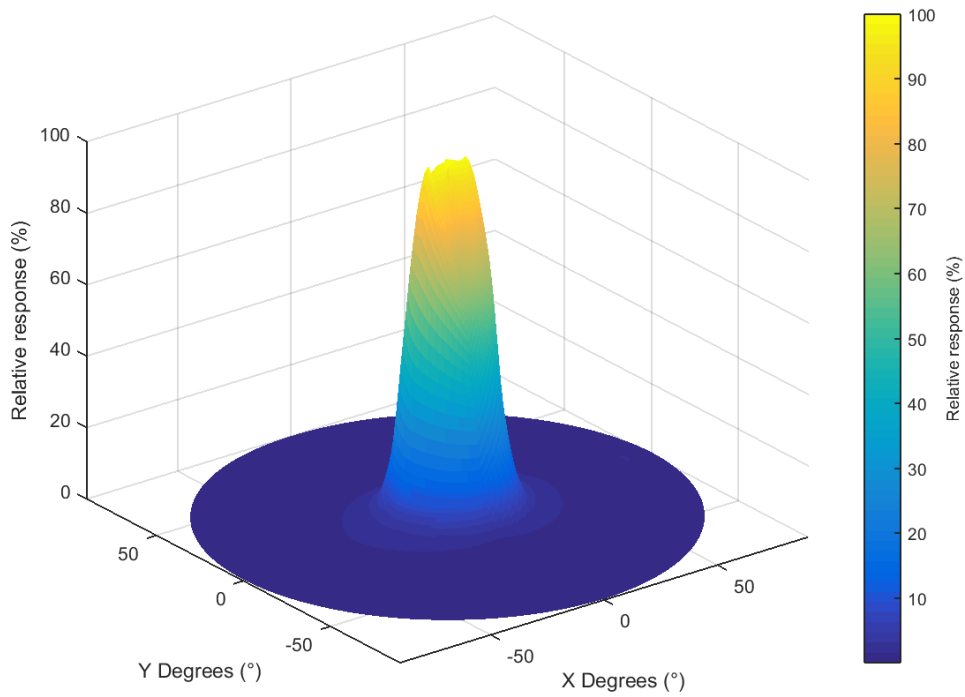
Figure 5 - 8. 3D model of the angular response of the Blue "Bright" LED.
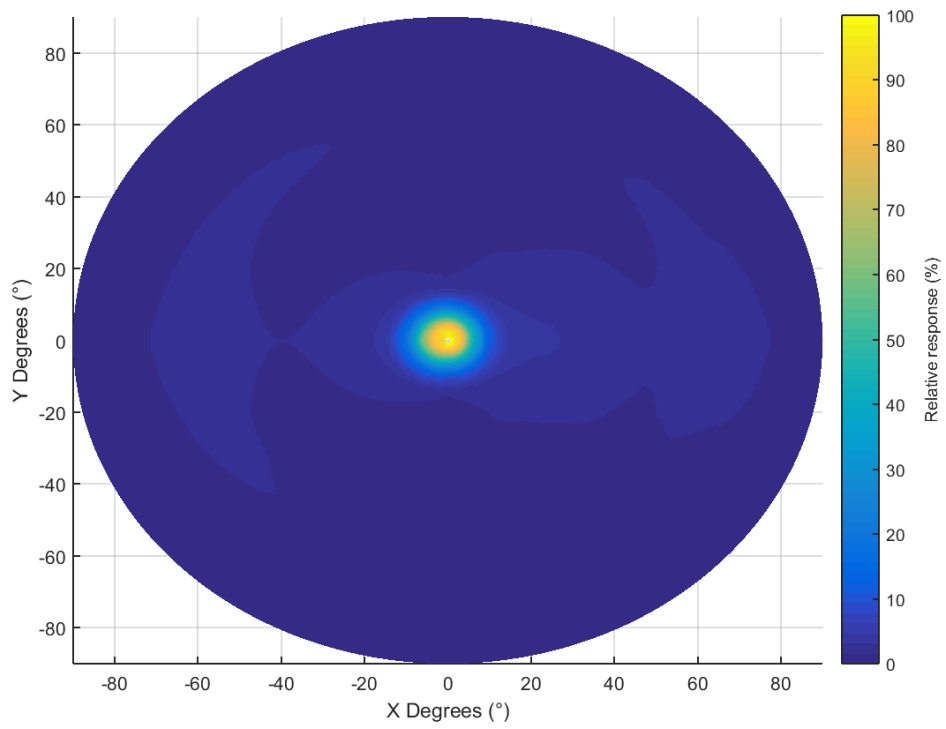
Figure 5 - 9. Top view of the 3D model of the angular response of the Violet "Bright" LED.
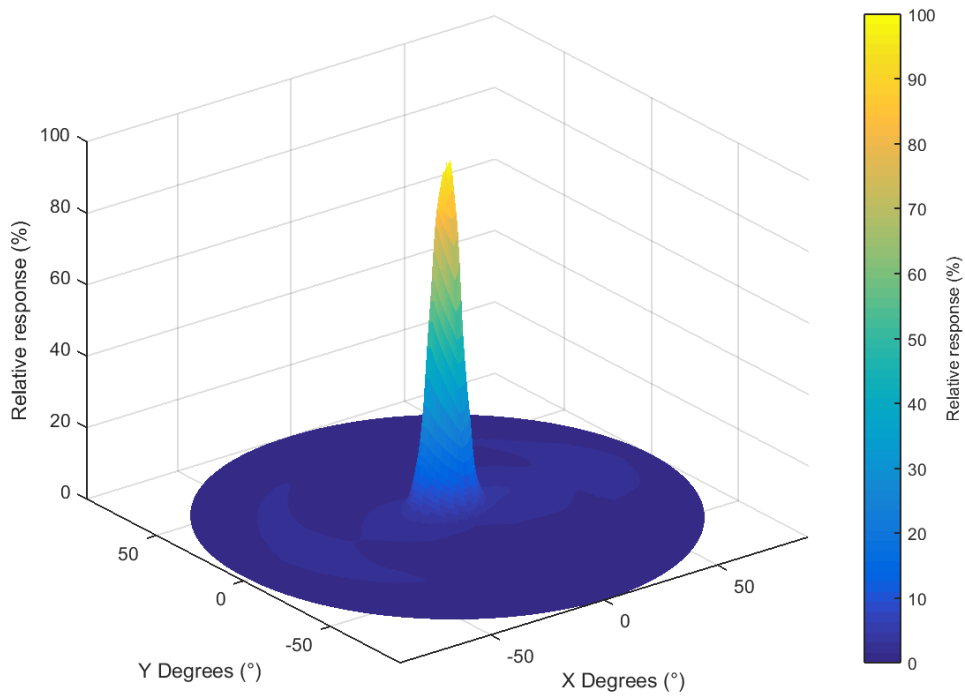
Figure 5 - 10. 3D model of the angular response of the Violet "Bright" LED.
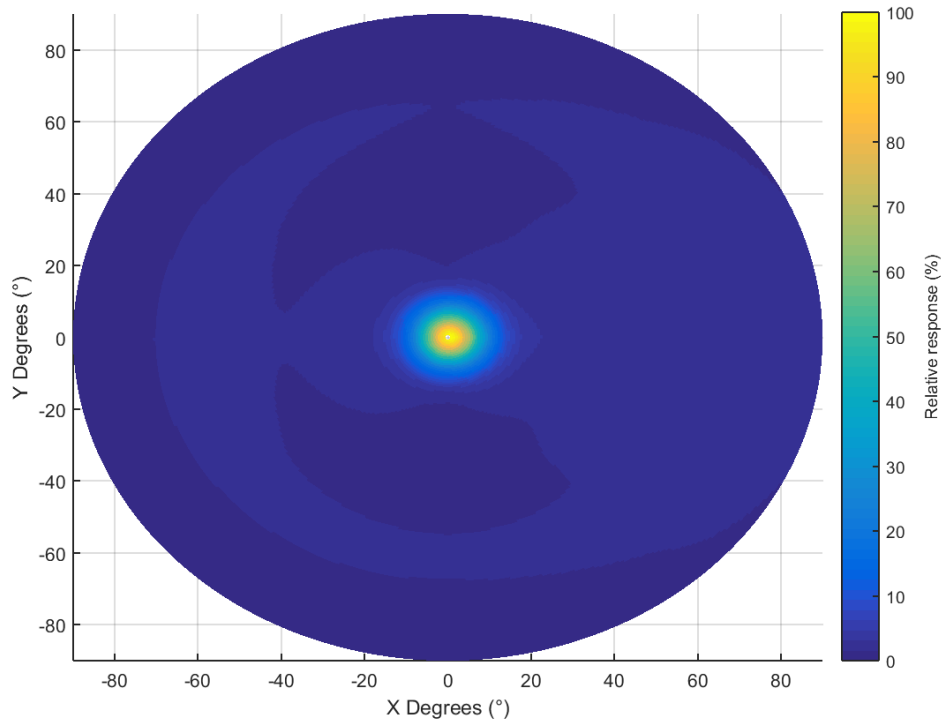
Figure 5 - 11. Top view of the 3D model of the angular response of the White "Bright" LED.
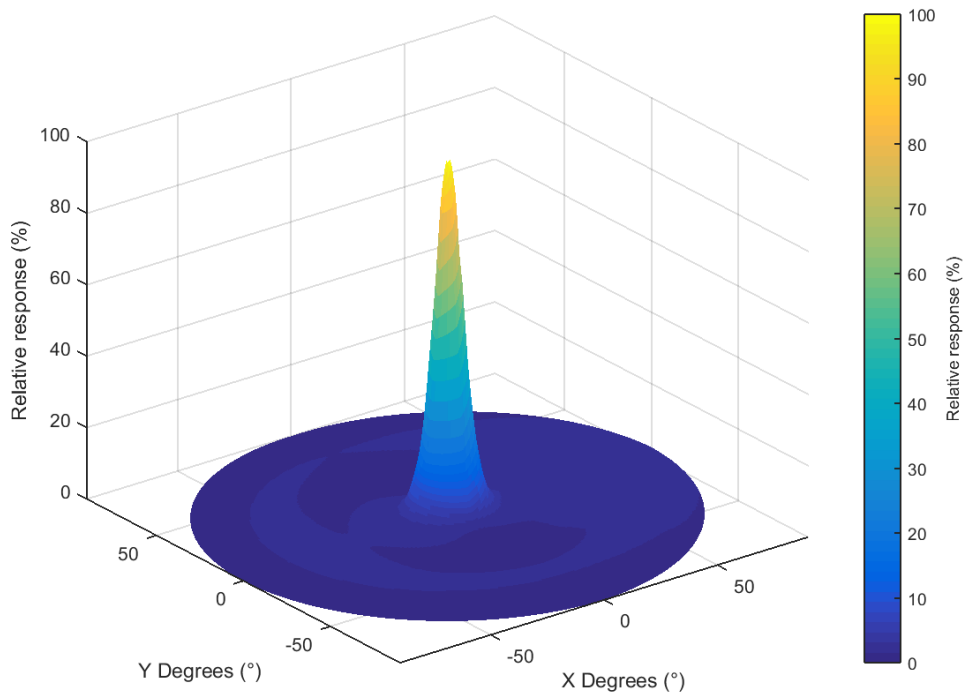
Figure 5 - 12. 3D model of the angular response of the White "Bright" LED.
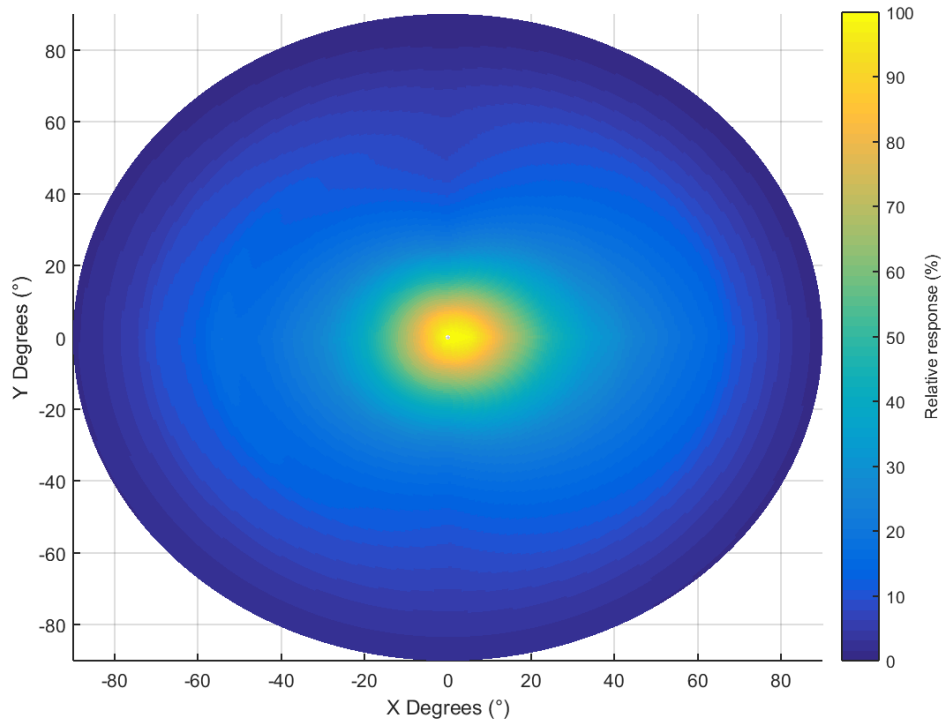
Figure 5 - 13. Top view of the 3D model of the angular response of the Red "Basic" LED.
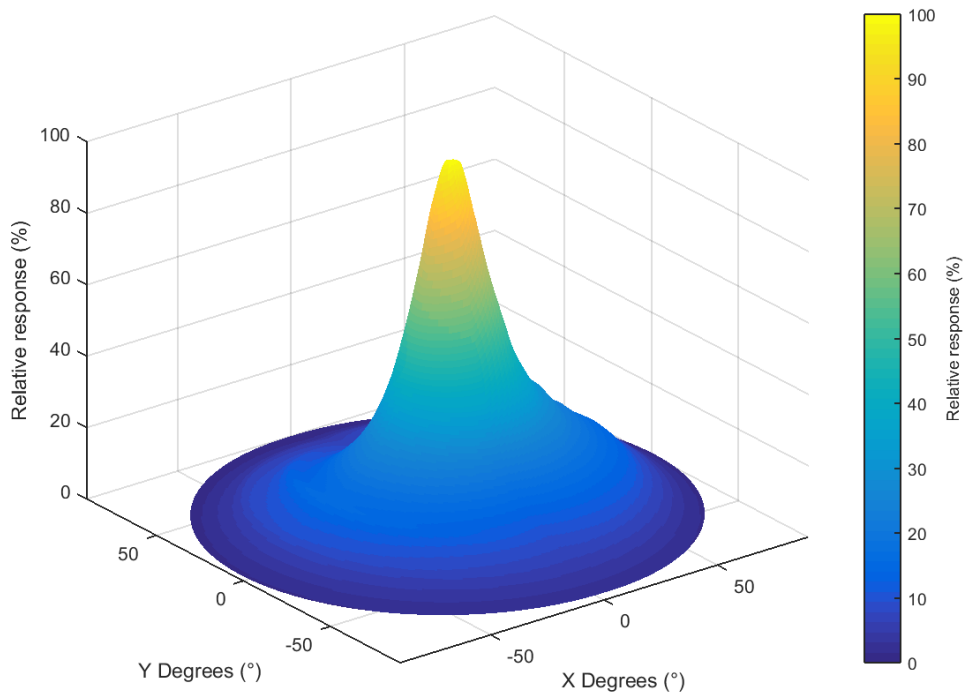
Figure 5 - 14. 3D model of the angular response of the Red "Basic" LED.
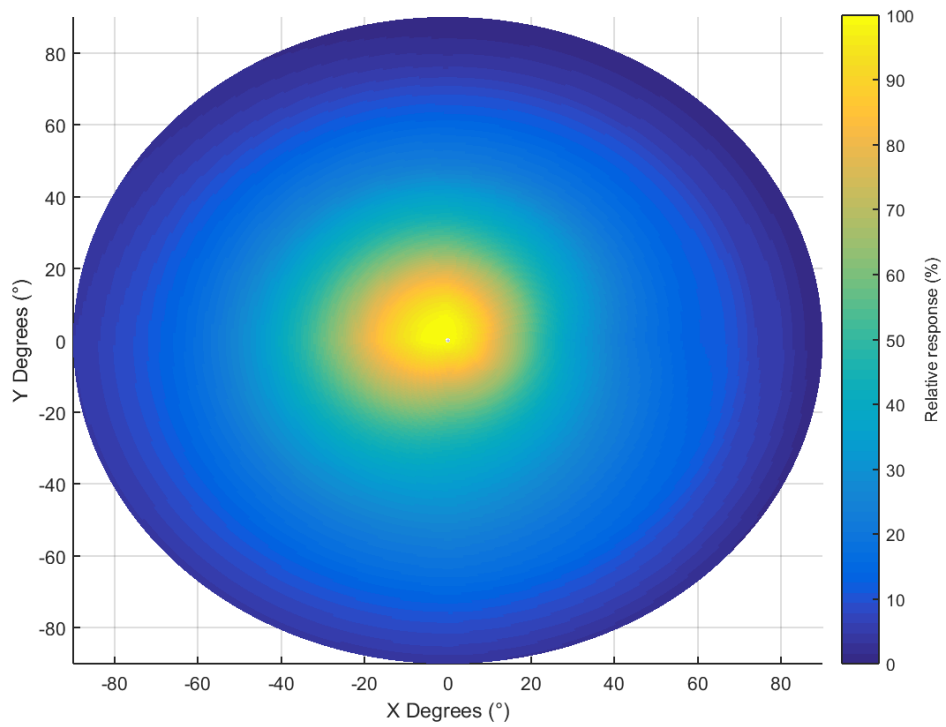
Figure 5 - 15. Top view of the 3D model of the angular response of the Orange "Basic" LED.
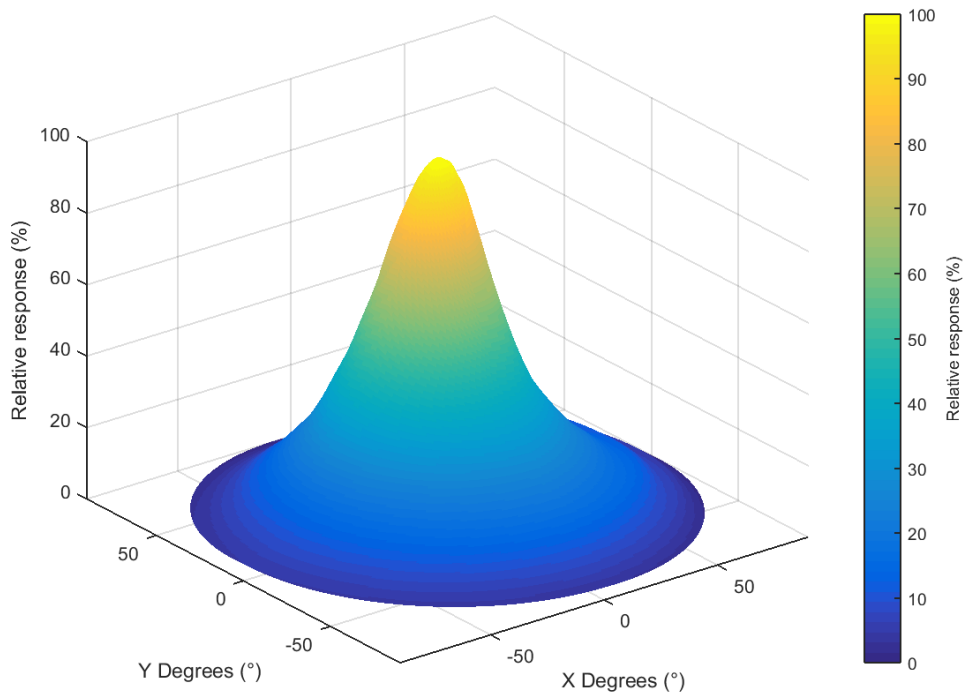
Figure 5 - 16. 3D model of the angular response of the Orange "Basic" LED.
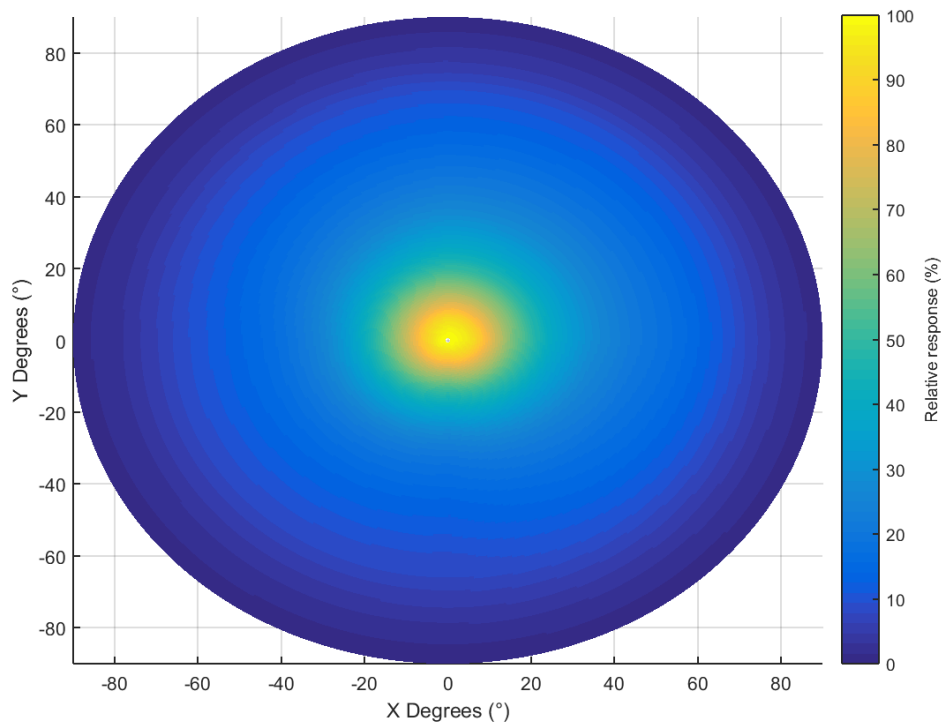
Figure 5 - 17. Top view of the 3D model of the angular response of the Yellow "Basic" LED.
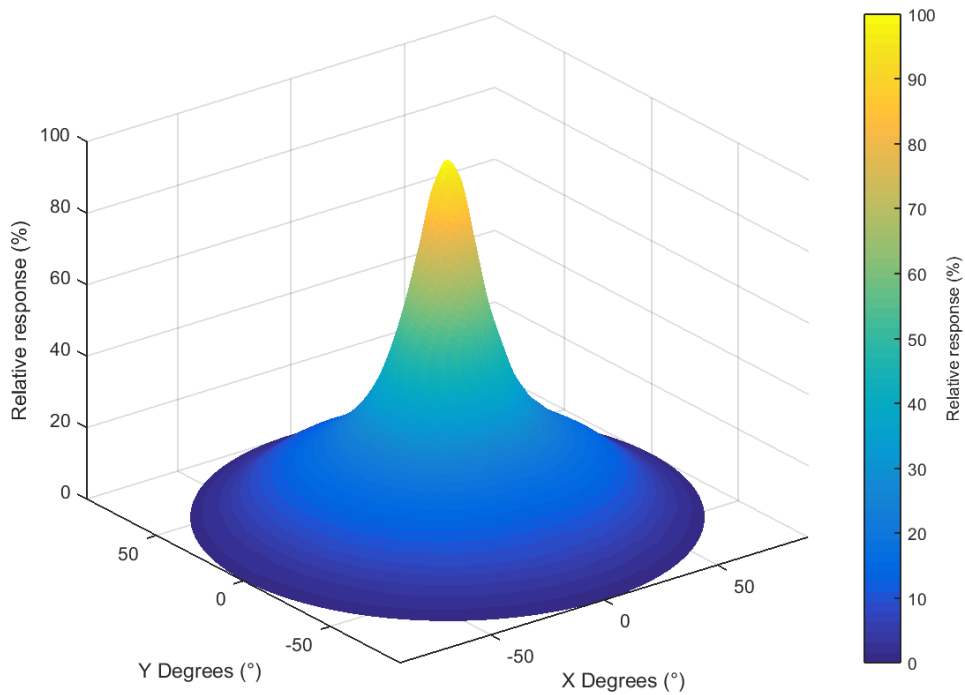
Figure 5 - 18. 3D model of the angular response of the Yellow "Basic" LED.
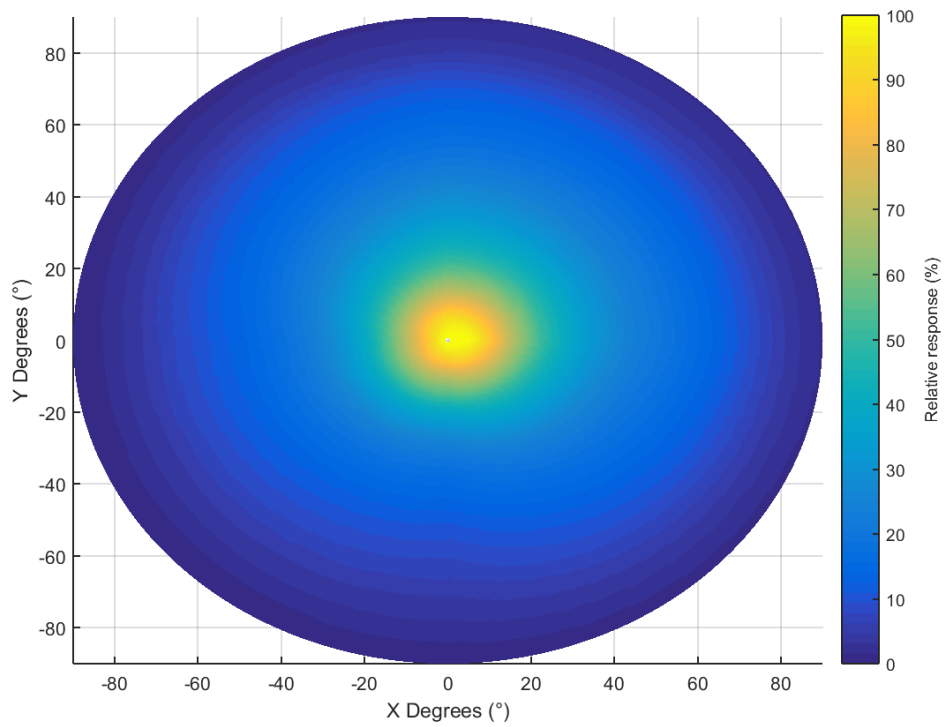
Figure 5 - 19. Top view of the 3D model of the angular response of the Green "Basic" LED.
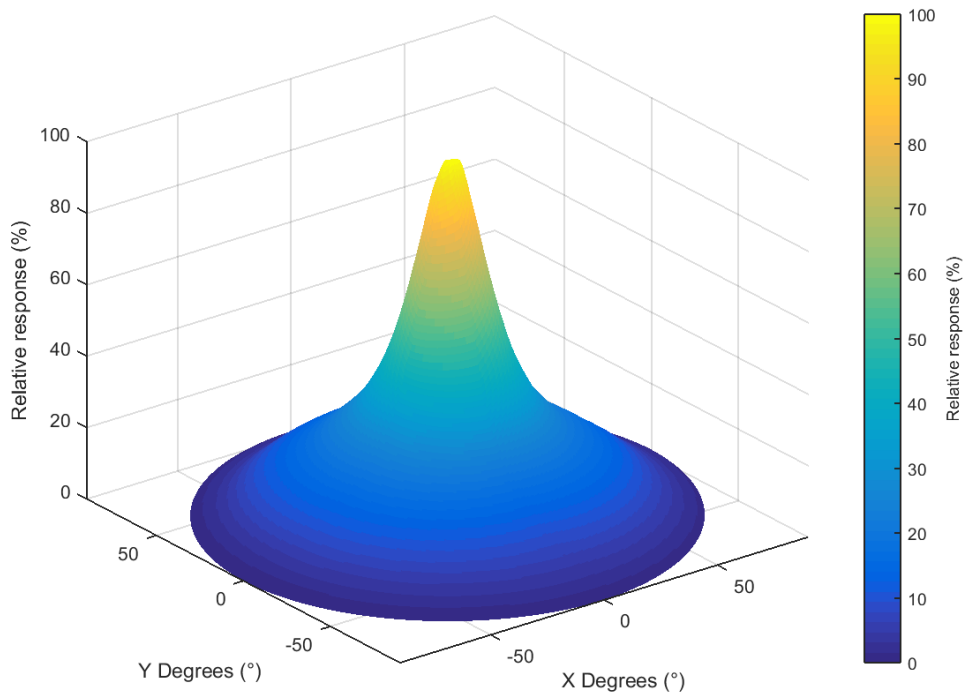
Figure 5 - 20. 3D model of the angular response of the Green "Basic" LED.
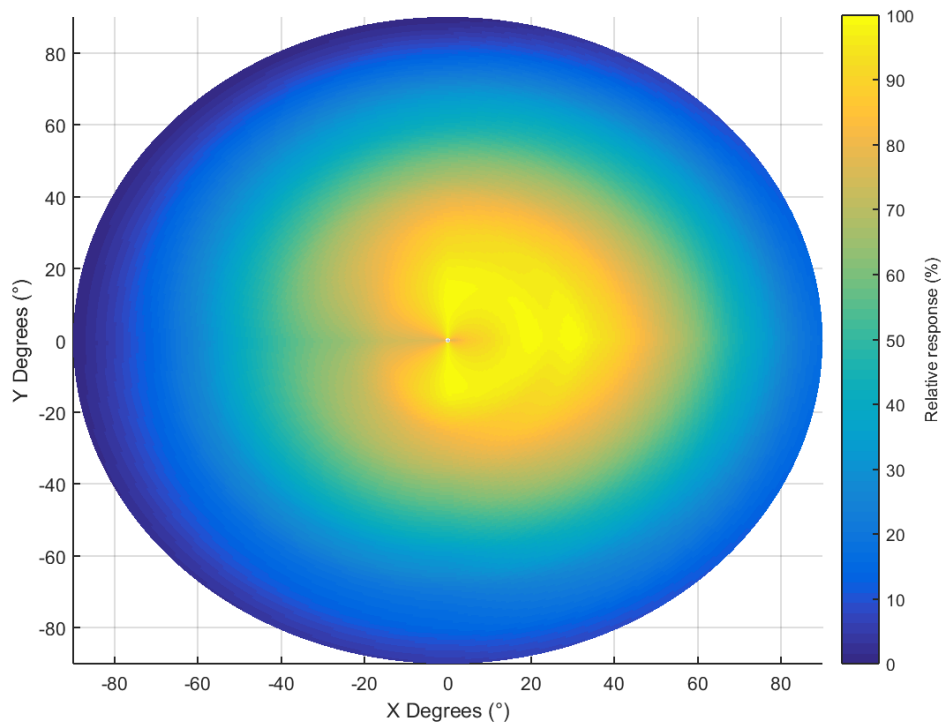
Figure 5 - 21. Top view of the 3D model of the angular response of the Blue "Basic" LED.
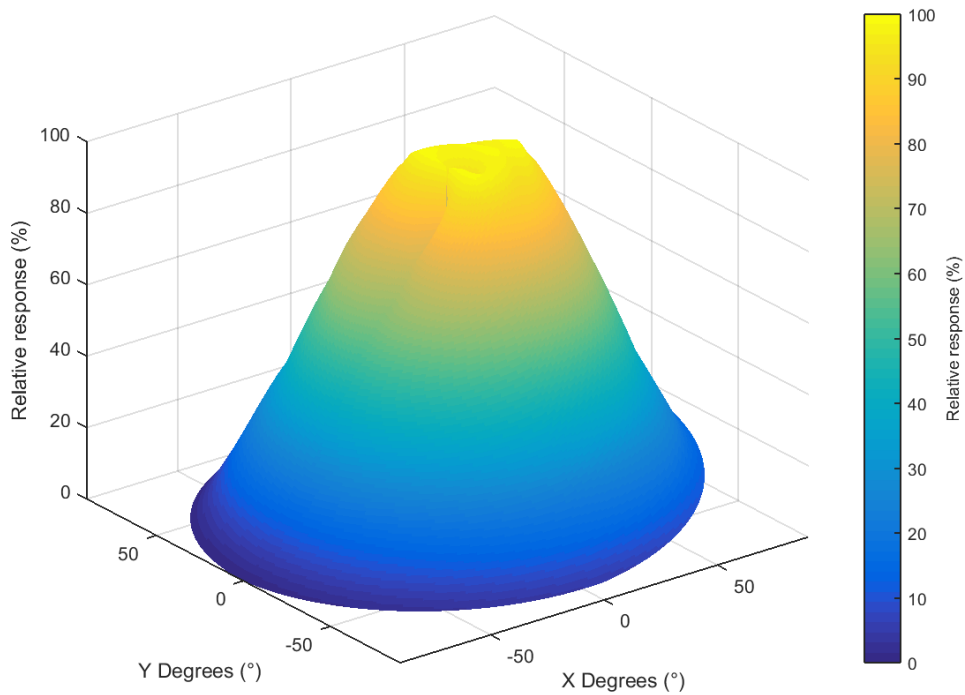
Figure 5 - 22. 3D model of the angular response of the Blue "Basic" LED.

127
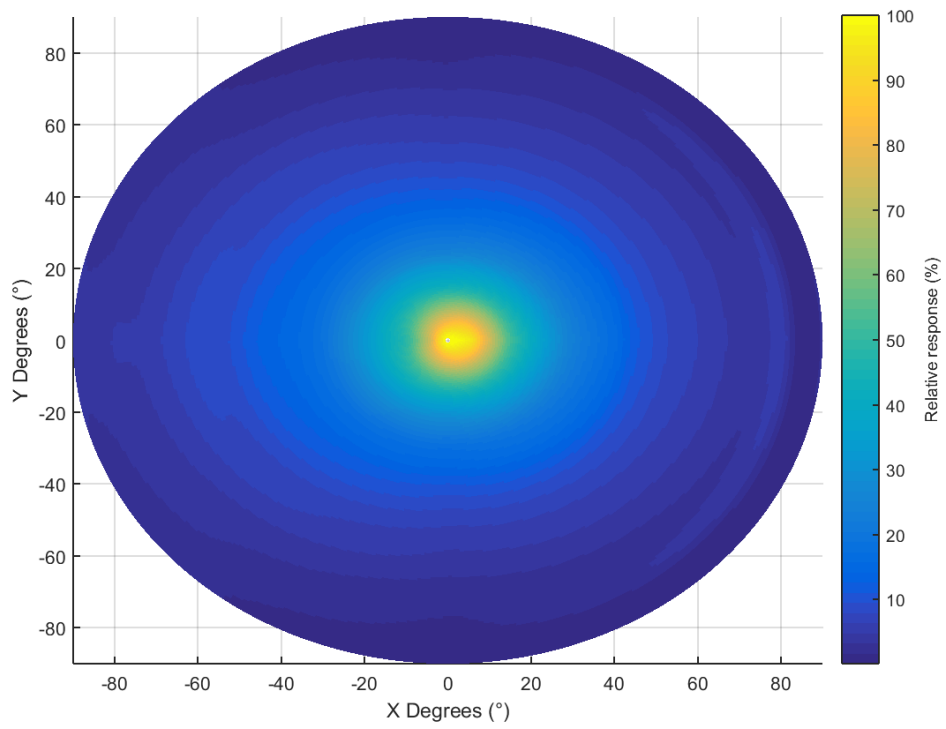
Figure 5 - 23. Top view of the 3D model of the angular response of the Violet "Basic" LED.
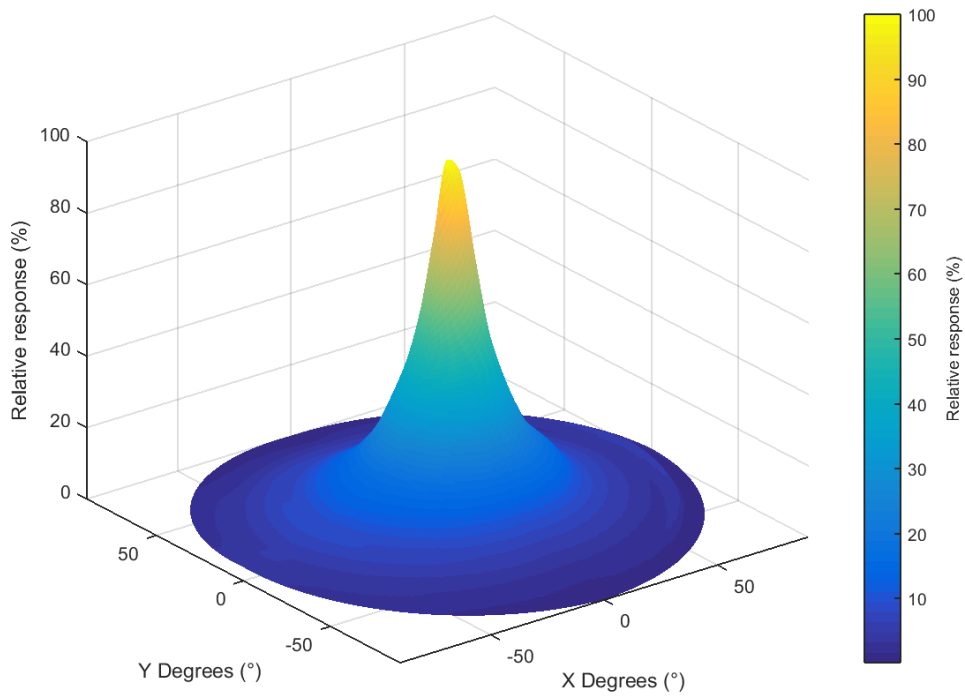
Figure 5 - 24. 3D model of the angular response of the Violet "Basic" LED.
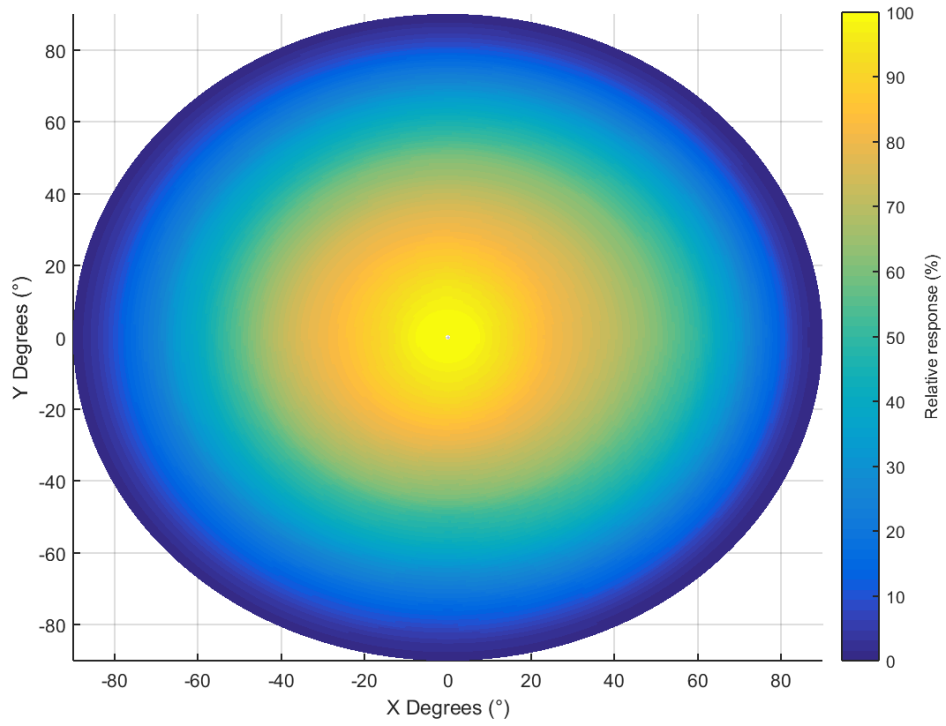
Figure 5 - 25. Top view of the 3D model of the angular response of the square-shaped White LED.
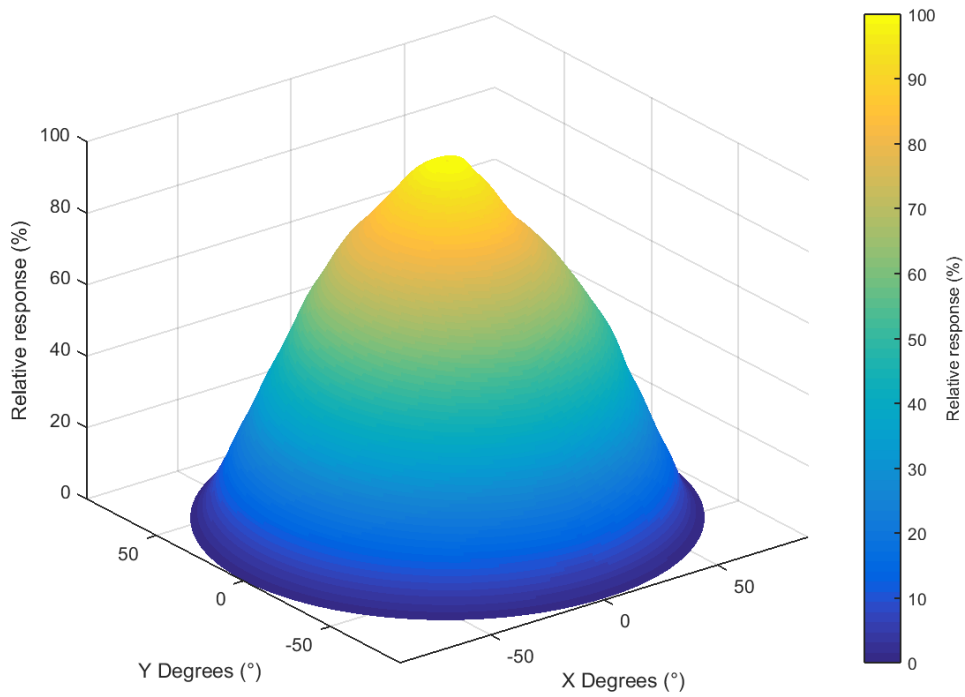
Figure 5 - 26. 3D model of the angular response of the square-shaped White LED.
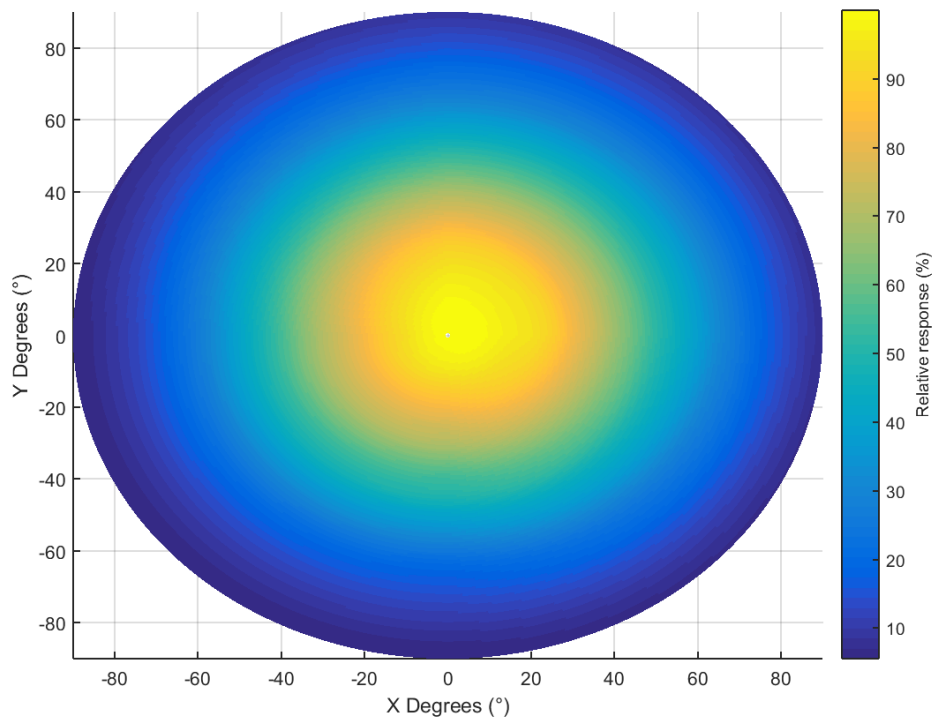
Figure 5 - 27. Top view of the 3D model of the angular response of the White LED with round lens.
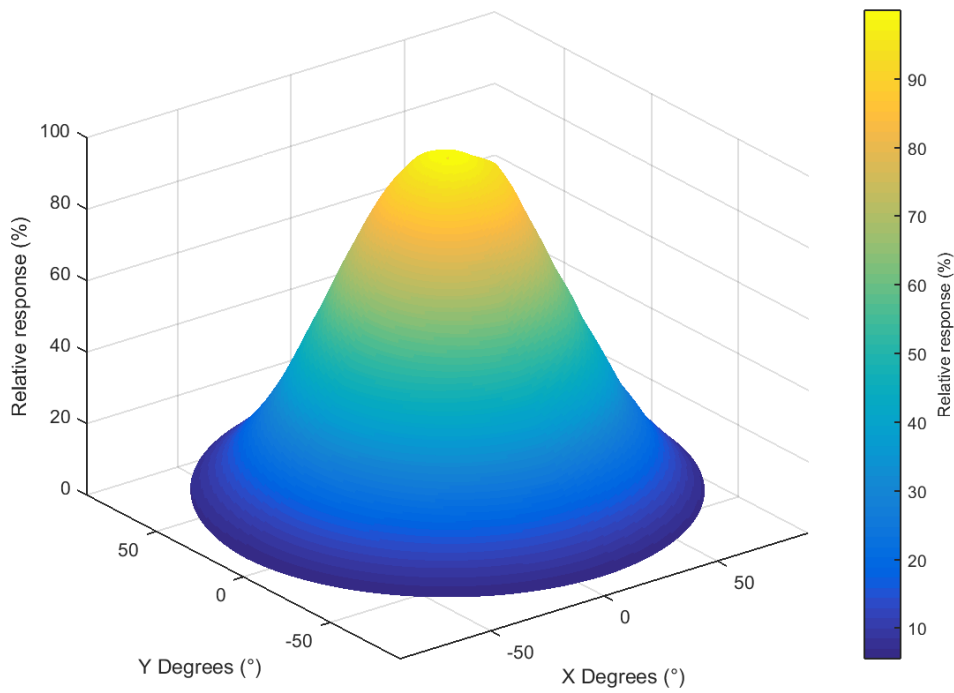
Figure 5 - 28. 3D model of the angular response of the White LED with round lens.

130

Appendix 6 – Results of the forward-bias and reverse-bias sensitivity measurements
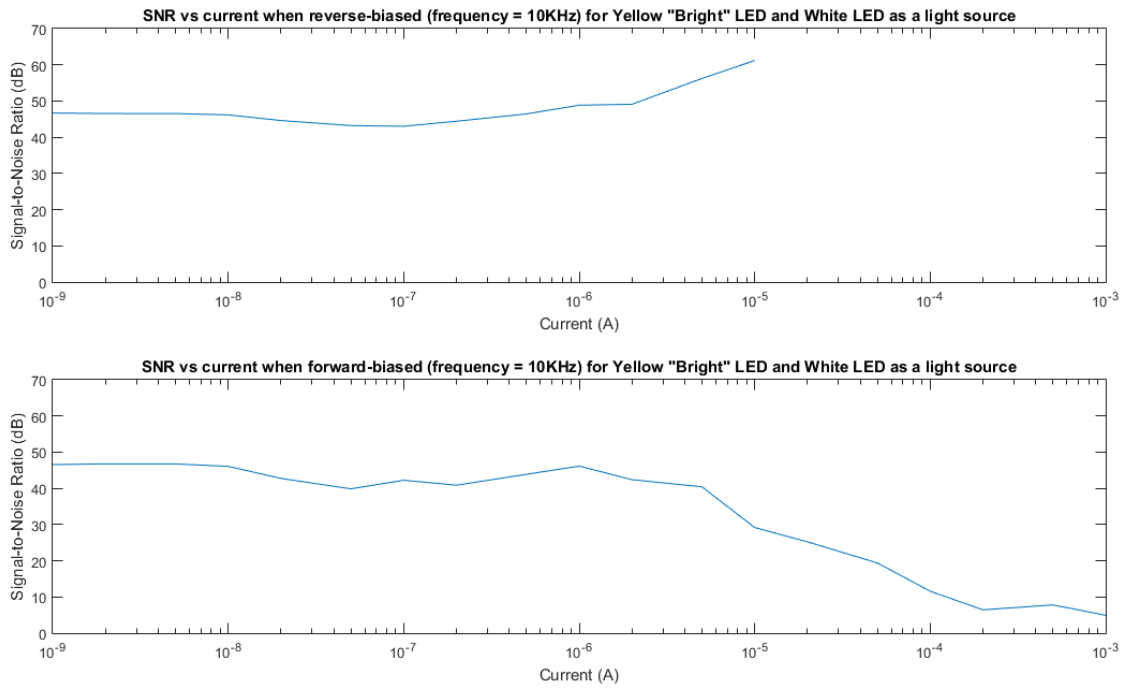
Figure 6 - 1. SNR versus current of the reverse-biased and forward-biased for Yellow 'Bright' LED and White LED as light source.
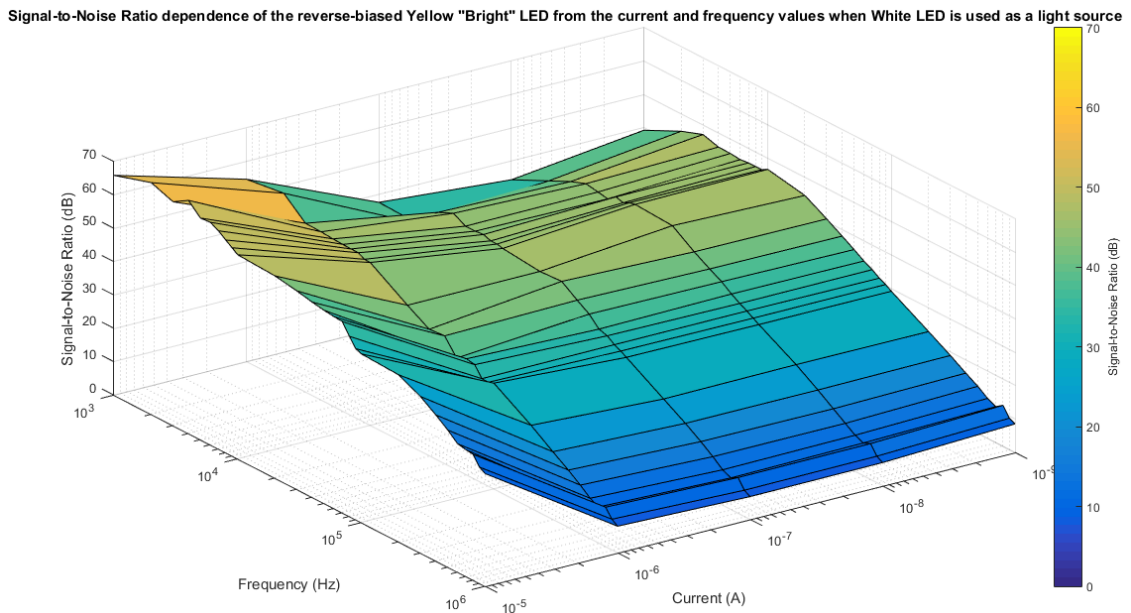
Figure 6 - 2. SNR dependence of the reverse-biased Yellow 'Bright' LED from the current and frequency values when White LED is used as a light source.

Figure 6 - 3. SNR dependence of the forward-biased Yellow 'Bright' LED from the current and frequency values when White LED is used as a light source.
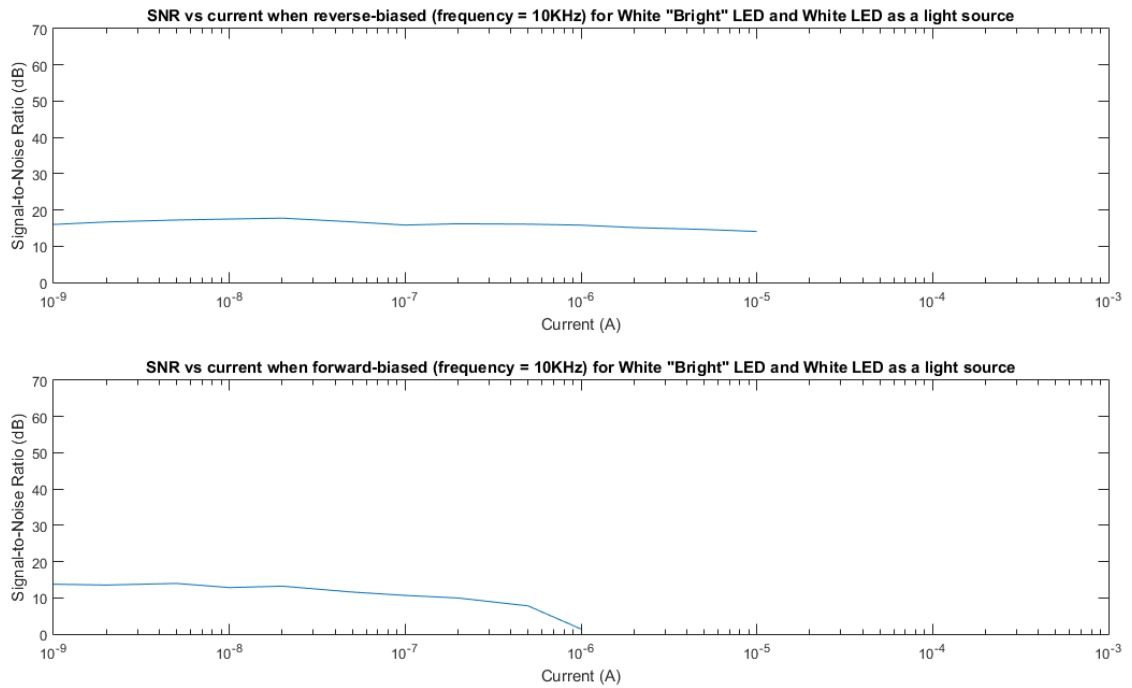
Figure 6 - 4. SNR versus current of the reverse-biased and forward-biased for White 'Bright' LED and White LED as light source.

Figure 6 - 5. SNR versus current of the reverse-biased and forward-biased for White 'Bright' LED and White LED as light source.
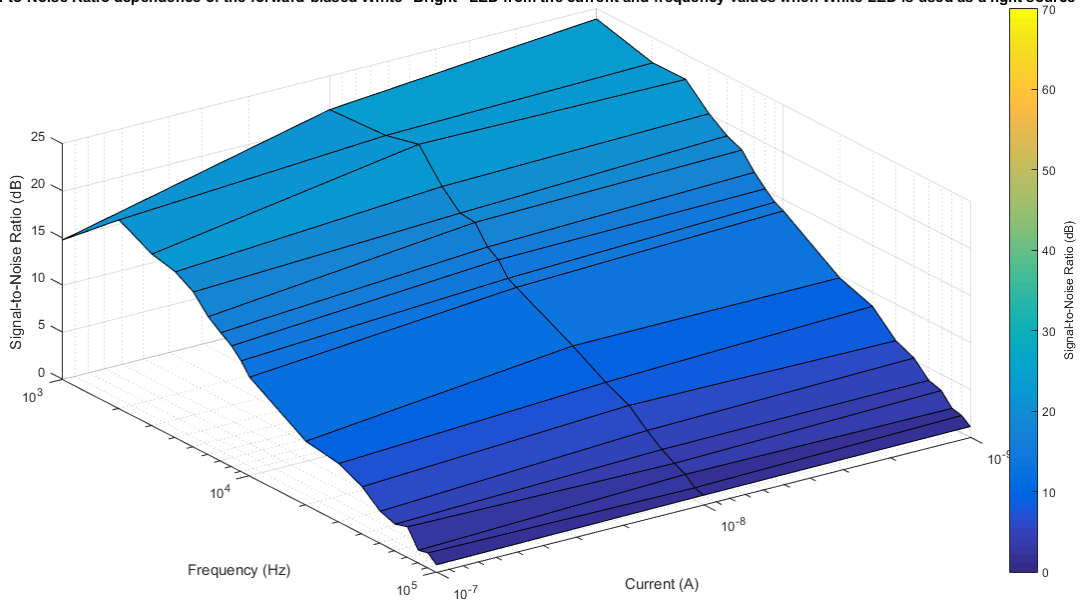
Figure 6 - 6. SNR dependence of the forward-biased White 'Bright' LED from the current and frequency values when White LED is used as a light source.
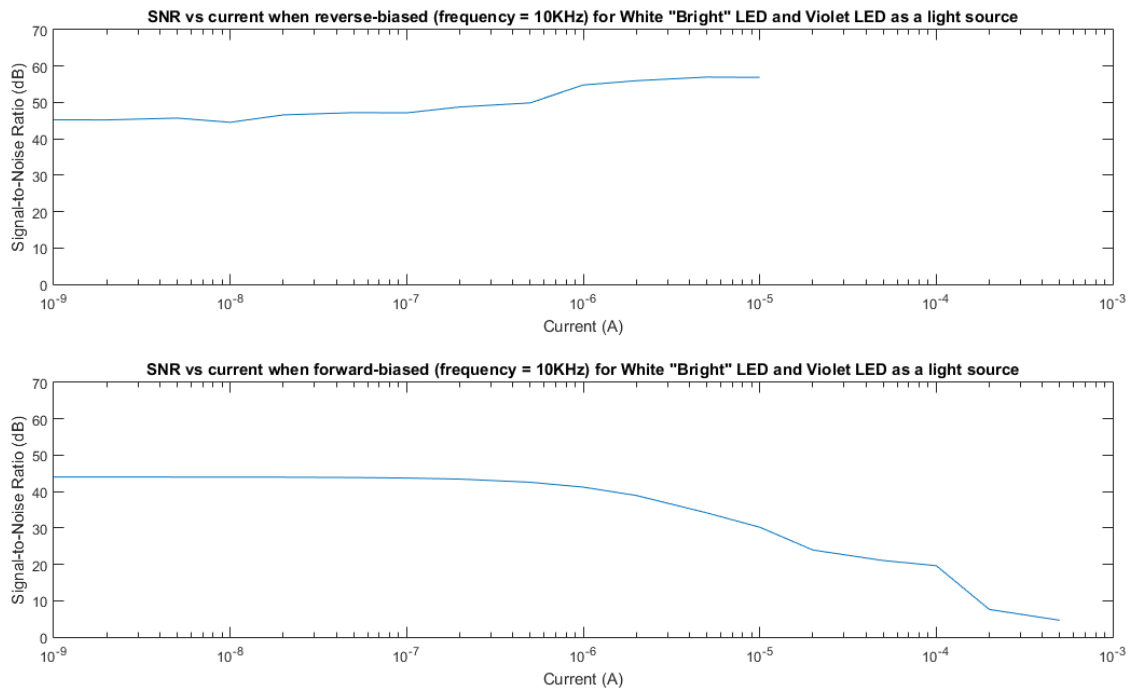
Figure 6 - 7. SNR versus current of the reverse-biased and forward-biased for White 'Bright' LED and Violet LED as light source.
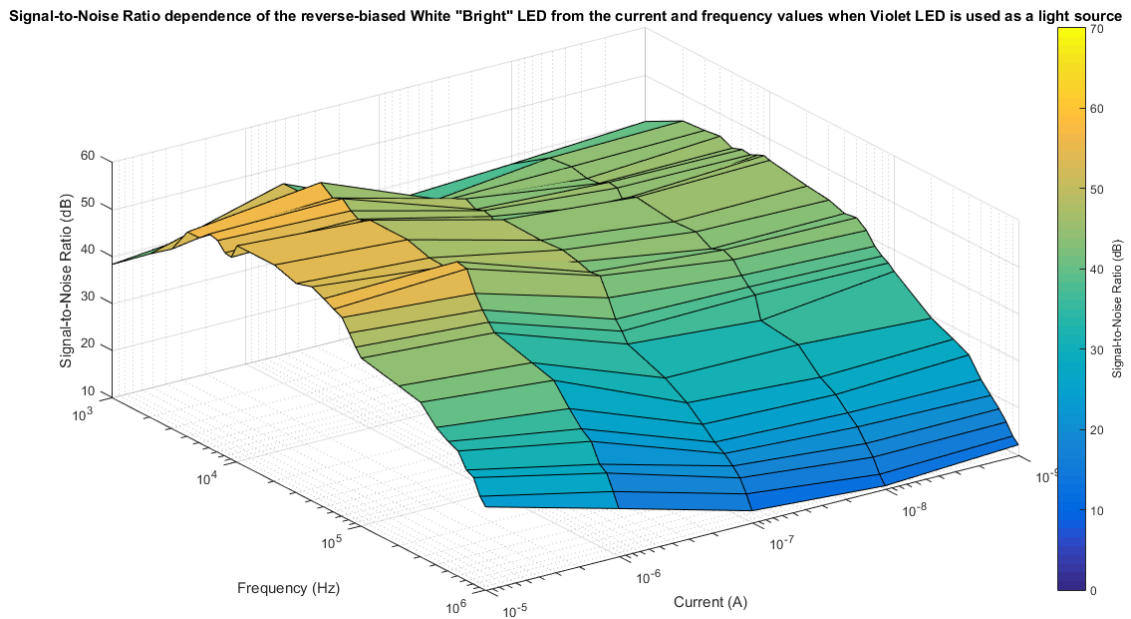
Figure 6 - 8. SNR dependence of the reverse-biased White 'Bright' LED from the current and frequency values when Violet LED is used as a light source.
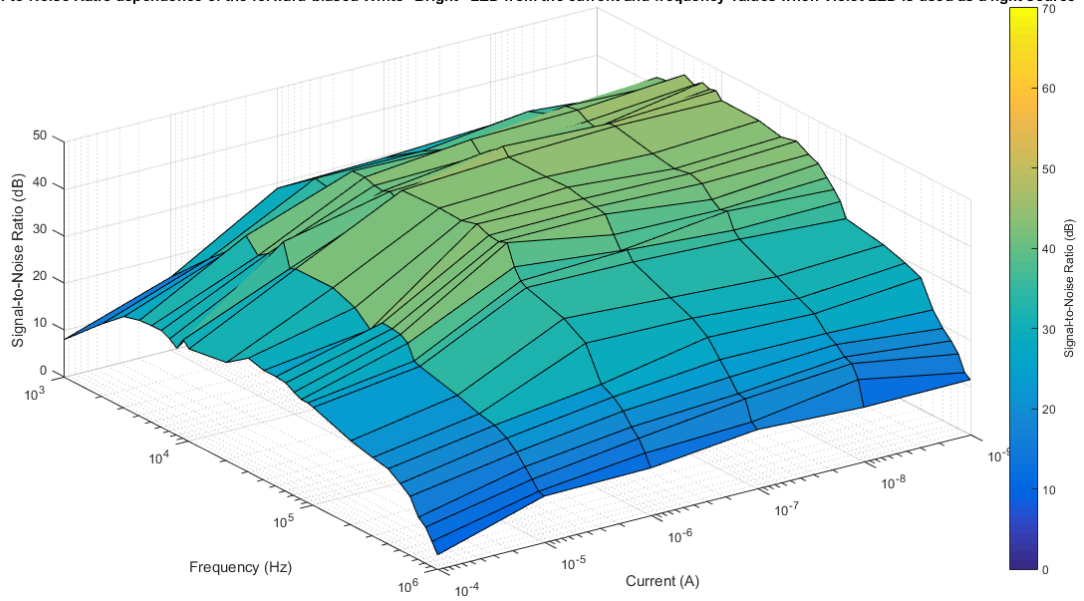
Figure 6 - 9. SNR dependence of the forward-biased White 'Bright' LED from the current and frequency values when White LED is used as a light source.

Appendix 7 – Simulation of the original EDN Networks design

The original circuit proposed in EDN Networks was simulated and analysed. The work is divided on multiple parts where the circuit was sending and receiving the signals and where multiple parts of the circuit were analysed in order to see how they are working. The simulation part was done in "Multisim" environment which is based on SPICE.

Sending signal

During the sequence when the device was sending signal, the TX controls the bipolar PNP transistor Q1 which turns the LED on and off. Due to no descriptions about the transistors characteristics or name, the ideal transistor was set. The resistor R1 limits the current at the transistors base and resistor R2 limits the current flowing through the LED. The circuit which was being used for the simulation is Figure 7 - 1.
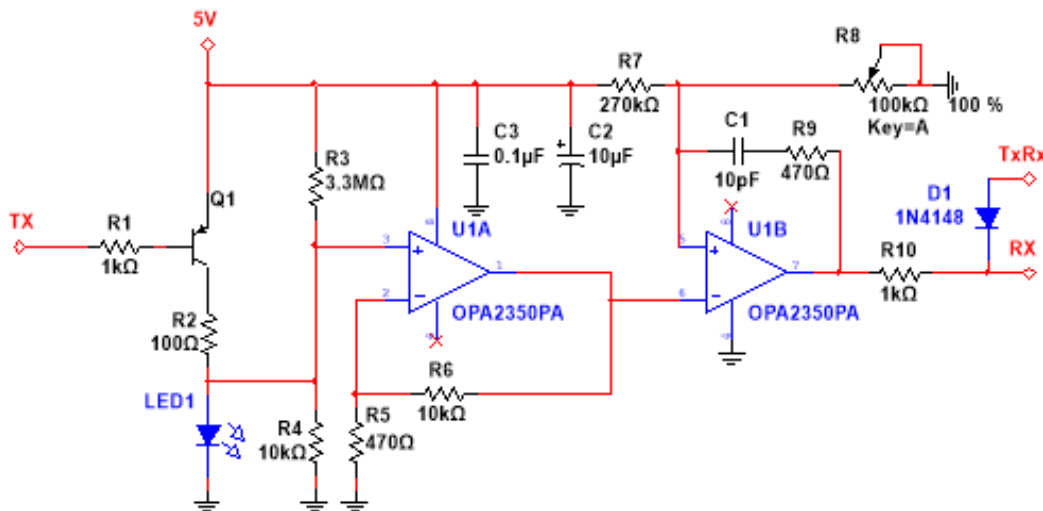
Figure 7 - 1. Circuit for the simulation when the device is sending signal.

The signal sending sequence was done at multiple frequencies to control how the circuit works. It was assumed that the input signal which was being sent was ideal and noiseless. The frequency values are 1kHz and 125kHz. The first result is shown in Figure 7 - 2. As it can be observed, the device is working as intended and the output signal is inverted due to the PNP transistor work. The output signal didn't have any distortions which could influence the shape of the signal.
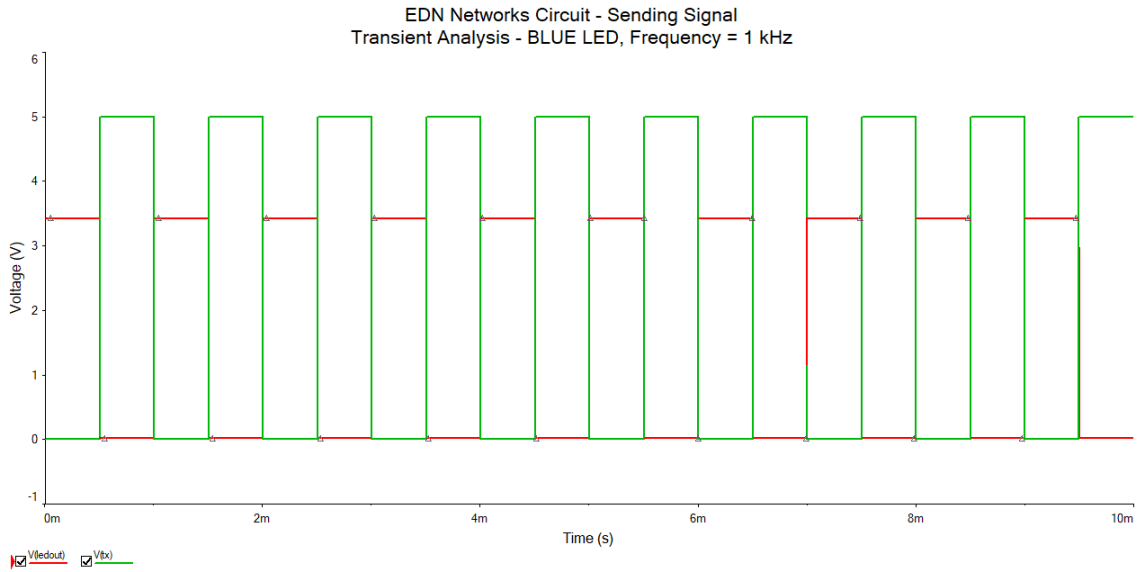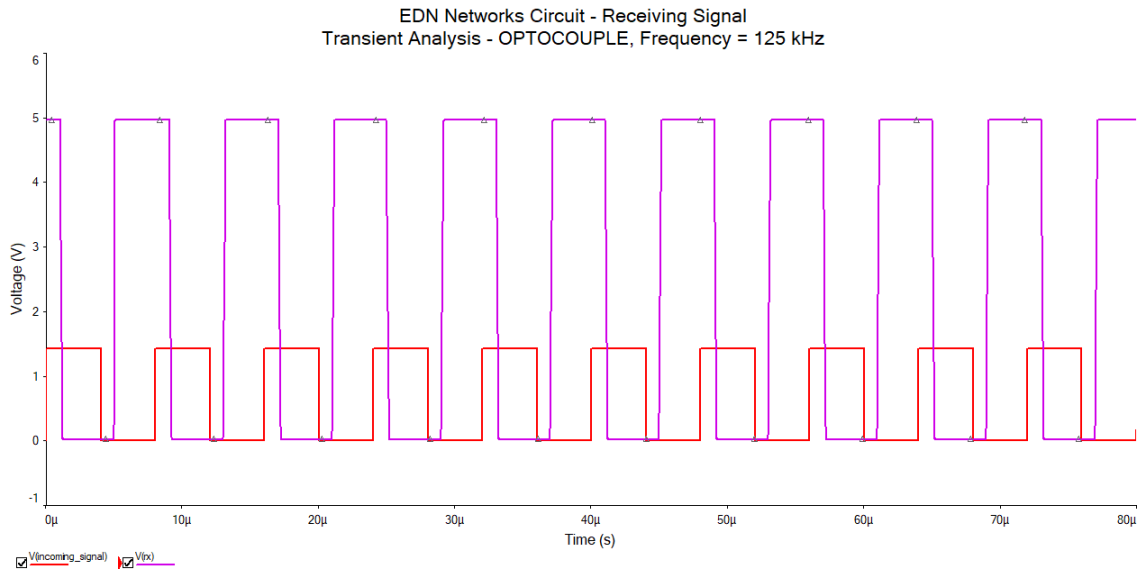
Figure 7 - 2. Input signal (green) and output signal (red) of the device when it was sending 1kHz frequency signal.

The results of the simulation with the 125kHz signal are shown in Figure 7 - 3. At higher frequencies the shape of the output signal changes dramatically. The reason is that LED has junction capacitance which is charged through the R2 resistor. Due to the low resistance value of the resistor R2 the diode's junction is charged fast, but during discharge part, the PNP transistor Q1 is closed, so the LED has to discharge through the load resistor R4 which has 100 times higher resistance value than the R2.
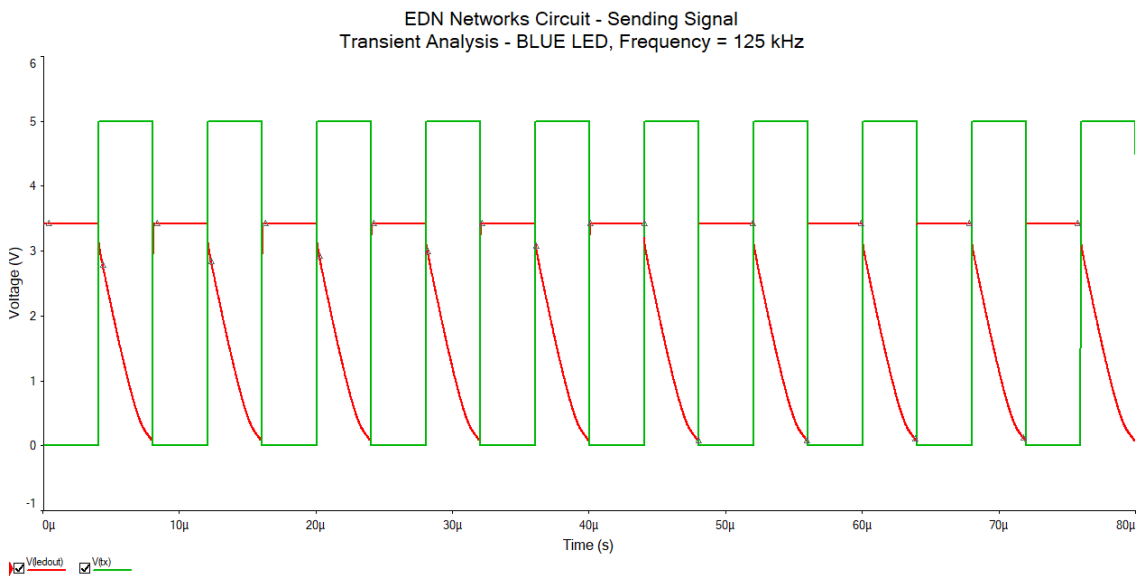
Figure 7 - 3. Input signal (green) and output signal (red) of the device when it was sending 125kHz frequency signal.

Receiving signal

In this part the LED was replaced with optocouple in order to imitate the work of the LED receiving the light signal. The circuit used for the simulation is shown in Figure 7 - 4. The transistor Q1 during receiving signal sequence is always closed and the current generated but the optocouple flows through the load resistor R4. Resistor R4 serves as the current-voltage converter and the voltage value is amplified by the non-inverting amplifier. The amplified signal is being sent to the negative pin of the comparator. The output signal would be inverted.
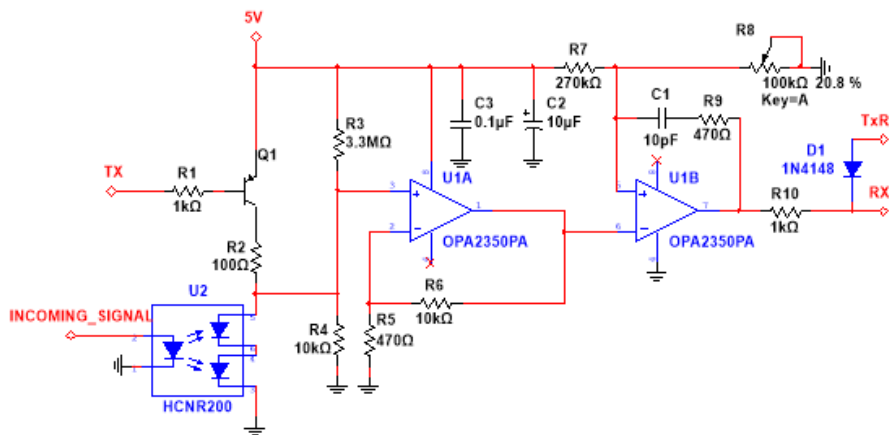
Figure 7 - 4. Circuit for the simulation when the device is receiving signal.

The simulated frequencies remain the same to control how the device is receiving signal. The received 1kHz signal is shown in Figure 7 - 5. The input signal was specifically set lower in order to imitate the distance between the devices. But the results show that output voltage at RX is close to be ideal. However, important note should be made that the shape of the output signal depends on the potentiometer R8 and accurate calibration is required. The next Figure 7 - 6 shows that changing the potentiometer value by, at least, 1kOhm may result in incorrect work of the device.
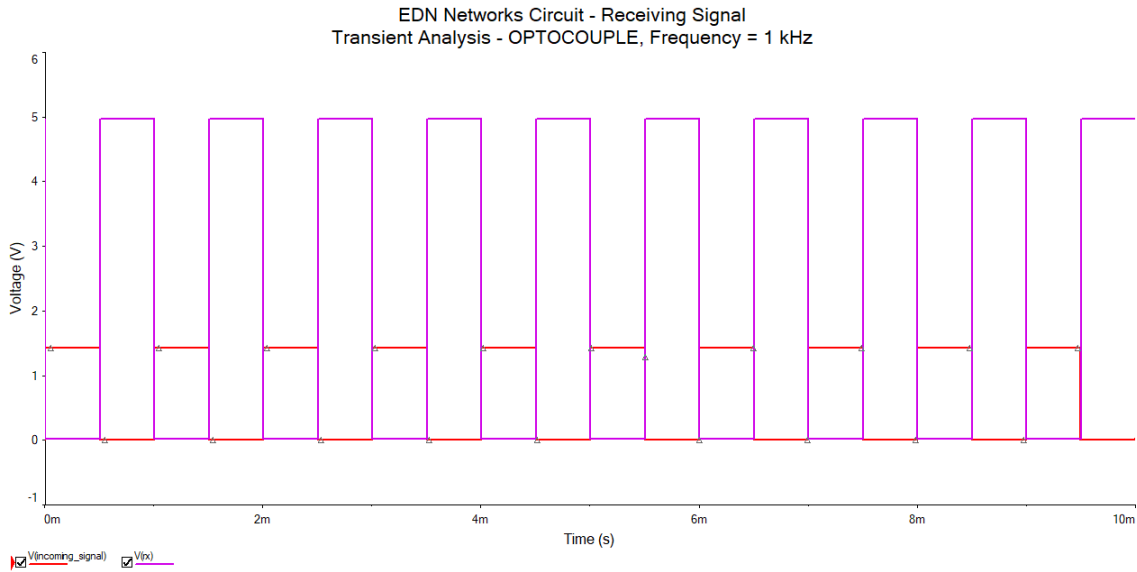
Figure 7 - 5. Input signal (red) and output signal (purple) of the device when it was receiving 1kHz frequency signal. The potentiometer was set to the most sensitive position.
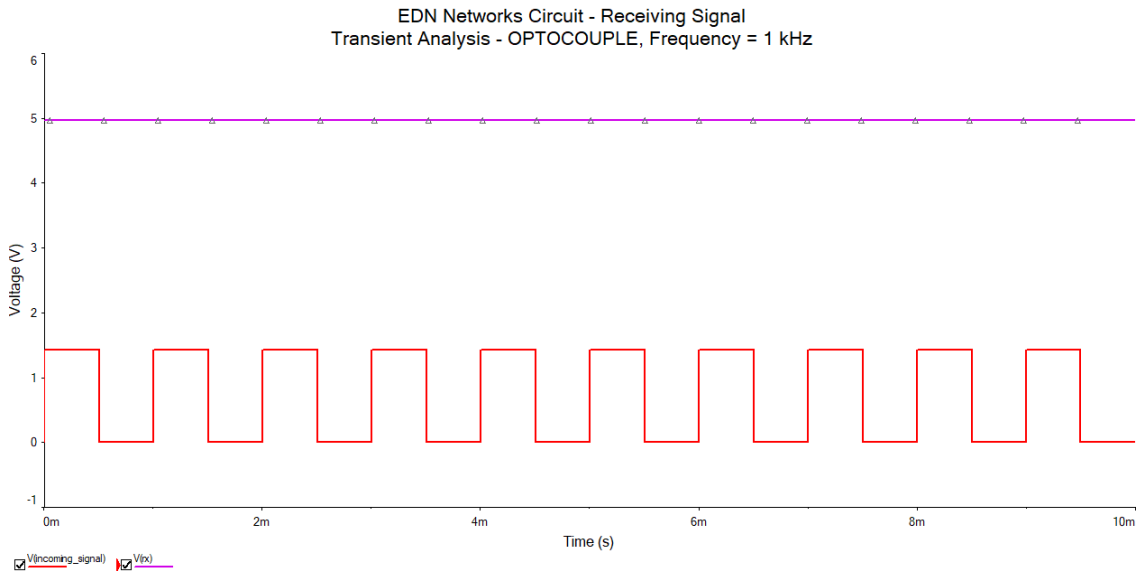
Figure 7 - 6. Input signal (red) and output signal (purple) of the device when it was receiving 1kHz frequency signal. The potentiometer value was increased by 1kOhm.

In case of 125kHz signal, the output signal at RX was shifted which means that the signal at the output of the non-inverting amplifier doesn't have ideal square shape. The potentiometer R8 in this case was also adjusted which means that at higher frequencies its value needs to be calibrated. The results with 125kHz signal are shown in Figure 7 - 7.

139

Figure 7 - 7. Input signal (green) and output signal (purple) of the device when it was receiving 125kHz frequency signal. The potentiometer was set to the most sensitive position.

Analysis of the non-inverting amplifier

The non-inverting amplifier part in the design is needed to amplify the incoming light signal. In order to analyse the AC characteristics of the OA, the circuit was modified. The modified circuit is presented in Figure 7 - 8. Resistors R1 and R2 give bias equal to half of the voltage supply on the input of the amplifier. Capacitor C1 is needed to amplify only AC signal. Capacitor C4 is needed to pass the AC signal on the input of the amplifier. All other parts remain the same which were taken from the original design.
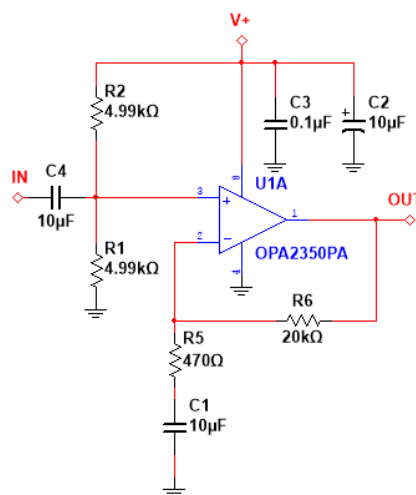
Figure 7 - 8. Non-inverting amplifier modified for the AC Response analysis.

140

The results in Figure 7 - 9 show that the circuit works as the band-pass filter with lower cut-off frequency at 36Hz and upper cut-off frequency at 929kHz. The gain of the amplifier is 32.8 dB. It should be noted that in the original design there was no capacitor C1, so the gain should remain the same even at the frequencies below 36Hz and the only cut-off frequency of the amplifier would be 929kHz which is the limitation of the OPA2350.
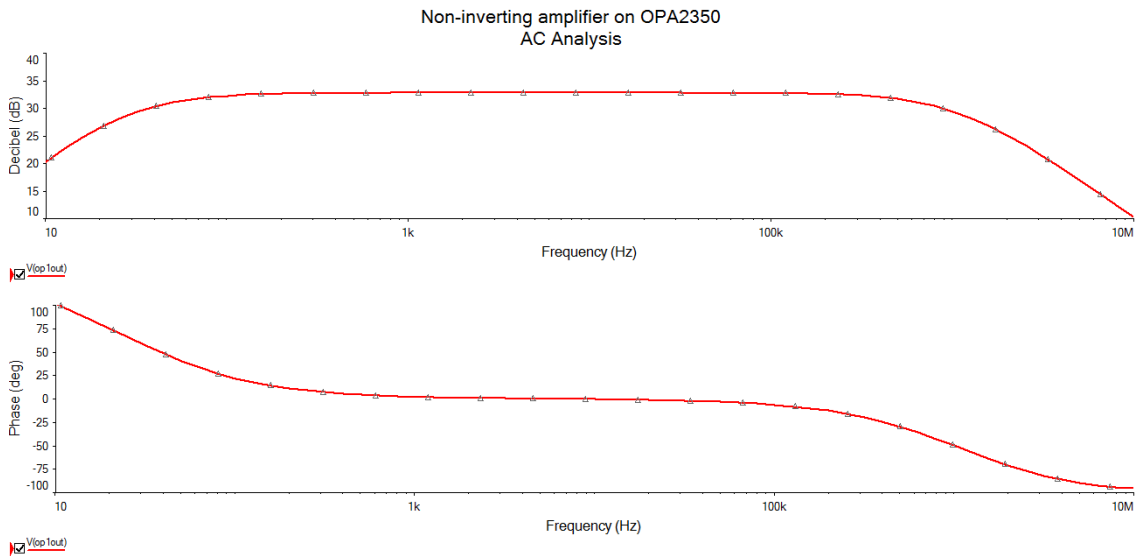
Figure 7 - 9. Results of the AC analysis of the non-inverting amplifier.

Analysis of the comparator

The comparator part of the original design was analyzed in order to overview it's work and behavior. The circuit under analysis is presented in Figure 7 - 10. The signal which was on input of the comparator is sinusoidal. The design was tested with two frequencies: 1kHz and 125kHz. The signal had the same DC bias voltage which was on the positive pin of the comparator.
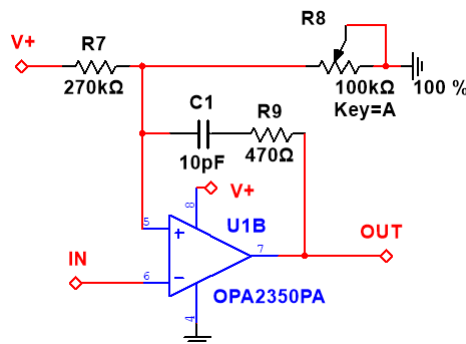
Figure 7 - 10. Comparator design part with adjustable reference.

141

The results of the simulation with 1kHz could be observed in Figure 7 - 11. It can be observed that switching output of the comparator between 'low' and 'high' levels cause distortions at the positive input of the comparator. This can be caused by the C1R9 chain which gives force effect for the comparator to switch faster, however, since the input signal frequency is low, it causes, instead, distortions. With 125kHz frequency however, the situation is different. The results could be seen in Figure 7 - 12. Due to high frequency of switching, higher frequency components of the pulse signal pass through the C1R9 chain which results in higher spikes on the positive input of the comparator. As a result, the comparator switches faster at higher frequencies.
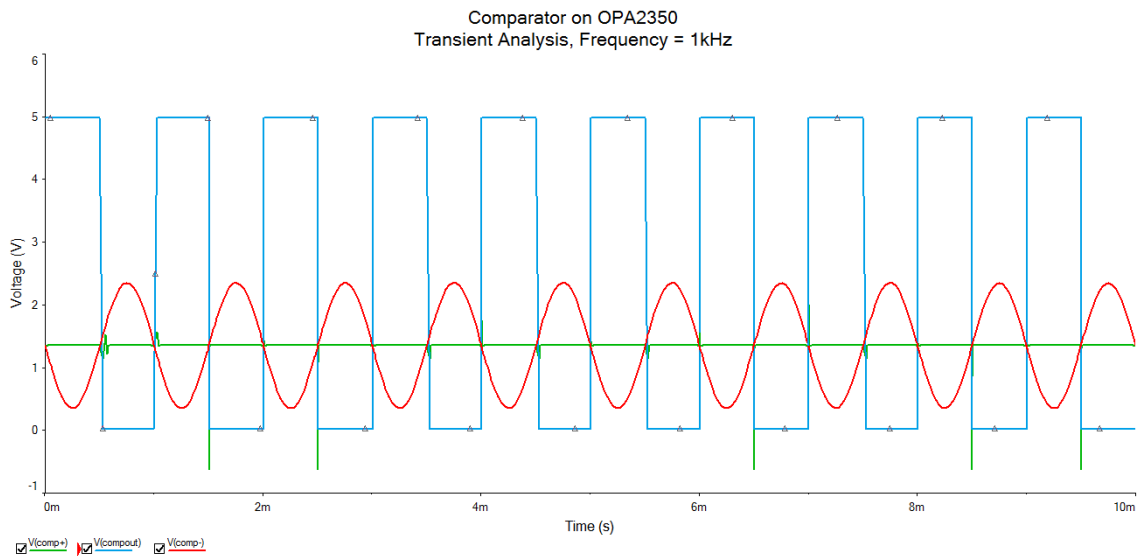
Figure 7 - 11. Input signal (red), reference voltage (green) and output signal (blue) of the comparator when the input signal frequency was 1kHz.
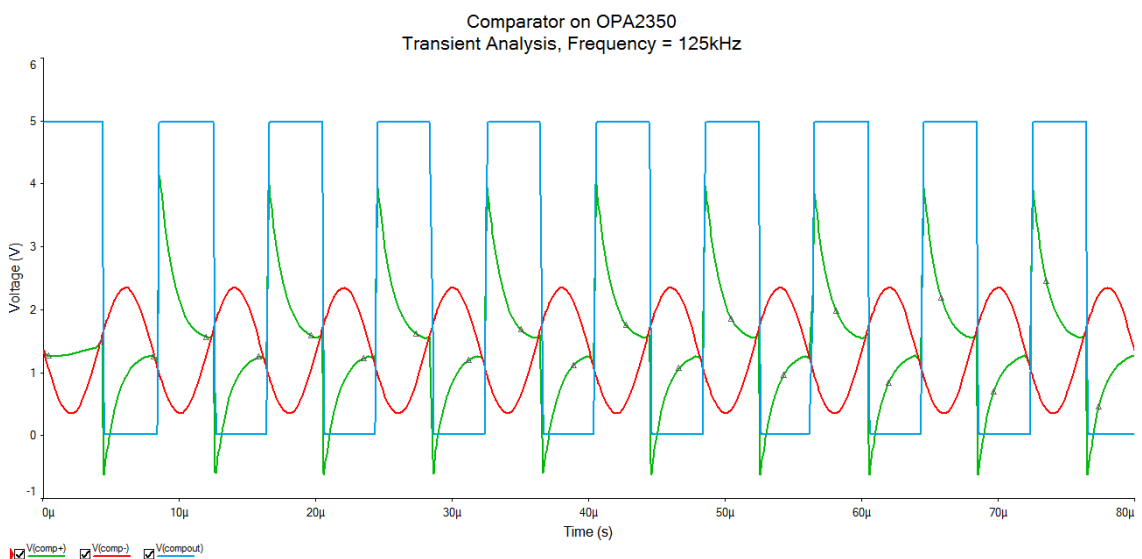
Figure 7 - 12. Input signal (red), reference voltage (green) and output signal (blue) of the comparator when the input signal frequency was 125kHz.

142

Appendix 8 – Simulation of the design proposed by Mitsubishi Electric Research laboratories

The circuit proposed by Mitsubishi Laboratories involves using microcontroller with the internal ADC. Due to lack of such microcontrollers in 'Multisim' simulation environment, the replacement was organized using discreet components. It assumed that sending signal part is working well without simulation and only receiving part needs to be researched if this actually possible to repeat the work of the LED sensor in the simulator. The circuit for the receiving part is proposed in Figure 8 - 1.
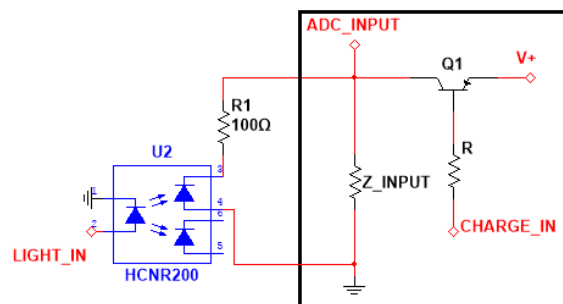
Figure 8 - 1. Circuit to imitate the work of the Mitsubishi Laboratories circuit during signal receiving.

The results of the simulation are shown in the next Figure 8 - 2. As it can be observed, when there is no light signal, the discharge rate of the LEDs junction capacitance is slower and doesn't cross the reference voltage. This can be represented by the microcontroller as logical '0'. When the light signal is high, the LED discharges faster and crosses the reference voltage. In this situation microcontroller represents it as logical '1'. So, the rate of discharge depends on the junction capacitance of the LED and input impedance of the ADC. The reference voltage could be adjusted in order to reduce ambient light noise influence.
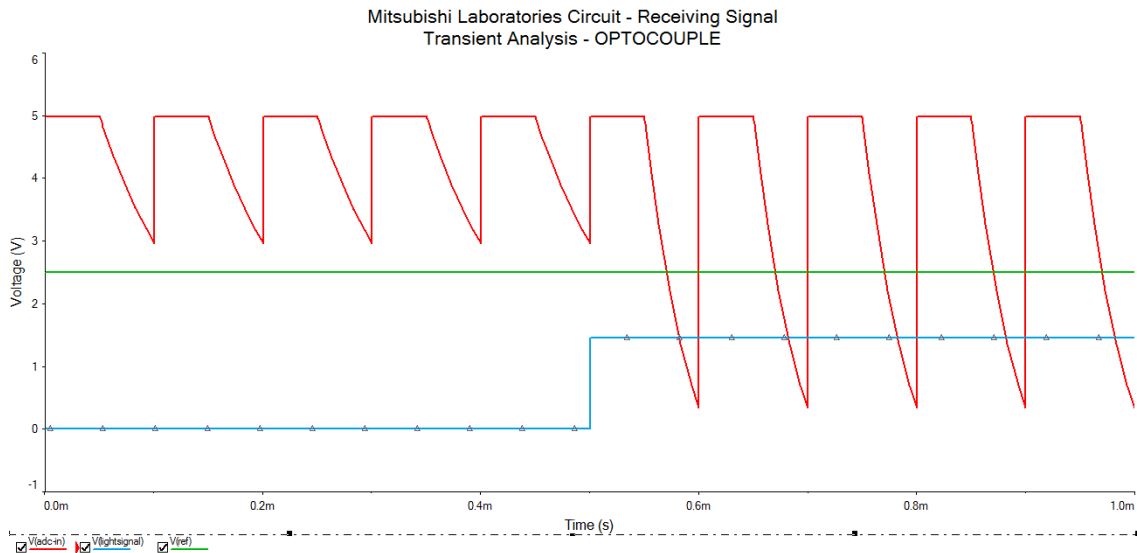
Figure 8 - 2. Results of the simulation of the circuit imitating the receiving part of the Mitsubishi Laboratories design. Input voltage for the ADC (red), reference voltage (green) and light signal (blue).

To conclude, though, there was no possibility to fully restore the work of the circuit and analyse it due to lack of the microcontrollers in the database, the simulator shows that this is still possible to rebuild it by using discreet components.

Appendix 9 – Calculation of the improved design components

The calculation was made only for the parts which are designed to improve original circuit's work. The list of the new parts is next:

- Passive high-pass filter with DC bias
- AC signal non-inverting amplifier
- Inverting Schmitt trigger
- 3rd order active low-pass filter

It should be noted that all calculations represent ideal cases and do not take into account limitations of the used active components.

Passive high-pass filter with DC bias

The idea of this part is to pass only AC part of the signal which should reduce the influence of the ambient light which is considered as the noise source. The circuit for this part is shown in Figure 9 - 1.
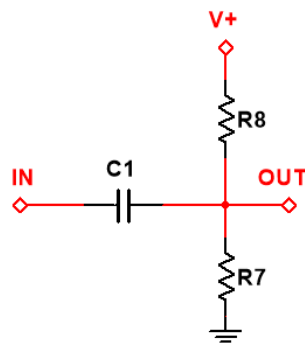
Figure 9 - 1. Passive high-pass filter with DC bias.

To reduce the influence on the load resistance of the LED sensor the resistors R7 and R8 were chosen 1MOhm and 1.5MOhm respectively. The capacitor C1 value was chosen 1nF. The resulting cut-off frequency equals:

$$f_{cut} = \frac{1}{2 \cdot \pi \cdot (R7||R8) \cdot C1} = 265.258 \, Hz \tag{9.1}$$

The calculated AC response of the filter is shown in Figure 9 - 2.
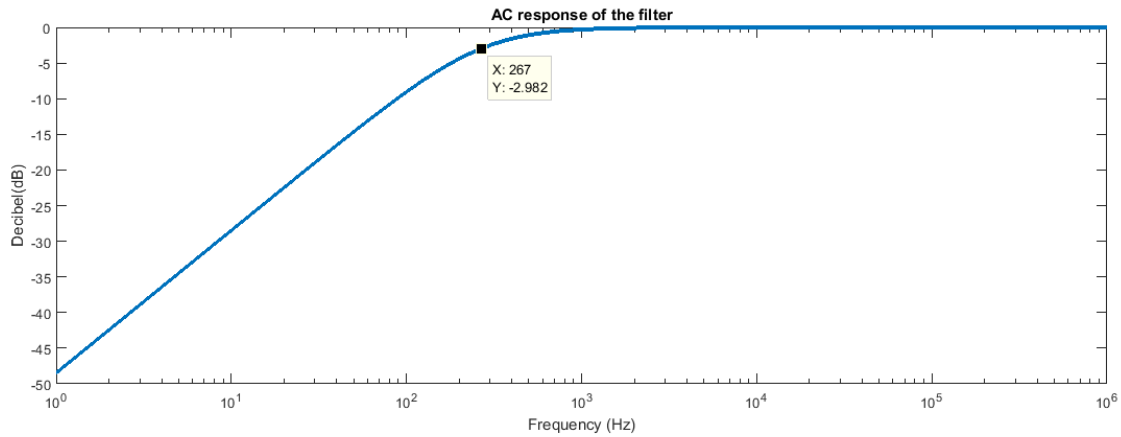
Figure 9 - 2. AC response of the filter with DC bias.

The sinusoidal signal lower than cut-off frequency would be attenuated. However, since the device works with the pulse signal which involves many frequency components, the higher frequency components won't be attenuated.

The R8 was chosen to be higher than R7 value on 50% and equals 1.5MOhm. The resulting DC bias:

$$V_{bias} = \frac{10^6 \cdot V_+}{1.5 \cdot 10^6 + 10^6} = \frac{2}{5}V_+ \tag{9.2}$$

The final bias value depends on the power supply voltage. If it equals 5V, the resulting DC bias would be 2V. In case it equals 3.3V, the resulting DC bias would be 1.32V. The resulting voltage on the output of the filter could be calculated with the next equation:

$$V_{out} = V_{DC} + V_{AC} = \frac{2}{5}V_+ + V_{in} \cdot \frac{(R7||R8)}{\sqrt{(R7||R8)^2 + (\frac{1}{2 \cdot \pi \cdot f \cdot C1})^2}} \tag{9.3}$$

AC signal non-inverting amplifier

The non-inverting amplifier from the original design was modified to amplify only AC part of the signal and pass DC part unamplified. The feedback resistor was replaced with one of higher resistance value. The resulting amplifier could be observed in Figure 9 - 3.

146
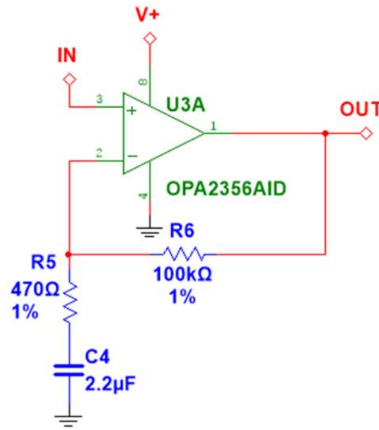
Figure 9 - 3. AC signal non-inverting amplifier.

The amplification for this filter equals:

$$\frac{V_{OUT}}{V_{IN}} = \frac{R6}{R5 - jX_{C4}} + 1 \qquad (9.4)$$

As it can be noted, the amplification of the amplifier depends on the frequency of the signal. At low frequencies the amplification falls until it reaches the minimum value of ~1. This will also mean that the DC voltage at the output would remain the same as it was on the input. At high frequencies the amplification reaches the maximum value of ~214. The AC response of the non-inverting amplifier could be observed in Figure 9 - 4.
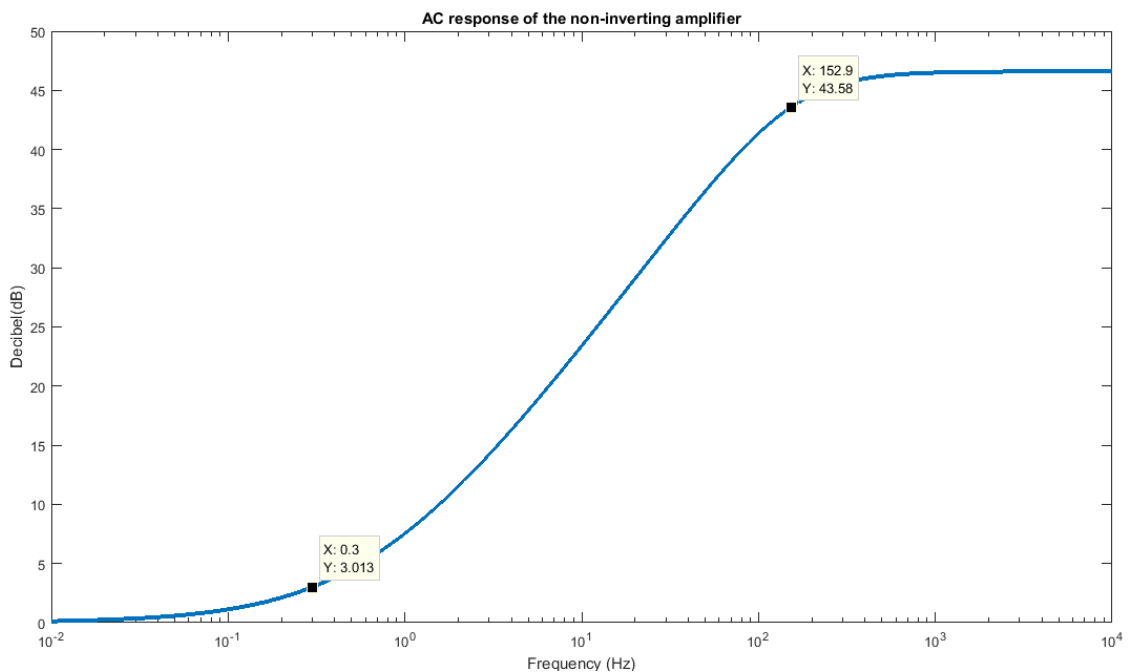
Figure 9 - 4. AC response of the non-inverting amplifier.

Inverting Schmitt trigger

The main idea of this circuit is to replace the comparator from the original design with the modified one which would also have hysteresis in order to reduce the noise influence. The new design could be observed in Figure 9 - 5.
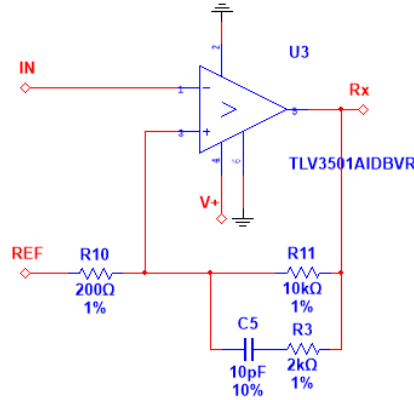
Figure 9 - 5. Inverting Schmitt trigger.

The hysteresis equation was taken from the provided datasheet [73] and for this circuit it equals:

$$V_{hys} = \frac{(V+) \cdot R10}{R10 + \dfrac{R11 \cdot \sqrt{R3^2 + X_{C5}^2}}{R11 + \sqrt{R3^2 + X_{C5}^2}}} + 0.006 \tag{9.5}$$

From equation it can be noted that the hysteresis value depends on the supply voltage and reactance of the capacitor which, in turn, depends on the frequency. These dependencies could be observed in Figure 9 - 6 and Figure 9 - 7. In the idle state, when no switching is performed, the hysteresis value equals 0.104V when the supply voltage is 5V and 0.071V when the supply voltage is 3.3V.

In case, when the circuit starts to switch, it's hysteresis changes to higher value providing a force effect and switching the comparator faster at higher frequencies. In that case during switching process the hysteresis value could change up to 0.542V when the supply voltage is 5V and 0.360V when the supply voltage is 3.3V. After switching the hysteresis returns back to the previous value.

148
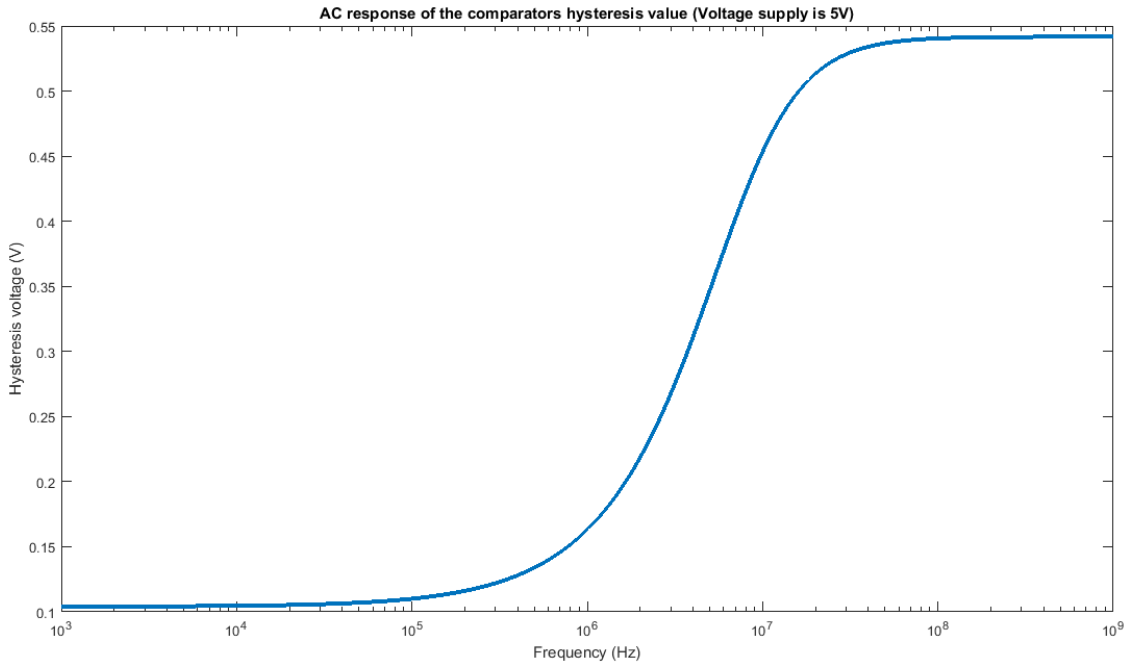
Figure 9 - 6. AC response of the comparators hysteresis when supply voltage is 5V.
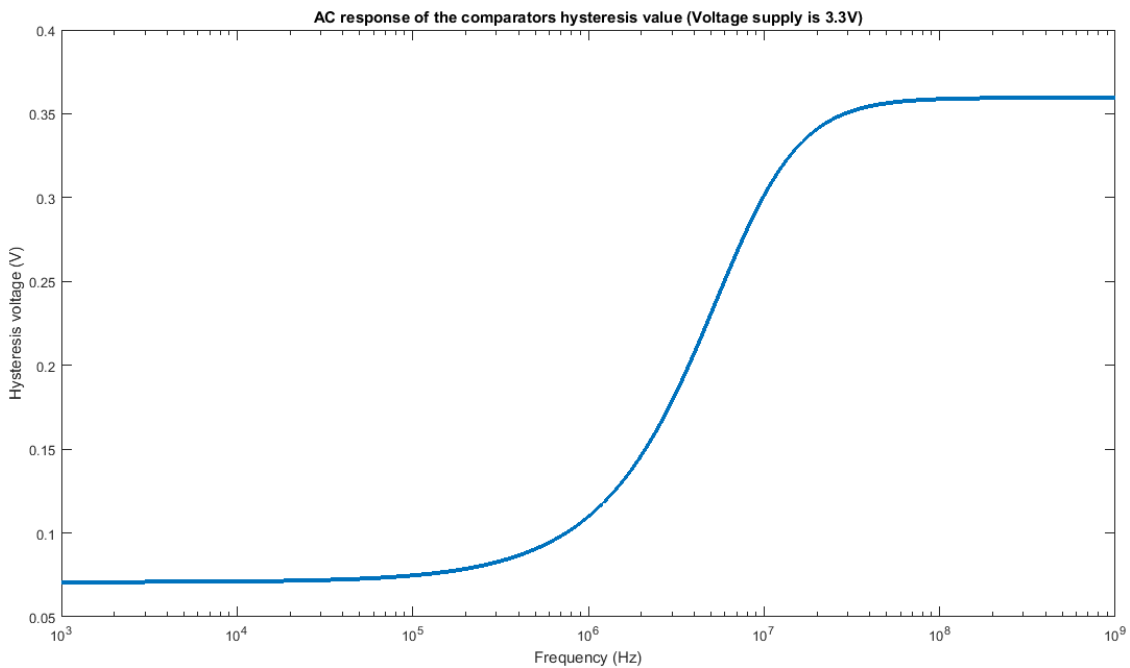
Figure 9 - 7. AC response of the comparators hysteresis when supply voltage is 3.3V.

3rd order active low-pass filter

The main idea of the design is to attenuate AC part of the signal higher than the cut-off frequency and pass only DC part. By passing the PWM signal through this filter, the DC voltage will be left on the output and by controlling the duty cycle of the PWM signal the DC value could be varied. The chosen circuit is shown in Figure 9 - 8.
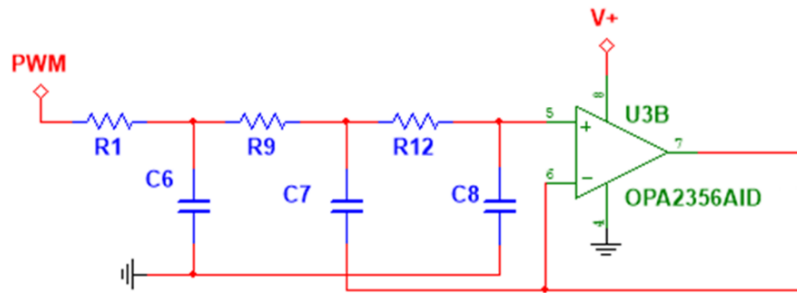
Figure 9 - 8. 3rd order low-pass filter.

The filter has 3rd order and made of Chebyshev type I with 1 dB pass band ripple due to the need of steeper roll-off. The cut-off frequency should be close to 1MHz. For easier calculation of the components values, the resistance values were taken the same and equal 10kOhm. The nominal capacitor value in this case equals:

$$C_{nom} = \frac{1}{2 \cdot \pi \cdot R1 \cdot f_{cut}} = \frac{1}{2 \cdot \pi \cdot 10^4 \cdot 10^6} = 15.924 \, pF \tag{9.6}$$

In order to determine all the capacitor values for the 3rd order filter, the coefficients [72] will be used, which are next: $C1_{coef} = 0.05872$, $C2_{coef} = 14.784$ and $C3_{coef} = 2.3444$. The first capacitor value equals:

$$C6 = C_{nom} \cdot C1_{coef} = 15.924 \cdot 0.05872 = 0.935 \, pF \tag{9.7}$$

All other values will be recalculated from the first capacitor value. The next values are:

$$C7 = \frac{C6 \cdot C2_{coef}}{C1_{coef}} = \frac{0.935 \cdot 10^{-12} \cdot 14.784}{0.05872} = 235.406 \, pF \tag{9.8}$$

$$C8 = \frac{C6 \cdot C3_{coef}}{C1_{coef}} = \frac{0.935 \cdot 10^{-12} \cdot 2.3444}{0.05872} = 37.324 \, pF \tag{9.9}$$

The final values should be rounded to more standard ones. Since the limit for cut-off frequency is 1MHz which shouldn't be exceeded, the values will be rounded to higher ones. The final capacitor values are: $C6 = 1 \, pF$, $C7 = 240 \, pF$ and $C8 = 39 \, pF$.

Appendix 10 – Simulation of the improved design of the communication device

The improved circuit based on EDN Networks was simulated and analysed. The work is divided on multiple parts where the circuit was sending and receiving the signals and where multiple parts of the circuit were analysed in order to see how they are working. The simulation part was done in "Multisim" environment which is based on SPICE.

Sending signal

During the sequence when the device was sending signal, the Tx sends the signal to the inverting buffer. The TxRx sets the inverting buffer enabled state and non-inverting buffer to logical '0' level. Resistor R2 limits the current flowing through the LED. The circuit which was being used for the simulation is Figure 10 - 1.
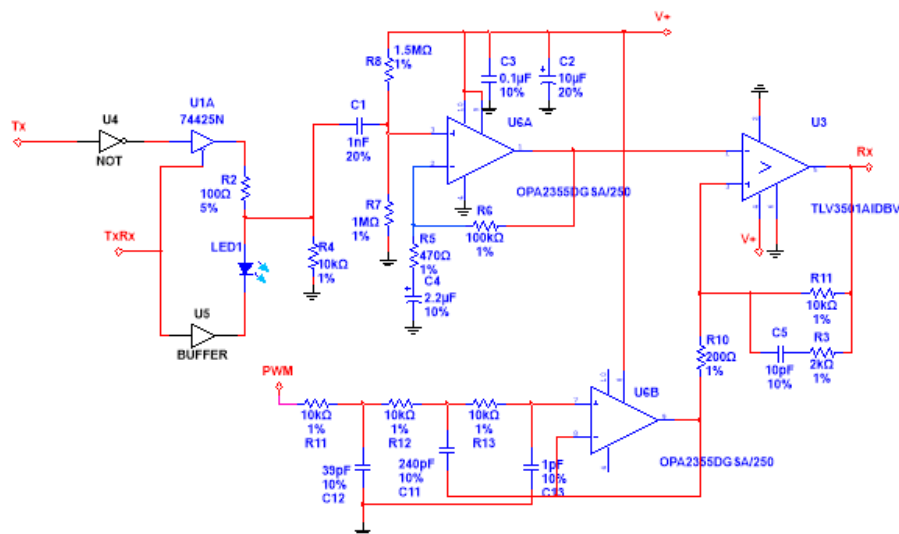
Figure 10 - 1. Circuit for the simulation when the device is sending signal.

The signal sending sequence was done at multiple frequencies to control how the circuit works. It was assumed that the input signal which was being sent was ideal and noiseless. The frequency values are 1kHz, 125kHz and 1.5MHz. The first results are shown in Figure 10 - 2 and Figure 10 - 3. As it can be observed, the device is working as intended and the output signal is inverted due to the inverting buffer. The output signal didn't have any distortions which could influence the shape of the signal, as it could be observed in signals Eye Diagram.
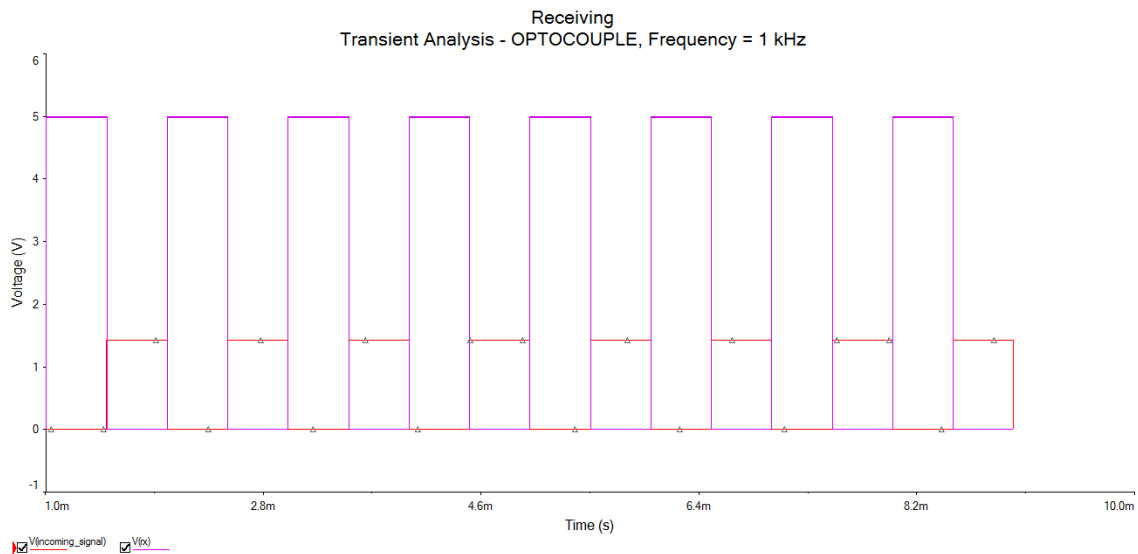
151
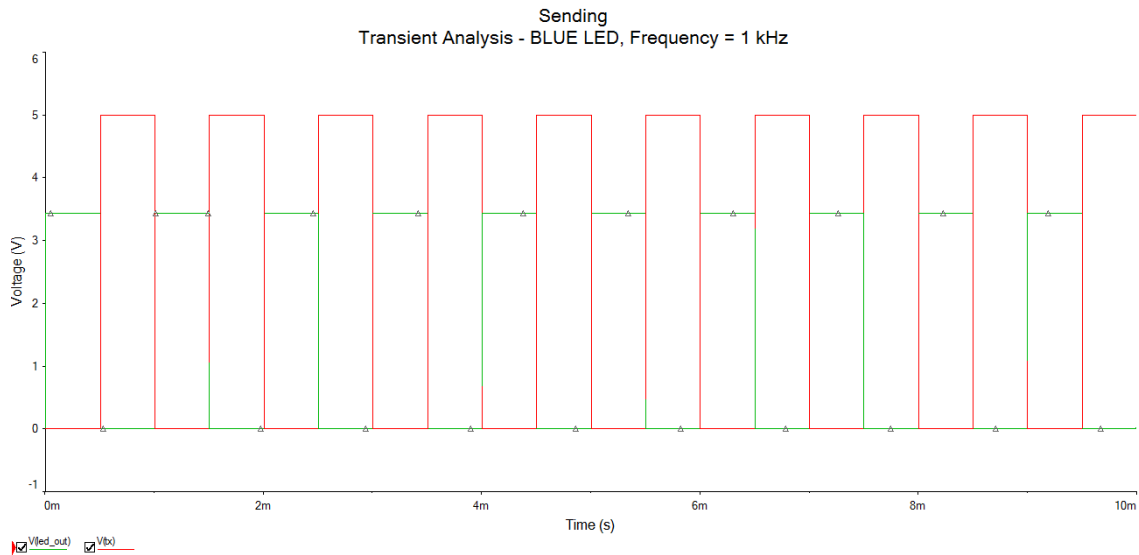
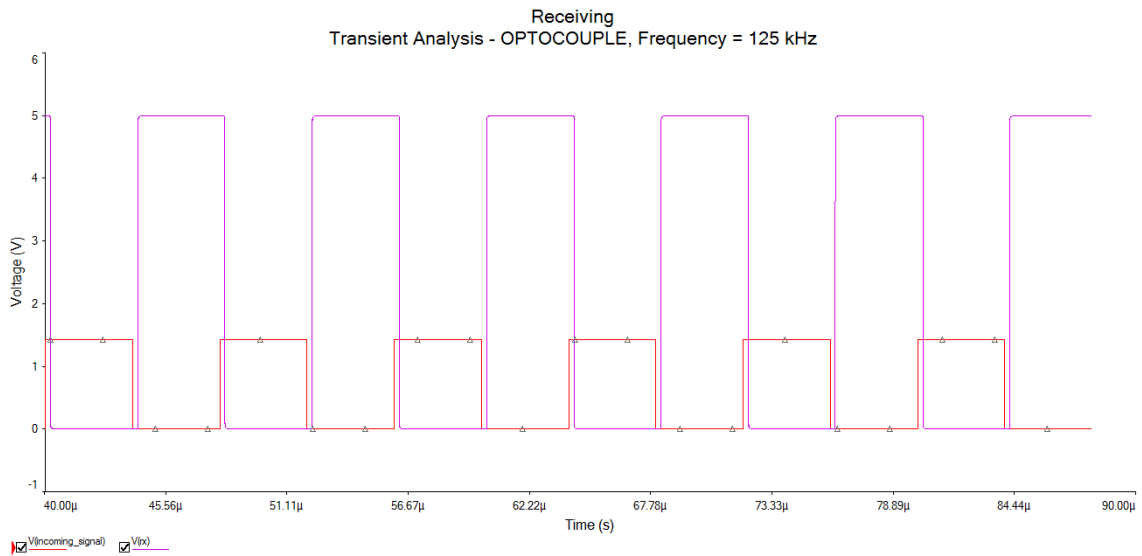Figure 10 - 2. Input signal (red) and output signal (green) of the device when it was sending 1kHz frequency signal.
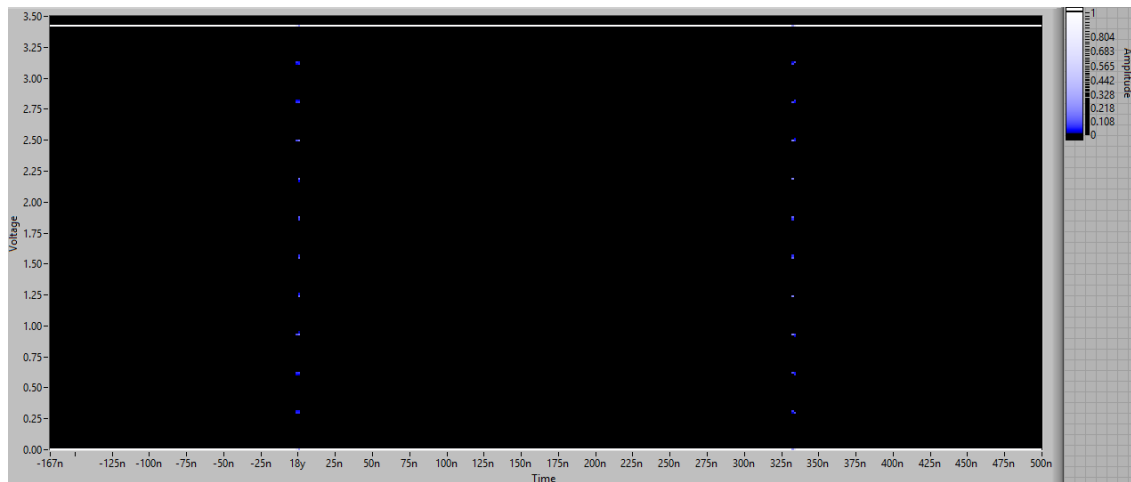
Figure 10 - 3. Eyediagram of 1kHz signal which was sent.

The results of the simulation with the 125kHz signal are shown in Figure 10 - 4 and Figure 10 - 5. At higher frequencies the shape of the output signal did change so dramatically as it was previously monitored in the original design. The problem was solved by adding buffer instead of PNP transistor which allows the LED to discharge through the resistor R2. The Eye Diagram shows that the signal still remains good square shape.
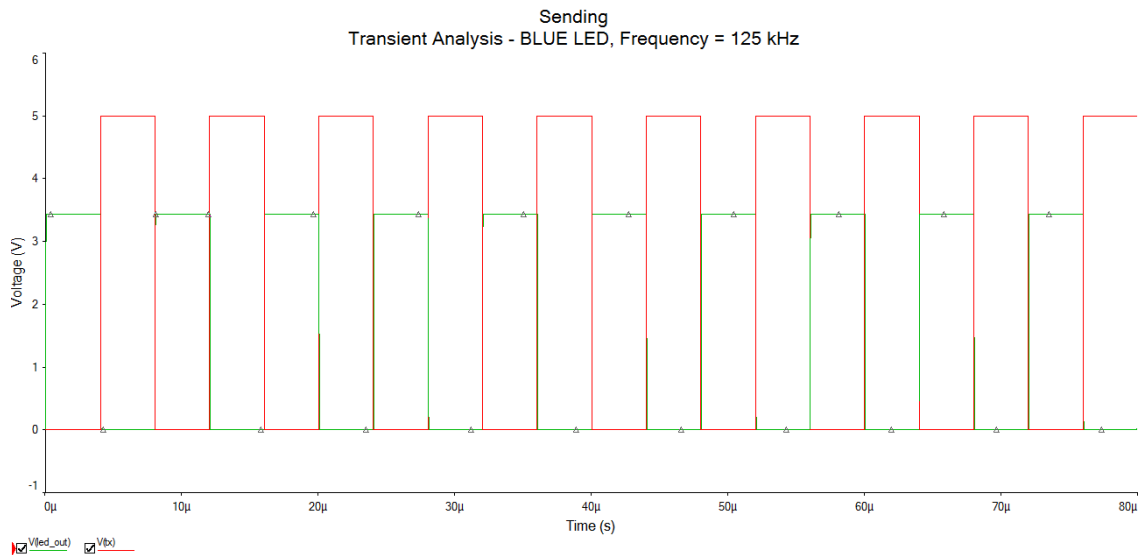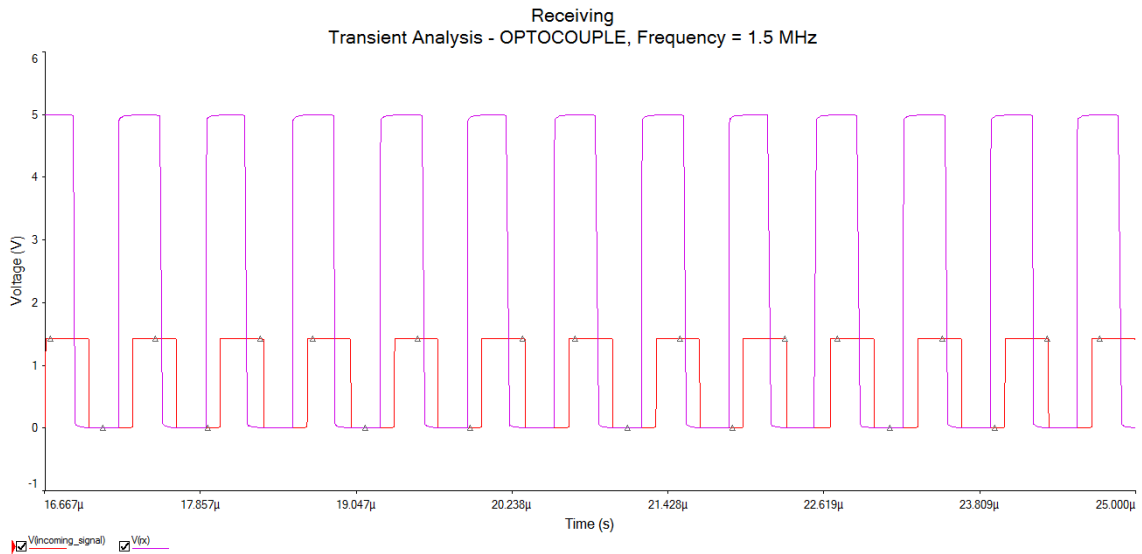
Figure 10 - 4. Input signal (red) and output signal (green) of the device when it was sending 125kHz frequency signal.
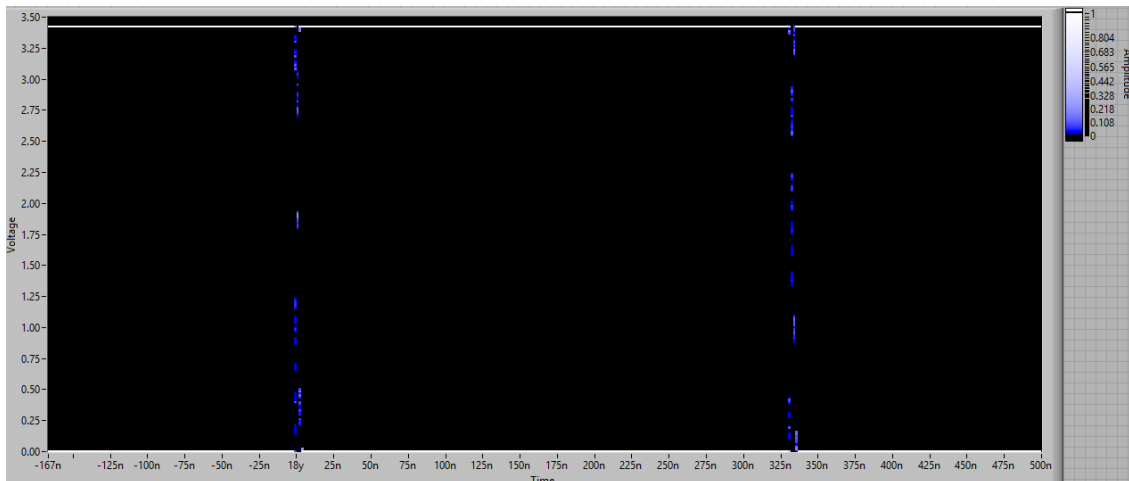
Figure 10 - 5. Eyediagram of 125kHz signal which was sent.

The results of the simulation with the 1.5MHz signal are shown in Figure 10 - 6 and Figure 10 - 7. At higher frequencies the shape of the output signal starts to change. The Eye Diagram shows that the rise and fall time is already not low enough to remain the square shape of the signal.
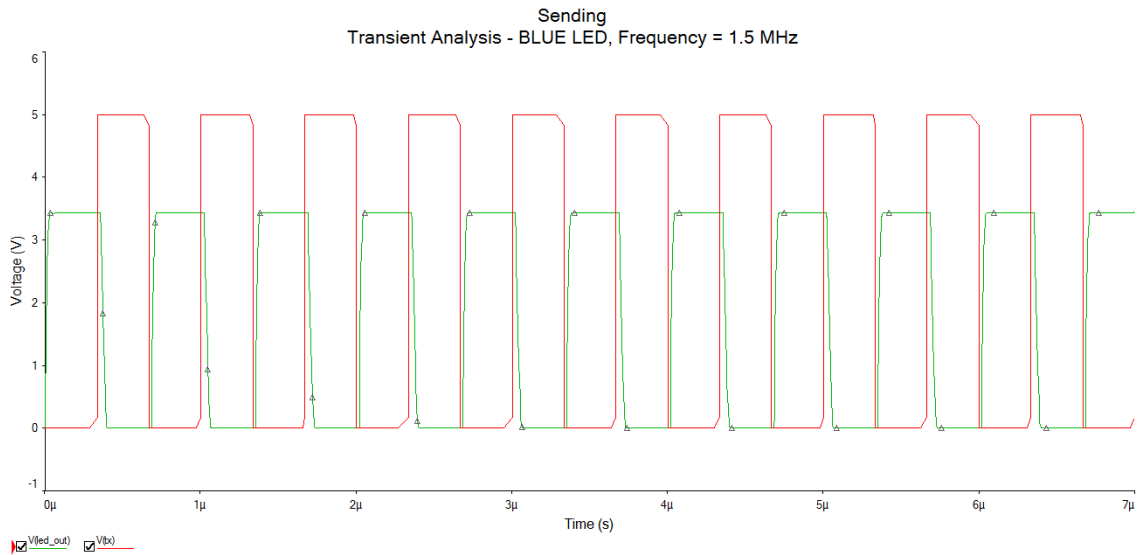
Figure 10 - 6. Input signal (red) and output signal (green) of the device when it was sending 125kHz frequency signal.
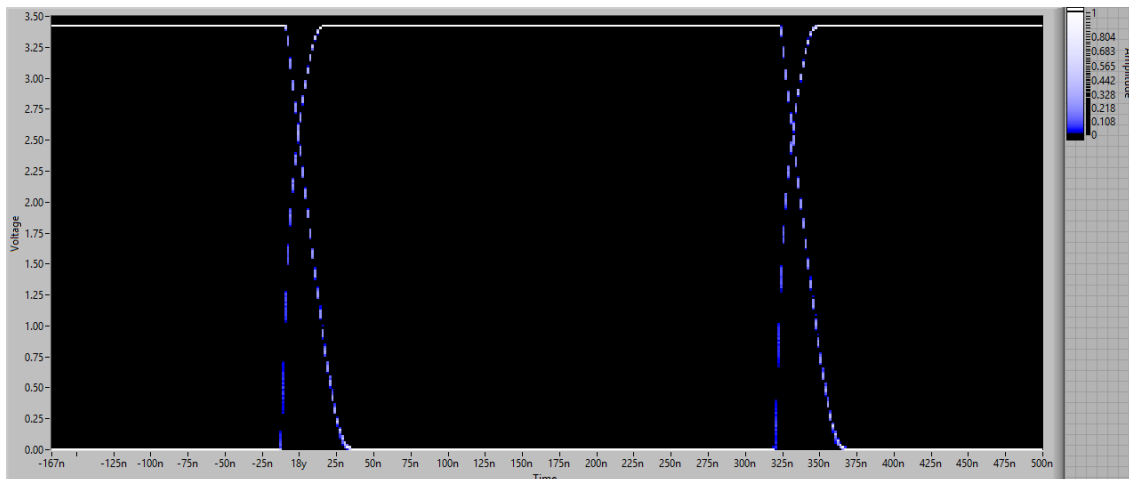
Figure 10 - 7. Eyediagram of 1.5MHz signal which was sent.

Overall results show that the sending part was improved and now the device is able to transmit signal at higher frequencies.

Receiving signal

In this part the LED was replaced with optocouple in order to imitate the work of the LED receiving the light signal. The circuit used for the simulation is shown in Figure 10 - 8. The inverting buffer is set to high impedance state and non-inverting buffer is set to logical "1" level in order to improve LEDs sensitivity. The current generated by LED flows through resistor R4. The voltage value of the AC signal is passed through high-

pass filter, amplified by modified non-inverting amplifier and sent to negative pin of the comparator. The output signal would be inverted.
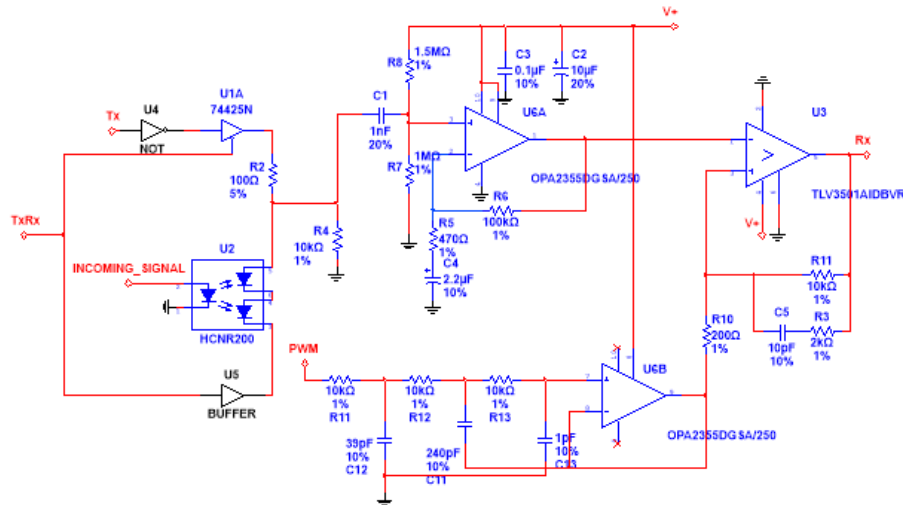
Figure 10 - 8. Circuit for the simulation when the device is receiving signal.

The simulated frequencies remain the same to control how the device is receiving signal. The received 1kHz signal is shown in Figure 10 - 9 and Figure 10 - 10. The input signal was specifically set lower in order to imitate the distance between the devices. But the results of the Eye Diagram show that the output voltage at RX is close to be ideal.

Figure 10 - 9. Input signal (red) and output signal (purple) of the device when it was receiving 1kHz frequency signal.
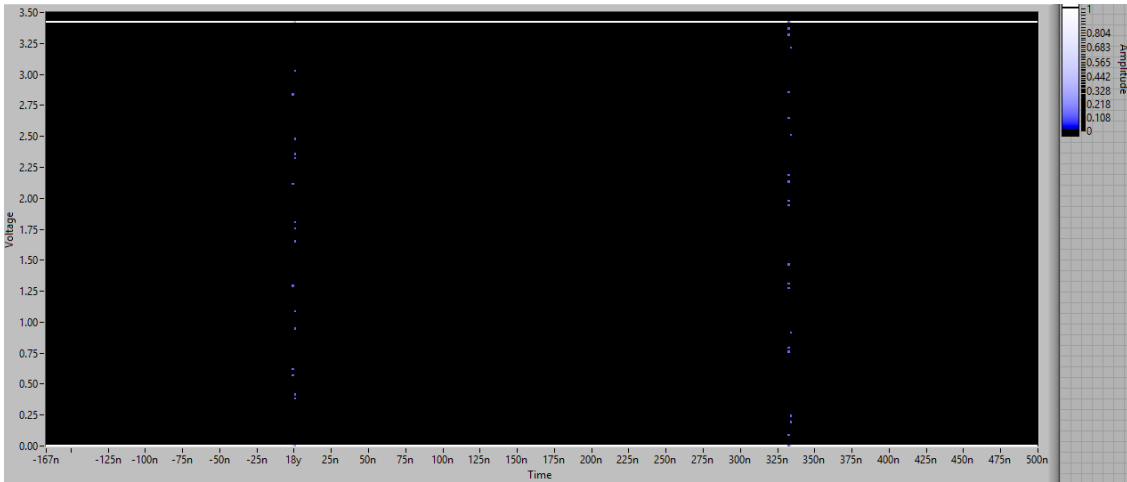
Figure 10 - 10. Eyediagram of 1kHz signal which was received.

The results with 125kHz signal are shown in Figure 10 - 11 and Figure 10 - 12. In case of 125kHz signal, the output signal at RX was shifted which means that the signal at the output of the non-inverting amplifier doesn't have ideal square shape. The reference voltage for the comparator was adjusted.

Figure 10 - 11. Input signal (red) and output signal (purple) of the device when it was receiving 125kHz frequency signal.

156
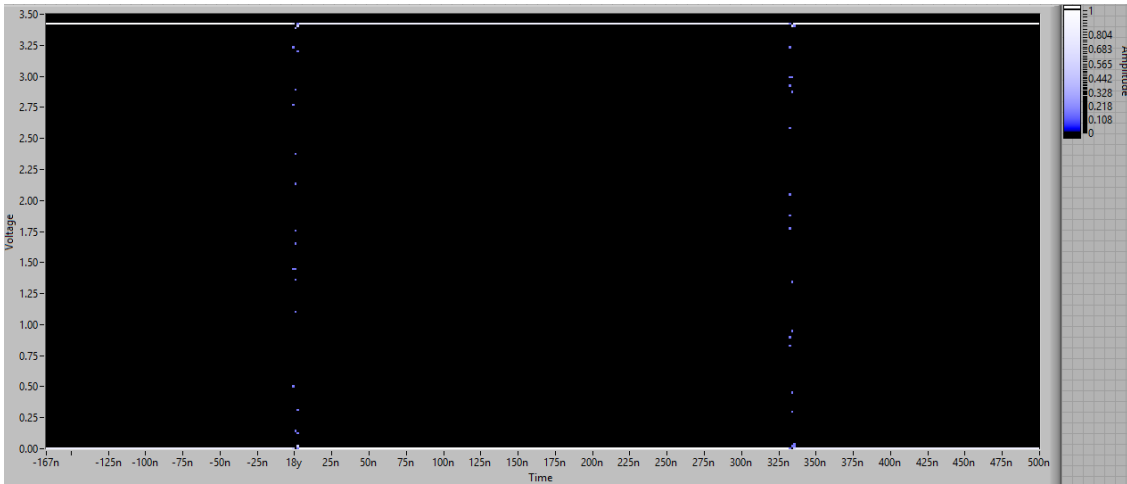
Figure 10 - 12. Eyediagram of 125kHz signal which was received.

The results with 1.5MHz signal are shown in Figure 10 - 13 and Figure 10 - 14. In case of 1.5MHz signal, the output signal at RX had bigger shift than in case with 125kHz frequency. The reference voltage for the comparator was adjusted again. At each frequency the reference voltage needs to be adjusted for better results.

Figure 10 - 13. Input signal (red) and output signal (purple) of the device when it was receiving 1.5MHz frequency signal.
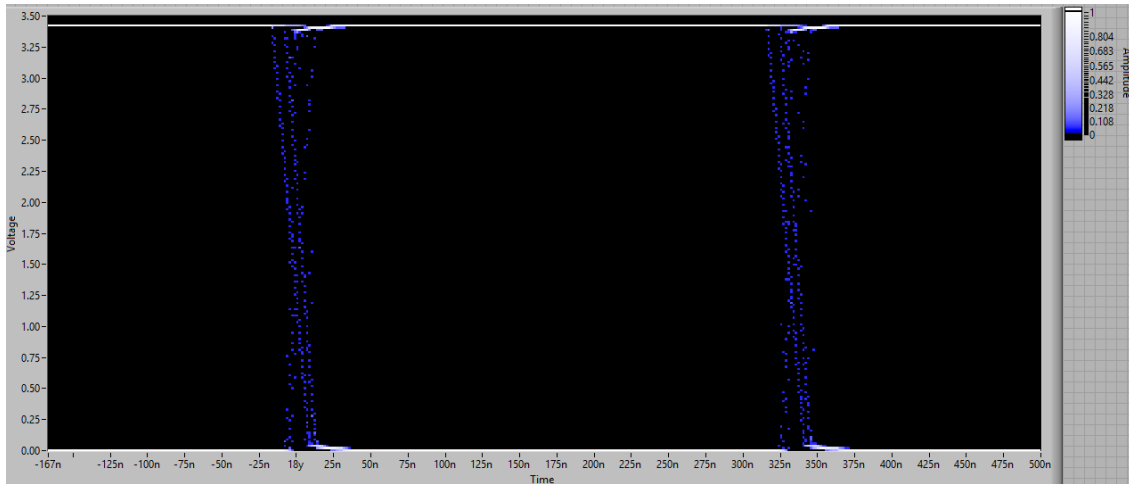
Figure 10 - 14. Eyediagram of 1.5MHz signal which was received.

Analysis of the non-inverting amplifier with high-pass filter with the DC bias

The non-inverting amplifier part in this design was modified in order to amplify only AC part of the signal. The modified circuit is presented in Figure 10 - 15. The DC bias voltage made by voltage divider using resistors R8 and R7 should be on the output of the circuit unamplified.
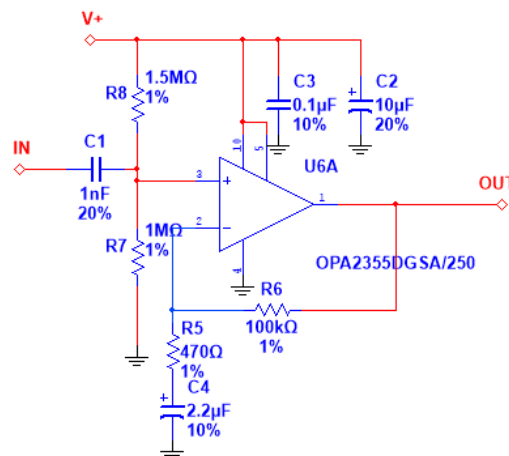
Figure 10 - 15. Circuit for the AC Response analysis.

The results in Figure 10 - 16 show that the circuit works as the band-pass filter with lower cut-off frequency at 330Hz and upper cut-off frequency at 1.16MHz. The gain of the amplifier is 46.6 dB. In Figure 10 - 17 is shown the comparison of the original non-inverting amplifier and the new one.

158
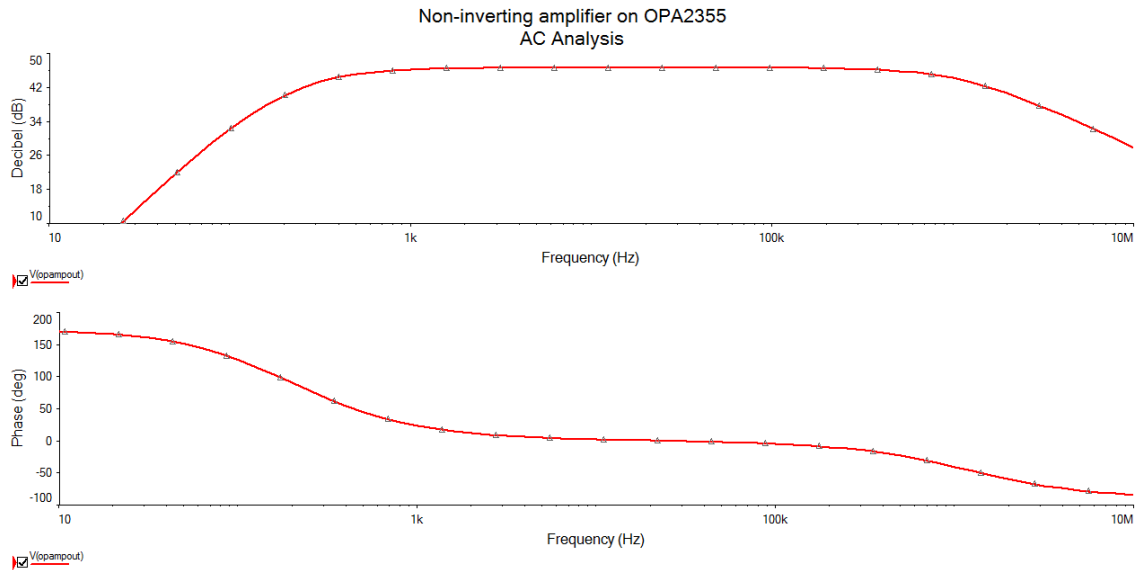
Figure 10 - 16. Results of the AC analysis of the non-inverting amplifier with high-pass filter with bias.
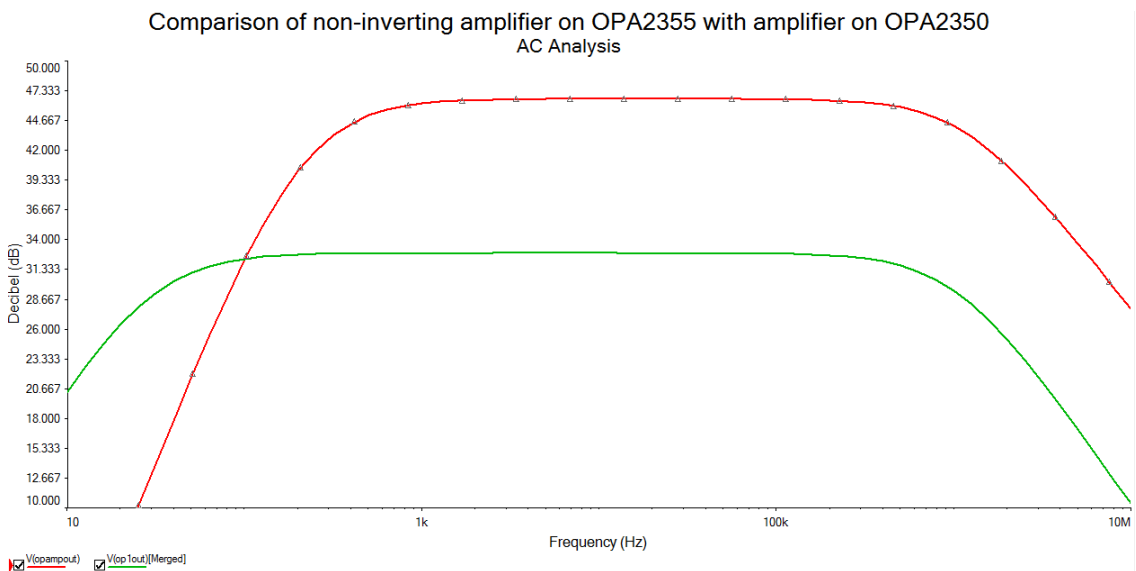
Figure 10 - 17. Comparison of previous non-inverting amplifier based on OPA2350 (green) and new one based on OPA2355 (red).

Analysis of the Schmitt trigger

The Schmitt trigger part of the new design was analyzed in order to overview it's work and behavior. The circuit under analysis is presented in Figure 10 - 18. The signal which was on input of the trigger is sinusoidal. The design was tested with two frequencies: 1kHz and 1.5MHz. The input signal had the DC bias voltage equal to the reference voltage.
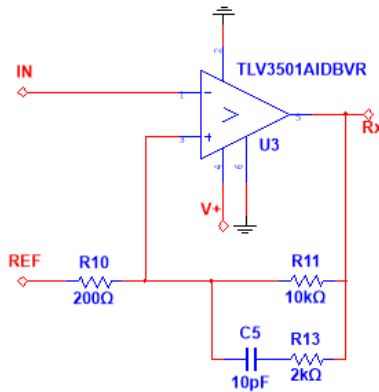
Figure 10 - 18. Comparator design part with adjustable reference.

The results of the simulation with 1kHz could be observed in Figure 10 - 19. It can be noted that positive input of the comparator has two different threshold voltages in order to switch. This should prevent from comparator from switching due to noise background. No oscillations like it was with previous design could be noted this time. The results for the 1.5MHz signal could be observed in Figure 10 - 20. Due to high frequency of switching, higher frequency components of the pulse signal pass through the C1R9 chain which results in spikes on the positive input of the comparator.
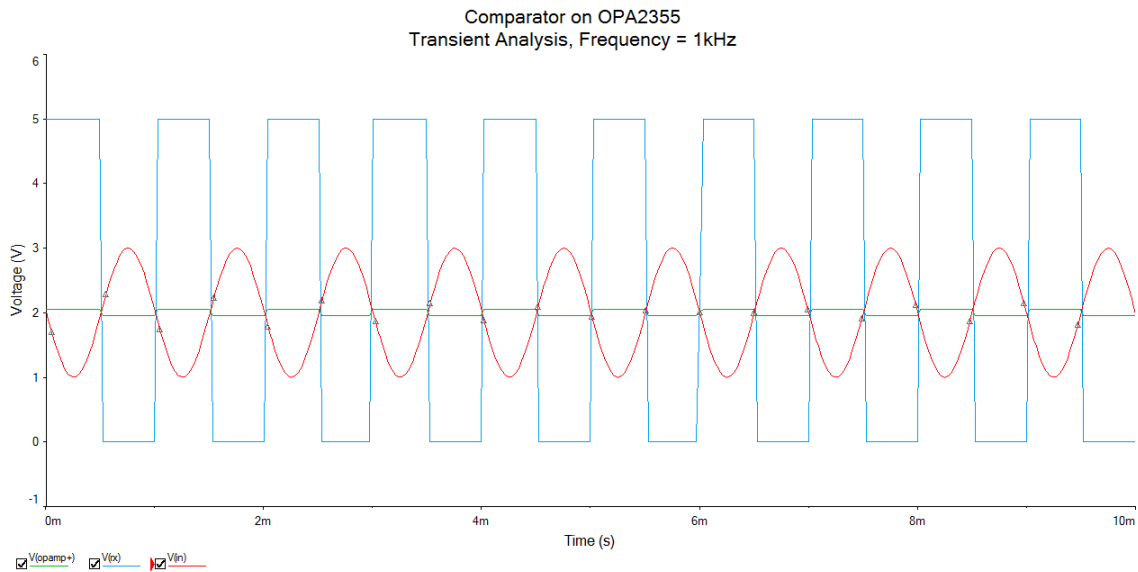
Figure 10 - 19. Input signal (red), reference voltage (green) and output signal (blue) of the comparator when the input signal frequency was 1kHz.

160
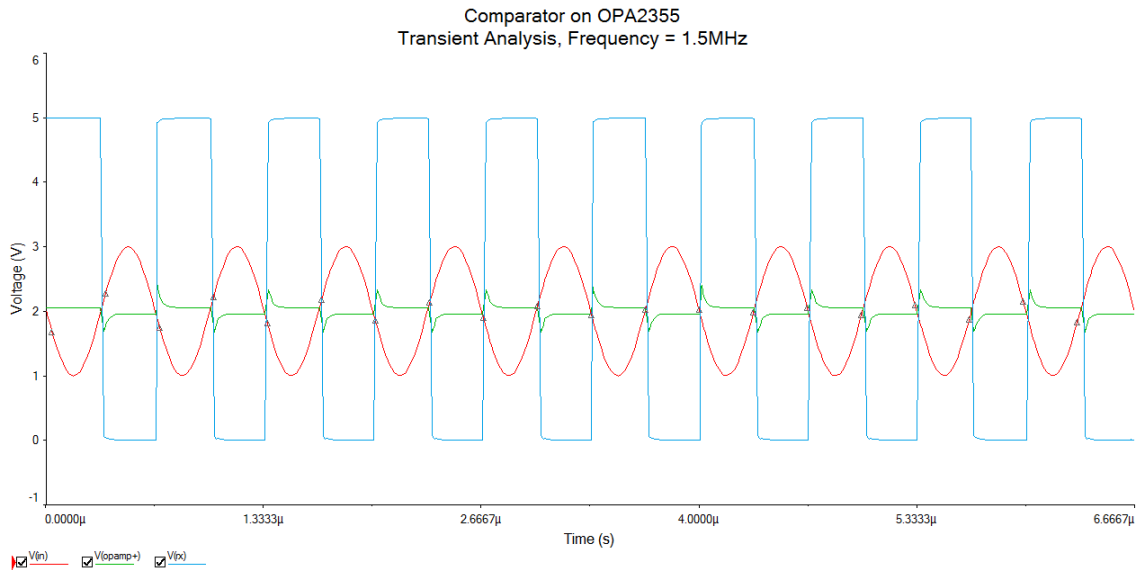
Figure 10 - 20. Input signal (red), reference voltage (green) and output signal (blue) of the comparator when the input signal frequency was 125kHz.

PWM signal to DC voltage converter

The circuit was designed to convert PWM signal to DC voltage. The circuit was built as 3rd order active low-pass filter Chebyshev type. The circuit is presented in Figure 10 - 21.
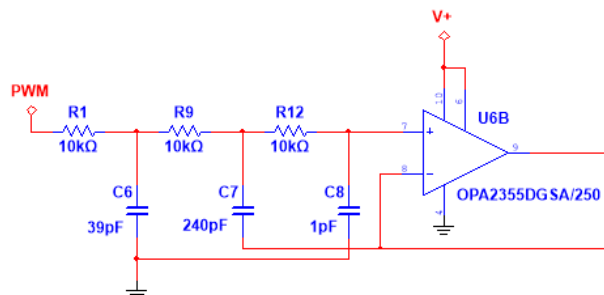
Figure 10 - 21. 3rd order active low-pass filter.

The results of the AC analysis in Figure 10 - 22 show that this low-pass filter with current component values have cut-off frequency equal to 593 kHz. The peak ripple at 394 kHz equals 2.68 dB. The previously estimated cut-off frequency was 1 MHz, but due to change of capacitor values to more standard ones, the final cut-off frequency value has shifted. Since the circuit is designed to work at higher frequencies starting from 4 MHz, the result is not considered as the downside. The resulting roll-off is close to be -80 dB/dec.

161
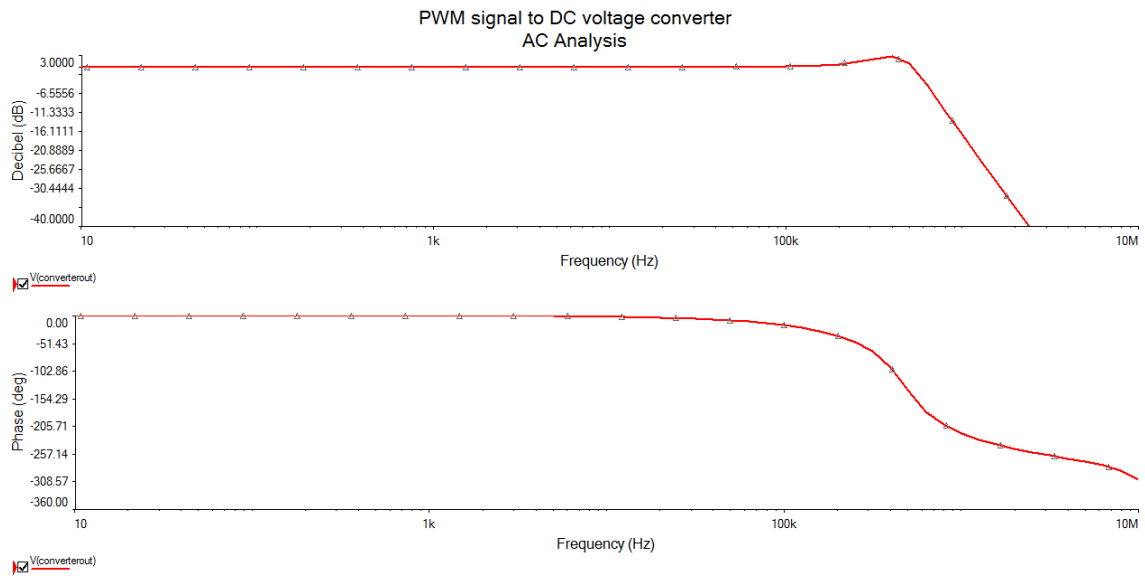
Figure 10 - 22. AC analysis of the 3rd order active low-pass filter Chebyshev type.

The next Figure 10 - 23 shows the transient simulation of the circuit where 4 MHz pulse signal with duty cycle 50% is passed to converter. The resulting output DC voltage should equal 2.5 V. As it can be observed, the output voltage oscillates and stabilizes only after 3.8 us. The main reason is that Chebyshev type filter frequency response has ripple which oscillates low frequency signals.
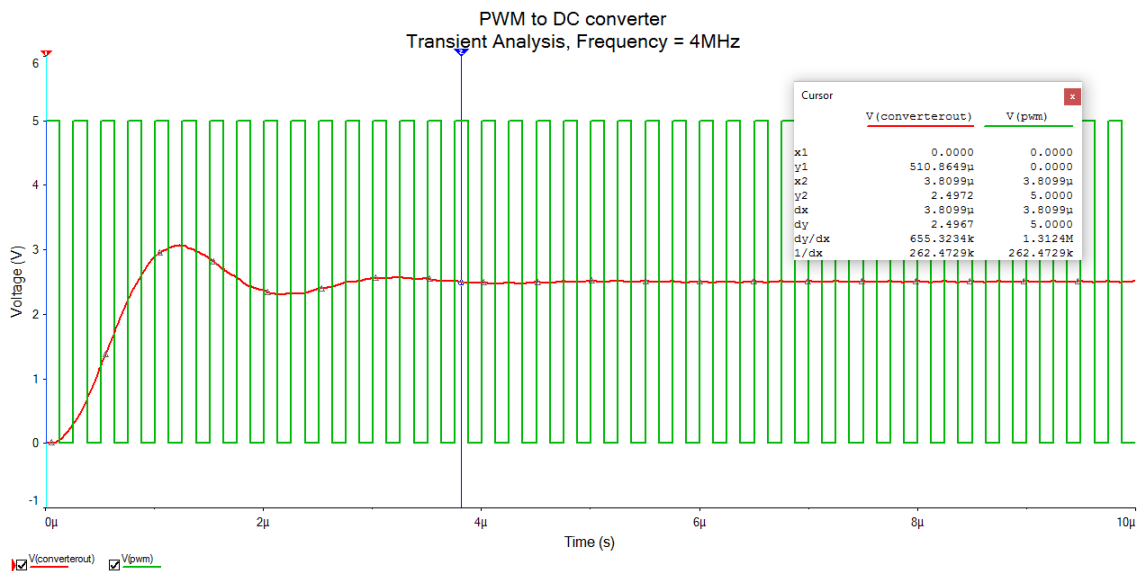
Figure 10 - 23. Transient analysis of the 3rd order active low-pass filter Chebyshev type. Green trace – input PWM signal, red trace – output of the converter.

162

Appendix 11 – Print Circuit Board of the improved communication device

The PCB design of the prototype board was made in the "Ultiboard" software, which allows to transfer the prepared circuit from the "Multisim" and design the PCB in more comfortable way.

All the components have their blueprints chosen and the input or output signals would have the connectors. During the design of the PCB board, next aspects were taken into consideration:

1. The board is only prototype and requires additional test points to control the correct values on the input and output.

2. The test points and connectors should be made with through-hole 2.54mm pins.

3. The traces and SMD components should be on one side.

4. It is likely that the board should have least THT components. They only could be used when the other traces are blocking the pass. The jumpers are final option.

'Ultiboard' software allows to autoplace all the parts and autoroute them, but in order to achieve all described tasks and recommendations which were described above, PCB was being designed manually. As a result, the board was designed with the length of 67mm and width of 40mm. The thickness of the board is 1.5mm. The width of the traces was set 0.5mm in order to prepare the board with improvised resources.

Since the top copper area wasn't used at all, there were placed all the THT components and 2 jumpers of different length. The pictures of the board with different layers and 3D models are shown in Figure 11 - 1 - Figure 11 - 5.
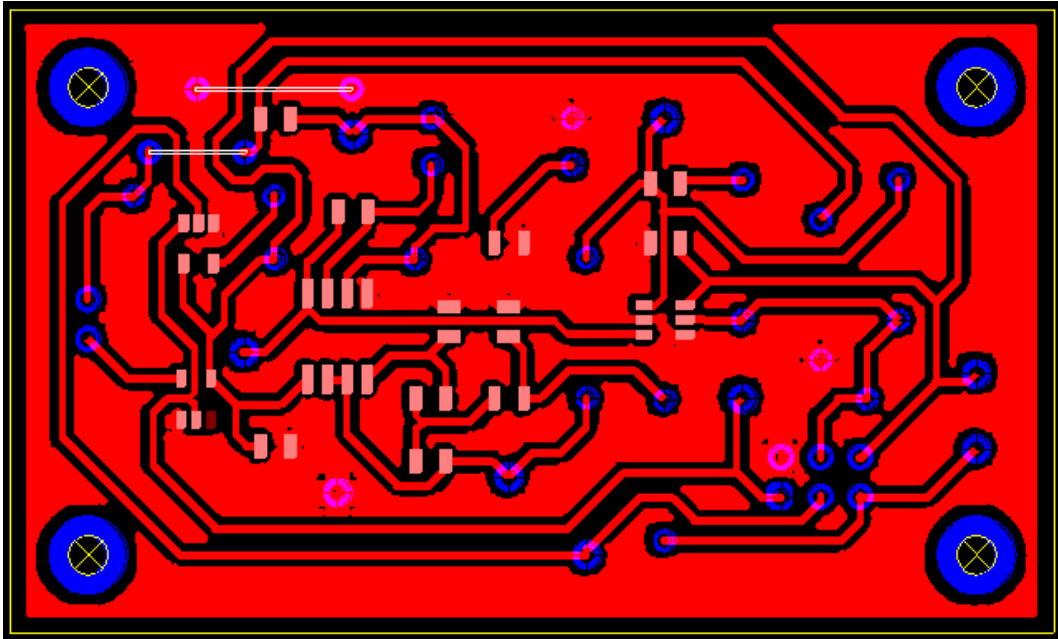
Figure 11 - 1. PCB with bottom copper cover.
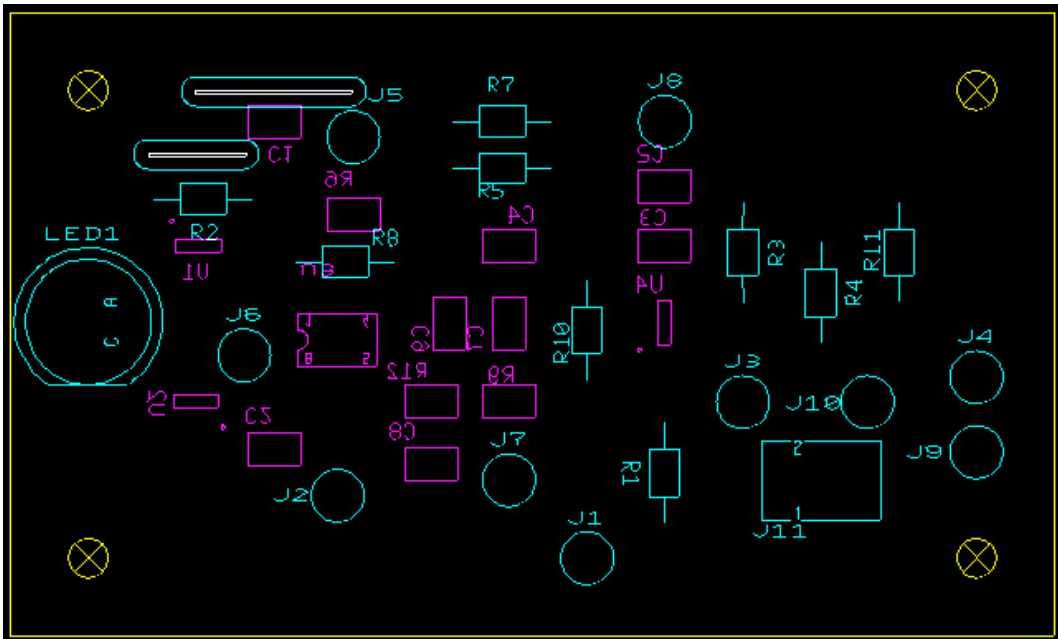
Figure 11 - 2. PCB with top and bottom silkscreens.

Figure 11 - 3. Board outlines and jumper positions.
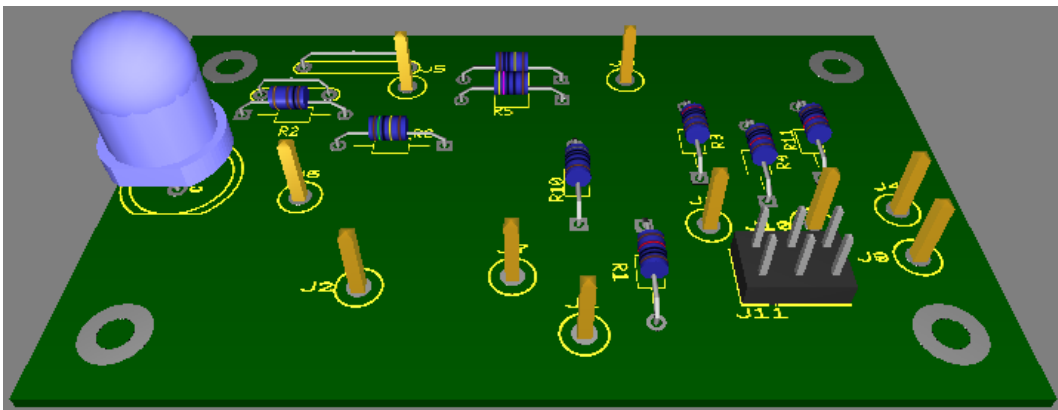
Figure 11 - 4. Top view of the prototype PCB 3D model.
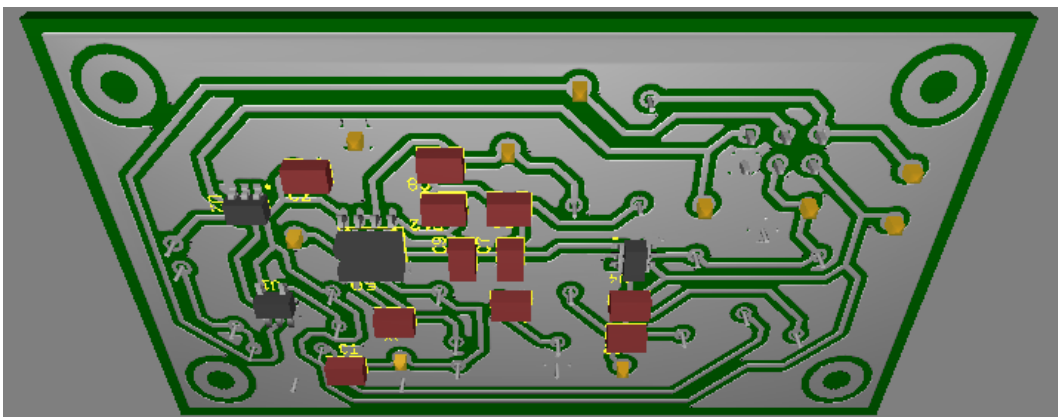
Figure 11 - 5. Bottom view of the prototype PCB 3D model.

Appendix 12 – Bill of materials for the improved communication device

All the components were purchased at Farnell. Note that some of the components could be only ordered in groups of multiple parts. The price regarding PCB is not included since the design could be constructed multiple ways. The price regarding LED is not included since the design is not tied to any particular LED.

Quantity	Description	Package	Reference Designator	Price for one	Total price
1	RESISTOR, 100kΩ 1%	0805	R6	0.0069	0.0069
1	RESISTOR, 470Ω 1%	RES900-300X200	R5	0.0553	0.0553
1	CAP_ELECTROLIT, 10μF 20%	0805	C2	0.847	0.847
1	CAPACITOR, 0.1μF 10%	0805	C3	0.0521	0.0521
1	CAPACITOR, 1nF 10%	0805	C1	0.0669	0.0669
1	RESISTOR, 1MΩ 1%	RES900-300X200	R7	0.058	0.058
1	RESISTOR, 1.5MΩ 1%	RES900-300X200	R8	0.0733	0.0733
1	CAPACITOR, 2.2μF 10%	0805	C4	0.0764	0.0764
3	RESISTOR, 10kΩ 1%	RES900-300X200	R1, R4, R11	0.0575	0.1725
1	RESISTOR, 100Ω 5%	RES900-300X200	R2	0.0418	0.0418
1	COMPARATOR, TLV3501AIDBVR	SOT-23-6(DBV)	U4	2.88	2.88
1	RESISTOR, 200Ω 1%	RES900-300X200	R10	0.058	0.058
2	RESISTOR, 10kΩ 1%	0805	R9, R12	0.0021	0.0042
1	CAPACITOR, 39pF 5%	0805	C6	0.231	0.231
1	CAPACITOR, 1pF 50%	0805	C8	0.0289	0.0289
1	CAPACITOR, 240pF 10%	0805	C7	0.493	0.493
1	RESISTOR, 2kΩ 1%	RES900-300X200	R3	0.0433	0.0433
1	CAPACITOR, 10pF 5%	0805	C5	0.0237	0.0237
1	OPAMP, OPA2356AIDGK	MSOP-8(DGK)	U3	3.49	3.49
1	3-STATE BUFFER, SN74LVC1G240	SOT-23-5(DBV)	U1	0.812	0.812
1	BUFFER, SN74LVC1G34	SOT-23-5(DBV)	U2	0.278	0.278
1	HEADERS, HDR2X3	HDR2X3	J1	0.304	0.304
				Totally:	10.0963

Table 12 - 1. Bill of materials for the improved communication device.

Appendix 13 – Results of the tests of the communication device

The improved visual light communicative device prototype was tested and its performance was monitored. The input signal type was square signal with duty cycle 50%. The supply voltage for the device was 5V. The test setup could be observed in next Figure 13 - 1.
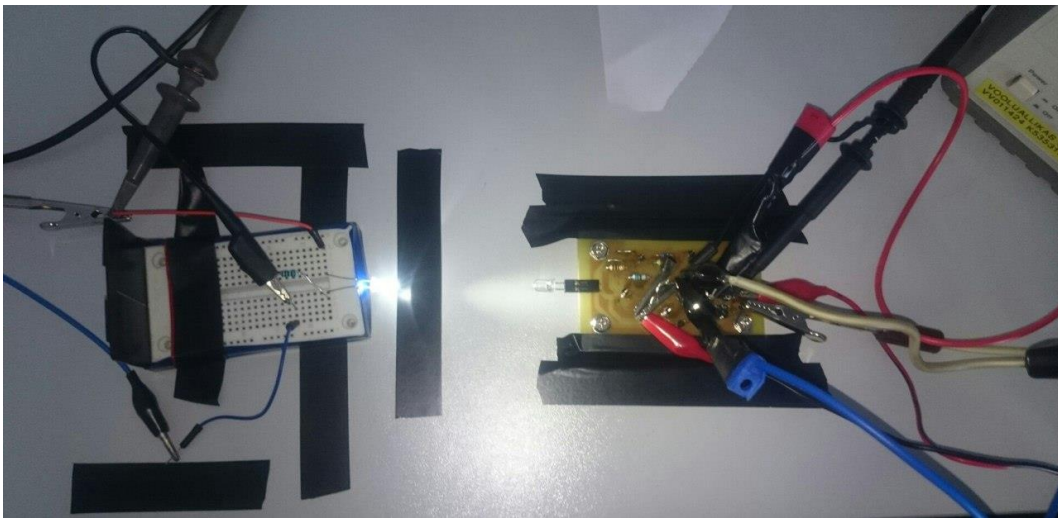
Figure 13 - 1. Picture of the test setup for the communication device.

Sending signal

Figure 13 - 2, Figure 13 - 3 and Figure 13 - 4 show the results where the device was sending signal. The TxRx pin was set to logical '0'. The Tx pin is marked with red colour and was connected to the function generator which generated 4.9 V peak-to-peak. The green trace represents the signal voltage on the Yellow Bright LED. The device sent the signal with different frequencies: 1kHz, 125kHz and 1.5MHz.

The results show that the output voltage on the LED is inverted as it was estimated. As it can be observed, the LED show good speed results, however, when the signal frequency is 1.5MHz, the oscillation could be observed. Additionally, at this frequency the shape of the output signal on the LED differs from the input signal and shows slope at the fall edge. The possible reason can be the length of the wires which connect the Tx pin to the generator.

Overall, the device able to send the signal at the desired speed and shows better results than in the simulation of the original design.
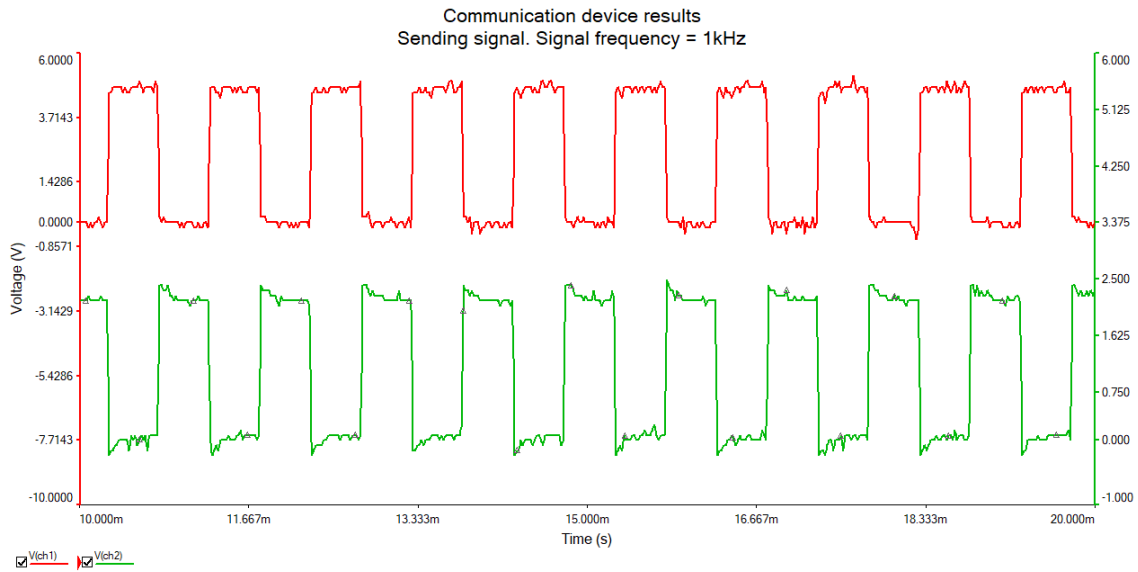
Figure 13 - 2. Communicative device sending signal with frequency 1kHz. Red trace – TX input signal, green trace – LED voltage.
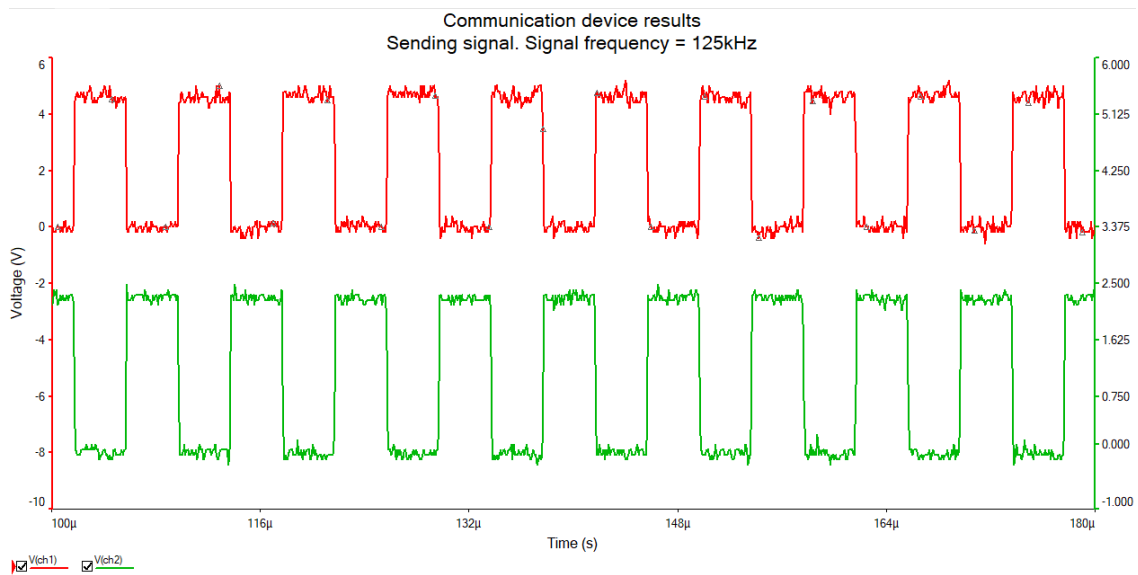
Figure 13 - 3. Communicative device sending signal with frequency 125kHz. Red trace – TX input signal, green trace – LED voltage.
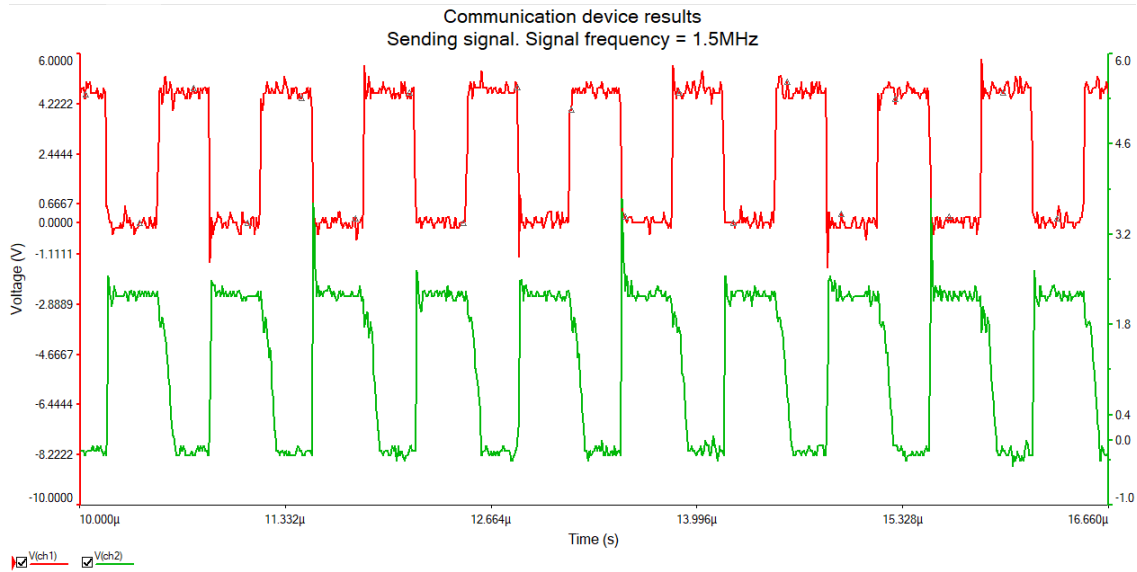
Figure 13 - 4. Communicative device sending signal with frequency 1.5MHz. Red trace – TX input signal, green trace – LED voltage.

Receiving signal

The next part was when the device needed to receive the signal. The higher the signal frequency, the smaller distance could be between the sender and the receiver. In case of the 1.5MHz the distance couldn't be longer than 30mm. The Figure 13 - 5 shows the results when the device was receiving the signal. The red trace represents the signal generated by the sender and the green trace represents the output signal of the device on the Rx pin. It was estimated that the output signal should be inverted, however, the results show that the output signal on Rx is in-phase to the in-phase with the input signal.
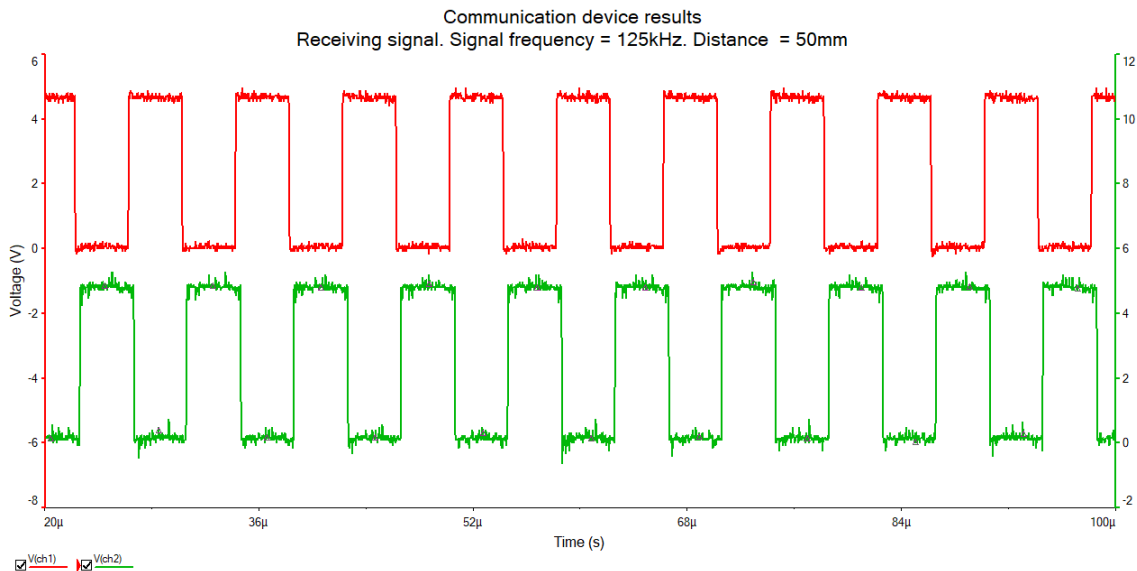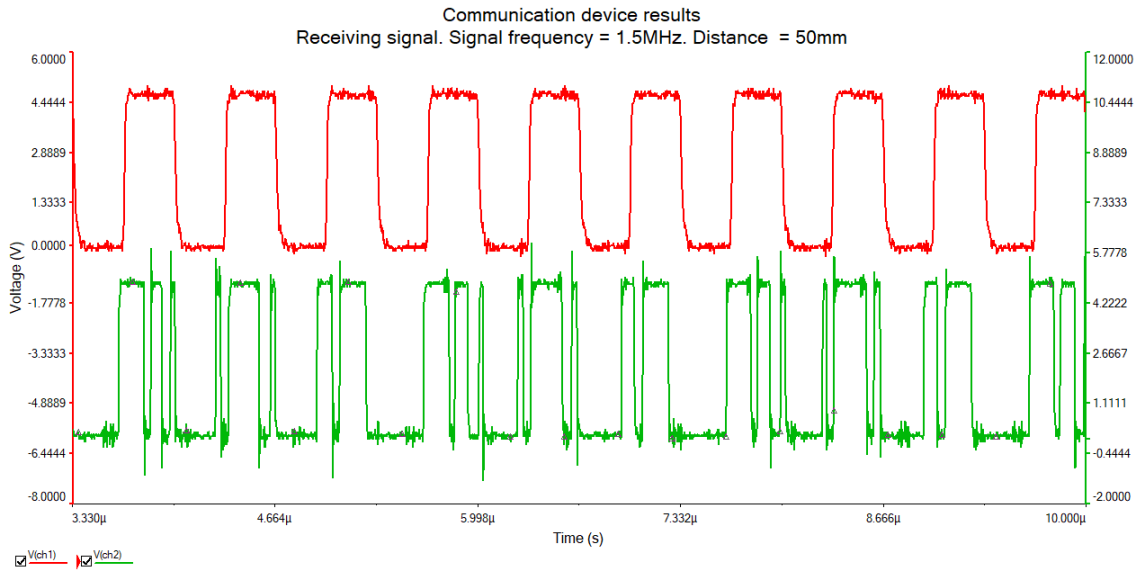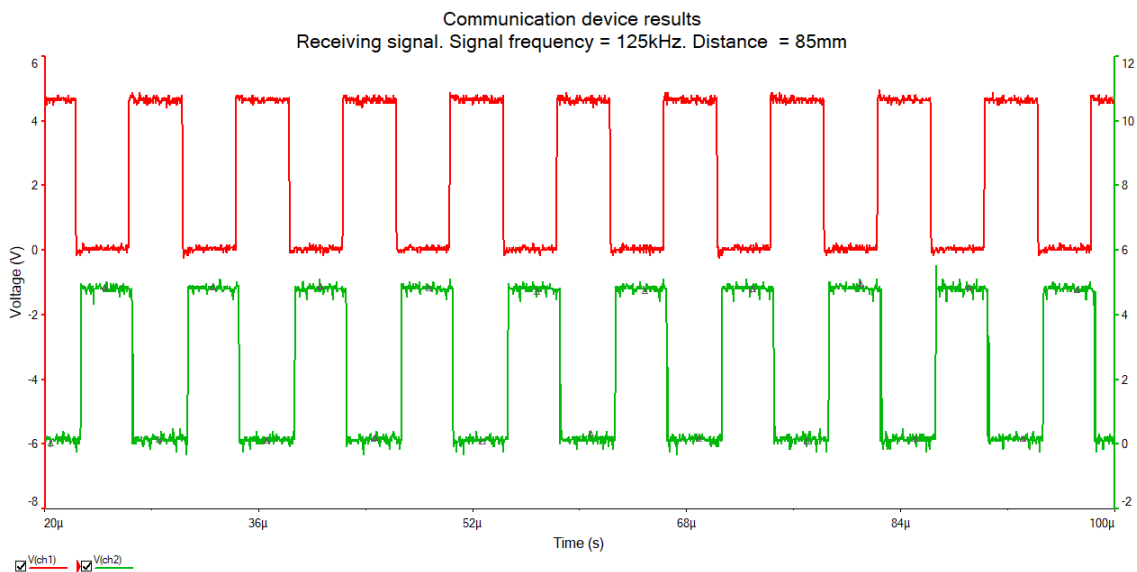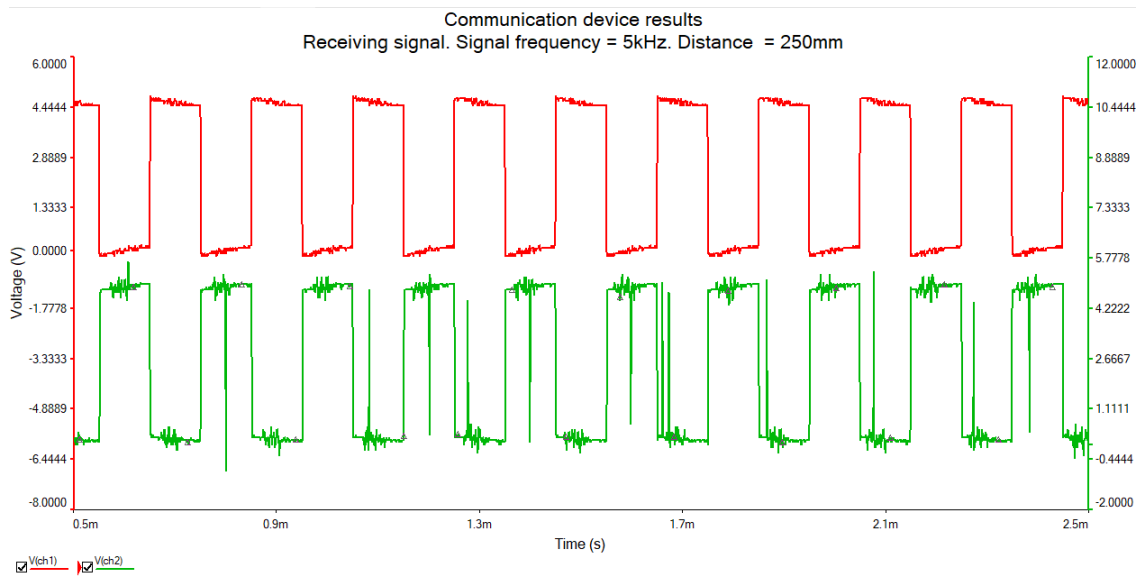
169
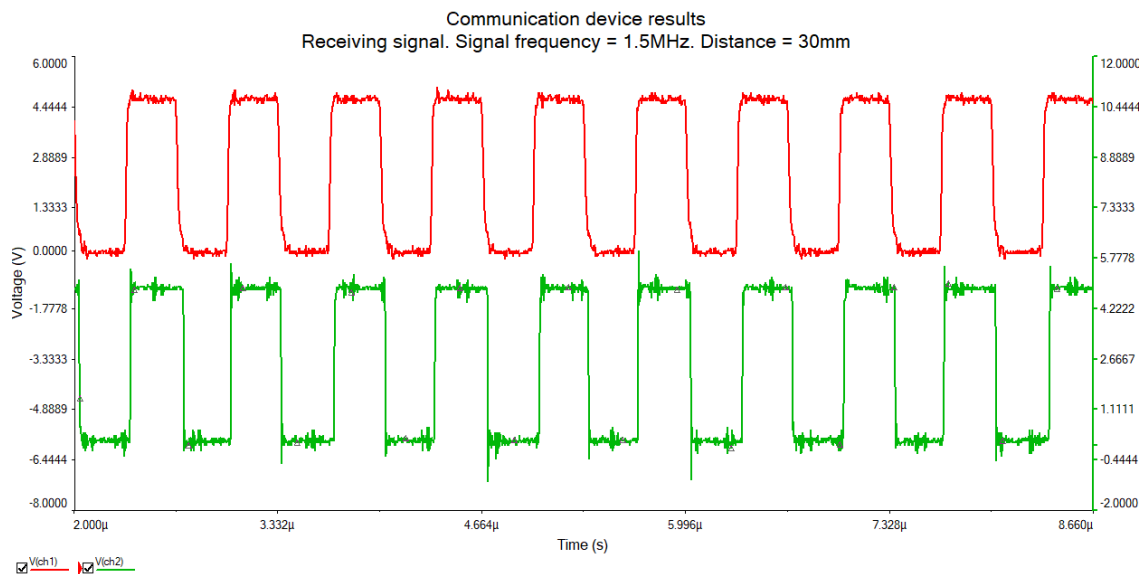
Figure 13 - 5. Communicative device receiving signal with frequency 1.5MHz. Distance between devices 30mm. Red trace – transmitter input signal, green trace – receiver output signal.

In order to understand why this condition appeared, the oscilloscope probe was connected to the output of the signal amplifier and the results could be seen in Figure 13 - 6. The voltage scale was set to 2V/div. The screen of the oscilloscope show that the output voltage appeared to be inverted. This means that it will be inverted again after the comparator and the phase of the output signal would be close to 0. The simulation showed that the phase shift at this frequency on the output of the amplifier should be close to $-90°$ and this means that the signal was shifted on $-90°$ one more time on the 10kOhm current-to-voltage converting resistor. To sum up, this resulted in setting the output signal at Rx pin in-phase with the signal which was generated.
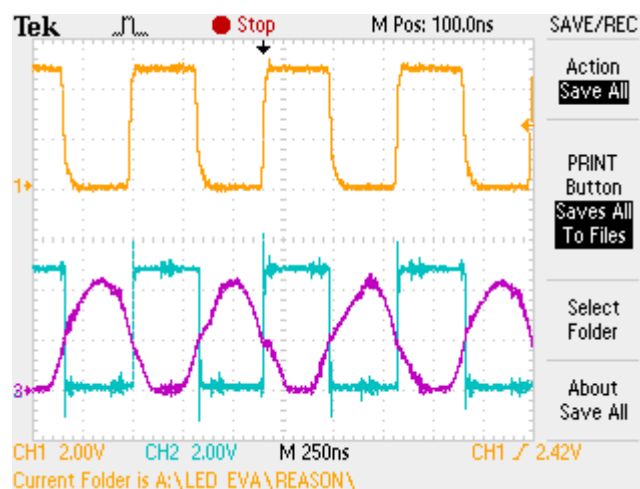
Figure 13 - 6. Oscilloscope picture with the output signal of the first operational amplifier. Distance between devices 50mm.

The Figure 13 - 7, Figure 13 - 8 and Figure 13 - 9 show the results when the distance between the sender and receiver was increased to 50mm. The good results were monitored with the signal frequencies 1kHz and 125kHz. In case of 1.5MHz signal it appeared to be distorted which means that the device cannot have stable output at this frequency with such distance.
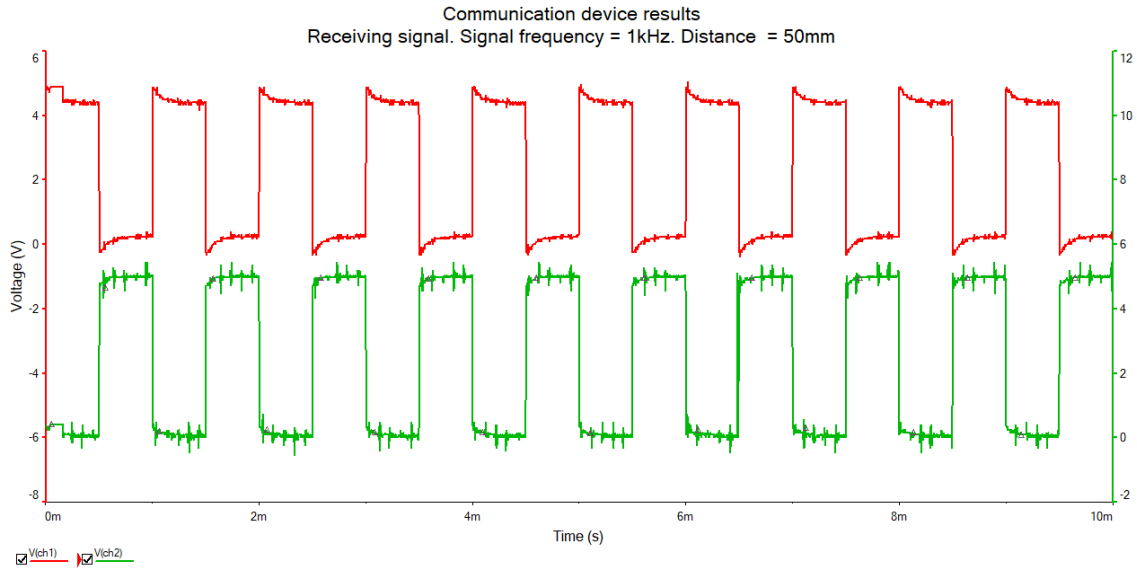
Figure 13 - 7. Communicative device receiving signal with frequency 1kHz. Distance between devices 50mm. Red trace – transmitter input signal, green trace – receiver output signal.
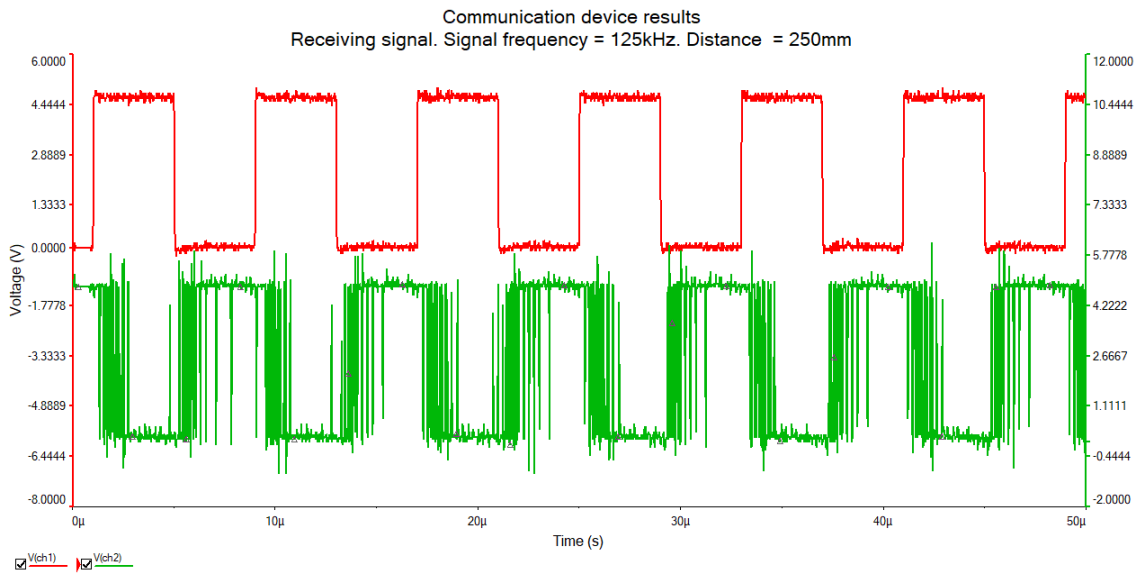

Figure 13 - 8. Communicative device receiving signal with frequency 125kHz. Distance between devices 50mm. Red trace – transmitter input signal, green trace – receiver output signal.

Figure 13 - 9. Communicative device receiving signal with frequency 1.5MHz. Distance between devices 50mm. Red trace – transmitter input signal, green trace – receiver output signal.

The next Figure 13 - 10 shows the results when the distance was increased again to the 85mm between the devices. This is the highest distance which could be set between the device and they could operate at the frequency of 125kHz. Further distance increase caused distortions on the output of the device.

Figure 13 - 10. Communicative device receiving signal with frequency 125kHz. Distance between devices 85mm. Red trace – transmitter input signal, green trace – receiver output signal.

The maximum distance at which the device could operate was 250mm. The frequencies which were tested at this distance were 5kHz and 125kHz. The reason why the 5kHz was set is that at this frequency the device had the most stable output for such distance. However, the distortions on the output still appeared. In case of the 125kHz, it could be observed that the device had too many distortions at the rise and fall edges, though, if

172

the signal could be filtered, the device would be still able to receive the incoming signal. The Figure 13 - 11 and Figure 13 - 12 show the results at 250mm distance.

Figure 13 - 11. Communicative device receiving signal with frequency 5kHz. Distance between devices 250mm. Red trace – transmitter input signal, green trace – receiver output signal.

Figure 13 - 12. Communicative device receiving signal with frequency 125kHz. Distance between devices 250mm. Red trace – transmitter input signal, green trace – receiver output signal.

Appendix 14 – Calculations of the transimpedance amplifier

For calculation, the parameters provided in the datasheet for OPA380 [85] will be used. The feedback resistor Rf for the circuit in Figure 14 - 1 was pre-chosen to be 100kOhm. The parasite capacitance of the diode is considered to be 50pF. The AD1580 [86] was used to settle the bias voltage on the positive pin of the transimpedance amplifier. The equations for calculations of the final parameters of the circuit were provided by TI Verified Design [74] and Application Notes [87].
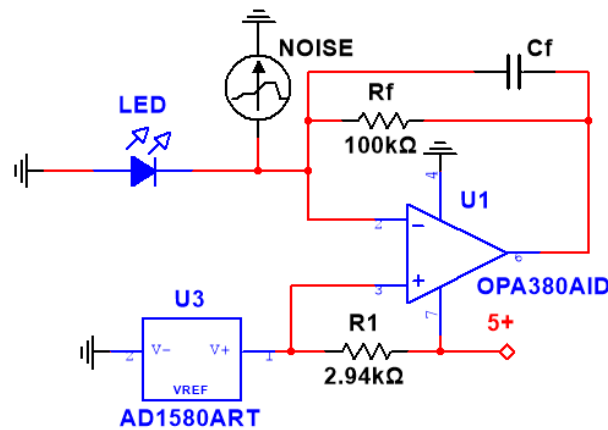
Figure 14 - 1. Transimpedance Amplifier Equivalent Circuit.

The specifications which would be used for calculations of the circuit parameters and component values are presented in Table 14 - 1.

Device	GBWP(MHz)	i_n $(\frac{fA}{\sqrt{Hz}})$	e_n $(\frac{nV}{\sqrt{Hz}})$	C_{diff} (pF)	C_m (pF)
OPA380	90	10	67	1.1	3

Table 14 - 1. Specifications of the OPA380

The Yellow Bright LED would be used as the light sensor which can output up to 1uA when the illuminance is 1000lx from White Bright LED and 20nA when the illuminance is 10lx. The output of the amplifier would be next:

$$V_{out} = i_{LED} \cdot R2 + V_B = 1.325V \qquad (14.1)$$

The total input capacitance of the device equals:

$$C_{in} = C_D + C_{diff} + C_m = 54.1\text{pF} \qquad (14.2)$$

174

The optimum compensation capacitor value equals next:

$$C_F = \sqrt{\frac{C_{in}}{2 \cdot \pi \cdot GBWP \cdot R_f}} = 978.05 \, fF \approx 1pF \tag{14.3}$$

And the resulting cut-off frequency of the bandwidth would be:

$$f_{-3dB} \cong \sqrt{\frac{GBWP}{2 \cdot \pi \cdot R_f \cdot C_{in}}} \approx 1.627 \, MHz \tag{14.4}$$

The input noise source could be calculated with next equation:

$$i_{ni} = \sqrt{i_n^2 + (\frac{e_n}{R_f})^2 + \frac{4 \cdot k \cdot T}{R_f} + \frac{(e_n \cdot 2 \cdot \pi \cdot f_{-3dB} \cdot C_{in})^2}{3}} \tag{14.5}$$

And the SNR is calculated with the following equation:

$$SNR = 20 \cdot \log(\frac{i_{min}}{i_{ni}}) \tag{14.6}$$

The i_{min} value in this case is the current value under 10lx illuminance and equals 20 nA. The final results of the noise source and SNR calculations are united in one Table 14 - 2.

Noise Current Term ($\frac{fA}{\sqrt{Hz}}$)	Noise Voltage Term ($\frac{fA}{\sqrt{Hz}}$)	Thermal Noise Term ($\frac{fA}{\sqrt{Hz}}$)	Input Capacitance Term ($\frac{pA}{\sqrt{Hz}}$)	SNR (dB)
10	670	405	21.4	59.4

Table 14 - 2. Noise source and SNR values.

The final result show quite high SNR, however, the output value of the amplifier may require additional amplification. Post amp gain also influences the SNR of the 1st stage amplifier and as a result next amplification stages should be taken with caution.

Appendix 15 – Simulation results of the transimpedance amplifier

The designed transimpedance amplifier was analysed in the simulation environment 'Multisim'. The circuit used for transient analysis is shown in Figure 15 - 1. The optocouple is used to imitate the LED receiving the light signal. The I1 current source is used as the noise source. The Gaussian white noise is generated from the previously calculated signal-to-noise ratio.
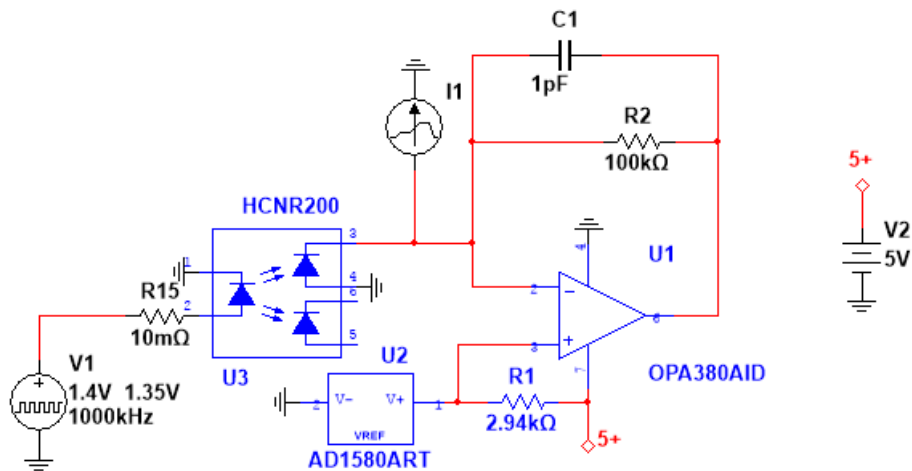
Figure 15 - 1. Circuit of the transimpedance amplifier for the transient analysis.

The transient analysis was done in order to see what voltage values are one the output of the amplifier and how amplifier respond to different photocurrents and signal frequencies. The Figure 15 - 2 shows the output of the amplifier when the peak-to-peak photocurrent was 90nA. The estimated peak-to-peak voltage value is 9mV. However, simulation output shows 7.287mV peak-to-peak value.
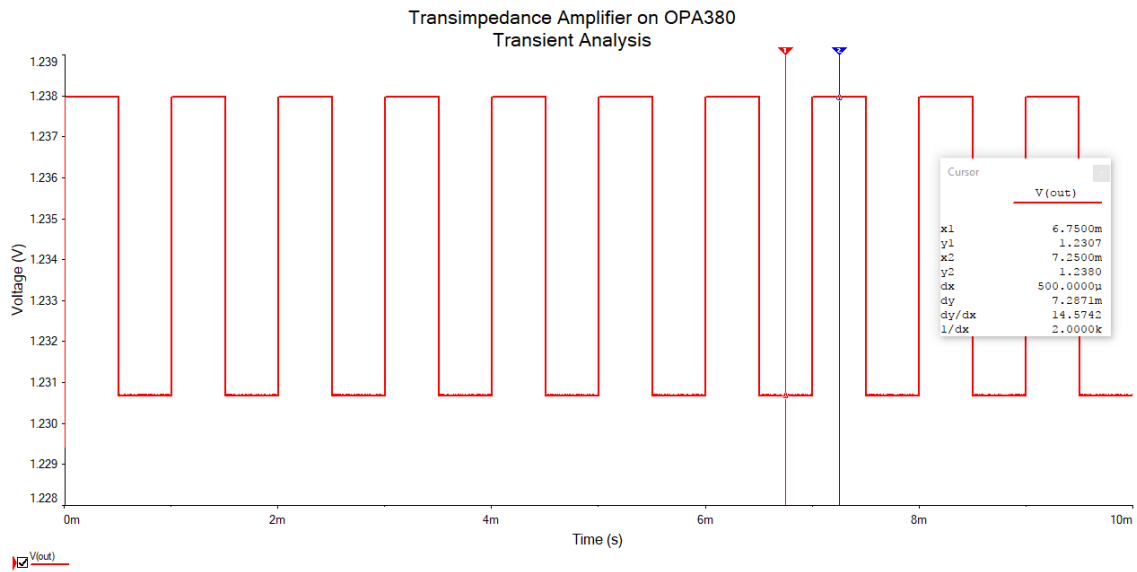
Figure 15 - 2. Output of the transimpedance amplifier with the signal frequency 1kHz and peak-to-peak value 90nA.

The next Figure 15 - 3 shows the results of the simulation when peak-to-peak value was increased to 990nA. The estimated peak-to-peak voltage output is 99mV. The results show that the peak-to-peak voltage output is 98.77mV.
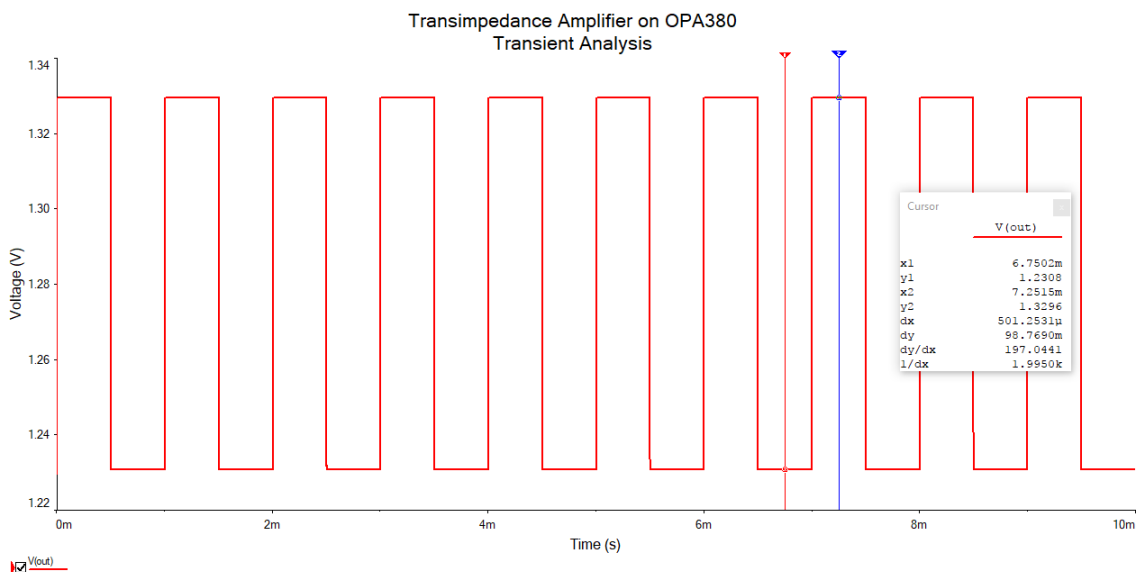
Figure 15 - 3. Output of the transimpedance amplifier with the signal frequency 1kHz and peak-to-peak value 990nA.

The results in Figure 15 - 4 show how the shape of the output signal changes when the signal frequency is 1MHz.
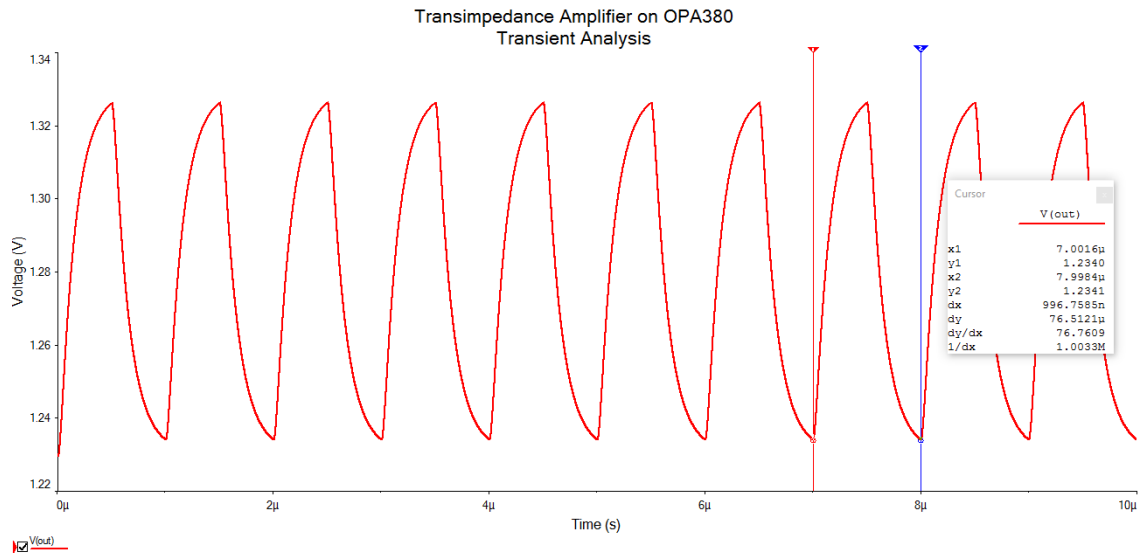
Figure 15 - 4. Output of the transimpedance amplifier with the signal frequency 1MHz and peak-to-peak value 990nA.

The AC transfer function was measured using AC Sweep analysis. The circuit which was used for the AC analysis is presented in Figure 15 - 5. The results are presented in Figure 15 - 6. The simulation shows that cut-off frequency was 1.327MHz.
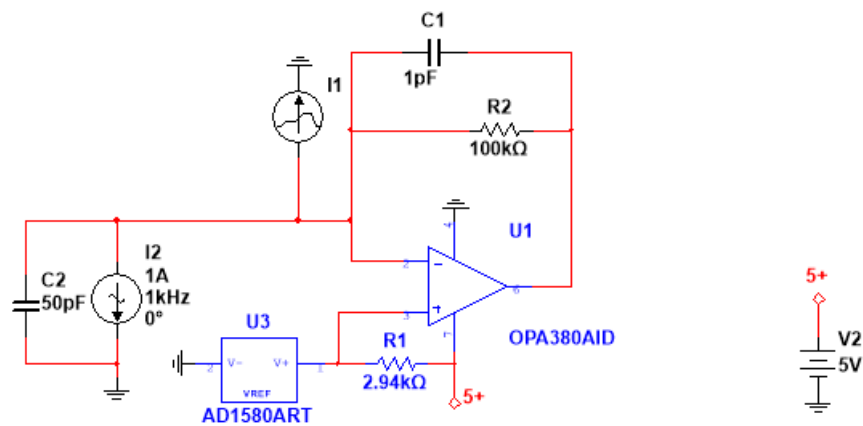
Figure 15 - 5. Circuit of the transimpedance amplifier for the AC analysis.

178
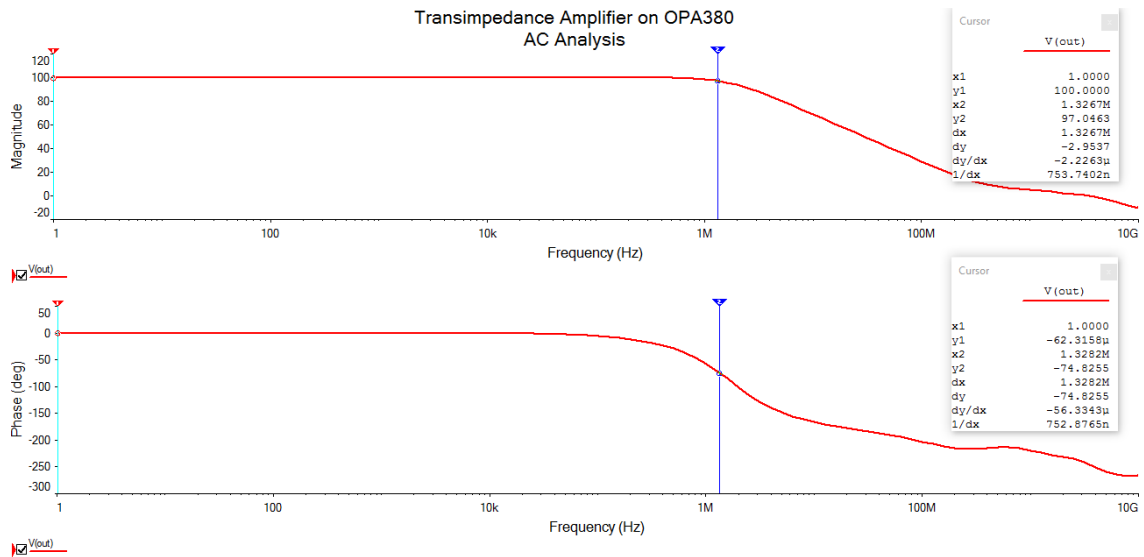
Figure 15 - 6. AC Analysis of the transimpedance amplifier.

The stability analysis in Figure 15 - 8 shows the loop closure point at 2.77MHz with 72.64 degrees of phase margin which means that the amplifier is stable. The circuit for the stability analysis is shown in Figure 15 - 7.
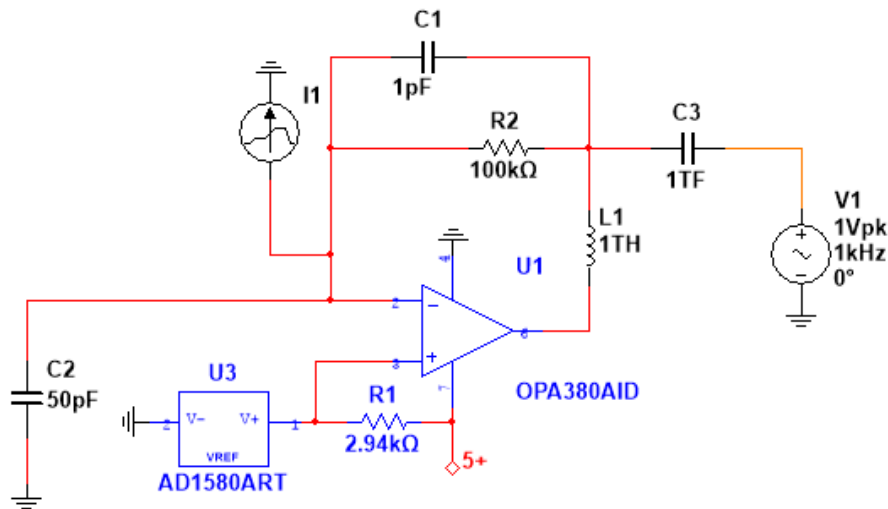
Figure 15 - 7. Circuit of the transimpedance amplifier for the stability analysis.
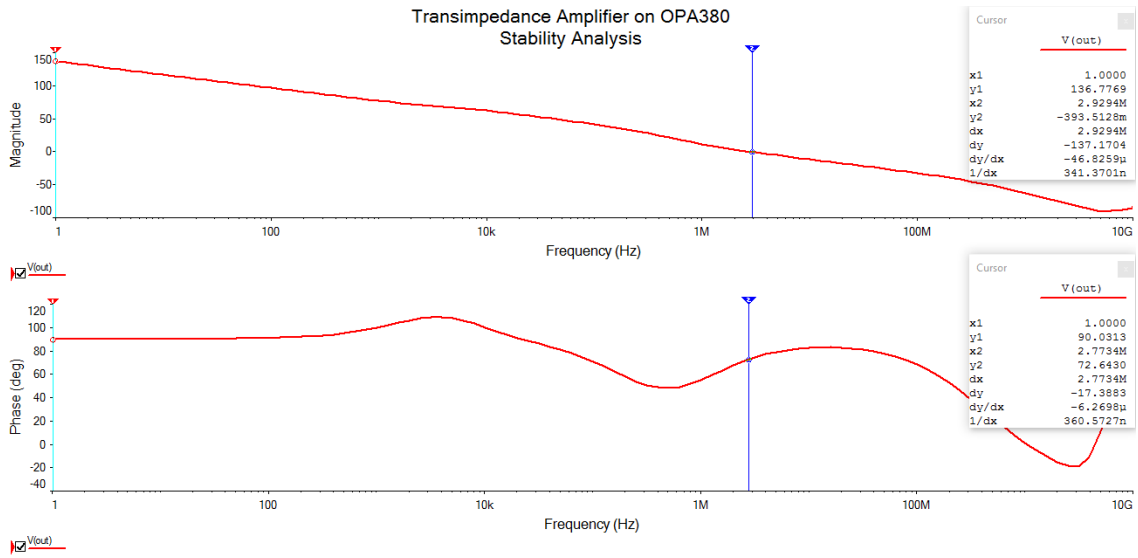
Figure 15 - 8. Stability Analysis of the transimpedance amplifier.

Appendix 16 – Print Circuit Board of the transimpedance amplifier

Before exporting the circuit to the 'Ultiboard' environment, it was modified by adding additional capacitor in parallel to the feedback resistor which could be observed in Figure 16 - 1. The reason is that the total value of the capacitor is low and the feedback resistor also contains parasitic capacitance which may result in overcompensation. During the assembly process only one capacitor would be added in parallel to the feedback resistor and, if any sort of instability would appear, additional one could be added later.
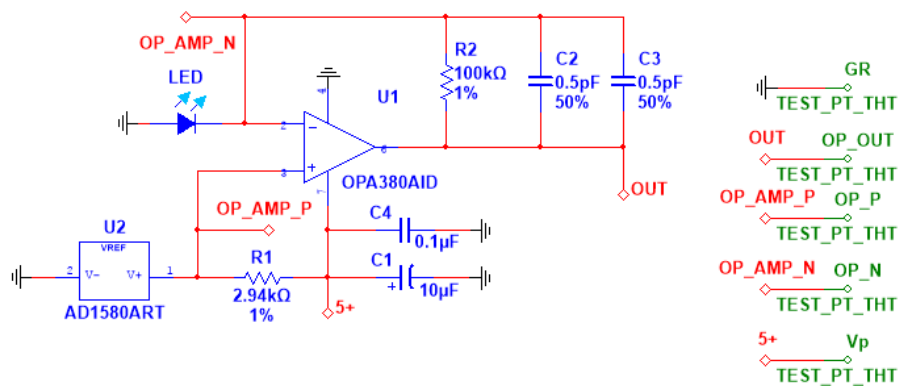
Figure 16 - 1. Modified circuit of the transimpedance amplifier.

The rules which were followed during construction of the PCB for the communication device in Appendix 11 – Print Circuit Board of the improved communication device also apply for the transimpedance amplifier. The board was designed with the length of 40mm and width of 30mm. The thickness of the board is 1.5mm and the width of the traces was set 0.5mm. The results of the PCB design with different layers and its 3D pictures could be found in Figure 16 - 2 - Figure 16 - 5.
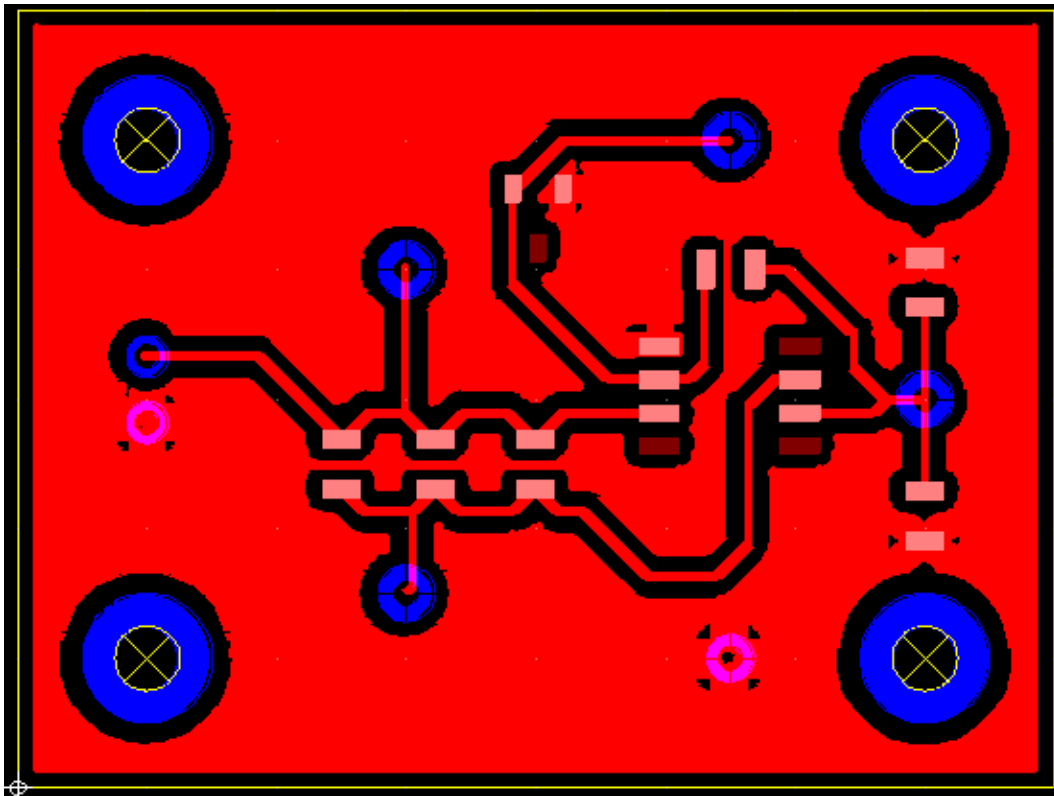
Figure 16 - 2. PCB with bottom copper cover.
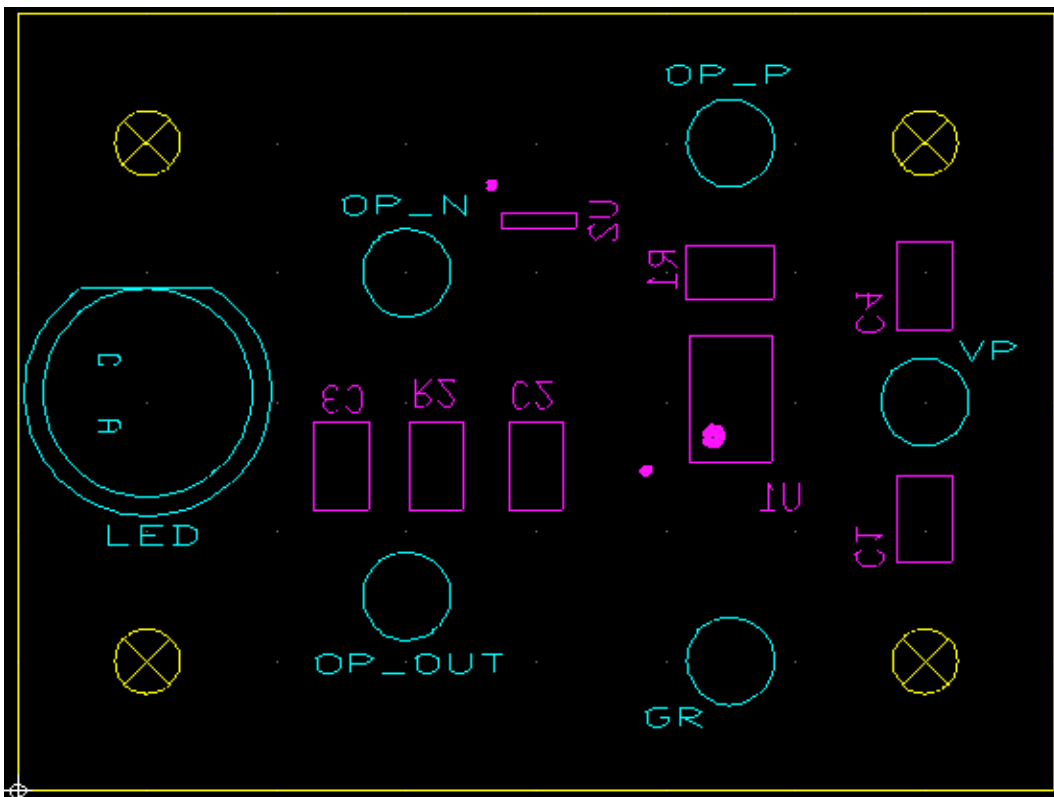
Figure 16 - 3. PCB with top and bottom silkscreens.
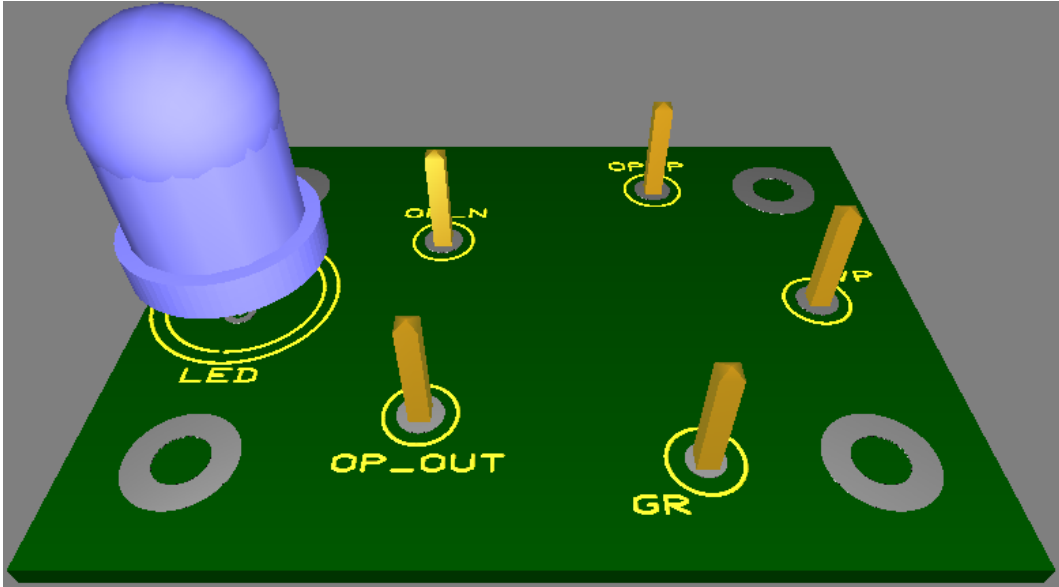
Figure 16 - 4. Top view of the prototype PCB 3D model.
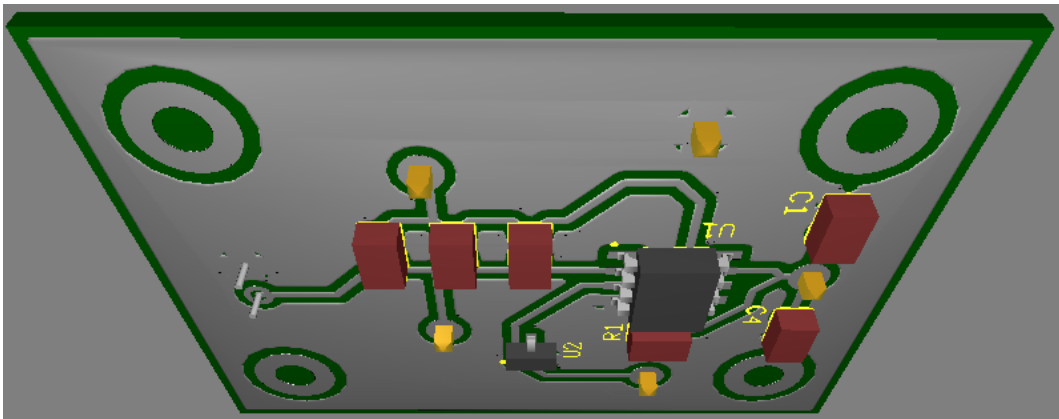
Figure 16 - 5. Bottom view of the prototype PCB 3D model.

Appendix 17 – Bill of materials for the transimpedance amplifier

All the components were purchased at Farnell. Note that some of the components could be only ordered in groups of multiple parts. The price regarding PCB is not included since the design could be constructed multiple ways. The price regarding LED is not included since the design is not tied to any particular LED.

Quantity	Description	Package	Reference Designator	Price for one	Total price
1	RESISTOR, 100kΩ 1%	0805	R2	0.0069	0.0069
1	CAP_ELECTROLIT, 10μF 20%	0805	C1	0.847	0.847
1	CAPACITOR, 0.1μF 10%	0805	C4	0.0521	0.0521
1	RESISTOR, 2.94kΩ 1%	0805	R1	0.0124	0.0124
1	OPAMP, OPA380AID	SOIC-D-8	U1	5.66	5.66
2	CAPACITOR, 0.5pF 50%	0805	C2, C3	0.0289	0.0578
1	VOLTAGE_REFERENCE, AD1580ART	SOT-23-RT-3	U2	2.22	2.22
				Totally:	8.8562

Table 17 - 1. Bill of materials for the transimpedance amplifier.

Appendix 18 – Results of the tests of the transimpedance amplifier

The transimpedance amplifier prototype was tested and its performance was monitored. The supply voltage for the device was 5V. The input signal type was square signal with duty cycle 50%. The frequency varied from 1kHz till 1.5MHz. The distance between the emitter and receiver was also changing. There were two types of device tested, one with 100kOhm feedback resistance and one with 3.3MOhm. The test setup could be observed in next Figure 18 - 1.

Figure 18 - 1. Picture of the test setup for the transimpedance amplifier.

Feedback resistance 100kOhm

The feedback resistor had additional 1pF compensation capacitor in parallel in order to prevent oscillations. The Figure 18 - 2, Figure 18 - 3 and Figure 18 - 4 show the performance of the transimpedance amplifier when the distance between the devices is only 3sm. The red trace represents signal to be transmitted and the green trace received signal.
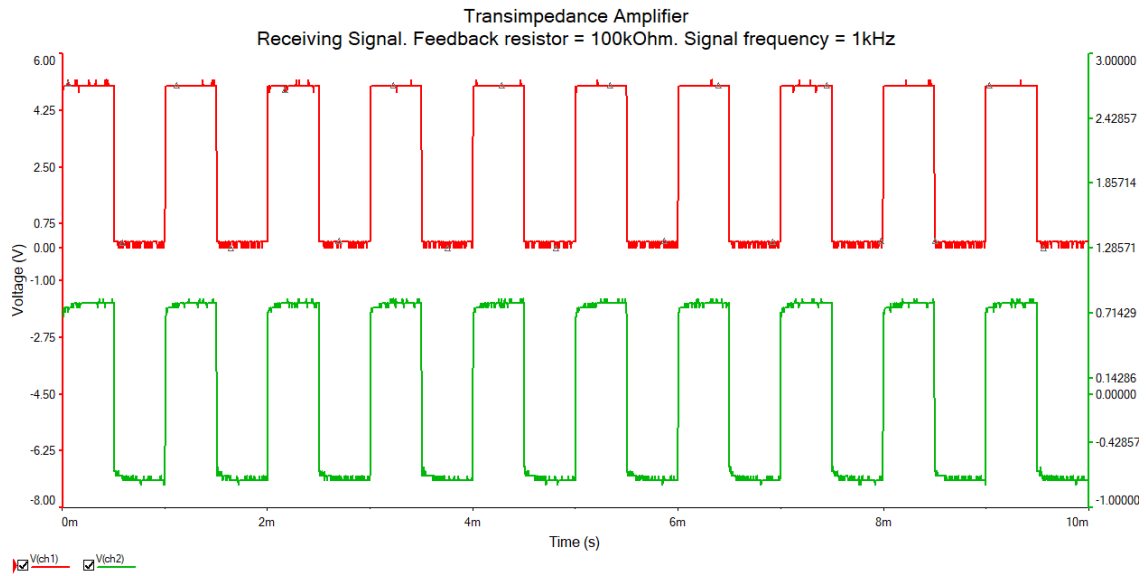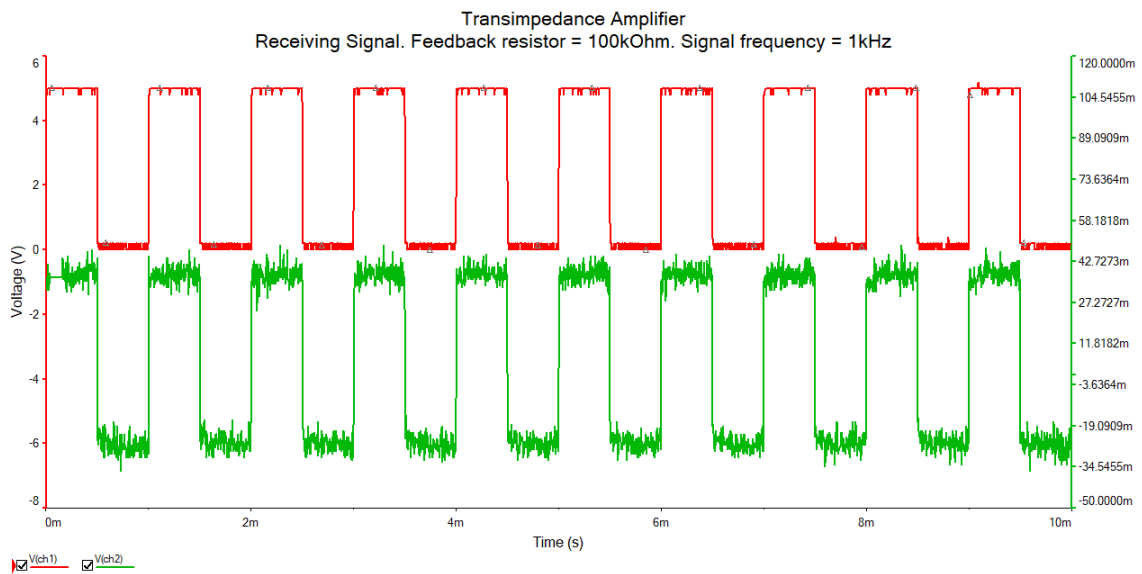
Figure 18 - 2. Results of the measurements when the distance between devices was 3sm and frequency signal 1kHz. Red trace – transmitter input signal, green trace – TIA output signal.
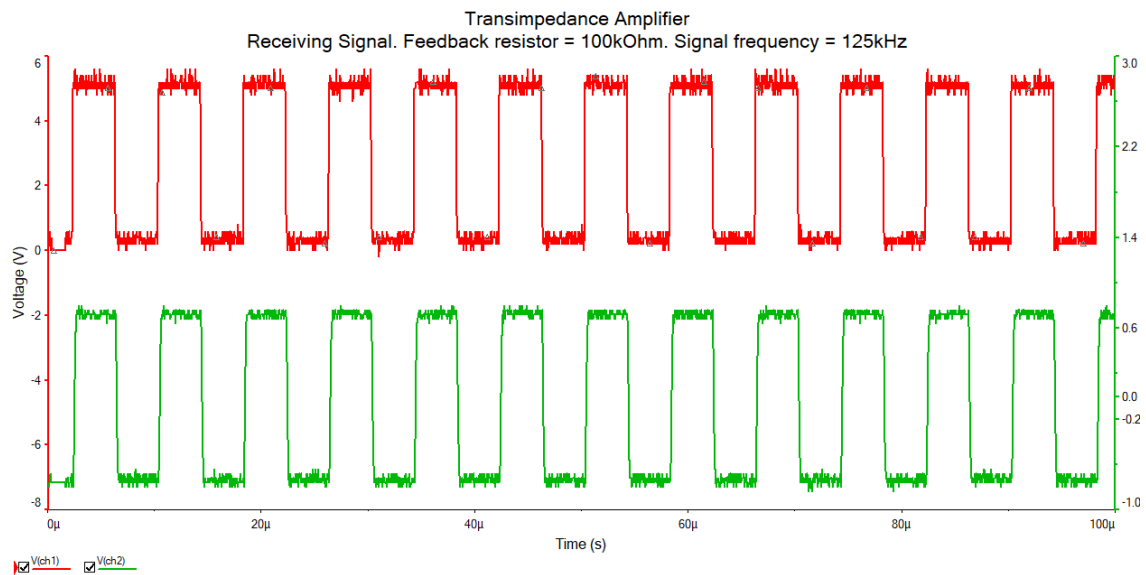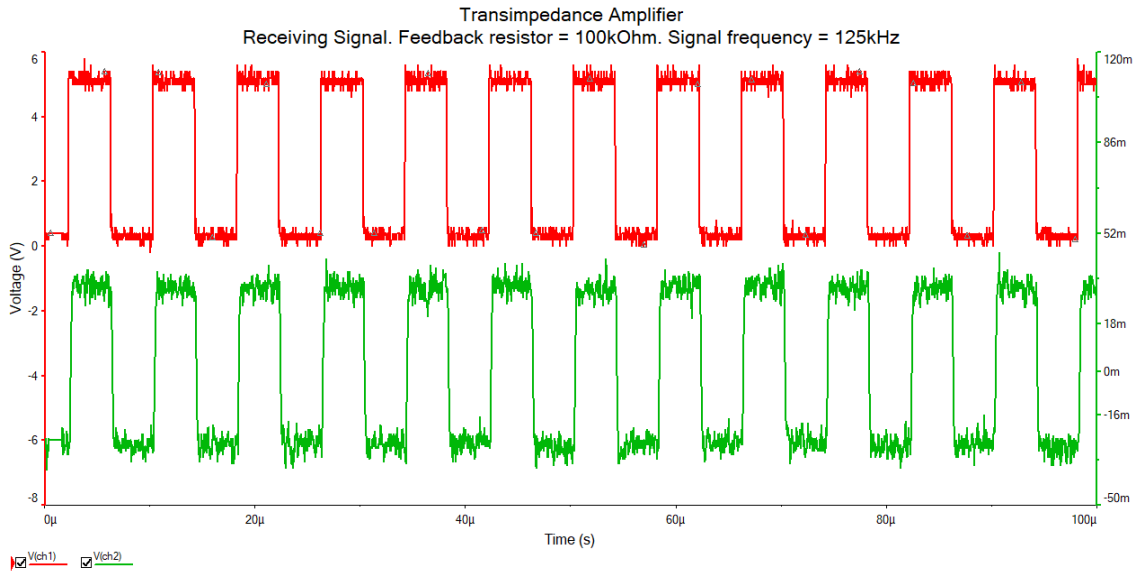

Figure 18 - 3. Results of the measurements when the distance between devices was 3sm and frequency signal 125kHz. Red trace – transmitter input signal, green trace – TIA output signal.
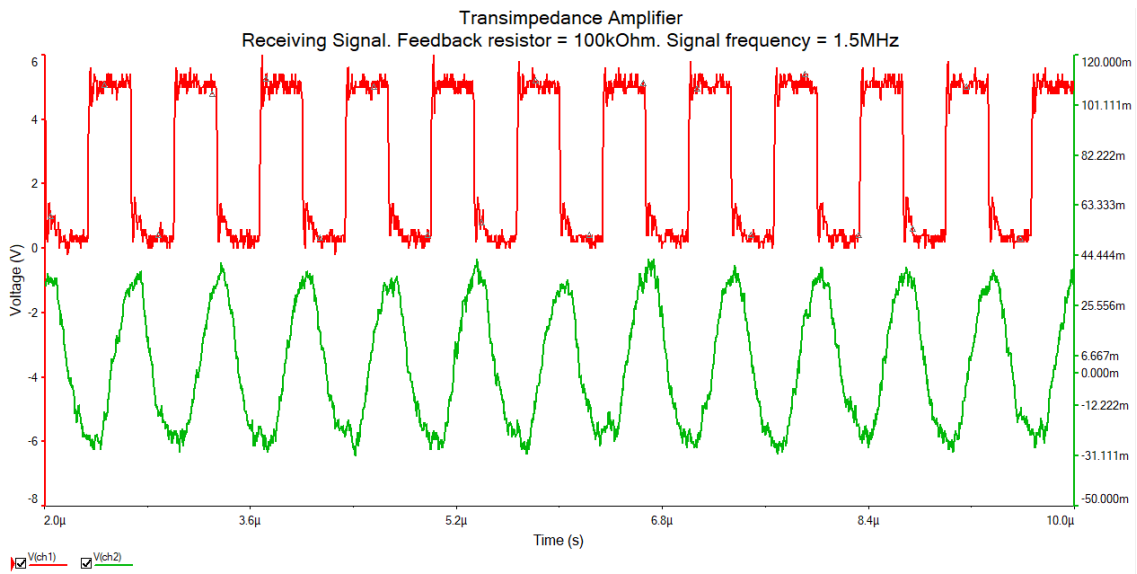
186
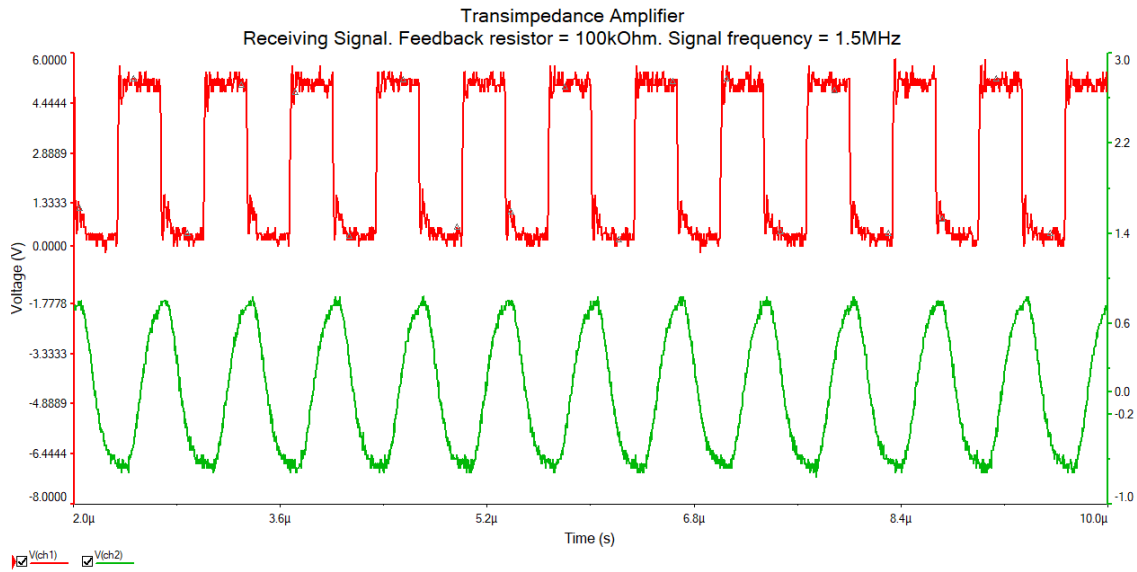
Figure 18 - 4. Results of the measurements when the distance between devices was 3sm and frequency signal 1.5MHz. Red trace – transmitter input signal, green trace – TIA output signal.

The Figure 18 - 5, Figure 18 - 6 and Figure 18 - 7 show the performance of the transimpedance amplifier when the distance between the devices is only 25sm. At this distance the lux-meter showed 190lx.
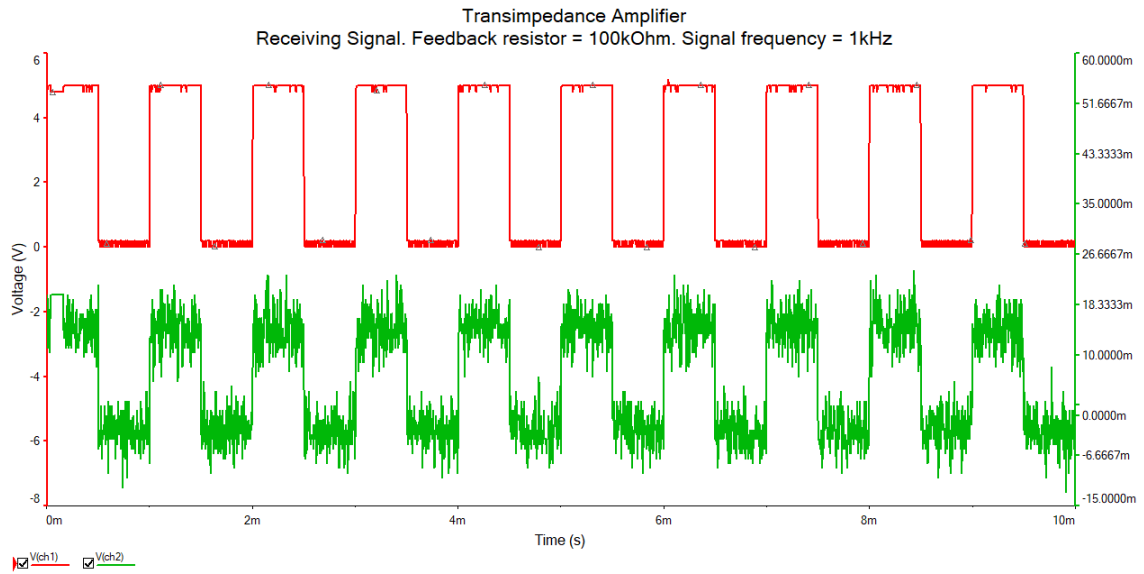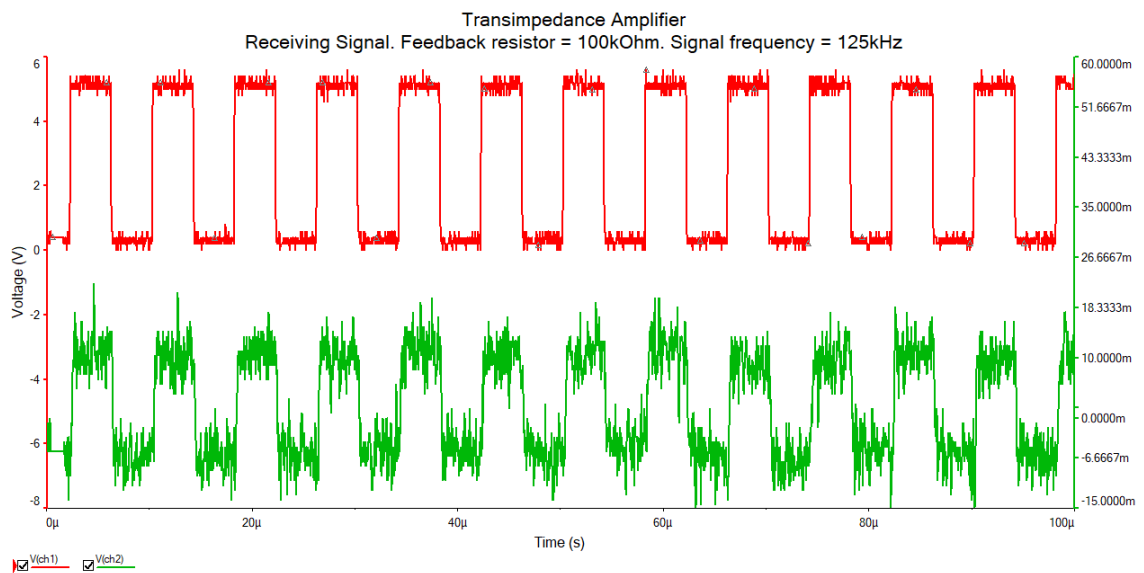

Figure 18 - 5. Results of the measurements when the distance between devices was 25sm and frequency signal 1kHz. Red trace – transmitter input signal, green trace – TIA output signal.

187

Figure 18 - 6. Results of the measurements when the distance between devices was 25sm and frequency signal 125kHz. Red trace – transmitter input signal, green trace – TIA output signal.
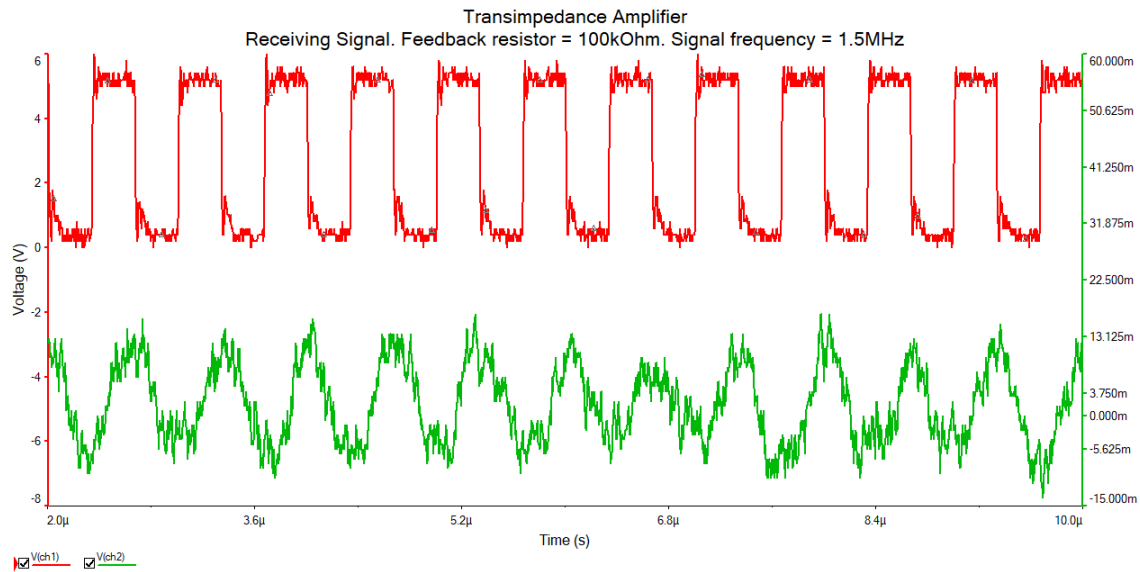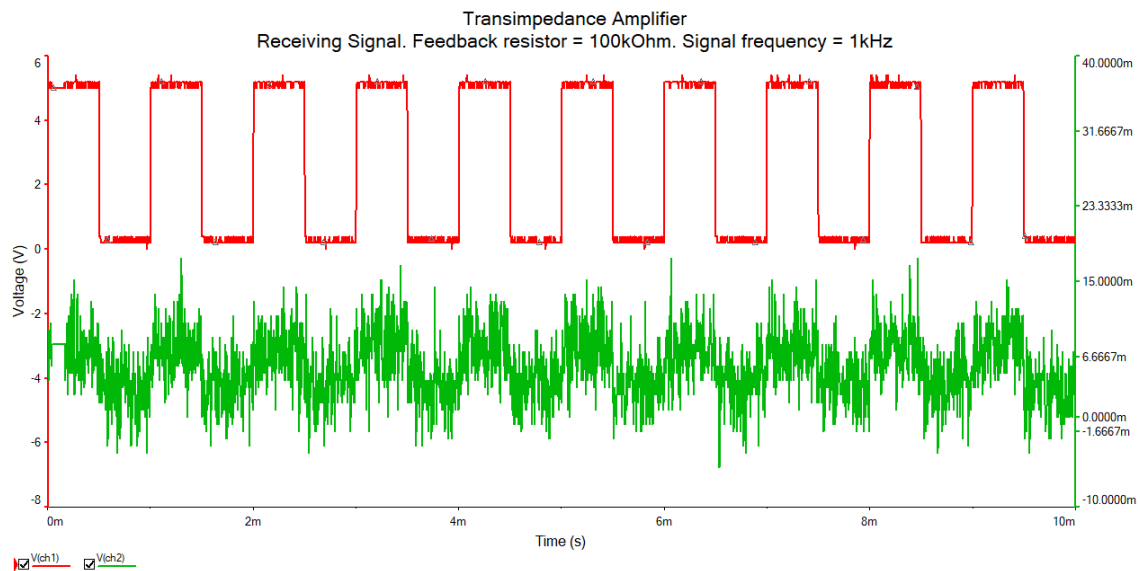

Figure 18 - 7. Results of the measurements when the distance between devices was 25sm and frequency signal 1.5MHz. Red trace – transmitter input signal, green trace – TIA output signal.

The Figure 18 - 8, Figure 18 - 9 and Figure 18 - 10 show the performance of the transimpedance amplifier when the distance between the devices is only 50sm. At this distance the lux-meter showed 80lx.

Figure 18 - 8. Results of the measurements when the distance between devices was 50sm and frequency signal 1kHz. Red trace – transmitter input signal, green trace – TIA output signal.
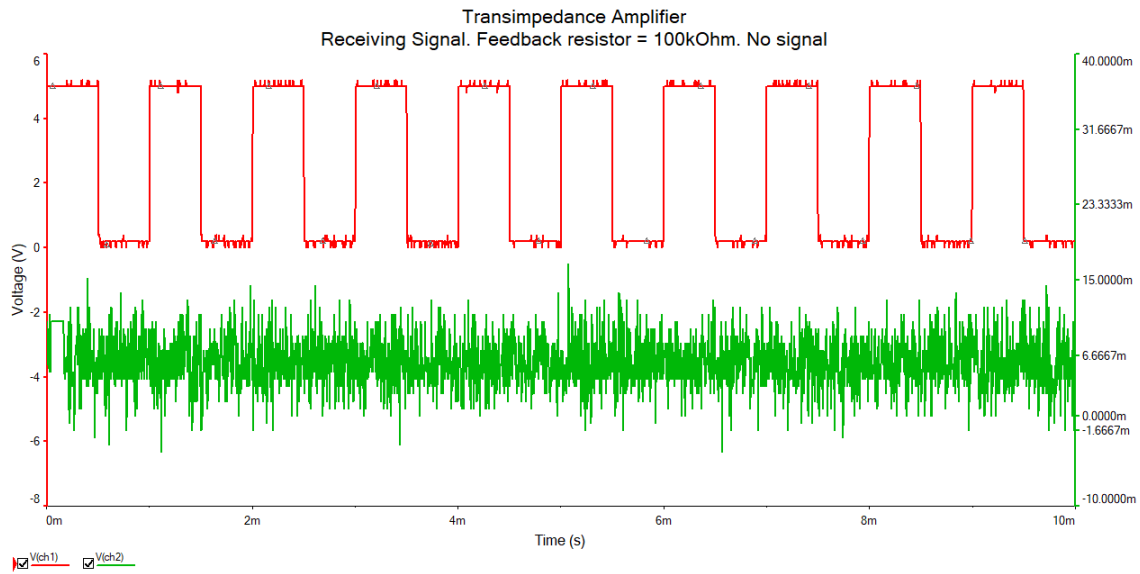

Figure 18 - 9. Results of the measurements when the distance between devices was 50sm and frequency signal 125kHz. Red trace – transmitter input signal, green trace – TIA output signal.
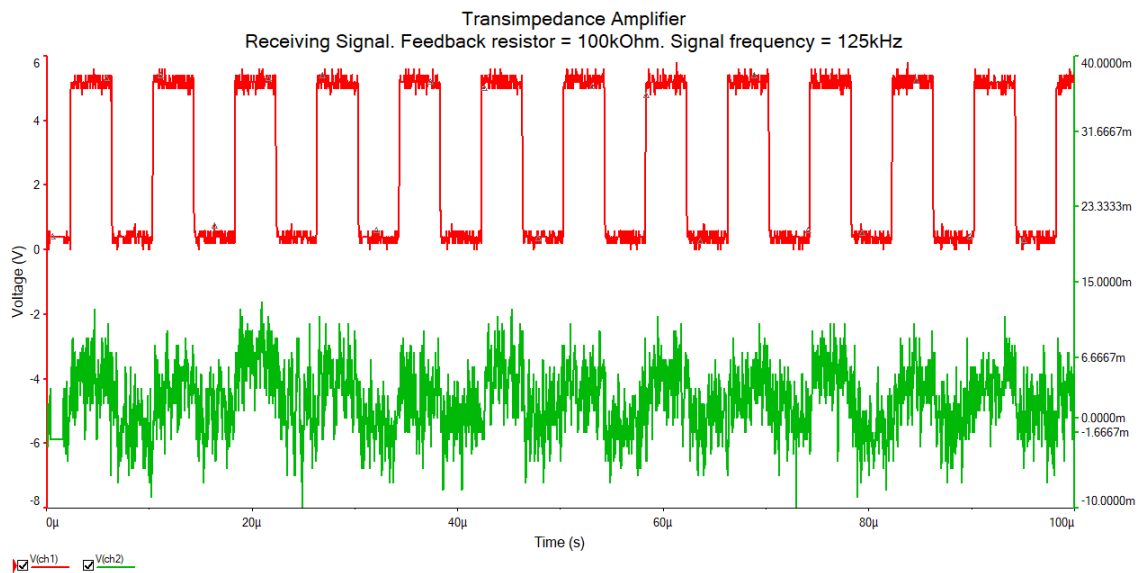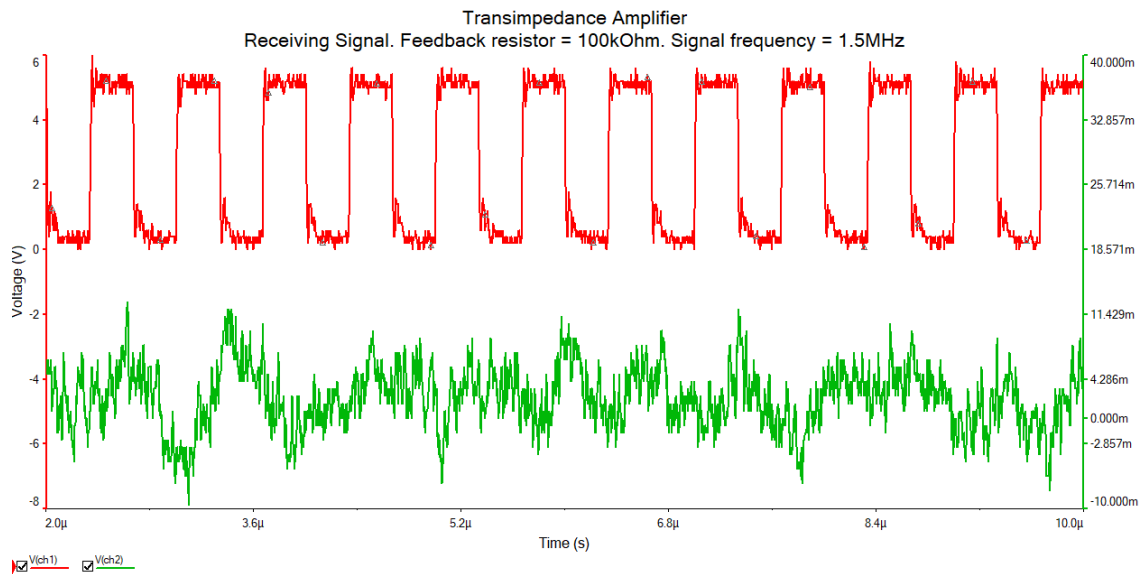
189

Figure 18 - 10. Results of the measurements when the distance between devices was 50sm and frequency signal 1.5MHz. Red trace – transmitter input signal, green trace – TIA output signal.

The Figure 18 - 11, Figure 18 - 13 and Figure 18 - 14 show the performance of the transimpedance amplifier when the distance between the devices is only 1m. At this distance the lux-meter showed 20lx.The Figure 18 - 12 shows the situation when there was no signal sent to compare with the situation when 1kHz signal was received.

Figure 18 - 11. Results of the measurements when the distance between devices was 1m and frequency signal 1kHz. Red trace – transmitter input signal, green trace – TIA output signal.

Figure 18 - 12. Results of the measurements when the distance between devices was 1m and no signal registered. Red trace – transmitter input signal, green trace – TIA output signal.
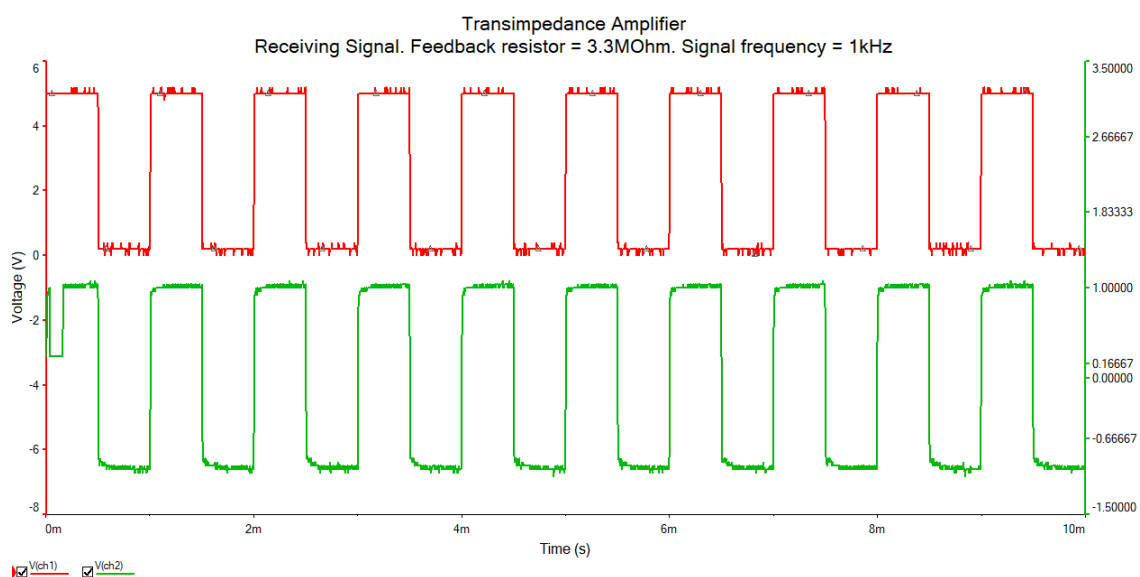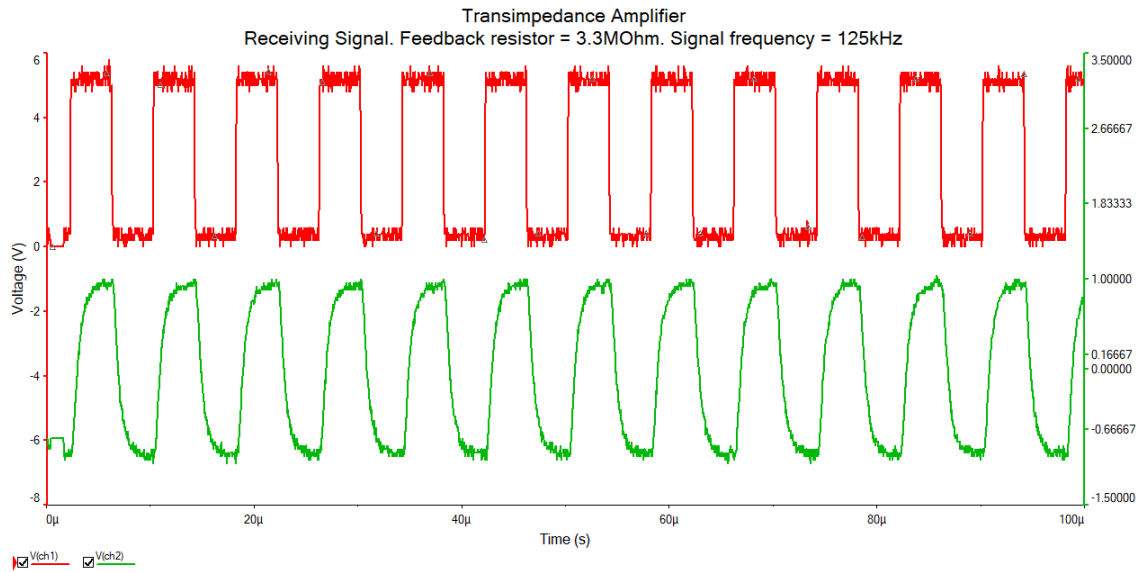

Figure 18 - 13. Results of the measurements when the distance between devices was 1m and frequency signal 125kHz. Red trace – transmitter input signal, green trace – TIA output signal.

191

Figure 18 - 14. Results of the measurements when the distance between devices was 1m and frequency signal 1.5MHz. Red trace – transmitter input signal, green trace – TIA output signal.

Feedback resistance 3.3MOhm

The feedback resistor didn't have any additional compensation capacitor in parallel the value of which was very low and in this case the parasitic capacitance of the resistor replace the compensation capacitor. The Figure 18 - 15, Figure 18 - 16 and Figure 18 - 17 show the performance of the transimpedance amplifier when the distance between the devices is only 25sm. The red trace represents signal to be transmitted and the green trace received signal.
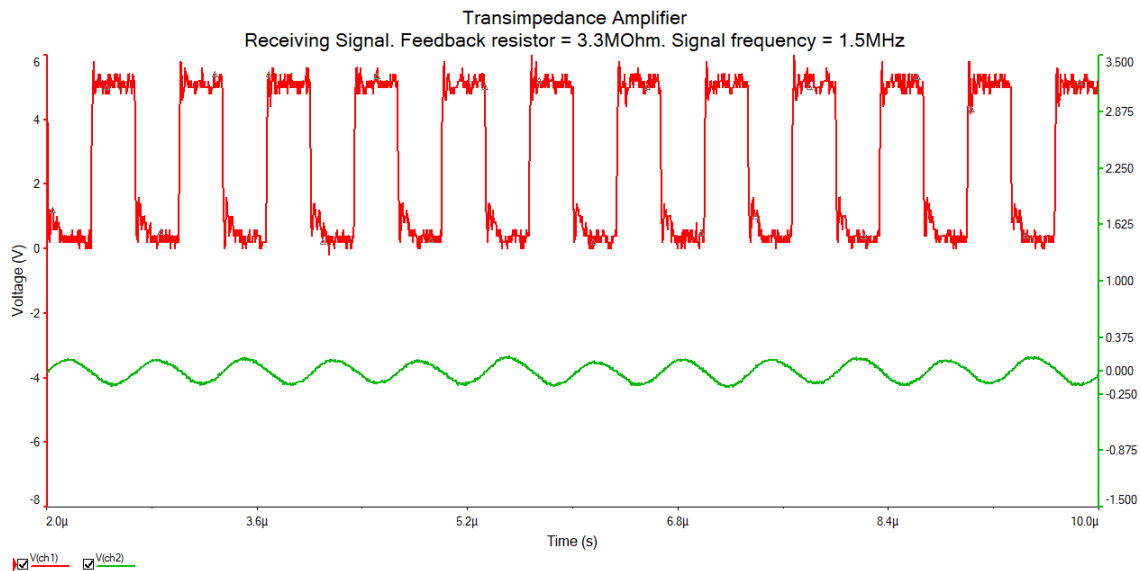

Figure 18 - 15. Results of the measurements when the distance between devices was 25sm and frequency signal 1kHz. Red trace – transmitter input signal, green trace – TIA output signal.
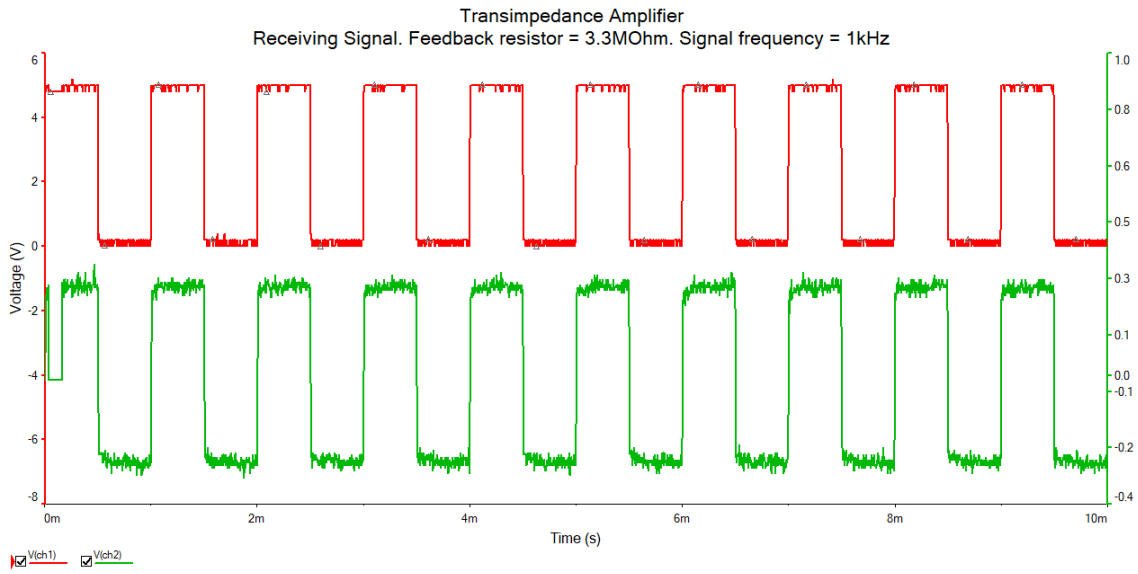
192

Figure 18 - 16. Results of the measurements when the distance between devices was 25sm and frequency signal 125kHz. Red trace – transmitter input signal, green trace – TIA output signal.
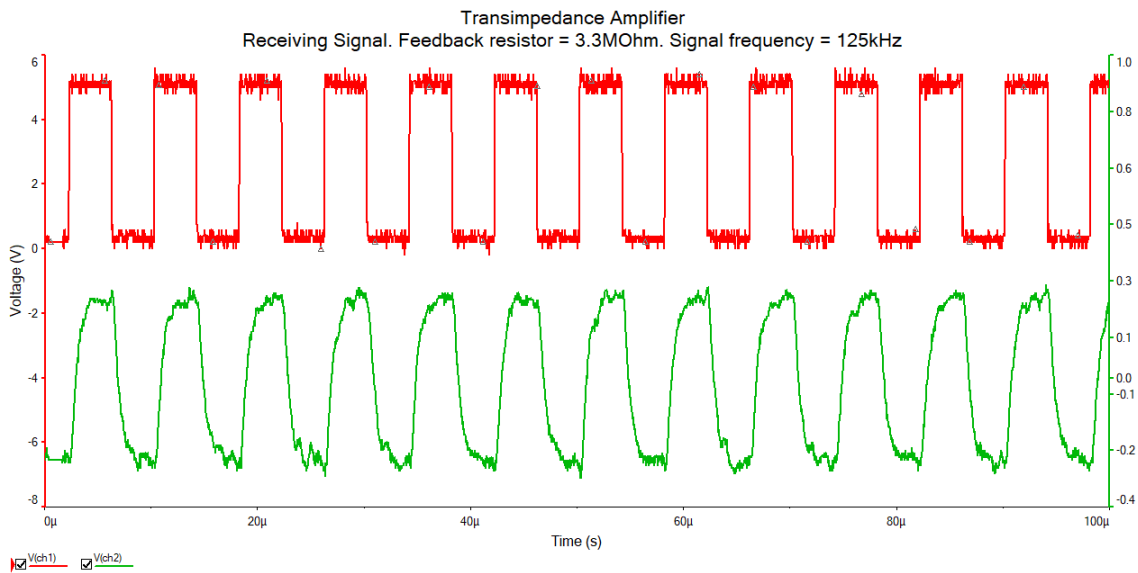

Figure 18 - 17. Results of the measurements when the distance between devices was 25sm and frequency signal 1.5MHz. Red trace – transmitter input signal, green trace – TIA output signal.

The Figure 18 - 18, Figure 18 - 19 and Figure 18 - 20 show the performance of the transimpedance amplifier when the distance between the devices is only 50sm.

Figure 18 - 18. Results of the measurements when the distance between devices was 50sm and frequency signal 1kHz. Red trace – transmitter input signal, green trace – TIA output signal.

Figure 18 - 19. Results of the measurements when the distance between devices was 50sm and frequency signal 125kHz. Red trace – transmitter input signal, green trace – TIA output signal.
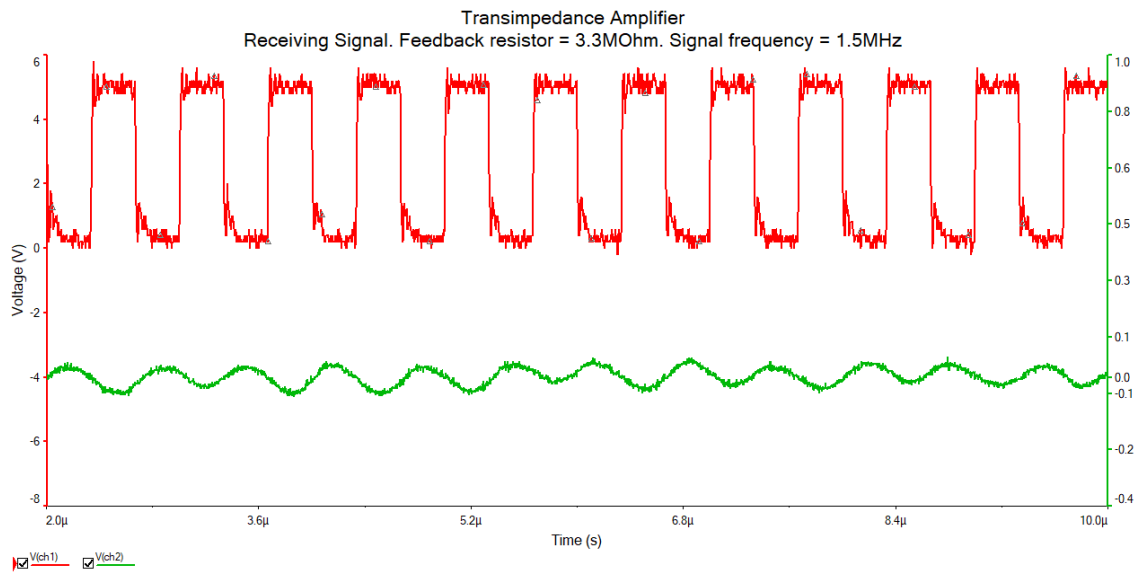
194

Figure 18 - 20. Results of the measurements when the distance between devices was 50sm and frequency signal 1.5MHz. Red trace – transmitter input signal, green trace – TIA output signal.

The Figure 18 - 21, Figure 18 - 22 and Figure 18 - 23 show the performance of the transimpedance amplifier when the distance between the devices is only 1m.
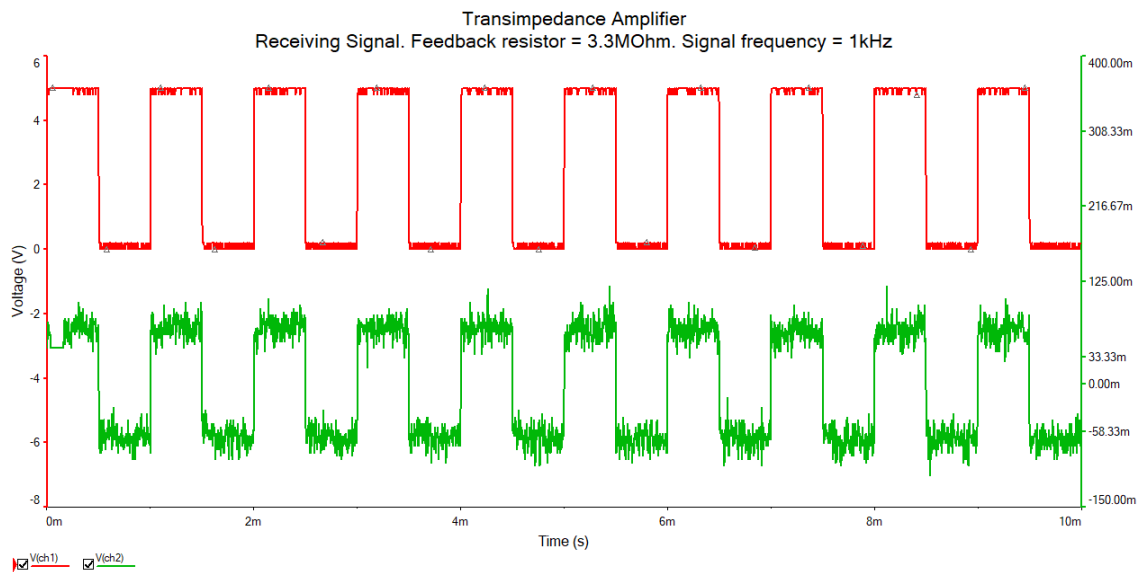

Figure 18 - 21. Results of the measurements when the distance between devices was 1m and frequency signal 1kHz. Red trace – transmitter input signal, green trace – TIA output signal.
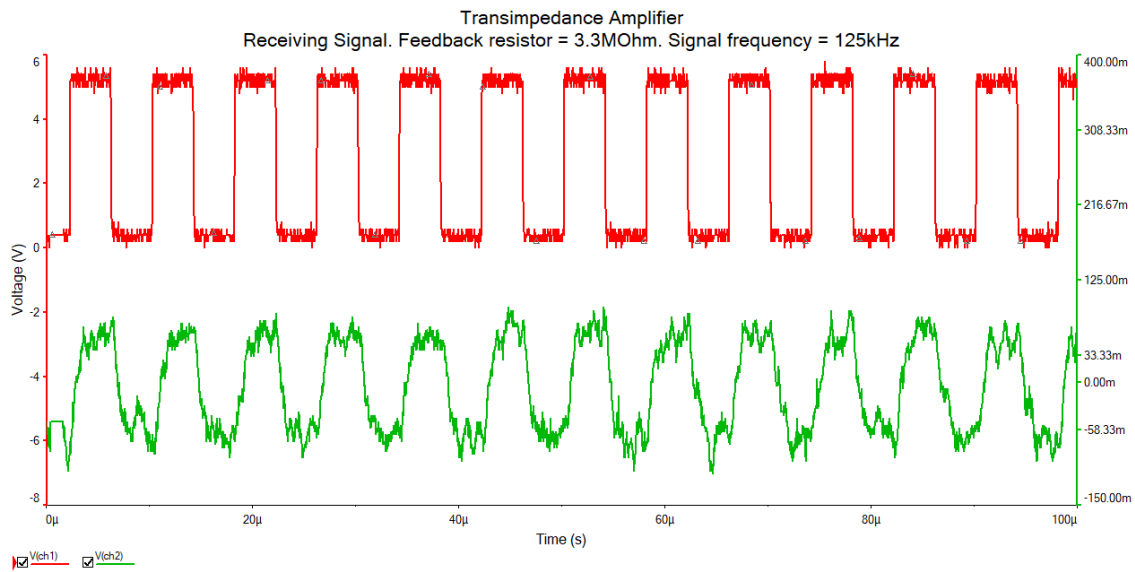
195

Figure 18 - 22. Results of the measurements when the distance between devices was 1m and frequency signal 125kHz. Red trace – transmitter input signal, green trace – TIA output signal.
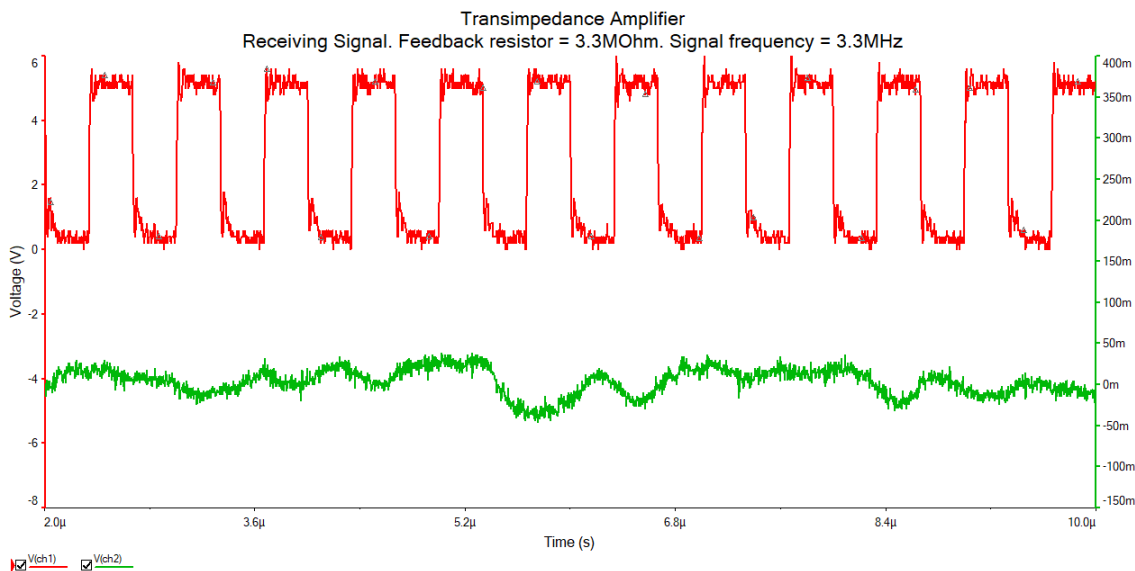

Figure 18 - 23. Results of the measurements when the distance between devices was 1m and frequency signal 1.5MHz. Red trace – transmitter input signal, green trace – TIA output signal.

Measured frequency response of the transimpedance amplifier

For this measurement lock-in amplifier with internal signal generator used. The White 'Bright' LED was used as light signal source connected in series with 150 Ohm resistance. The DC voltage offset was set to 5V. The sine wave with amplitude of 1V was generated and frequency of the signal increased from 300Hz to 5MHz. The distance between the

detector and emitter was measured to be 25sm. The frequency response with the lock-in amplifier was measured and the results are presented in Figure 18 - 24.
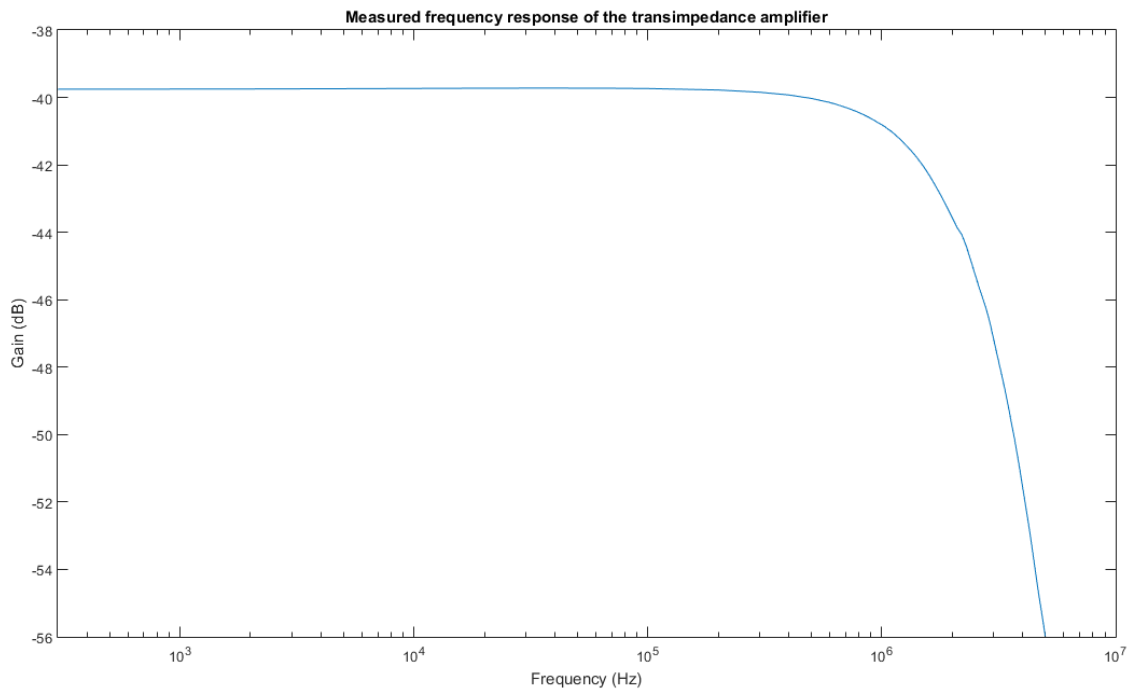

Figure 18 - 24. Results of the frequency response measurements of the transimpedance amplifier.

The results show that the cut-off frequency to be very close to the calculated value which show that calculations were made very accurate. The received results show that the selected feedback resister gives good gain for the transimpedance amplifier circuit and high bandwidth.

On-off keying analysis

In previous measurements the square shape signal was used to imitate data transmission. In this analysis lock-in features were used to lock-in to certain frequency and analyse the circuit when the modulation is used in order to increase SNR and, as a result, possible distance increase between the devices.

The sending device was set to 5V DC. The amplitude of the carrier frequency varied from 1V to 25mV. The frequency value was chosen to be 1.7MHz which is the cut-off frequency of the circuit. The lock-in amplifier senses only AC part of the signal and the root-mean square value of the output signal should increase when the device senses the carrier frequency. When the carrier signal is sent, the output voltage rises and if not, then only noise could be registered. The results of the measurements could be observed in Figure 18 - 25, Figure 18 - 26 and Figure 18 - 27.
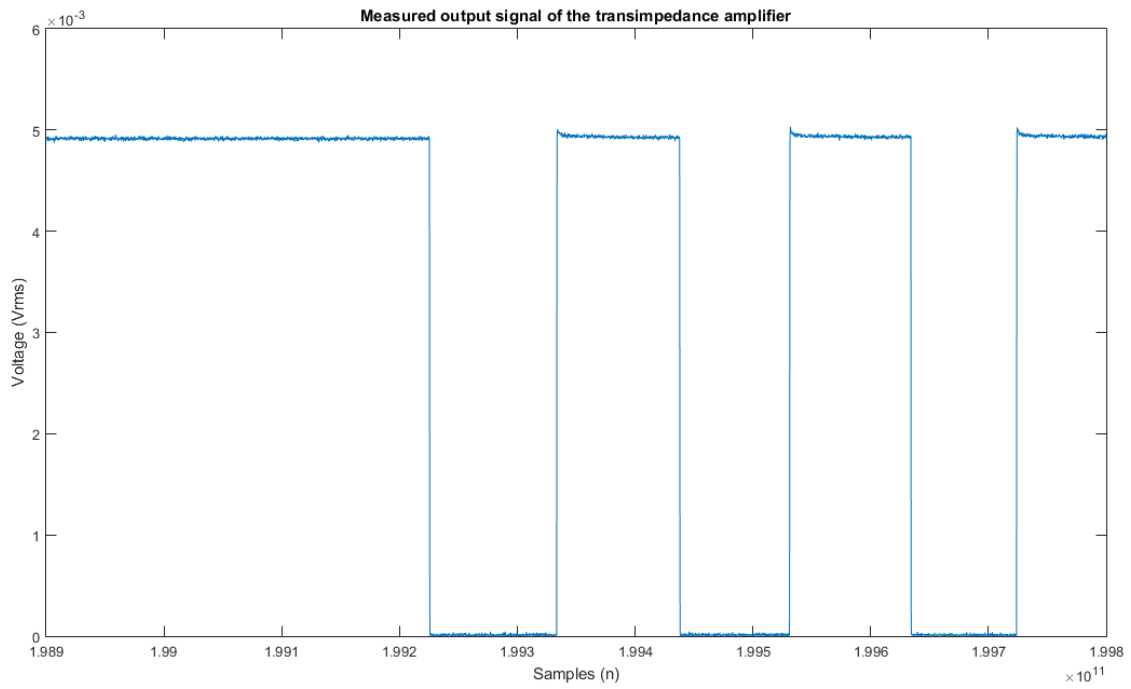
197

Figure 18 - 25. Results of the measured output signal of the transimpedance amplifier with 335uW power of the signal.
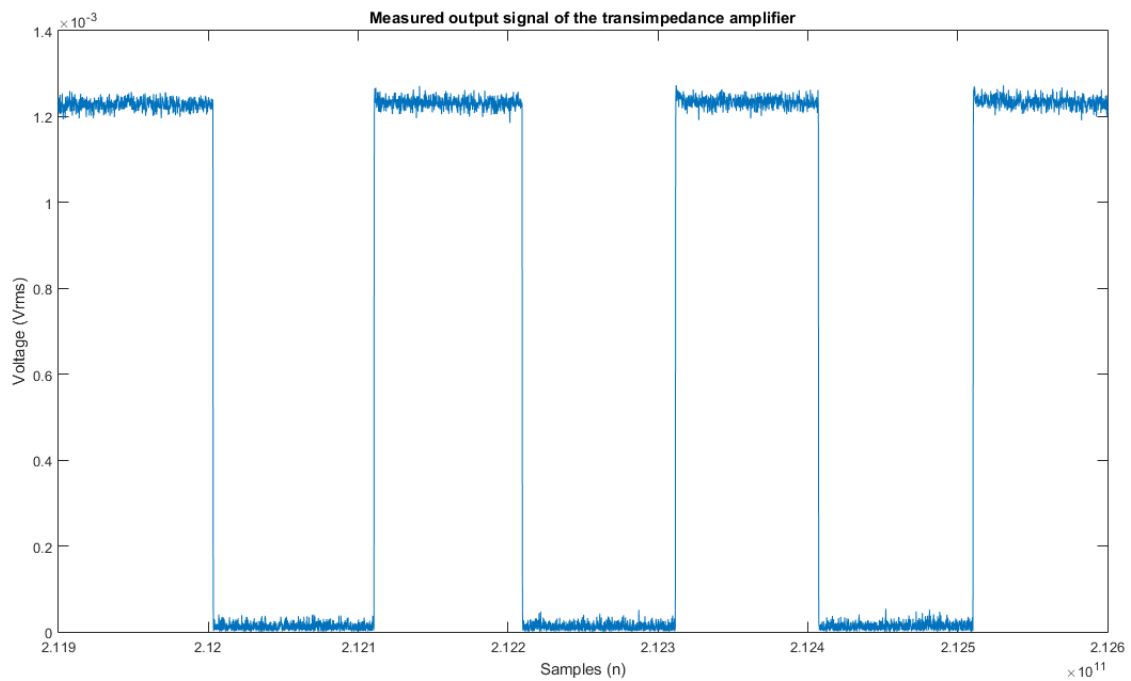

Figure 18 - 26. Results of the measured output signal of the transimpedance amplifier with 20uW power of the signal.
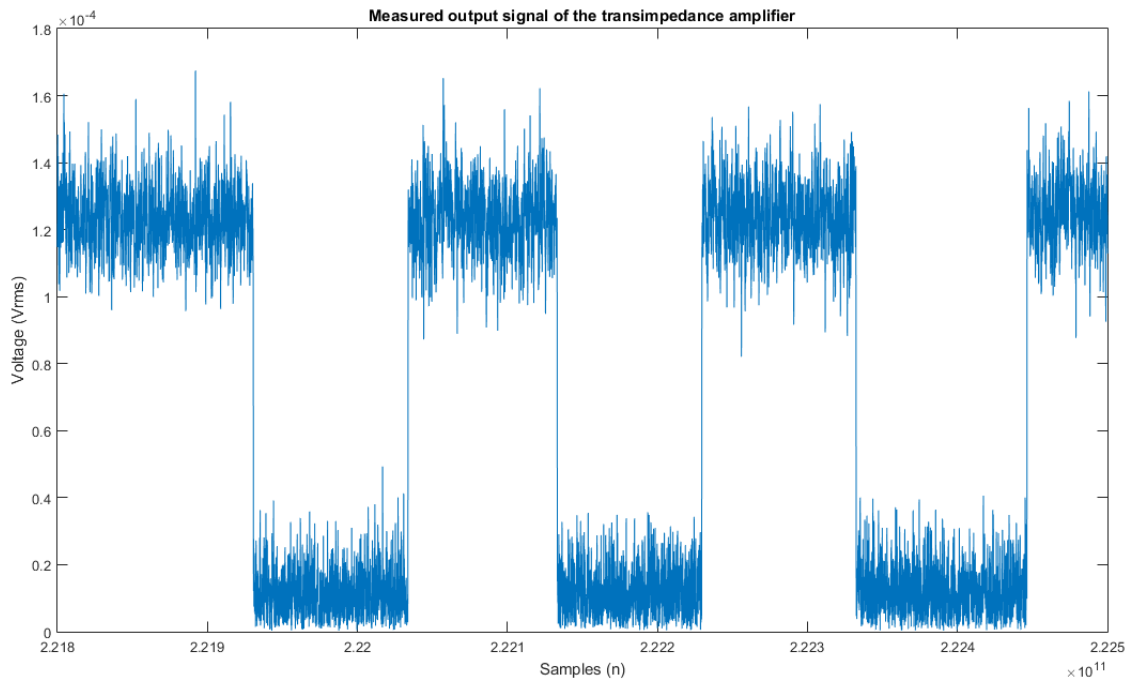
Figure 18 - 27. Results of the measured output signal of the transimpedance amplifier with 0.2uW power of the signal.

The results show that using lock-in feature and signal modulation allow to register the incoming signal even in range of microvolts which allows to significantly increase the sensitivity of the device and, as a result, the distance between communicating devices.